Università degli Studi di Napoli Federico II

Dottorato di Ricerca in Biologia

XXXII ciclo

Effect of Light, Iron and Vitamin B_{12} Co-limitation on Phytoplankton Species of the Ross Sea (Antarctica). Ecological implications.

Effetto della co-limitazione luce, ferro e vitamina B_{12} su specie fitoplanctoniche del Mare di Ross (Antartide). Implicazioni Ecologiche

Coordinatore:

Prof. Salvatore Cozzolino

Dottorando:

Dott. Francesco Bolinesi

Tutor:

Prof.ssa Olga Mangoni

Dott.sa Maria Saggiomo

A.A. 2016-2017

The problem **Page 1**

Rationale, working hypotheses and activities articulation of the thesis **Page 1**

BACKGROUND AND OVERVIEW **Page 4**

MATERIAL AND METHODS **Page 11**

Field activities **Page 11**

P-ROSE and CELEBER Cruise (PNRA expedition) **Page 11**

CICLOPS Cruise (NSF expedition) **Page 13**

Laboratory procedures **Page 13**

- ***Pigment analysis*** **Page 13**
- ***Nutrient Analyses*** **Page 14**
- ***Photosynthetic efficiency and physiological status of phytoplankton cells*** **Page 15**
- ***Molecular analysis*** **Page 15**
- ***Statistical analysis*** **Page 16**

Phytoplankton culturing and manipulative experiments **Page 16**

- ***Species isolation and maintenance of monospecific culture*** **Page 16**
- ***Experimental Set-Up*** **Page 17**

RESULTS

P-ROSE and CELEBER Cruise (PNRA expedition) **Page 19**

CICLOPS (NSF expedition) **Page 28**

- ***Shipboard co-limitation experiments on natural populations*** **Page 29**

The discovery of a *Prorocentrum* sp. in association with gelatinous colonies of *Phaeocystis antarctica* **Page 31**

Manipulative experiments **Page 34**

Experiment 1 - ANEMIA **Page 34**

Experiment 2 – High Light –Low Light **Page 39**

DISCUSSION AND CONCLUSIONS **Page 44**

Concluding remark **Page 47**

Acknowledgments **Page 48**

REFERENCES **Page 49**

To my family,

nature,

and fundamentals of life.

EFFECT OF LIGHT, IRON AND VITAMIN B_{12} CO-LIMITATION ON PHYTOPLANKTON SPECIES OF THE ROSS SEA (ANTARCTICA). ECOLOGICAL IMPLICATION.

The problem

The Southern Ocean represents an important area for the uptake and storage of atmospheric CO_2 via primary production. For this reason, the Southern Ocean is considered a key area for studying and monitoring global climate change.

Primary production in the Antarctic Ocean is essentially driven by phytoplankton production and this attracts the attention of wide array of Antarctic researchers. The physical-chemical factors affecting the availability of energy (light) and materials (macro- and micro-nutrients) for the phytoplankton are therefore central to the comprehension of the ecology of the Antarctic Ocean.

Phytoplankton communities of the Ross Sea are dominated by the haptophyte *Phaeocystis antarctica* Kersten and diatoms. Production processes are characterized by the incomplete utilization of macronutrients and limited by the availability of micro nutrients, mainly iron. This latter is involved as the main cause of the "High Nutrient – Low Chlorophyll *a*" condition of Antarctic primary production. Diatoms and the haptophyte *Phaeocystis antarctica* show different spatial-temporal patterns and show a different trophic fate. However, the complete regulatory mechanisms of these patterns are still poorly understood. Understanding the dynamics controlling the influence of bottom-up factors such as iron and vitamin B_{12} availability on phytoplankton species composition in Antarctic coastal waters, as well as the open Southern Ocean, still represents an important research area, given the impact of primary production on biogeochemical cycles in the Southern Ocean and their influence on climate change.

Rationale, working hypotheses and activities articulation of the thesis

This thesis aimed at understanding the ecophysiological mechanisms implied in primary production processes in Antarctic waters, addressing aspects related to structural and functional biodiversity of phytoplankton, their production efficiency and the limiting role of iron and vitamin B_{12} in determining rates and timing of production. The specific hypotheses (H) to be tested in the proposed study include the following:

H1: The phytoplankton community structure in the Ross Sea vary in space and time.

H2: The continental melting processes play a pivotal role in primary production processes during summer.

H3: Light availability and Mixed Layer depth control the vertical distribution of phytoplankton groups.

H4: Iron and vitamin B_{12} availability play a key role in the ecology of Antarctic phytoplankton productivity.

The thesis can be divided into two phases.

In the first phase, problems of phytoplankton ecology have been addressed in situ, namely the role of macro- and micro-nutrients and the structural and functional aspects of phytoplankton communities in terms of functional groups, size classes (data not showed), and aspects of the photosynthetic process with particular attention to photosynthetic efficiency. Field activities have been carried out in the Antarctic waters of the Ross Sea and Marie Byrd Land. The field work has been carried out personally by the candidate in the frame of the Italian project for Antarctic research (PNRA) and within a formal collaboration with a research group supported by the National Science Foundation (USA) focused on the role of iron and vitamin B_{12} co-limitation in regulating primary production processes and an aspects of community structure.

The above activity has been the object of the following papers:

1. Mangoni O., Saggiomo M., **Bolinesi F.**, Castellano M., Povero P., Saggiomo V., DiTullio G.R. (2019). *Phaeocystis antarctica* unusual summer bloom in stratified Antarctic coastal waters (Terra Nova Bay, Ross Sea). Marine Environmental Research, 151, 104733. doi: 10.1016/j.marenvres.2019.05.012 (attachment 1).

2. Rivaro P., Ardini F., Grotti M., Aulicino G., Cotroneo Y., Fusco G. , Mangoni O., **Bolinesi F.**, Saggiomo M., Celussi M. (2019). Mesoscale variability related to iron speciation in a coastal Ross Sea area (Antarctica) during summer 2014. Chemistry and Ecology, 35 (1-2): 1-19 (attachment 2).

3. Escalera L., Mangoni O., **Bolinesi F.**, Saggiomo M. (2019). Austral Summer Bloom of Loricate Choanoflagellates in the Central Ross Sea Polynya. Journal of Eukaryotic Microbiology. doi: 10.1111/jeu.12720 (attachment 3).

4. Mangoni O., Saggiomo V., **Bolinesi F.**, Escalera L., Saggiomo M. (2018). A review of past and present summer primary production processes in the Ross Sea in relation to changing ecosystems. *Ecological Questions*, 29 (3): 75-85 (attachment 4)

5. Mangoni O., Saggiomo V., **Bolinesi F.**, Margiotta F., Budillon G., Cotroneo Y., Misic C., Rivaro P., Saggiomo M. (2017). Phytoplankton blooms during austral summer in the Ross Sea, Antarctica: driving factors and trophic implications. PLoS ONE, 12(4): e0176033. doi: 10.1371/journal.pone.0176033 (attachment 5).

The collaboration carried out with the American colleagues during the cruise in the Amundsen and Ross Seas, has continued in a research project, funded and organized by the National Science Foundation (USA) and the Swedish Polar Secretariat and centred on the problem of the role of phytoplankton in the formation of marine aerosol and cloud nuclei condensation, in the frame of a cruise to the geographic North Pole for two months during the summer 2018.

In this frame, the contribution of the candidate was that of the study of the photophysiological responses of phytoplankton community in conditions of light and nutrient limitation by seven *in situ* experiments and two weeks of in vivo experimentation of board. The results have been submitted with 2 manuscripts to the special issue *Arctic Aquatic Ecosystems in the 21st century* of Limnology and Oceanography:

- Torstensson A., Margolin A.R., Showalter G.M., Smith W.O., Shadwick E.H., Carpenter S.D., **Bolinesi F.,** Deming J.W. (*submitted*). Sea-ice microbial communities in the central Arctic Ocean: limited responses to short-term pCO_2 perturbations. Limnology and Oceanography.

- DiTullio G.R., Schanke N., **Bolinesi F.**, Mangoni O., Lee P. (*submitted*). Light, Nitrogen and trace Metal Co-Limitation of Marine Phytoplankton at the North Pole. Limnology and Oceanography.

In the second phase, thanks to the collection of live samples of phytoplankton community in different ecological sub-system of the Ross Sea, and the isolation of key species performed by the candidate in the laboratory of Marine Ecology at Department of Biology, experiments on monospecific cultures have been performed in order to evaluate the response of single species to different irradiance and in presence of iron and vitamin B_{12} limitation.

BACKGROUND AND OVERVIEW

Antarctic continental shelves are the most productive areas in the Southern Ocean and play a central role in sustaining the larger Antarctic ecosystem (Arrigo *et al*., 2008a; Smith *et al*., 2007).

Antarctic margins also provide the unique set of physical conditions that allows the formation and subduction of dense shelf waters, which is mediated by the formation of sea ice during winter. These dense shelf waters contribute to the formation of Antarctic Bottom Water (AABW), which impacts global climate through its roles in the global overturning circulation and the ocean carbon cycle (Orsi and Weiderwohl 2009; Marinov *et al*., 2006; Budillon *et al*., 2011).

In this context, the Ross Sea is an area of particular interest in that large phytoplankton blooms can trigger significant biological sequestration of atmospheric CO_2 via the formation and export of particulate organic carbon to the deep waters where AABW moves northwards (Arrigo *et al*., 2008b).

For the mechanisms implied in the production processes, the Antarctic waters are considered a key point for evaluating the evolution of climate change. Indeed, physical processes such as irradiance, vertical mixing and sea ice formation directly impact the magnitude of the biological pump. However, there are also important chemical and biological controls on the magnitude of export production. The Ross Sea area includes a mosaic of functionally different ecosystems such as polynyas, marginal ice zones, coastal and offshore waters, which altogether contribute, over different spatial-temporal scales and with different mechanisms, to primary production processes.

Phytoplankton communities in the Ross Sea have been studied intensively for decades. In general, phytoplankton biomass and composition are coupled to ice distribution, the variation in mixed-layer depth (UML), and irradiance availability. In spring, impressive phytoplankton blooms are observed at ice melting in offshore areas (Carrada *et al*., 2000; Saggiomo *et al*., 2000; Smith *et al*., 2000). The production of meltwater is related to the generation of a stratified surface layer and to the release of micronutrients and epontic algae into the water that can increase primary production within marginal ice zones (Smith and Nelson, 1985, Arrigo *et al*., 1998; Mangoni *et al*., 2004; Geibert *et al*., 2010; Taylor *et al*., 2013). Although satellite observations of ocean colour during this period are often obscured by clouds (Arrigo and McClain, 1994), these data also confirm that chlorophyll begins to increase in November (Arrigo and van Dijken, 2004).

In this period, large numbers of organisms of different trophic levels (krill, birds, seals, whales) converge along the ice margins (Saino and Guglielmo, 2000).

During the austral summer, a sharp drop in primary production is observed after pack ice dispersal due to two major processes: the deepening of the UML and micronutrients limitation

(Martin *et al*., 1990; Boyd *et al*., 2000; Sedwick *et al*., 2011; Alderkamp *et al*., 2012; Moore *et al*., 2013; Smith and Jones, 2014). In this regard, it must be noticed that the availability of micronutrients such as dissolved iron, an essential trace metal that can severally limits phytoplankton growth (Martin *et al*., 1990; Sedwick *et al*., 2000). This aspect may also explain why offshore waters during summer show "high nutrient low chlorophyll (HNLC)" conditions in ice-free areas (Saggiomo *et al*., 1998, 2002; Peloquin and Smith, 2007; Wang and Moore, 2011). Shields and Smith, (2009) have modelled on the seasonal development of phytoplankton blooms in the central Ross Sea and the relationships between environmental factors (irradiance, Fe availability), growth rates and relative concentration of both colonial and single-cell *Phaeocystis antarctica* during the spring-summer period (Fig. 1). Because of phytoplankton uptake, dissolved iron concentrations (brown line) decrease rapidly from November to early December, remaining lower (~0.1 nM) throughout the growing season, limiting the blooms during summer. According to this model, the growth of colonial forms can be controlled by bottom-up factors (selected iron, increased aggregates with reduced buoyancy), while the abundance of solitary cells is limited by the transformation into new colonies and by the grazing by primary consumers.

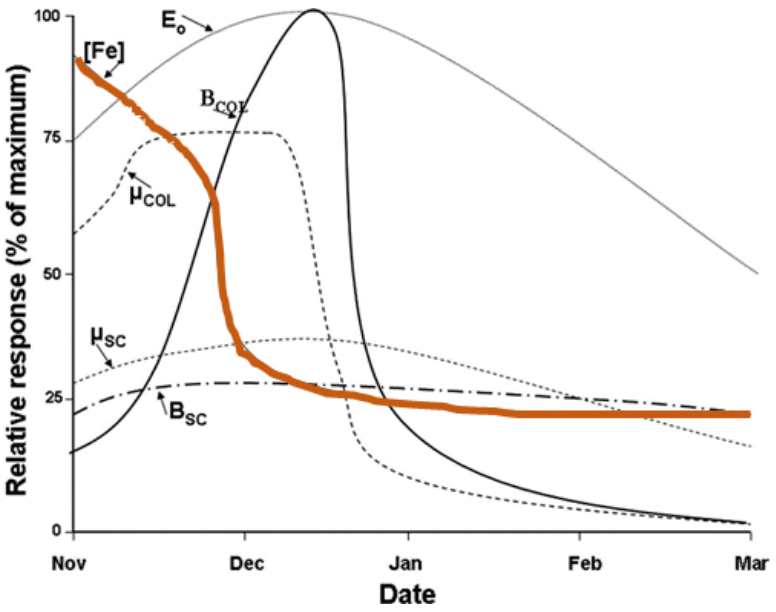

Figure 1 – From Shields and Smith (2008). E_0, surface irradiance; [Fe]-brown line, concentration of iron; B_{COL} colony biomass; μ_{COL}, colony growth rate; B_{SC} biomass of the solitary cells; μ_{SC} growth rate of single cells.

The basal level of the pelagic trophic web is remarkably simple with two main groups of phytoplankton that typically dominate the primary producers community composition,

characterized by the seasonal alternation of haptophytes (*Phaeocystis antarctica*) and diatoms (e.g. *Fragilaripsis curta*, *Fragilaripsis cylindrus*, *Chaetoceros* spp.) (Gibson *et al*., 1990; DiTullio and Smith, 1996; Alderkamp *et al*., 2012).

The temporal dynamics of phytoplankton communities in the Ross Sea have been well documented in the past two decades. El-Sayed et al. (1983, 1987) described large accumulations of the haptophyte *Phaeocystis antarctica* near the Ross Ice Shelf, and Smith and Nelson (1985) reported massive accumulations (the largest accumulations of biogenic silica ever observed) of a diatom bloom off the coast of Victoria Land, both emphasizing the wide variability of this species in space and time. Blooms of haptophytes (*Phaeocystis antarctica*) have been found to dominate the larger Ross Sea polynya during spring and early summer, whereas blooms of diatoms (such as *Fragilaripsis cylindrus*) usually dominated production in open waters of the western Ross Sea during summer (DiTullio and Smith, 1996; Arrigo *et al*., 1999-Fig. 2).

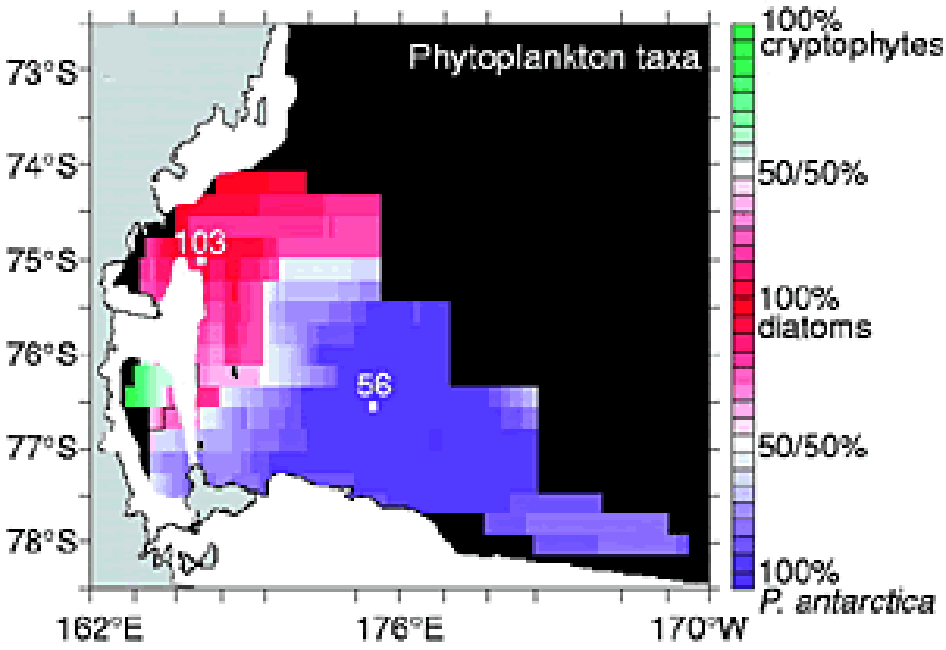

Figure 2 - Spatial patterns of phytoplankton taxa (from Arrigo *et al*., 1999).

These two taxa coexist throughout the Ross Sea (Garrison *et al*., 2003), although each taxon can form nearly monospecific blooms that leave distinctive biogeochemical imprints (Boyd et al., 1999; DiTullio *et al*., 2000; Smith et al., 2010; Mangoni *et al*., 2017). For example, per unit of phosphorus, *Phaeocystis antarctica* populations assimilate nearly twice the carbon and nitrogen with respect to diatoms (Bates et al., 1998; Arrigo *et al*., 1999; Dunbar et al., 2003;

Hales and Takahashi 2004). The Ross Sea during the spring bloom presents DMS and DMSP concentrations more than two orders of magnitude higher than average global ocean values (DiTullio et al., 2000; Lee et al., 2015).

Moreover, because their relative dominance varies on different temporal and spatial scales, diatoms and haptophytes can have also major implications on trophodynamics (Schoemann et al., 2005; Peloquin and Smith, 2007; Smith *et al*., 2014). The phytoplankton community structure in fact play also a pivotal role in the POM composition, which shows high mesoscale variability in the Ross Sea, influencing the amount of biomass recycled in the photic layer and therefore the quality of the POM exported to the bottom (Misic *et al*., 2017; Fabiano and Pusceddu 1998).

Phaeocystis antarctica populations can exist as both solitary cells (3–4 μm in size) and palmelloid colonies (> 2 mm) that can differ in size by several orders of magnitude (Mathot *et al*., 2000; Schoemann *et al*., 2005), with seasonal changes in the relative numbers of each form (Mathot *et al*., 2000). The two forms have separate trophic fates, with solitary forms being ingested by heterotrophic microplankton (Dennett *et al*., 2001, Smith *et al*., 2003), while colonies sink and are remineralized at depth, because grazing rates of mesozooplankton on colonial *Pheocystis antarctica* are low due to the large size of colonies (Caron *et al*., 2000; Lonsdale *et al*., 2000; Tagliabue and Arrigo, 2003; Tang *et al*., 2008). Pteropods may consume both solitary cells and colonies (Elliott *et al*., 2009). In contrast, diatoms are grazed at significant rates by zooplankton, such as copepods and krill, so that diatom blooms represent a crucial ecological link between primary production and higher trophic levels in the Ross Sea.

To date, the environmental factors that determine the distribution and seasonal evolution of *Phaeocystis antarctica* and diatom populations in the Ross Sea remain poorly known. Generally, UML has been correlated with phytoplankton community structure, with diatoms and *Phaeocystis antarctica* populations dominating under shallower and deeper UML conditions, respectively (DiTullio and Smith, 1996; Arrigo *et al*., 2000). Spring biomass is generally dominated by *Phaeocystis antarctica* (Smith and Gordon, 1997, Arrigo *et al*., 1999). After the seasonal decline of *P. antarctica*, phytoplankton assemblages are dominated by diverse populations of diatoms, which tend to dominate assemblages in summer in the shallower mixed layers and are often associated with sea- and glacial-ice melt (Smith *et al*., 2014 – Fig. 3). Other groups (dinoflagellates, cryptomonads, and silicoflagellates) occur in spatially restricted locations (Arrigo *et al.*, 1999). Although this overall pattern is relatively predictable, significant interannual variations exist in the contributions of the various functional groups to total phytoplankton biomass (Smith *et al*., 2011b).

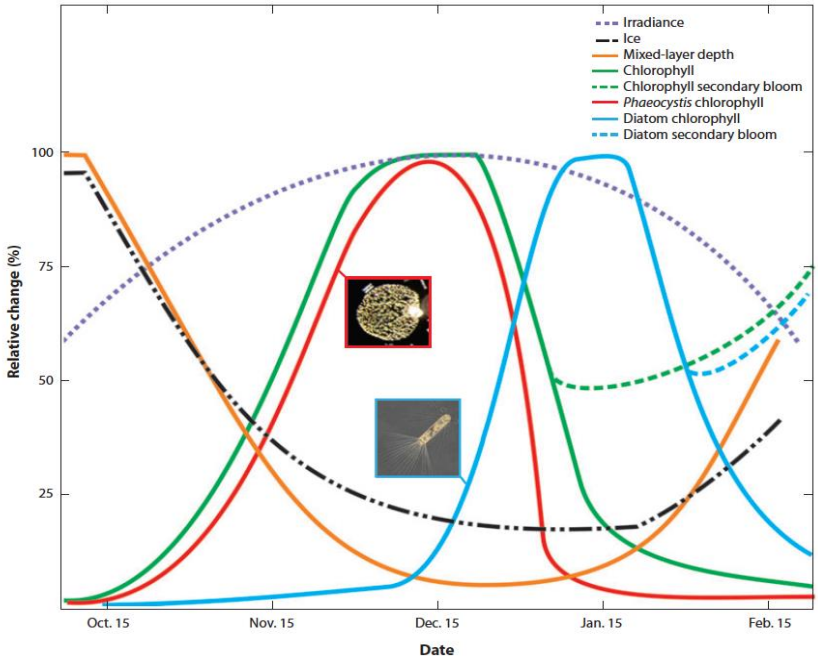

Figure 3 - Conceptual representation of the temporal progression of several environmental variables and phytoplankton composition in the southern Ross Sea (from Smith *et al*., 2014).

Nevertheless, the currently accepted paradigm for the Ross Sea posits that water column stratification favors diatom dominance under high light conditions due to their physiological advantage in photoprotection and high tolerance to photoinhibition compared to *Phaeocystis antarctica* (Kropuenske *et al*., 2009; Mills *et al*., 2010; Arrigo *et al*., 2010). Diatom dominance, however, is dependent on water column iron availability (Martin *et al.*, 1990). Consequently, diatom populations typically dominate in stratified waters in relatively high iron regions near the Victoria Land Coast such as Terra Nova Bay (TNB) (DiTullio and Smith, 1996), in marginal ice zones (Smith and Nelson, 1985), and especially near melting sea ice (Sedwick and DiTullio, 1997). Distinct iron transport mechanisms by which both diatoms and *Phaeocystis antarctica* acquire organically bound iron may also influence community growth rates (Hatta *et al*.,2017; Kouth *et al*., 2017; Strzepek *et al*., 2011). Laboratory and field data show that *P. antarctica* can grow at significantly lower iron concentrations when irradiance levels are near saturation but suboptimal irradiance levels cause an increase in their iron requirement (Sedwick *et al*., 2007; Garcia *et al*., 2009).

Although photo-physiological processes are important for sustaining diatom blooms in stratified surface waters of the Ross Sea, the phytoplankton growth could also be co-limited by B_{12} and iron, especially during summer (Bertrand *et al*., 2007, 2011). The extent of Fe- B_{12} stimulation can be inversely related to heterotrophic bacterial abundances (Bertrand *et al*., 2011b),

whose growth and resultant B_{12} biosynthesis are dependent on seasonal DOM production (Ducklow *et al*., 2001). Field studies conducted in HNLC areas, including those in the polar regions, indicate that the addition of vitamin B_{12} alone or with another limiting nutrient, can potentially shape the phytoplankton community structure (Bertrand *et al*., 2007; Koch *et al*., 2011). Vitamin B_{12} is a cobalt-containing organometallic compound, only produced by archea and some bacteria (Guillard, 1969; Swift and Guillard, 1977), that enables the activity of methionine synthase, class II ribonucleotide reductase (RNRII) and methylmalonyl-CoA-mutase (MMCM).

In a study conducted in the coastal area of the Gulf of Alaska by Kock *et al*. (2011), the addition of B_{12} combined with NO_3^- yielded an algal community dominated by dinoflagellates (Tang *et al*., 2010) which were nearly absent in the diatom dominating with only the NO_3^- treatment, and stimulated also the growth on large phytoplankton cells.

Recent evidence suggests that algal-bacterial interactions involving iron and B_{12} could be important in driving micronutrient co-limitation in the Ross Sea, with the possibility that a mutualistic symbiosis may develop between certain bacterial groups (e.g., SAR 92, *Oceanospirillaceaea* spp. and *Cryomorphaceae* spp.) and colonial *Phaeocystis* cells (Bertrand *et al*., 2015; Delmont *et al*., 2014). Recently Nef *et al*., (2019), demonstrated that haptophytes can mitigate the vitamin B_{12} limitation by an increase in dissolved methionine assimilation, or regulating genes involved in methionine cycle and B_{12} transport or limit B_{12} transport to the mitochondrion (Nef *et al*., 2019). Despite this, to date, it remains unclear how the vitamin B_{12} limitation can influence the relationship between haptophytes and other phytoplankton species in the Ross Sea.

After the discover of the ozone hole over Antarctica, in addition to micronutrient limitations, concerns were expressed about the impact of increased UV radiation on phytoplankton productivity. Many studies revealed in fact that high UV-B radiation affects the survival of phytoplankton by inhibiting their phototactic and photophobic responses (Diffey, 1991; Karentz *et al*., 1991). One of the molecular mechanisms used by Antarctic phytoplankton cells to contrast the effect of UV radiation is the production of Mycosporine-like amino acids (MAAs), that have been reported to be abundant especially in *Phaeocystis* (Marchant *et al*., 1991; Vernet *et al*., 1994) and the diatom *Thalassiosira* (e.g., *Thalassiosira gravida*; Ferreyra *et al*., 1994). Contrasting to bloom-forming algae, MAAs seem to play a minor role as photoprotectants in sea ice algae, where they are found in low amounts.

The effects of UV-R on phytoplankton species depend also on the light attenuation along the water column, that in turn depends on the optical properties of seawater itself, dissolved material, concentration of phytoplankton and suspended particles (Häder *et al*., 2011). Considering

the poor understanding of rates of vertical mixing and phytoplankton recovery from photochemical damage (Neale *et al*., 2012) as well as the lack of adequate methodological procedures to assess the damage, an accurate assessments of UV effect on Antarctic phytoplankton species remain difficult to obtain.

Climate change affects the Ross Sea shelf largely through the physical forcing of the environment; some ecological and oceanographic changes that have been observed in the West Antarctic Peninsula (Montes-Hugo *et al*., 2009) may occur in the Ross Sea, albeit with substantial regional differences. For example, the sea-ice seasonality is also changing rapidly (Stammerjohn *et al*., 2008, 2012; Comiso *et al*., 2011). Ice concentrations in the Ross Sea have been significantly increasing in extent and duration (Stammerjohn *et al*., 2012), and they are responsible for the modest net increase in Southern Ocean ice extent since 1979. Models of future ice conditions (Bracegirdle *et al*., 2008) suggest that this trend is transient and that in 50 years the Ross Sea will experience a substantial reduction in sea ice during austral summer driven by increased atmospheric temperatures and changes in winds. Some changes in the physical-chemical characteristics in the Ross Sea have already been documented (Turner *et al*., 2013), but, to date, current variations affecting the pelagic food web are mostly unknown (Constable *et al*., 2014; Xavier *et al*., 2016).

In recent years, an increasing number of studies reported a dramatic shift in phytoplankton communities composition of the Ross Sea. For example, many studies have reported *Phaeocystis antarctica* bloom in coastal areas generally characterized by the dominance of diatoms (Smith and Asper, 2001; Mangoni *et al*., 2019). In addition, Italian researchers found an under-ice bloom of small phytoflagellates in late austral spring 2016 in Terra Nova Bay during the ice continental melting season (Saggiomo *et al*., in preparation), a fact never reported so far. Therefore, all these aspects suggest that even after several decades of study, spatial and temporal uncoupling of diatom and *Phaeocystis* blooms obscures our understanding of bloom dynamics in the Ross Sea and based on recent observation new question arise on the drivers regulating primary production processes in this area.

This thesis fits within the vast framework of the background discussed above, and aims to study the structural and functional biodiversity of phytoplankton, their production efficiency and the limiting role of iron and vitamin B_{12} in determining rates and timing of production in a changing Southern Ocean.

MATERIAL AND METHODS

Field activities

Two oceanographic cruises were carried out in the Ross Sea. The first one from January 1 to February 11, 2017 on board the R/V *Italica* as part "P-ROSE project - *Plankton biodiversity and functioning of the Ross Sea ecosystems in a changing southern ocean*", and "CELEBeR project - *CDW Effects on glaciaL mElting and on Bulk of Fe in the Western Ross sea*" and the second one from December 27, 2017 to February 20, 2018 on board of the R/V *Nathaniel B. Palmer* as part of the "*CICLOPS Project - Cobalamin and Iron Co-Limitation of Phytoplankton Species*". The cruises followed two tracks of different spatial scales: the first within the Ross Sea (Fig. 4) and the second over a much longer spatial scale stretching from Lat. -59° 14.586 S, Long. 68°22.682 W, crossing the Amundsen Sea, coastal waters of Marie Burd Land and reaching the inner part of the Ross Sea. (Fig. 5).

P-ROSE and CELEBER Cruise (PNRA expedition)

Water samples were collected using a carousel sampler (Sea-Bird Electronics 32) equipped with 24 (12-L) Niskin bottles, and a CTD sensor (9/11 Plus; Sea-Bird Electronics) with a fluorimeter. In order to investigate on the vertical distribution of phytoplankton biomass in the first 100 m of the water column, water sampling depths (6-7 for each station) were chosen according to the fluorescence profile, in addition with the physical structure of the water column. In this regard, physical and chemical vertical profiles down to 100 m have been elaborated.

At each depth 5 liters of seawater were collected for the analyses of i) total phytoplankton biomass, ii) diagnostic pigments in order to obtain information on the chemotaxonomic composition, photo-protection index and grazing activity by herbivores, iii) taxonomic identification, iv) inorganic nutrient concentrations and dissolved iron. Sea water samples for the analysis of points i and ii were filtered on glass fiber filters and rapidly frozen at -80 °C until laboratory analysis. For the phytoplankton taxonomic identification, samples were fixed and preserved in formalin solution (final concentration, 4%), buffered with $CaCO_3$. Cell counts were performed with an inverted light microscope (Zeiss Axiophot). For the determination of nutrients concentration, samples were taken directly from the Niskin bottles, stored at -20°C in 20 mL low-density polyethylene containers until laboratory analysis. In addition, at selected stations seawater samples were collected by a 20-L teflon-lined GO-FLO bottle (which was deployed on a kevlar 6 mm diameter line and closed using a PVC messenger) for dissolved iron analysis. Seawater was transferred in

acid-cleaned 2-L low-density polyethylene (LDPE) bottles and immediately treated as reported by Rivaro *et al.*, 2019. In order to set up a series of monospecific culture of phytoplankton species of the Ross Sea in Italy, 30 ml of sea water from the Niskin bottle were pre-filtered with 300 µm mesh Nitexs, to remove most metazoan plankton, and inoculated in 60 ml flasks filled up with natural sterilized Ross Sea water enriched with L1 media 20%. After inoculum, flasks were placed in a specific incubator at 3°C and 24 h of continuous light period at 40 µmol photons m^{-2} sec^{-1}. All samples were checked periodically by optical microscope and refreshed every 2 weeks until the end of the cruise. Once the R/V *Italica* arrived in Italy, flasks with live samples were checked out with microscope and the incubator was transferred in a refrigerated vehicle and transported to the laboratory. Here, all flasks were transferred in refrigerate cells at 1.5°C and 40 µmol photons m^{-2} sec^{-1} in continuous light period (24h) and refreshed with 50% L1 media at 34 salinity, generating a series of replicates for each sample. The refrigerate cell allowed to store the samples under manipulative controlled conditions thanks to the possibility to modulate light intensity, temperature and light cycles.

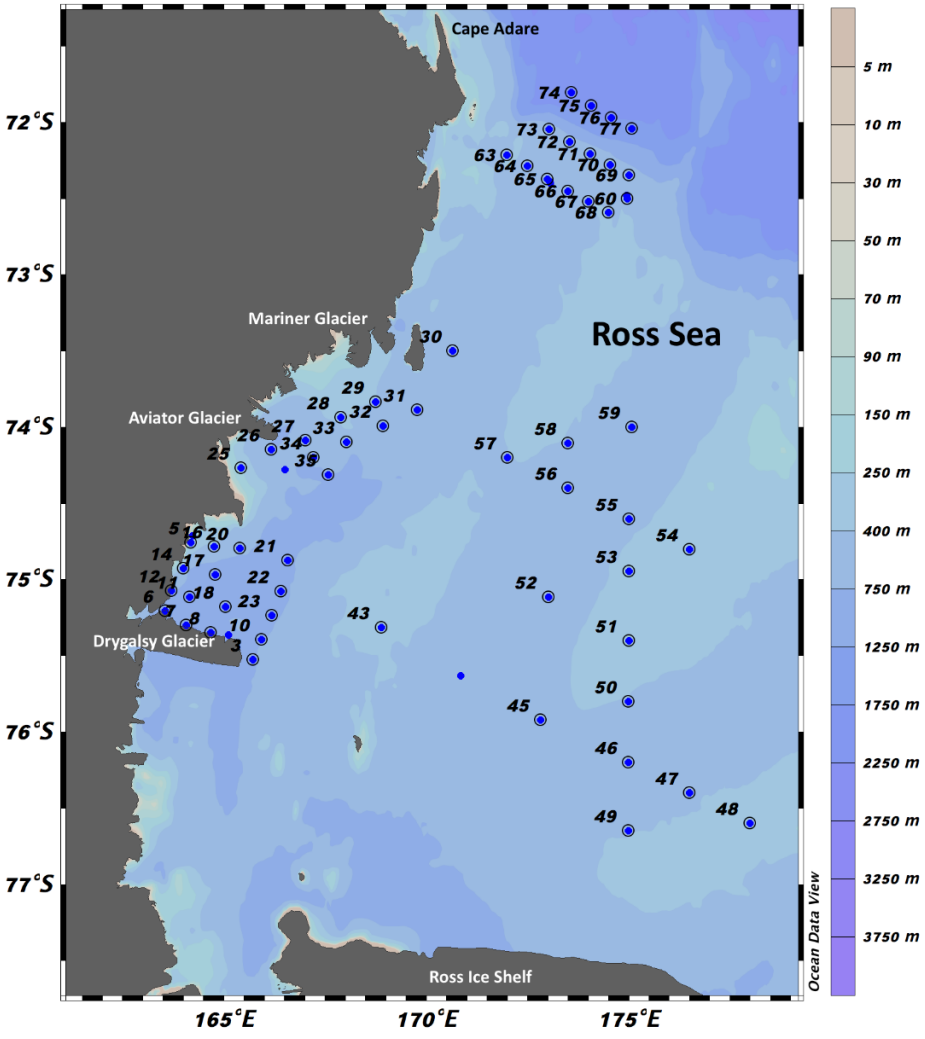

Figure 4 - Map of the stations sampled during the research activities P-ROSE and "CELEBeR projects.

CICLOPS Cruise (NSF expedition)

In order to study the effect of continental melting on primary production processes, stations from 10 to 17 have been sampled in the coastal area of Marie Byrd Land (Fig 5), that is considered to produce more freshwater than any other region in Antarctica (Rignot *et al*., 2013; Jacobs *et al*., 2013; Assmann et al., 2019). Samples of sea water were collected at different depths (~5 depths) along the first 100 m of the water column according to the fluorescence profile and the physical structure of the water column. At each depth, 10 liters of sea water were collected for the analysis of the following parameters: i) total phytoplankton biomass, ii) diagnostic pigments in order to obtain information on the chemotaxonomic composition of phytoplankton community and photo-protection processes, grazing activity by herbivores, iii) maximun quantum yield (Fv/Fm) and non-photochemical quenching (NPQ) in order evaluate the photosynthetic capacity and physiological status of phytoplankton cells. Sea water samples for the analysis of points i, ii were filtered on glass fiber filters and rapidly frozen at -80 °C until laboratory analysis. Fv/Fm and NPQ were measured directly on board (the full description of the method is described in the following section "*Photosynthetic efficiency and physiological status of phytoplankton cells".*

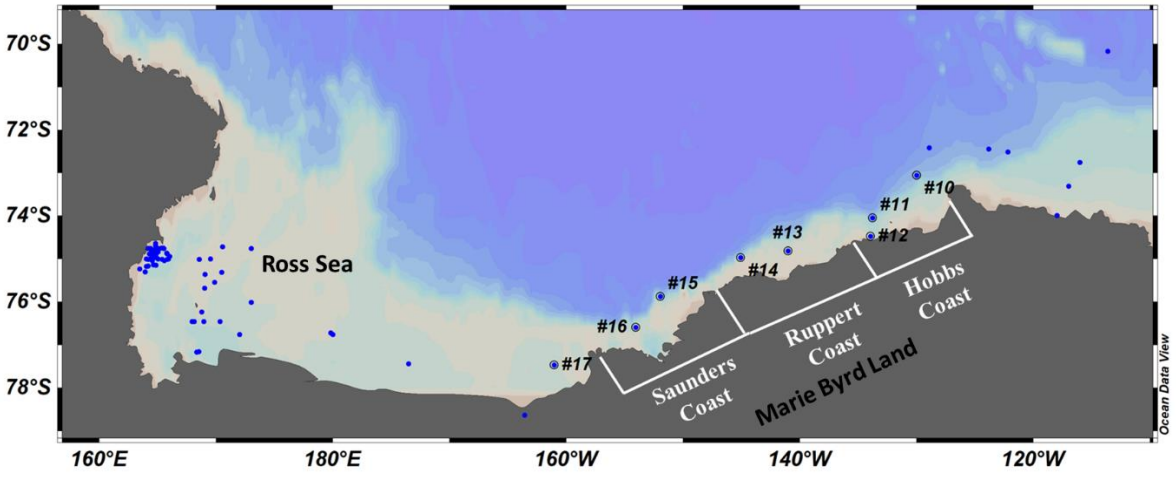

Figure 5 - Map of the stations sampled during the CICLOPS cruise along different sub-regions of the Marie Byrd Land. Saunders Coast (158°00'W - 146°31'W), Ruppert Coast (146°31'W - 136°50'W), Hobbs Coast (136°50'W - 127°35'W).

Laboratory procedures

Pigment analysis

- *Phytoplankton biomass* - 500 ml of sea water were filtered through Whatman GF/F filters (25-mm diameter) for analyses of chlorophyll a (Chl-a) and phaeopigments (Phaeo) according to Holm-Hansen et al. (1965) using a Shimatzu spectrofluorometer calibrated and checked daily with

a Chl-a standard solution (*Anacystis nidulans*, Sigma).

- *Functional phytoplankton groups by chemotaxonomic criteria* - For the analyses of accessory pigments, two liters of seawater were filtered onto Whatman GF/F filters (47 mm diameter) and stored at -80° C until onshore pigment HPLC analysis was performed back in Italy. HPLC pigment separations were made on an Agilent 1100 HPLC according to the method outlined in Vidussi *et al*., (1996) as modified by Brunet and Mangoni (2010). The system was equipped with an HP 1050 photodiode array detector and a HP 1046A fluorescence detector for the determination of chlorophyll degradation products. Instrument calibration was carried out with external standard pigments provided by the International Agency for 14C determination-VKI Water Quality Institute. The relationship between spectrofluorimetric Chl-a and HPLC Chl *a* for all samples was very close ($p < 0.001$, $y = 1.28 x + 0.26$, $R2 = 0.82$, $n = 198$). The concentrations of pigments were used to estimate the contributions of the main functional groups to the total Chl-a using the matrix factorisation programme CHEMTAX 1.9.5.
- *Photo-protective pigment* - The carotenoids partecipating in the photoregulatory processes through the xanthophyll cycle were analyzed according to Demers *et al*., 1991; Meyer *et al*., 2000; Mangoni *et al*., 2009. The photo-protective pigment ratio was calculated as the ratio of the sum of diadinoxanthin (Dd) and diatoxanthin (Dt) to Chl-a (Dd+Dt/Chl-a). The de-epoxidation state of the xanthophyll cycle was expressed as the ratio between the Dt and Dd+Dt concentrations (Dt/[Dd+Dt]).

Nutrient Analyses

For the determination of the nutrient concentrations (NO_3-, NO_2-, NH_4+, $Si(OH)_4$, PO_4^3-), samples were taken directly from the Niskin bottles, stored at -20°C in 50 mL low-density polyethylene (LDPE) containers until laboratory analysis. The analyses were performed using a five-channel continuous flow autoanalyser (Technicon Autoanalyser II), according to the method described by Hansen et al., (1983). The accuracy and the precision of the method were checked by Certified Reference Material (CRM) MOOS- 3 (Seawater Certified Reference Material for Nutrients; http://www. nrc-cnrc.gc.ca/obj/inms-ienm/doc/crm-mrc/eng/MOOS-3_e.pdf). The measured nutrient concentrations in the CRM were not significantly different ($p<0.05$) from the certified values. For the analysis of total dissolved iron, seawater samples were filtered through 0.4 μm pore-size PC membranes, collected in 200-mL PP bottles and stored at -20 °C until analysis. The total dissolved Fe was determined by ICP-MS after a metal pre-concentration procedure through co-precipitation with Mg(OH)2, based on a previous work by Wu and Boyle (1998) and following

as descripted in Rivaro et al., 2018. Seawater was transferred in acid-cleaned 2-L LDPE bottles and immediately treated as reported by Rivaro et al., 2018.

Photosynthetic efficiency and physiological status of phytoplankton cells

The maximum PSII photochemical efficiency (Fv/Fm) and the maximum PSII effective absorption cross section (σPSII), which describes the functional 'target area' of the light harvesting antenna that is energetically coupled to the O_2-evolving reaction centres (RCIIs) (σPSII; Mauzerall and Greenbaum, 1989; Falkowski and Raven 2007), have been determined using a Phyto_PAM II compact unit (Walz). All samples were acclimated at the dark for 30 minutes before analysis to minimize the non-photochemical dissipation of excitation, and measurements were blank corrected filtering the sample through 0.2 μm filter (Cullen and Davis, 2003). As regard Fv/Fm, samples were illuminated with a saturating pulse as reported in Maxwell and Johnson (2000), and values derived from the formula Fv/Fm = (Fm-F0)/Fm. For the determination of σPSII at 440 nm we used the fast kinetics windows (Phyto Win_3 software) for the analysis of the wavelength dependent O-I1 fluorescence rise kinetics upon onset of pulses of strong actinic light. All samples were far-red pre-illuminated before the analysis to inhibit the PS I response (Schreiber *et al*., 2012).

Molecular analysis

Total DNA was extracted from the separate clonal cultures of *P. antarctica* and the unknown dinoflagellate found in its association using the CTAB method (Doyle and Doyle, 1990). Regions of the 18S and 28S ribosomal RNA genes were PCR amplified using the primer pairs 18SF1/18SR1 (5'-TACCTGGTTGATCCTGCCAG-3' and 5'-ACTACGAGCTTTTTAACYGC-3', respectively), 18SF2/18SR2 (5'-AGGGCAAGTCTGGTGCCAG-3' and 5'-CCTTCCGCAGGTTCACCTAC-3', respectively) and 28SF/28SR (5'-CCGCTGAATTTAAGCATAT-3' and 5'-CTTGGTCCGTGTTTCAAGAC-3', respectively) (Wakeman *et al*., 2018). Amplification reactions were conducted in a final volume of 50 μL using 10 ng of DNA, 0.3 μM of each primer, 200 μM dNTPs, 1U *Xtra Taq Pol White* (Genespin) in 1X Reaction buffer. Amplification reactions consisted in an initial denaturation step at 95°C for 1 min followed by 35 cycles of 30 s at 95°C, 30 s at 52°C, 1 min at 72°C and a final elongation step at 72°C for 10 min. The amplification products were cloned into the pSC-A-amp/kan vector (Agilent), sequenced using the specific primers and analyzed using an ABI 310 Genetic Analyzer (Applied Biosystems). The obtained sequences were examined through BLASTn analysis and deposited in GenBank under the accession numbers (*in course*).

Statistical analysis

In order to evaluate the relationship between variables physic (Temperature, Salinity, UML), chemical (Dissolved Inorganic Nitrogen, $Si(OH)_4$, PO_4^{3-}), and biological (Chl *a*, %Diatoms, %Haptophytes) a multivariate analysis was performed through a Principal Component Analysis (PCA) method. Data were standardized with a Pearson correlation prior to computations to avoid inflating the impact of variables with high variances on the result, and variables were graphed in a correlation circle chart. The software utilizes for all statistical analysis was XL-STAT Ecology 2019.

Phytoplankton culturing and manipulative experiments

Species isolation and maintenance of monospecific culture

Once the R/V *Italica* arrived in Italy, flasks containing natural live samples of phytoplankton collected during P-ROSE Project, and stored within a specific incubator, were checked out by microscope and transferred in a refrigerated vehicle to the laboratory of Marine Ecology at Department of Biology (University of Naples –Federico II) . Here, all flasks were transferred in refrigerate cells at 1.5°C and 40 μmol phtons m^{-2} s^{-1} in continuous light period (24h) and refreshed with 50% L1 media at 34 salinity, generating a series of replicate for each sample. The refrigerate cell allowed to store the samples under manipulative controlled conditions thanks to the possibility to modulate light intensity, temperature and light cycles.

After 2 weeks of adaptation, we started to isolate single species of phytoplankton from mixed live samples in order to obtain monospecific cultures. The isolation procedures were performed following as suggested by C. Tomas - Center for Marine Science, University of North Carolina, Wilmington, USA- (personal communication), and consisted of both serial dilution and single cells collection by hand held micropipettes and optical inverted microscopes (Zeiss Telaval 31 and Leica DMIL led).

The serial dilutions have been made in sterile conditions under a laminar hood (ASALAIR 700) using a multiwell rack (24 and 96 well) and micropipettes (P1000, P200 Gilson) following 1:10 diluting factor, moving from the most to the less concentrate well containing sample. This procedure was carried out until obtained only one cell in the less concentrate well. As regard palmelloid *Phaeocystis antarctica*, single balloon-like colony were picked up with a modified micropipette and transferred to a multiwall rack 24 position following the procedure descripted above. Subsequently, once achieved the maximum growth rate, few ml from each well were inoculated together in 60 ml flasks, adding 50 % the volume of new media.

In addition to the microscopic control, we also performed HPLC analysis using marker pigments –such as 19'-Hexanoyloxyfucoxanthin, that is the marker pigment of *Phaeocystis antarctica* (Wright *et al*., 1996) - to define the pigment spectra composition of each species.

Experimental Set-Up

In order to study the photo-physiological responses of species isolated and cultivated in monoclonal culture in presence of iron and vitamin B_{12} starvation, and at different intensities of light irradiance, two different experiments have been made on *Phaeocystis antarctica* and *Prorocentrum* sp. comparing growth, pigment spectra composition and photosynthetic efficiency of these two species. In addition, to shed light on the possible interaction between *Phaeocystis antarctica* and *Prorocentrum* sp., mixed flasks containing 50 % of the volume of *Phaeocystis antarctica* and 50% of *Prorocentrum* sp. were prepared to investigate which species dominated under stressful conditions. Before the start of the experiments species were acclimated to each experimental condition for 12 weeks.

Experiment 1 ANEMIA - A 2 litre non axenic monospecific culture of *Prorocentrum* sp. and 2L non axenic monospecific culture of *Phaeocystis antarctica* grown up in L1 media at salinity 34 and 40 μmol photons m^{-2} sec^{-1} were used as main inoculants, in presence of nutrient starvation conditions, to generate three lines of growth:

1- *Phaeocystis antarctica (monospecific culture)*

2-Prorocentrum sp. *(monospecific culture)*

3-Prorocentrum sp. *+ Phaeocystis antarctica (mixed culture)*

Each line of growth has undergone three different treatments

- *Treatment +dFe+B_{12}*: species were grown in L1 media 100%
- *Treatment -B_{12}*: species were grown in L1 media 100% without vitamin B_{12}
- *Treatment -dFe*: species were grown in L1 media 100% without vitamin dissolved iron

The treatments have been prepared in triplicate for a total of 135 flasks analyzed in the entire experiment. The flasks used for the incubations were trace metal soaked overnight in 1% citranox (Alconox), rinsed six times with Milli-Q water, then soaked for at least 3 days in 10% HC1 (Baker Instra-analyzed), then rinsed three times with pH 2 Milli-Q water prior to use. Single time-point incubations were represented by 60 ml polycarbonate flask TPP. The flask incubations were prepared in a positive-pressure trace metal clean area using trace-metal clean techniques.

Data reported derived from sampling occurred in triplicate at time 0 (Start), time 6 (T6) and time 12 (T12) for each treatment and each line of growth.

As regard the treatment -B_{12}, modified L1 media 100% was prepared excluding the vitamin B_{12} from the vitamin stock solution. The amount of vitamin B_{12} in the pre-filtered (0.2 μm) seawater used as culture medium before the addition of L1 nutrient (under a laminar hood) can be considered negligible thanks to the sterilization by autoclaving at 1.06 kg cm^{-2} for 20 minutes. For the treatment -dFe, DFB [desferoxamine B] has been used in the ratio of 100DFB : 1dFe to chelate dissolved iron (~2 nM) present in the sea water. As regard the treatment +dFe+B_{12}, flasks were filled up with L1 media 100%, as normal growth condition for both species.

Experiment 2 Light-light – In order to study the photo-physiological responses of *Phaeocystis antarctica* and *Prorocentrum* sp. at different levels of light intensity in presence of non-limiting nutrient concentrations, two lines of growth (*Phaeocystis antarctica and Prorocentrum* sp.) were prepared following the inoculating procedure descripted above. Each line of growth has undergone four different light intensities descripted below:

High Light (**HL**) = 110 μmol phtons m^{-2} s^{-1}

Low Light 1 (**L1**) = 60 μmol phtons m^{-2} s^{-1}

Low Light 2 (**L2**) = 36 μmol phtons m^{-2} s^{-1}

Low Light 3 (**L3**) =19 μmol phtons m^{-2} s^{-1}

Each treatment was prepared and analysed in triplicate for a total of 120 flasks in the entire experiment. The light inside the culture flasks was measured with a spherical sensor (Biosperical Instruments Inc. QSL-100). The cultures were grown in TPP flasks at 4°C and kept in suspension by daily shaking. L1 medium 100% was prepared as described by Guillard, 1995.

RESULTS

P-ROSE and CELEBER Cruise (PNRA expedition)

The distribution of integrated values of chl a in the first 100 m of the water column, shows the presence of areas with different productivity, that identify different sub-systems of the Ross Sea discussed below (Fig. 6a). Figure 6b gives a comparative picture of the vertical distribution of the water column structure (UML) in the sampled area. For a better explanation of results, in each area data will be discussed starting from the physical structure of the water column, followed by the distribution and composition of phytoplankton biomass, distribution of inorganic nutrients, and a principal component analyses.

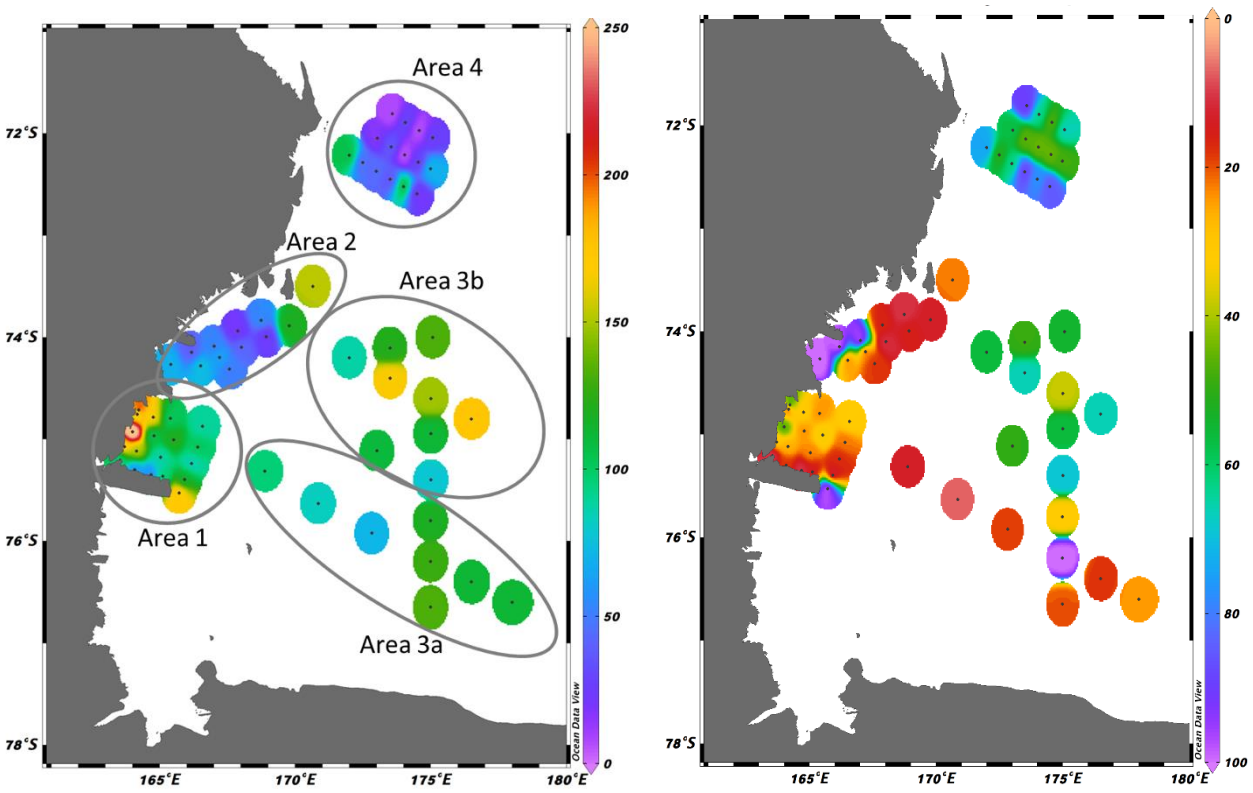

a **b**

Figure 6: a) Spatial distribution of integrated chl a value (µg/L) in the first 0-100 m of the water column; b) Upper mixed layer depth (m). Area **1**: St. 3-23 – Area **2**: St. 25-36 – Area **3a**: St. 43-51 - Area **3b**: St. 52-59 – Area **4**: St. 60-79.

Area 1. The Area 1 includes stations distributed along the northern shores of the Drygalsky ice tongue, and the interpretation of the data collected must be carried out keeping in mind the influence of this coastal feature on the forcing factors influencing the structural and functional

characters of phytoplankton communities. The vertical structure of the water column (Fig. 6b) is not homogeneous in the entire area, varying in terms of UML from 9 to 57 m, while at some stations (3 and 4) UML exceeds the depth considered by sampling. Of the above stations only station 3 was sampled for the entire list of factors considered, while the adjacent station 4 only for its physical structure, here considered as an indicator of the horizontal extent of the water column characteristics. The observed range of UML was roughly distributed along a gradient going from the shores of Drygalsky to north-west. Considering the distribution of integrated 0-100 m values of chl a, higher levels of biomass were reported in the polynya of Terra Nova Bay, particularly near the coastline where a maximum of (271.81 mg chl a m^2) was recorded at station 14 (Fig. 6a). In this area, an eastwards decreasing gradient of concentration was present, and a relative maximum was recorded in proximity of the Drygalsky ice tongue, probably as consequence of the melting inflow processes. The point distribution of chl a in the first 100 m reached the maximum concentration of 4.6 µg/L at 0 m, in the coastal area of TNB (Fig. 7a). The mean vertical profile of chl a presented a linear decrease toward the bottom, with mean values ranged from ~2.1 µg/L at surface to 0.3 at 100 m. In the first 20 m, mean values exceed always 2 µg/L, decreasing down to 0.81 µg/L at 50 m. Points with highest chl a concentration in the layer 0-40 m all belongs to the station 14, near the coast (Fig. 7a). As regards the vertical distribution of nutrients (data not showed), DIN showed within the upper 20 m a variation from 9.1 to 20.0 µmol/L; at deeper levels exceeded 27.0 µmol/L. PO4 displayed the variation range analogous to that of DIN, from 0.45 to 1.5 µmol/L in surface waters and concentrations up to 2.29 µmol/L below UML. Mean dissolved iron concentration reported in this area at ˜30 m was 0.9 (±0.37) nM. Figure 7b describes the percentage contribution of the main functional groups to the total biomass. Diatoms were the main functional group, with a mean of 67%, while haptophytes contribute with 26% to total biomass. As regard other minor groups, chlorophytes show a mean of 3%, while other groups are poorly represented, with dinoflagellates characterized by high variance and a not significant mean value. The results obtained using a PCA (Fig. 12) explained 75.28% of the total variance, with F1 axis accounting for 61.55% and F2 axis for 13.73% of total variance. Diatoms, Temperature, UML and chl a are negatively correlated with F1 axis, and a strong correlation suggesting the dominance of diatoms in surface waters where biomass reached higher concentration. On the contrary, haptophytes were strongly correlated with salinity along the positive F1 axis, showing an inverse correlation with the variables descripted before, indicating that haptophytes were most abundant below the UML. As regards inorganic nutrients, DIN and PO4 displayed the same correlation as haptophytes and salinity along the negative F1 axis, while SiO2 was much more correlated along the positive F2 axis.

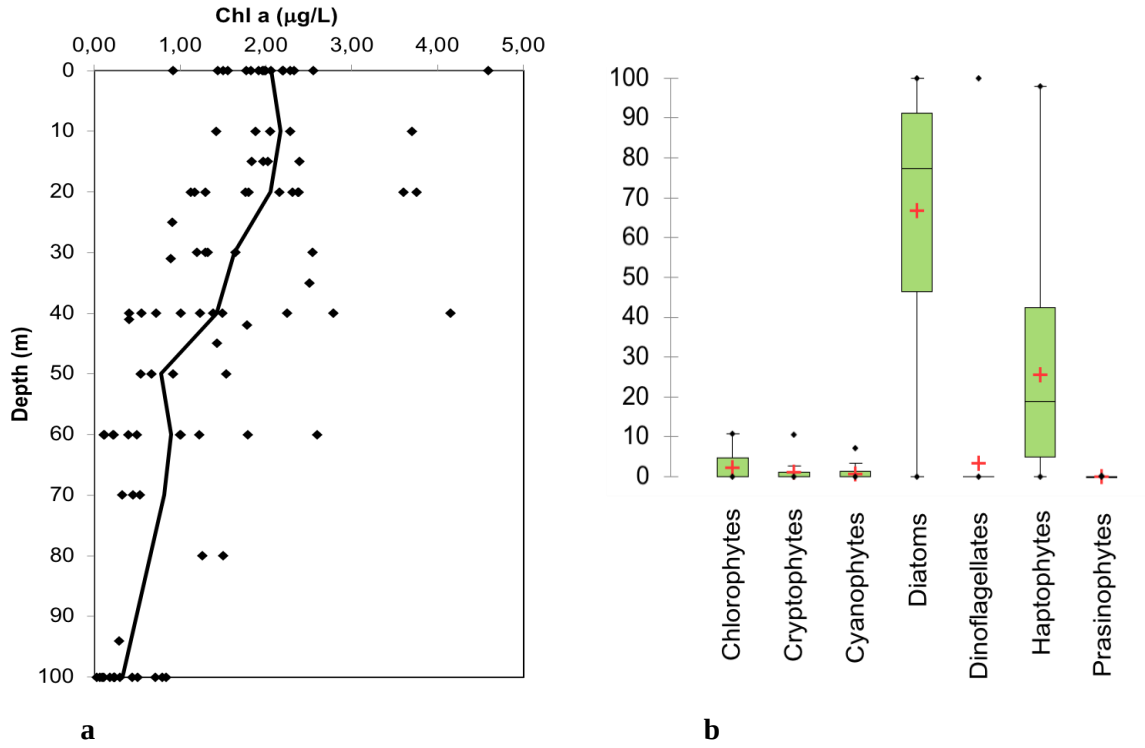

Figure 7 – **Area 1**: **a**) vertical distribution of chl a at each sampled depth (dots) , and mean vertical profile of concentration (black line)**; b**) Percentage contribution of the main functional groups to total biomass; red cross represents the mean value.

Area 2. Area 2 has been covered by a cruise track stretching from the Aviator ice tongue to Coulman island. The water column structure (Fig. 6b) shows a completely mixed water column in the inner stations by Aviator islands; the other stations show a UML ranging from 18 to 13 m in the more external stations cluster, while in the isolated northernmost station 30 it reached 23 m. The overall picture shows a stratified water column for the first 10 m, while the deepening of the mixed layer of station 30 indicate that its waters are "uncoupled" with respect to the others, pointing to the presence of a gradient from clearly characterized shore waters to open ones. Values of chl a in the first 100 m were low in the entire area, except at the northern stations 30 and 31 where relative maximum were 152.40 and 119.56 mg chl a m^2 respectively (Fig. 6a). A slight decreasing gradient of concentration is present moving from coastal stations to those located northward. The point distribution of chlorophyll a along the water column, shows higher values in the first 35 m (Fig. 8a). In this layer, the mean value of chl a exceed 1 µg/L between 10 and 25 m, displaying a sub-surface maximum, while in other depths values were less than 0.6 µg/L reaching a minimum of 0.24 µg/L at 100 m. The group of points that exceed 2 µg/L in the 10-30 layer belongs to the station 31 located near Coulman Island. Nutrients in terms of DIN show an

inverse trend from surface to deeper waters in all stations (12.94 to 24.35 µmol/L) except station 30 where high levels of DIN were present with constant values (25-30 µmol/L) along the entire water column. PO4 ranged from 0.82 to 1.64 µmol/L at the surface, and up to 2.08 µmol/L at deeper levels. Mean dissolved iron concentration reported in this area at ˜30 m was 1.02 (±0.4) nM. The percentage contribution of the main functional groups to the total biomass (Fig. 8b) shows the dominance of diatoms with a mean percentage of 64% while haptophytes account only for 16% of total biomass. Other groups are nearly completely absent except cryptophytes (4.7%) and cyanopthytes (2.3%). The results obtained through PCA (Fig. 12) explained only 59.43 % of the total variance, with the F1 axis accounting for 43.76% and the F2 axis for 15.67% of the total variance. Chl a and diatoms were strongly correlated, placing both in the fourth quadrant. Temperature was correlated with UML along the negative F1 axis, salinity, DIN and PO4 were strictly correlated along the positive F1 axis. Haptophytes were more correlated along the positive F1 axis, and showed a weak negative correlation with negative axis F2. SiO2 places in the first quadrant, displaying the same positive correlation with positive F1 and F2 axis.

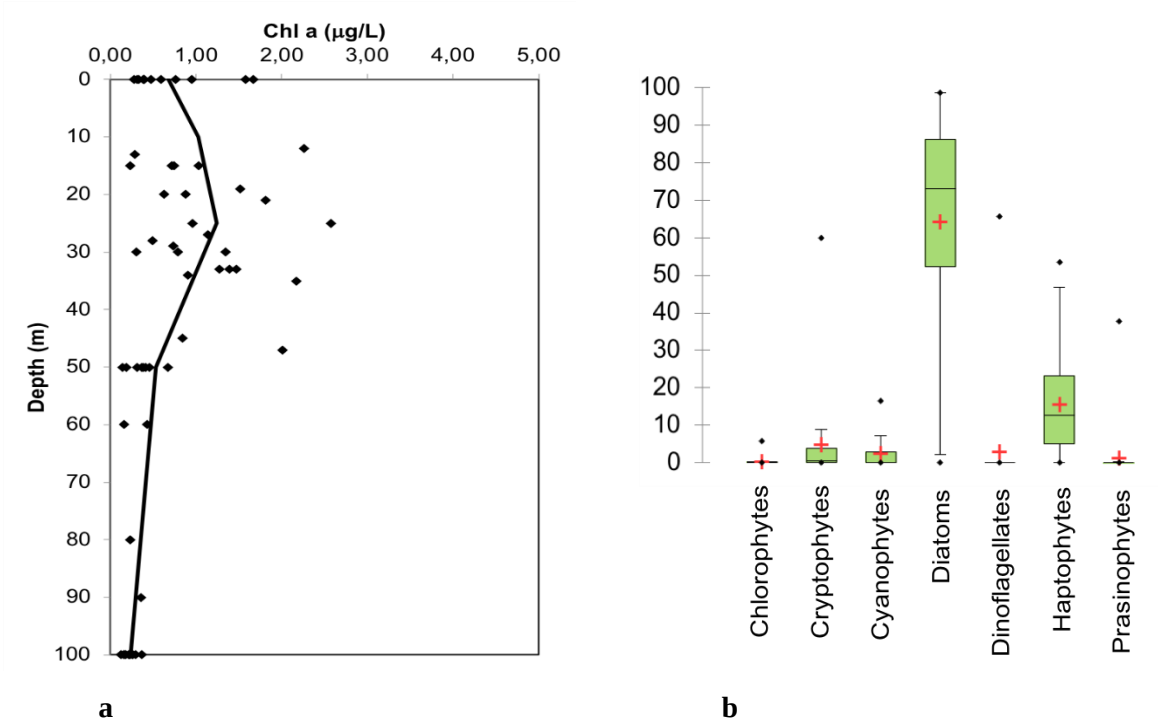

Figure 8 – **Area 2**: **a**) vertical distribution of chl at each sampled depth (dots), and mean vertical profile of concentration (black line)**; b**) Percentage contribution of the main functional groups to total biomass; red cross represents the mean value.

Area 3 – Stations were distributed within a large area representing an off-shore system of the Ross Sea polynya, which has been subdivided into two subareas (Area 3a, b) threated separately

due to the different levels of synoptic sampling. The Area 3a was sampled between January 26-27, 2017 and include stations from 43 to 50; the Area 3b was sampled between January 29-30, 2017 and include stations from 51 to 59. This cluster of stations has been sampled after two days with respect to those of 3a due to the ship standing at heave to due to heavy seas.

Area 3a - The water column structure (Fig. 6b) in this area shows the presence of a shallow UML < 25 m, except at stations 50 (32 m) and station 46, both located between Glomar Challenger Trough and Pennel Bank. The values of concentrations of chl *a* ranged from 176.59 mg chl a m^2 at station 54, to 79.39 mg chl a m^2 at station 51, with the presence of an increasing gradient of concentrations moving from station 57 in the northwestern part, to the station 54 in the south-eastern part (Fig. 6a). Values of chl a reported at station 54 represent the highest maximum value recorded in the off-shore area of the Ross Sea. The vertical distribution of chl a show the presence of higher levels of biomass in the first 50 m, with a mean profile of concentration reaching the maximum of 1.96 µg/L at 20 m, and values that exceed 1.77 µg/L in the 10-40 m layer (Fig. 9a). Below 50 m, chl a decreased sensibly down to 0.2 µg/L at 100 m. The maximum values of concentration reported in this area was 2.6 µg/L at 14 m. The nutrient distributions in terms of DIN showed lower concentrations in the first 50 m of the water column, with values ranging from 15.04 to 22.63 µmol/L, while at deeper levels concentrations increased up to 31.56 µmol/L. PO4 displayed the same pattern of distribution of DIN, with values ranging from 0.86 µmol/L to 1.97 µmol/L in first 50 m that increased up to 2.5 µmol/L at 100 m. As regards the concentration of dissolved iron at ˜30 m, mean values was 1.07 (±0.4) nM. Box plots in Fig. 9b show the dominance of diatoms with 62%, followed by haptophytes with 36% of total biomass. Among minor groups, chlorophytes were recorded with 3.5%, while other groups were nearly completely absent. Figure 12 shows the results of PCA analysis, that explained 67.44% of the total variance, with the F1 axis accounting for 43.7% and the F2 axis for 23.74 % of total variance. The position of active variables reveals a weak correlation with chl a, that was inversely correlated with UML along F2 axis, suggesting the presence of relative higher amount below this layer. SiO2 showed the same trend of chl a. Salinity, PO4 and DIN were correlated along positive F1 axis, while Temperature and diatoms displayed the same correlation with negative F1 axis and were inversely correlated with F2 axis. Haptophytes and diatoms were inversely correlated.

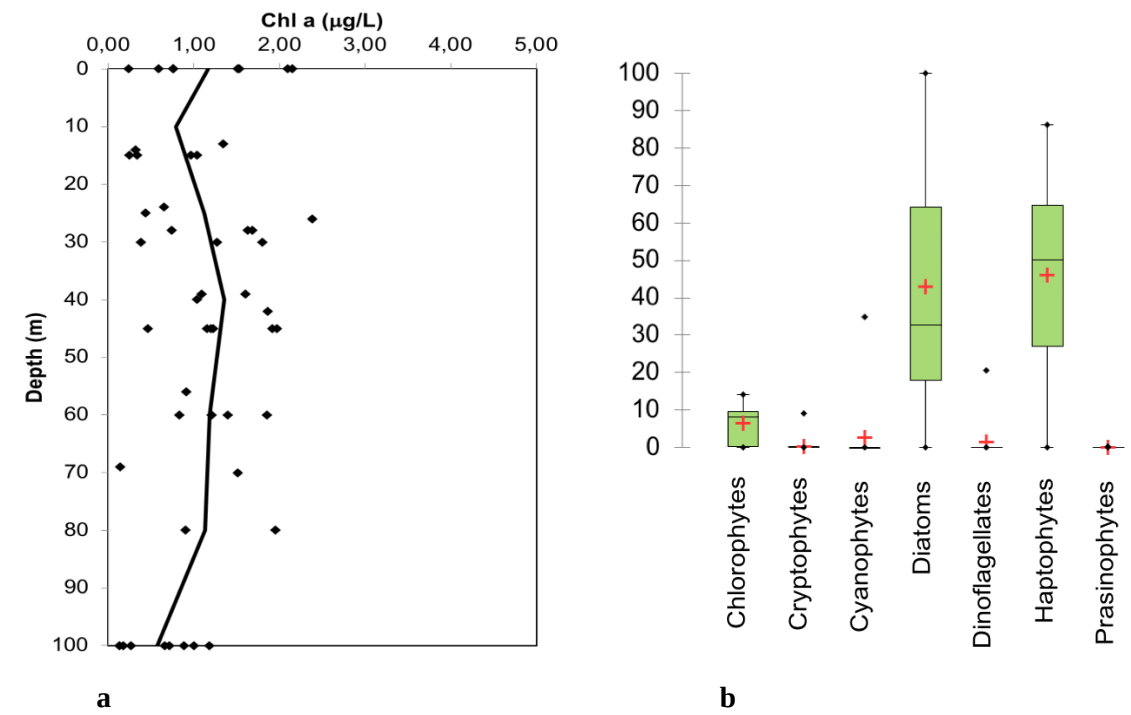

Figure 9 – **Area 3a**: **a**) vertical distribution of chl at each sampled depth (dots), and mean vertical profile of concentration (black line)**; b**) Percentage contribution of the main functional groups to total biomass; red cross represents the mean value.

Area 3b - Area 3b was sampled two days later than Area 3a due to adverse meteorological situation, which certainly contributed to the vertical structures of the water column found. UML, in fact, displayed a homogeneous distribution being 55 (±9) m in the entire area sampled area (Fig. 6b). As regard total the distribution of integrated chl a in the first 100 m, values ranged from a maximum of 132.13 mg chl a m^2 at station 49 to a minimum of 71.74 mg chl a m2 at station 45, with presence of relative higher values moving south-eastward (Fig. 6a). The point distribution of chl a was rather homogeneously in the first 70 m of the water column (Fig. 10a). The mean vertical profile of chl a, in fact, showed values of ~1.2 µg/L between the surface and 80 m, except at 10 m and 100 m where values were 0.8 and 0.57 µg/L respectively. The maximum recorded in this area was 2.39 µg/L at 26 m (Fig. 10a). The vertical distribution of DIN showed lower values in the first 50, where concentrations ranged from 21.58 to 26.67 µmol/L, and increased up to 32.07 µmol/L at 100 m. Like DIN, PO4 were more abundant in the 0-50 layer, with concentrations ranging from 1.10 to 2.01 µmol/L, and up to 2.47 µmol/L at deeper levels. Mean concentration of dissolved iron at ˜30 m was 0.73 (±0.4) nM. The percentage contribution of the main functional groups to the total biomass (Fig. 10b) shows the presence of haptophytes and diatoms with similar percentages, 46% haptophytes and 43% diatoms respectively. Among minor groups, chlorophytes represent 6% of the biomass and cyanophytes only the 2.5%. Other groups are nearly completely absent. PCA

analysis (Fig.12) on this system explained 70.73% of the total variance, with the F1 axis accounting for 48.22% and the F2 axis only for 22.51 % of total variance. Temperature and UML overlapped along positive F1 axis; also chl a and, to a lesser extent SiO2, displayed a strong correlation with positive F1 axis. Diatoms and haptophytes were inversely correlated, while salinity, DIN and PO4 showed a similar correlation with negative F1 axis.

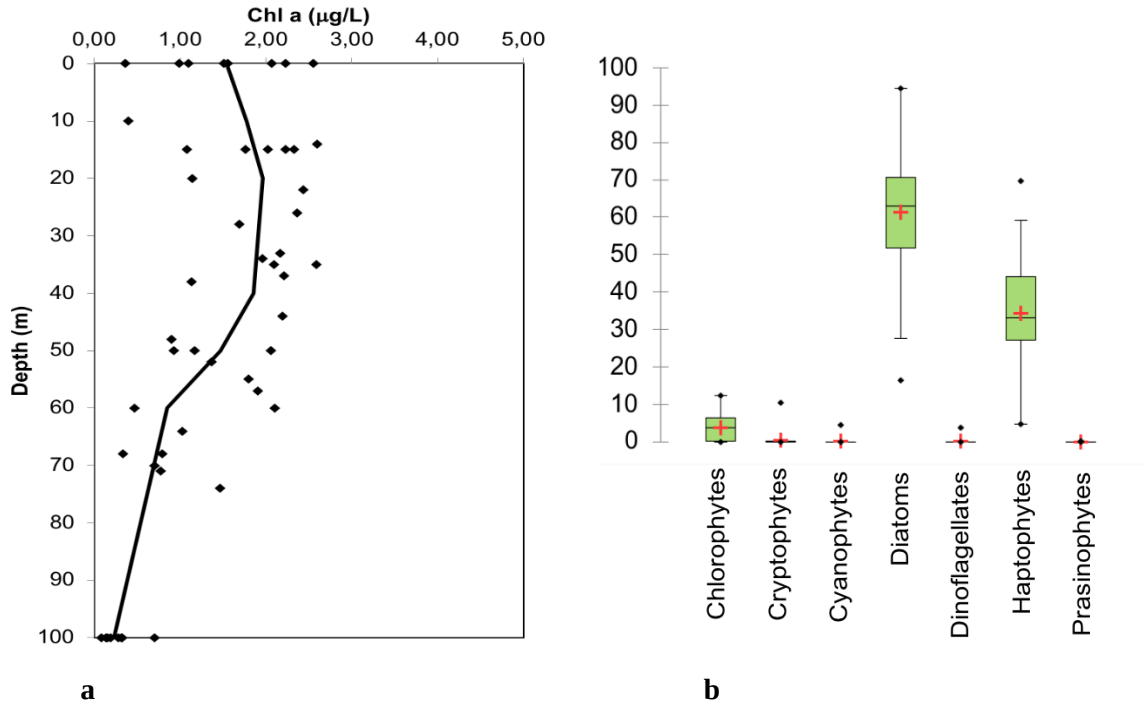

Figure 10 – Area 3b: **a**) vertical distribution of chl at each sampled depth (dots), and mean vertical profile of concentration (black line)**; b**) Percentage contribution of the main functional groups to total biomass; red cross represents the mean value.

Area 4 - This area represents the northernmost sampling site of the cruise, whose stations distributed along three short transect at the interface with the open Southern Ocean waters. The UML shows a pronounced variation increasing toward the more external station in a range from 45 to 90 m. The integrated chl a concentration in the first 100 m of the water column ranged from 106.80 mg chl a m^2 at station 63, to 6.63 mg chl a m^2 at station 74 (Fig. 6 a). Relatively higher levels of biomass were observed in the southern zone of the area, while in the northern side values of biomass were close to 0. The distribution of chl a slightly decreased from the surface, where it reached a mean maximum of 0.83 µg/L, to the deeper layer with a mean minimum of 0.22 µg/L; a subsurface maximum was not present (Fig. 11a). The maximum values of chl a reported in this area was 2.27 µg/L at 20 m. DIN values ranged from 21.5 µmol/L to 27.0 µmol/l for all station, except for station 65, where an increase of concentrations up to 31.8 was observed (Fig. 6b). PO4 shows a distribution analogous to that of DIN both in terms of extent of variation and depth profile.

Mean value of dissolved iron concentration was 0.74 (±0.43) nM. Figure 11b shows the percentage composition of phytoplankton community in terms of main functional groups. Diatoms represent the most abundant group with 52.6% but, surprisingly, dinoflagellates were the second most abundant one with 23.5%, followed by haptophytes with 22.6%. Other groups were close to 0. PCA analysis (Fig. 12) explained 64.15 % of the total variance, with the F1 axis accounting for 42.10 % and the F2 axis only for 22.04 % of total variance. Salinity and temperature placed in the first quadrant and were strongly correlated, being almost overlapped. Diatoms and haptophytes did not show an inverse correlation with first group strongly correlated with chl a along positive F2 axis, while haptophytes showed the same correlation of DIN along positive F1 axis, and to lesser extent with positive F2 axis. SiO2 and PO2 placed in the second quadrant and were inversely correlated with chl a and diatoms. As regard UML, it was the only variable placing in the third quadrant, and was inversely correlated with DIN and to a lesser extent with temperature, salinity and haptophytes.

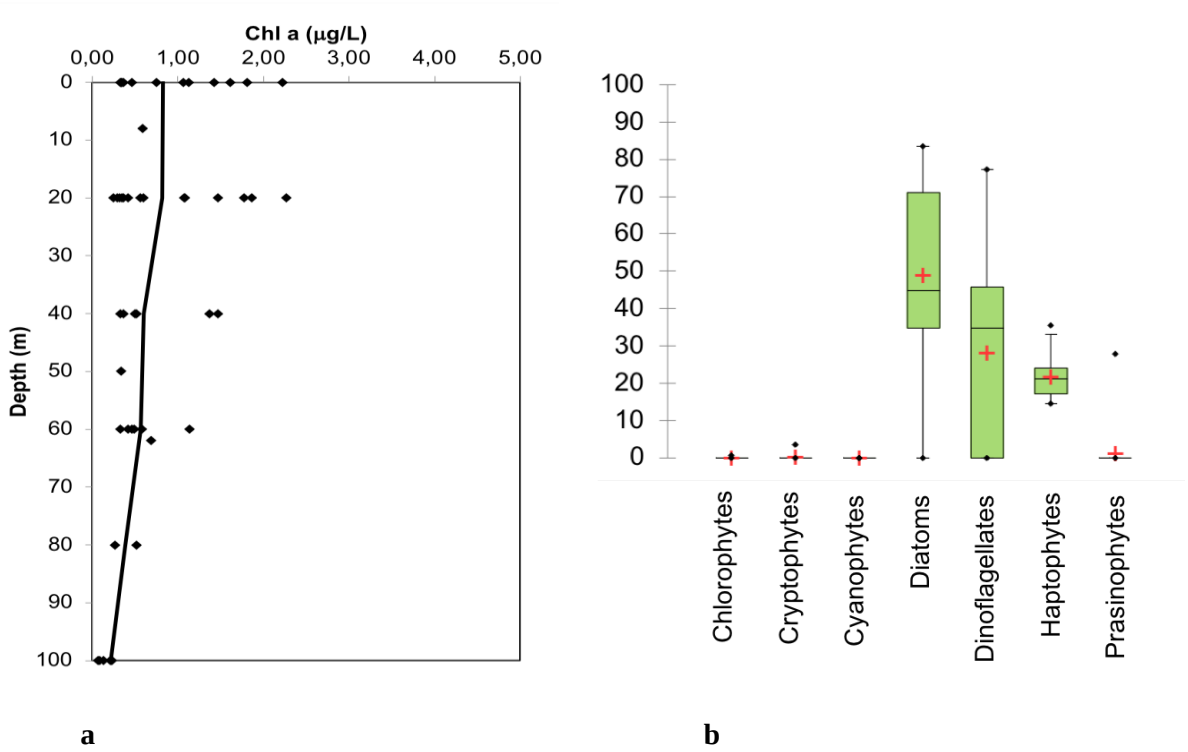

Figure 11 – Area 4: **a**) vertical distribution of chl at each sampled depth (dots), and mean vertical profile of concentration (black line)**; b**) Percentage contribution of the main functional groups to total biomass; red cross represents the mean value.

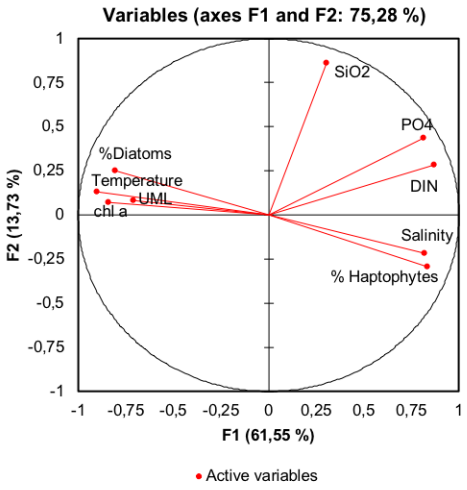

Area 1

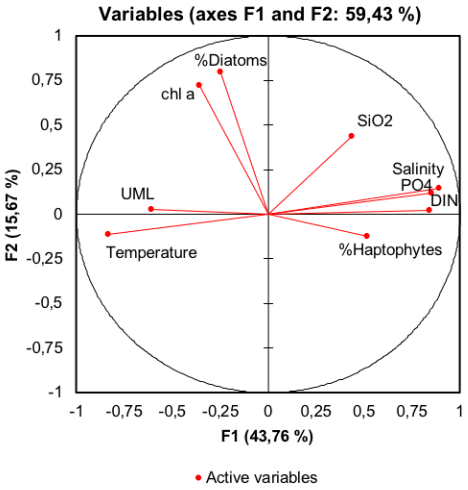

Area 2

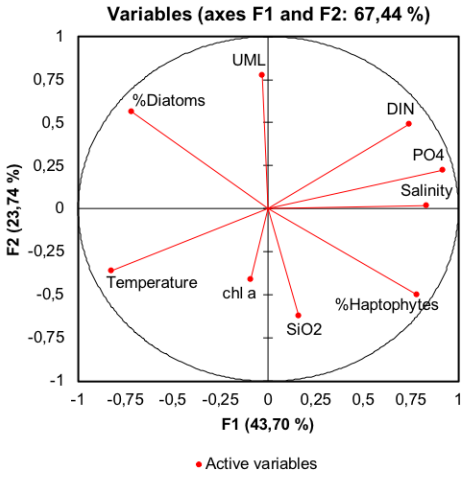

Area 3a

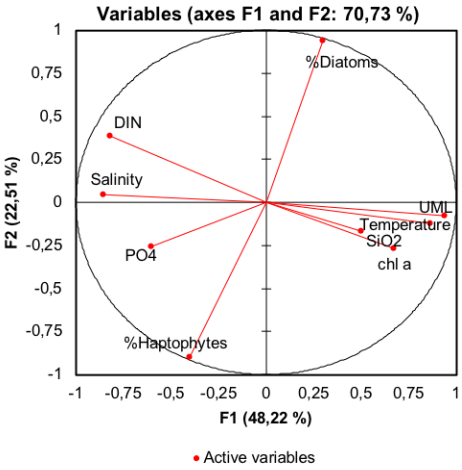

Area 2b

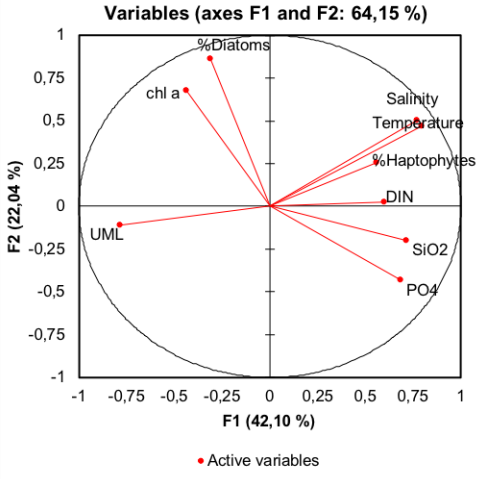

Area 4

Figure 12 - Output of the Principal Component Analysis (PCA) between biological [chl a, percentage contribution of diatoms and haptophytes to total biomass) and environmental variables (salinity, temperature, dissolved inorganic nitrogen (NO2+NO3), silicate (SiO2), phosphate (PO4), upper mixed layer (UML)].

CICLOPS (NSF Expedition)

The vertical profiles of salinity and temperature (Fig. 13), show different pattern of distribution along the water column moving Eastward from station 10 to station 17. In particular, at station 10 isohalines were grouped at ~ 20 m ranging from 33.9 to 34.1 between 10 and 18 m, respectively. In the same layer, water temperature ranged from -0.82°C at surface to -1.6 °C at 18m, remaining almost constant in deeper layers and reaching -1.79°C at 100 m. At stations 11,12,13 and 14 isohalines were distributed more homogeneously along the water column, and slightly decreased from the surface to the bottom. Temperature was higher at stations 11 and 12 (-0.58°C at surface) and decreased toward the bottom following the isohaline of 34.05; below 70 m, in fact, at station 10 temperature was -1.8°C while at station 12 temperature was -1.11°C at 100 m and salinity did not reach 34.05. Stations 13 and 14 showed a similar pattern of distribution of salinity, although temperature was relatively higher at station 13 where it changed with salinity and displaying an irregular profile from the surface to the bottom. In particular, at station 13 temperature decreased from the surface to the bottom, while at station 14 temperature did not decrease uniformly being higher at 80 m (-1.50) than 45 m (-1.60). Stations 15, 16 and 17 displayed a different thermohaline profile, especially with respect to temperature that exceed +0.4°C in the first 20 m at station 17. The lowest value of salinity of the transect was observed at station 15 (33.75) in the first 20 m. Below 20 m, temperature sensibly decreased in the three stations up to -1.77 at 100 m. A strong stratification emerged at the western side of the sampled area, where salinity and temperature strongly changed between 20 and 30 m.

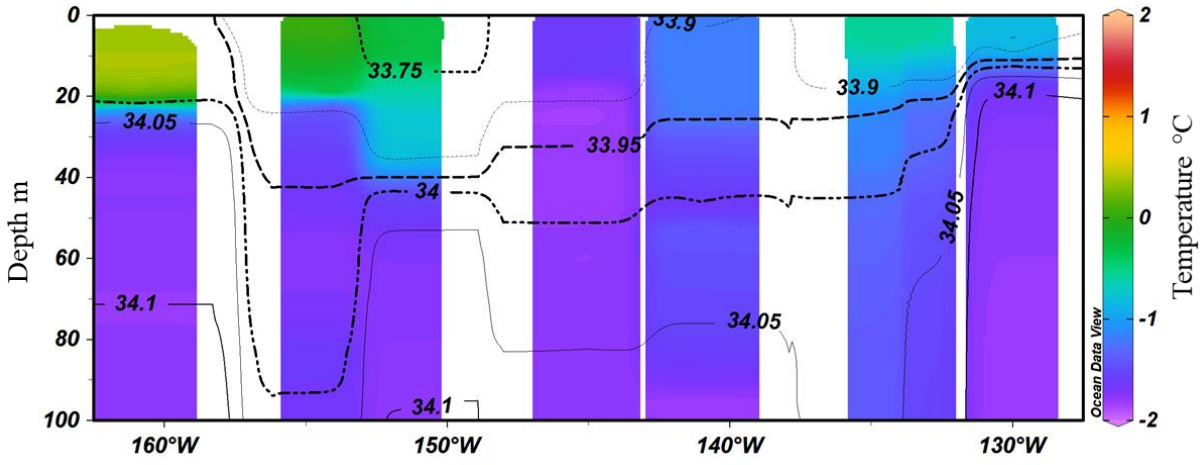

Figure 13 - Vertical distribution of salinity (isohaline, black lines) and temperature (z axis) crossing Saunders Coast (158°00'W - 146°31'W), Ruppert Coast (146°31'W - 136°50'W), Hobbs Coast (136°50'W - 127°35'W) of Marie Byrd Land.

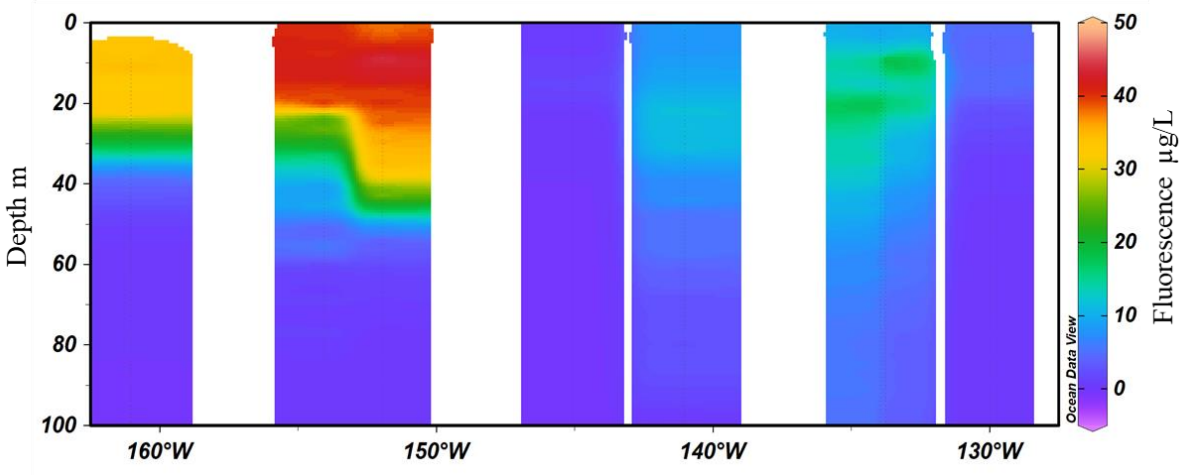

Figure 14 - Vertical distribution of fluorescence (µg/L) and temperature (z axis) crossing Saunders Coast (158°00'W - 146°31'W), Ruppert Coast (146°31'W - 136°50'W), Hobbs Coast (136°50'W - 127°35'W) of Marie Byrd Land.

The distribution of fluorescence profile (Fig. 14) – as indicator of phytoplankton biomass - clearly shows the presence of two distinct areas with higher fluorescence, that can be identified in association with lower salinity and higher temperature. In particular, at stations 11 and 12 fluorescence exceed 20 µg/L in the first 20 m, although at station 11 values sensibly decreased up to 0 at 100 m, while at station 12 fluorescence was ~8.5 ah 100 m. The second area was represented by stations 15,16,17 located in coastal area of Saunders Coast, near the Ross Sea borderline, were values of fluorescence exceed 40 µg/L in the first 20 m and followed the thermohaline profile, thus highlighting the role of melting processes and the continental input on primary production in this area. The analyses of phytoplankton biomass between stations 15 and 17 through chemotaxonomic approach, revealed that haptophytes (*Phaeocystis antarctica*) represented the dominant functional groups, with a mean percentage that exceeded 85%. Dinoflagellates and diatoms instead only accounted for 10% and 5% respectively.

Shipboard co-limitation experiments on natural populations

Considering such an intense phytoplankton bloom in an area strongly subjected to freshwater inputs, as consequence of continental melting, and the net dominance of *Phaeocystis antarctica*, an experiment was carried out using the water collected at the Deep Chlorophyll Maximum (DCM) according to the vertical fluorescence profile, in order to evaluate the effect of the addition of iron and vitamin B_{12} on the natural phytoplankton community, in presence and absence of UV radiation.

The different treatments were: **1**) iron (+dFe), **2**) vitamin B_{12} (B_{12}), **3**) iron and vitamin B_{12} (+Fe+B_{12}), **4**) absence of iron (-dFe), **5**) control (CTRL).

Each line of growth was set up in triplicate and analysed at time 0 (T0), time 2 (T2, 2 days later the start) time 5 (T4, 4 days later the start). Further details are reported in the section Material and Methods.

Figure 14 clearly shows that after 5 days, the addition of iron and Fe+B_{12} stimulated the growth of diatoms, whose percentage reached 25% in dFe treatment and 23 in treatment B_{12}+Fe. The percentage of *Phaeocystis antarctica* was instead 75% (dFe) and 77% (Fe+B_{12}) respectively. Treatments CTRL, B_{12} and –dFe, did not show significant differences between T0 and T5.

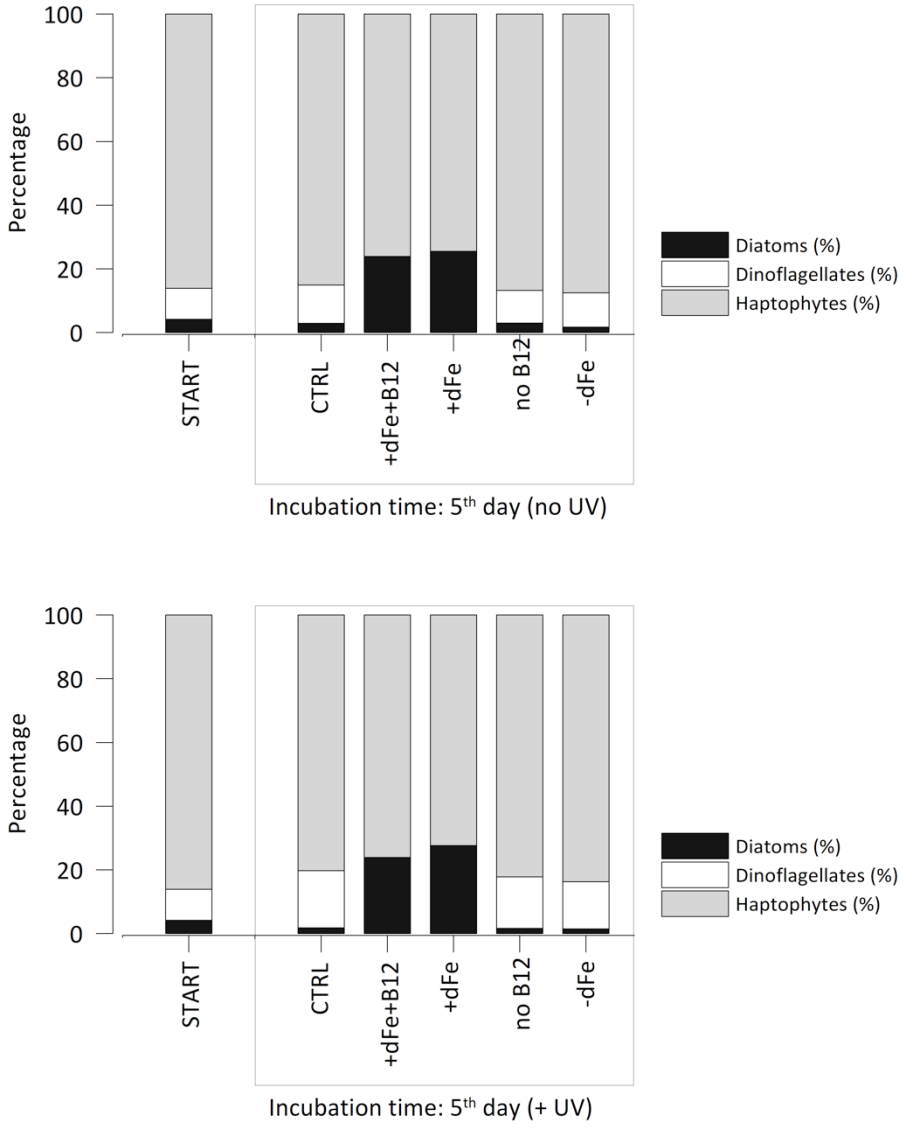

Figure 14 – Shipboard co-limitation experiments on natural populations (irradiance = 50 µmol photons m^{-2} s^{-1}).

The effect of iron addition is particularly evident also in terms of quantum efficiency (Fm/Fm), at T2 and T5. The highest values of Fv/Fm were in fact reported both presence and absence of UV in the iron treatments. In particular, Fv/Fm for dFe and +Fe+B_{12} in absence of UV at T2 was 0.55 (± 0.036 and 0.03 respectively), while in absence of iron value reached 0.34±0.012. As regard CTRL and B_{12}, Fv/Fm was 0.39±0.09 and 0.42±0.074 respectively. Also in presence of UV radiation, +Fe and +Fe+B_{12} showed the highest Fv/Fm values (0.45±0.021 and 0.45±0.042 respectively). In CTRL Fv/Fm was 0.31±0.028, in the treatment without iron 0.29±0.085 and in B_{12} was observed the lowest value of 0.25±0.028.

At day 5, in presence of UV light Fv/Fm displayed a pattern similar to that observed at time 2. Values reported in different treatments were 0.45±0.026 for +Fe+B_{12}, 0.453±0.05 for +dFe, 0.35±0.044 in absence of iron (-dFe), 0.31±0.072 for -B_{12} and 0.343±0.058 for CTRL. In absence of UV, the highest value was observed in dFe 0.38±0.076; CTRL and +Fe+B_{12} showed similar values (0.317±0.021 and 0.317±0.031 respectively); +B_{12} and –dFe displayed instead the lowest Fv/Fm (0.277±0.031 and 0.273±0.035, respectively) (Fig. 14).

The discovery of a *Prorocentrum* sp. in association with gelatinous colonies of *Phaeocystis antarctica*

During attempt to get single palmelloid colonies of *Phaeocystis antarctica* into culture, unexpectedly flasks left for 2 weeks under nutrient starvation changed colour (Image 1). The first investigation by microscopic observations on the contaminant, revealed the presence of a species of dinoflagellate that initially appeared to be a *Prorocentrum minimum*-like cell, attached to the gelatinous colonies of *Phaeocystis.* Thanks to serial dilutions, and with the help of a modified micropipette, single cells of *Prorocentrum* sp. have been isolated from stressed colonial *Phaeocystis antarctica* culture. Eight weeks later, *Prorocentrum* sp. and *P. antarctica* were successfully established in monospecific cultures (Image 2). Both species were grown in L1 media and under 20 µmol phtons m^{-2} s^{-1} as descripted in Material and Methods. In order to shed light on the pigment spectra composition of *P. antarctica* and *Prorocentrum* sp. an HPLC analyses has been performed on monospecific cultures of the two species (Fig. 15). Each peak of the chromatograms (in absorbance) represents an eluted pigment and the elution time is reported in Table I. *P. antarctica* was characterized by the presence of 19'-exanoyloxyfucoxanthin (its marker pigment), while *Prorocentrum* sp., in addition with high concentrations of peridinin that represents

the major marker pigment of dinoflagellates, was also characterized by a distinct peak of a secondary pigment associated with diadinoxanthin (minute 7.7). Further investigation will allow to evaluate if this pigmentary characteristic represents a complementary identification tool of the species.

Image 1– Change of culture colors after 1 month in condition of nutrient starvation.

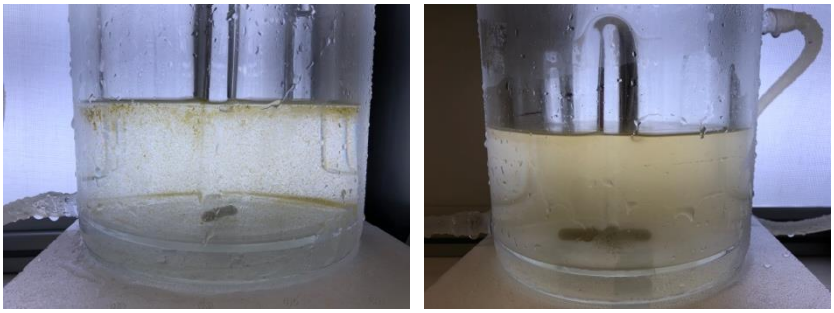

Image 2 – The color difference of two monospecific culture of *Phaeocystis antarctica* (left) and *Prorocentrum* sp. (right).

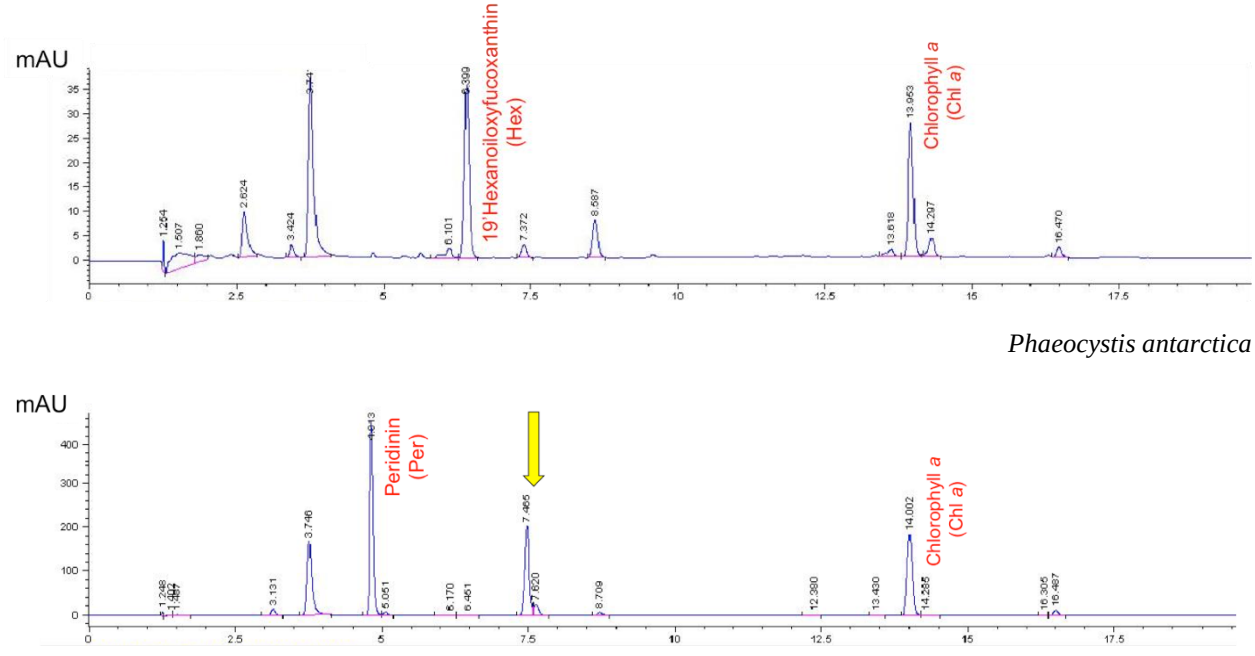

Figure 15 - Pigment spectra (chromatograms in absorbance).

Retention time (minutes)	Pigment
2.7	Chlorophyll C3
3.9	Chlorophyll C2
4.9	Peridinin
6.1	Butanoyloxyfucoxanthin
6.6	19'Hexanoyloxyfucoxanthin
7.6	Diadinoxanthin
7.7	Simil-Allox**
8.4	Diatoxanthin
14.1	Chlorophyll *a*
16.5	B-carotene

Table I - The elution time of pigments in the two chromatograms.

To better investigate on the two species, molecular analysis were performed to define the genetic sequences profile of *P. antarctica* and *Prorocentrum* sp. BLASTn analysis of the algal 18S and 28S nucleotide sequences confirmed that the species identified as *P. antarctica* belongs effectively to the species *Phaeocystis antarctica,* showing high nucleotide identity (18S 99.77% and 28S 99.54%) with the homolog sequences of this species present in GenBank. The 18S and 28S nucleotide sequences of the dinoflagellate gave the best BLASTn hits with homologous sequences of the genus *Prorocentrum*; however, the highest values of nucleotide identity range between 96,19% (18S) and 96.65% (28S). This result indicates that the isolated dinoflagellate belongs to *Prorocentrum* genus and suggests it could be a still not described species.
Genera form of *Prorocentrum* sp. with hearth around the shape (Image 3).

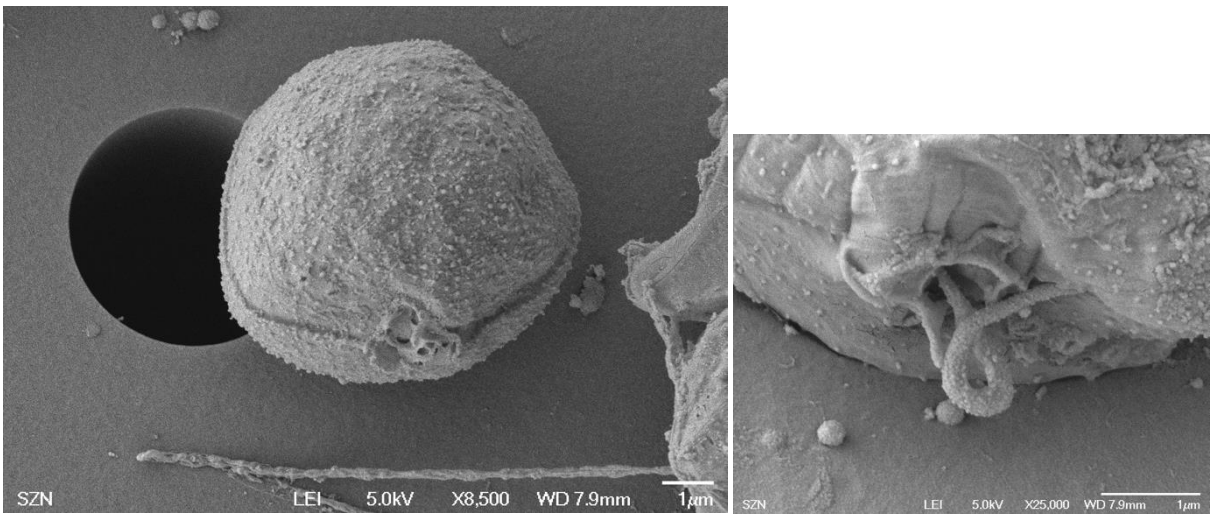

Image 3 – SEM microscopy.

Manipulative experiments

Experiment 1 - ANEMIA

The main objective of the experiment was to evaluate the response of *P. antarctica* and *Prorocentrum* sp., in terms of photosynthetic efficiency and growth, to the addition of medium L1 without B_{12} (-B_{12}), without dissolved Fe (-dFe) and medium L1 with the entire stock of nutrients (+dFe+B_{12}) in both monospecific and mixed cultures. At the beginning of the experiments, cells used for the inoculum were grown under nutrient starvation conditions (START) (see details in Material and Methods). Figure 16 shows the chl a concentrations in *Phaeocystis antarctica*, *Prorocentrum* sp. and mixed cultured under different treatments.

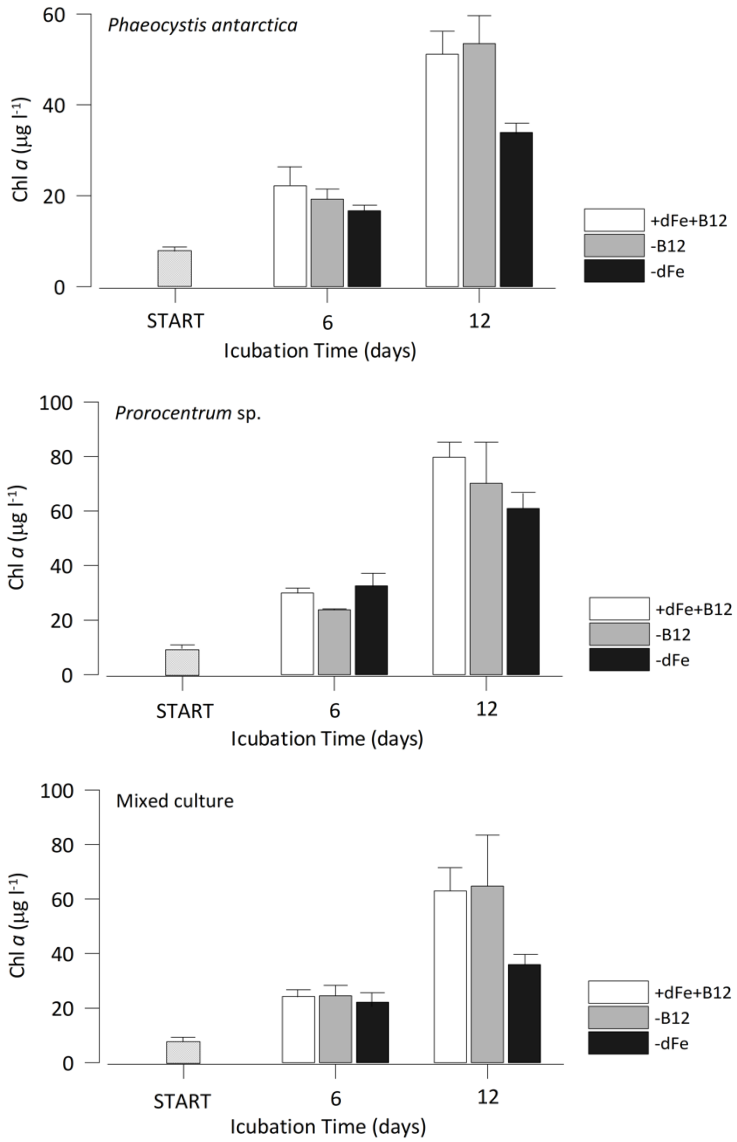

Figure 16 – Changes in chl a concentrations for amended treatments over time for Experiment 1 – ANEMIA in *Phaeocystis antarctica*, in *Prorocentrum* sp. and in mixed culture (incubation light = 40 µmol phtons m^{-2} s^{-1}).

• *Phaeocystis antarctica* - In the treatment +dFe+B_{12}, chl a increased from 7.24 µg/L (±0.08), at time 0, to 51.17 µg/L (±7.68) at time 12. In absence of -dFe, values of chl a increased from 7.24 µg/L (±0.04), at time 0, to 33.95 µg/L (±2.18) at time 12. In absence of B_{12} (-B_{12}), values of chl a increased from 7.24 µg/L (±0.06), at time 0, to 53.49 µg/L (±6.15) at time 12.

• *Prorocentrum* - In the treatment dFe+B_{12}, values of chl a increased from 8.7 µg/L (±0.04), at time 0, to 79.75 µg/L (±10.07) at time 12. In the treatment without Fe (-dFe), values of chl a increased from 8.7 µg/L (±0.05), at time 0, to 60.96 µg/L (±6.08) µg/L at time 12. In the treatment without B_{12} (-B12), values of chl a increased from 7.24 µg/L (±0.06), at time 0, to 70.14 µg/L (±15.14) at time 12.

• Mixed culture - In the treatment with dFe+B_{12}, values of chl a increased from 7.99 µg/L (±0.01), at time 0, to 63 µg/L (±7.66) µg/L at time 12. In the treatment with -dFe, values of chl a increased from 7.99 µg/L (±0.01), at time 0, to 35.98 µg/L (±4.88) at time 12. In absence of B_{12}, values of chl a increased from 7.99 µg/L (±0.02), at time 0, to 64.79 µg/L (±18.68) µg/L at time 12.

Figure 17 shows the photosynthetic efficiency and Fig. 18 shows the σPSII regulation in *Phaeocystis antarctica, Prorocentrum* sp. and mixed cultures under different treatments.

• *Phaeocystis antarctica* - As regards the quantum efficiency (Fv/Fm), before the addition of nutrients the initial value was 0.25 (±0.02). Once cultures were refreshed, a strong increase was observed in all treatments after 6 days, with net differences that emerged between +Fe+B_{12} (0.61±0.02), -B_{12} (0.55±0.02) and –dFe (0.49±0.02) (Fig. 17). At T12, Fv/Fm in +dFe+B_{12} and -B_{12} decreased to 0.53±0.03 and 0.52±0.02, respectively, probably as consequence of nutrient depletion due to high growth rate, while Fv/Fm in -dFe was (0.49±0.03). As concern σPSII, dFe+B_{12} showed the same value of the inoculum at T0 (12.95±0.83). B_{12} and -dFe showed instead values of 12.58±0.52 and 12.40±0.35 respectively. At T12 was observed a general decrease in σPSII, and the highest value was observed in the B_{12} (9.95±0.20) while -dFe and +dFe+B_{12} displayed the same values (9.36±0.62 and 9.38±0.24, respectively) (Fig. 18).

• Prorocentrum sp. - In *Prorocentrum sp*. Fv/Fm increased from 0.18±0.03 (inoculum) to 0.42±0.05 at T6 in all treatments. At T12, Fv/Fm was lower in -B_{12} (0.54±0.04) than -dFe (0.60±0.04) and +dFe+B_{12} (0.62±0.05) (Fig. 17). σPSII changed from 10.79±0.02 (inoculum) to 10.90±0.09 (+dFe+B_{12}), 11.08±0.25 in -dFe and 10.62±0.45 in -B_{12} at T6. At T12 values decreased in all treatments, showing the same pattern observed in *P. antarctica*. In particular, 7.87±0.12 in +dFe+B_{12}, 8.11±0.17 in –B_{12} and 7.73±0.13 in –dFe treatment (Fig. 18).

• Mixed culture - The value of Fv/Fm at time 0 was 0.23±0.02. Six days after the addition of micronutrients, measurements in the three treatments were similar (0.39±0.02). At T12, -dFe displayed the highest Fv/Fm (0.71±0.02) while in -B_{12} and +dFe+B_{12} it was similar, 0.55±0.03 and 0.54±0.02 respectively (Fig. 17). Values of σPSII showed small differences between treatments at T6. In this case, +dFe+B_{12} displayed the highest values and -dFe the lowest ones. At T12, the general decreased observed reflects the trend reported at T6, although a more pronounced difference can be observed between -dFe (7.11±0.02) and treatments -B_{12} (8.54±0.04), +dFe+B_{12} (8.66±0.02) (Fig. 18).

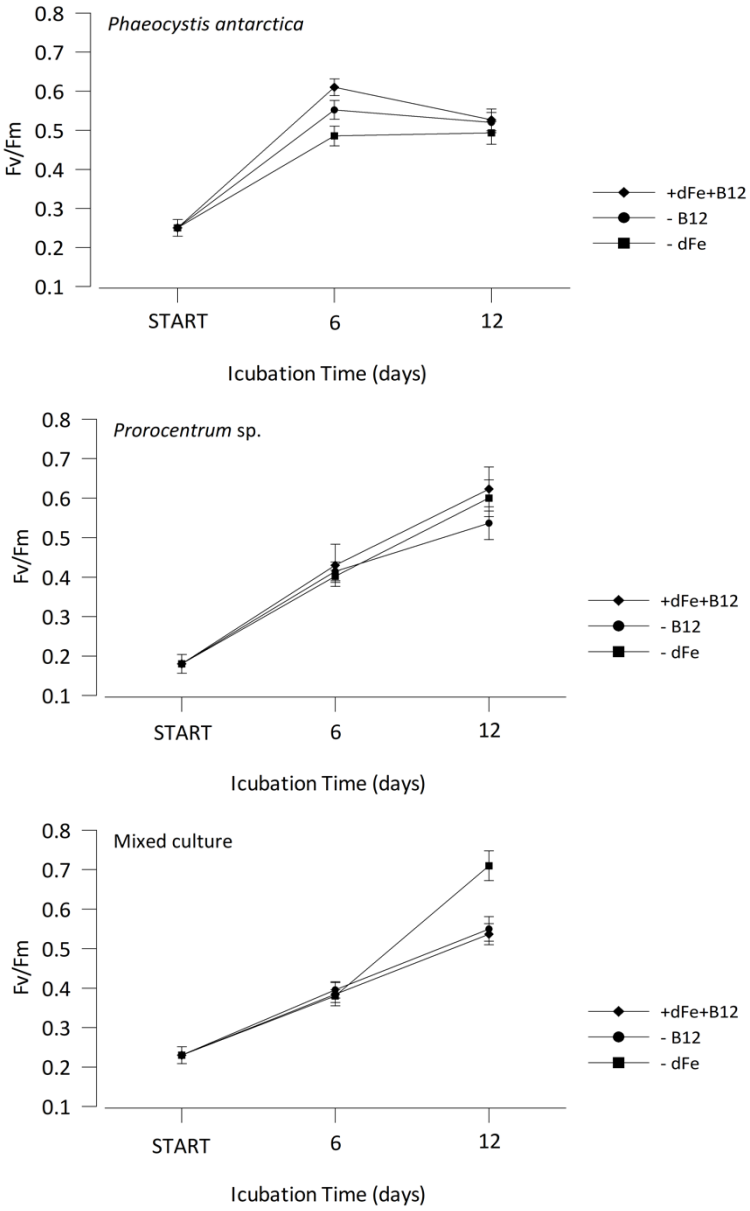

Figure 17 - Changes in photosynthetic efficiency for amended treatments over time for ***Experiment 1 – ANEMIA*** in *Phaeocystis antarctica*, in *Prorocentrum* sp. and in mixed cultures (incubation light = 40 μmol phtons m^{-2} s^{-1}).

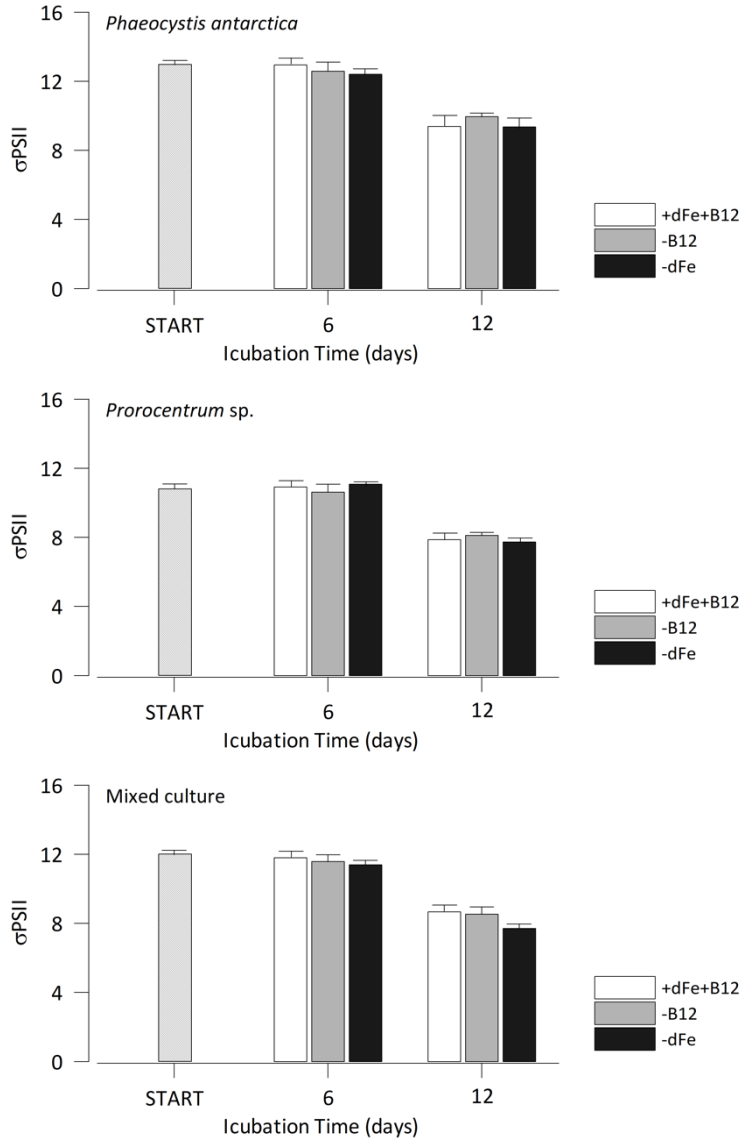

Figure 18 - Changes in σPSII regulation for amended treatments over time for ***Experiment 1 – ANEMIA*** in *Phaeocystis antarctica*, in *Prorocentrum s*p. and in mixed cultures (incubation light = 40 µmol phtons m^{-2} s^{-1}).

In order to understand which species, between *Prorocentrum* sp. and *Phaeocystis antarctica* prevails over the other in different micronutrient limitations at T12, the marker pigment ratio Per:Hex was used to describe the dominance of *Prorocentrum sp*. over *Phaeocystis antarctica*. In addition, the ratios Per:chl a and Hex:chl a were used to describe changes in marker pigments concentration in the two monospecific cultures (Fig. 19). While the ratio Per:Hex in +dFe+B_{12} and -B_{12} treatments was similar (9.5), in -dFe it was more than twice (21.2), suggesting clearly the dominance of *Prorocentrum* sp. over *Phaeocystis antarctica* in presence of iron limitation (Fig. 19).

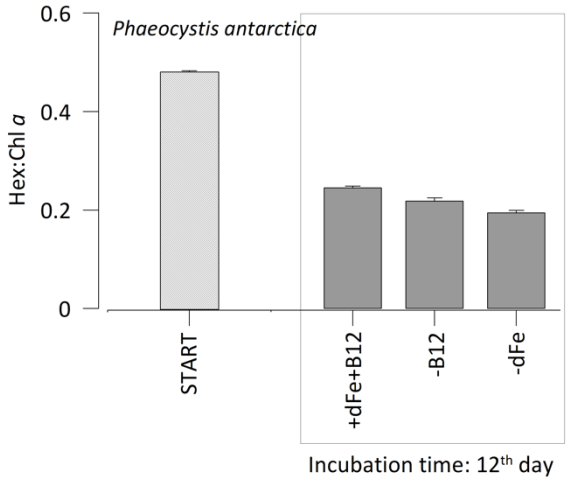

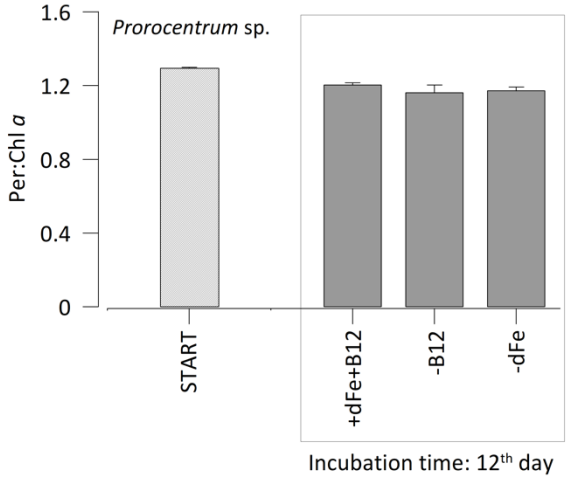

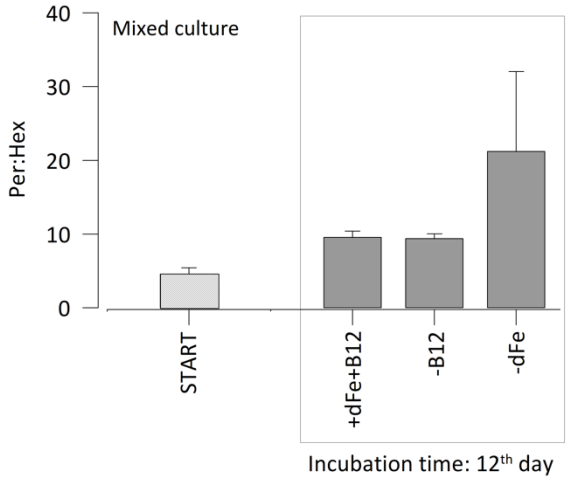

Figure 19 - Changes in pigment ratios for amended treatments over time for ***Experiment 1 - ANEMIA*** in *Phaeocystis antarctica*, in *Prorocentrum* sp. and a mixed culture of both (incubation light = 40 µmol phtons m^{-2} s^{-1}).

Experiment 2 – High Light –Low Light

In order to evaluate the response of *Phaeocystis antarctica* and *Prorocentrum* sp. to different levels of irradiance, the two species - previously adapted at 40 µmol photon m-2 s-1 in a continuous light period (24h) - have been exposed for 12 days at the following light intensity:

- 110 µmol phtons m^{-2} s^{-1} (treatment HL)
- 60 µmol phtons m^{-2} s^{-1} (treatment L1)
- 30 µmol phtons m^{-2} s^{-1} (treatment L2)
- 19 µmol phtons m^{-2} s^{-1} (treatment L3)

Phaeocystis antarctica

At T 0, chl a concentration was 16±0.92 (HL), 9.02±0.5 (L1), 8.16±1.76 (L2) and 6.55±0.31 (L3). At T 6, treatments showed a different increase in chl a, with values of 19.92±10 (HL), 17.7±0.85 (L1), 13.58±0.3 (L2) and 11.24±0.1 (L1) respectively, although the general pattern was similar to that observed at T0 as consequence of the presence of mucilage colonies during inoculum activities (Fig. 20a). However, at the end of the experiment -T12- a significant change was observed between HL and L1. Values of chl a were 58.11±3.89 (HL), 59.28±11.03 (L1), 81.21±3.54 (L2), 75.48±1.84 (L3), respectively.

To better illustrate changes in chl a concentration over the entire duration of the experiment, a linear equation has been calculated for each treatment. Figure 20b clearly shown differences in terms of chl a between treatments, with L3 and L2 characterized by a strong increase in chl a concentrations, and L1 and HL by a completely different trend.

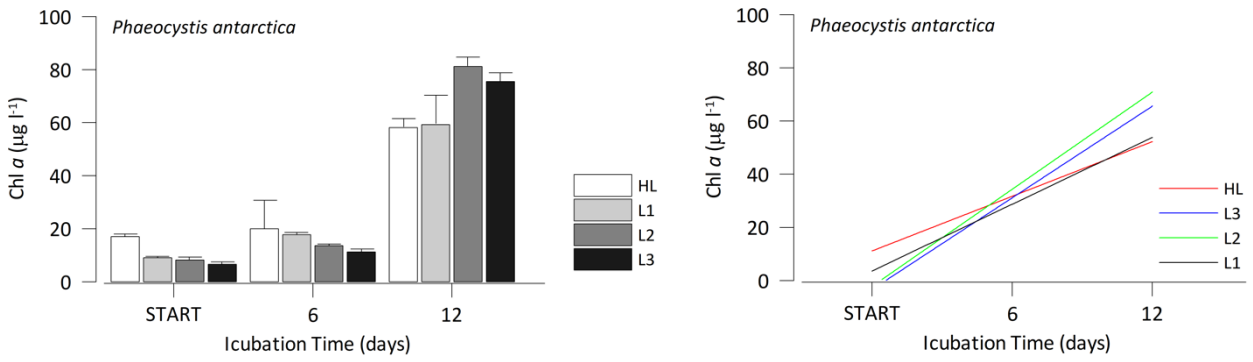

a **b**

Figure 20 – Changes in chl a concentrations (**a**) histograms, and b) linear equations for amended treatments over time in the ***Experiment 2 – High Light –Low Light*** in *Phaeocystis antarctica*. Incubation light (µmol phtons m^{-2} s^{-1}): HL = 110, L1 = 60, L2 = 36, L3 =19.

As regards the maximum quantum efficiency (Fig. 21a), at day 6 Fv/Fm increased in all treatments as consequence of the initial culture refresh. Except little differences due to the highest value observed in HL, treatment displayed a similar value of quantum efficiency. At T12, Fv/Fm in HL and L1 showed a weak decrease, contrarily to what observed in L2 and L3, but no big differences emerge between treatments in the entire duration of experiment. As regard σPSII, a general decrease of values was observed at the end of the experiment, and strong differences emerged between treatments at T6 and T12. σPSII strongly varied according to light intensity, with lowest values in HL, and highest values in L3. At T12 the trend was the same, with a general decrease of values except in HL (Fig. 21b).

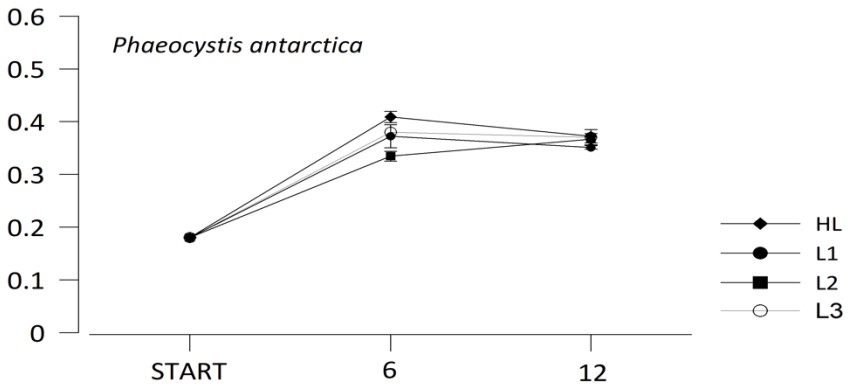

a

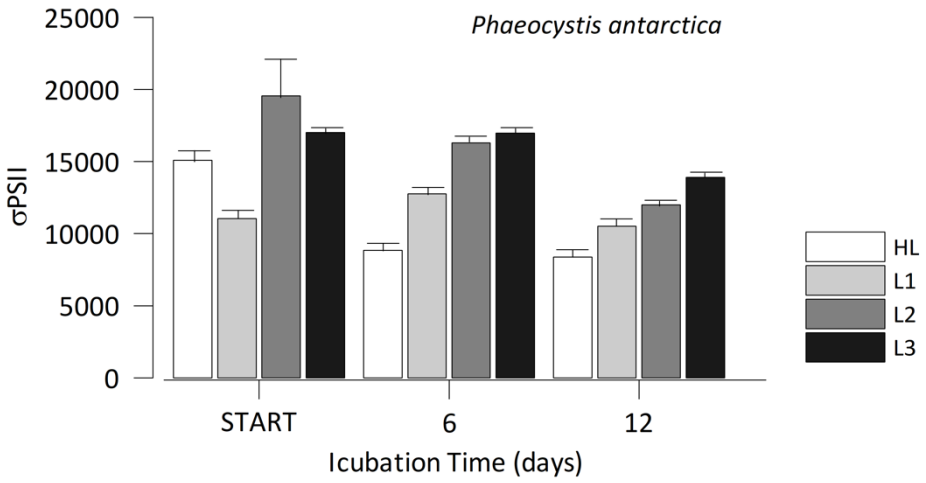

b

Figure 21 - Changes in Fv/Fm (**a**) and sPSII (**b**) for amended treatments over time for ***Experiment 2 – High Light-Low Light***. Incubation light (µmol phtons m^{-2} s^{-1}): HL = 110, L1 = 60, L2 = 36, L3 =19.

***Prorocentrum* sp.**

At T0, chl a concentration in different treatments was 79.72±1.25 (HL), 77.12±0.96 (L1), 78.29±0.79 (L2), 85.07±0.9 (L3) (Fig. 22a). At T6, differences emerged especially between HL and other treatments, with values of 92±0.3 (HL), 107±6.4 (L1), 106.49±4.73 (L2) and 106±1.97 (L3) respectively. At T12, chl a concentration in each treatment was inversely correlated with light intensity, being 171.53±5.85 (HL), 180.19±2.23 (L1), 194.84±0.64 (L2), 220.81±5.18 (L3). To better illustrate changes in chl a concentration over the duration of the experiment, were reported specific linear correlations for each treatment in Fig. 22b. Linear equations show a decrease in chl a concentration with increasing light irradiance.

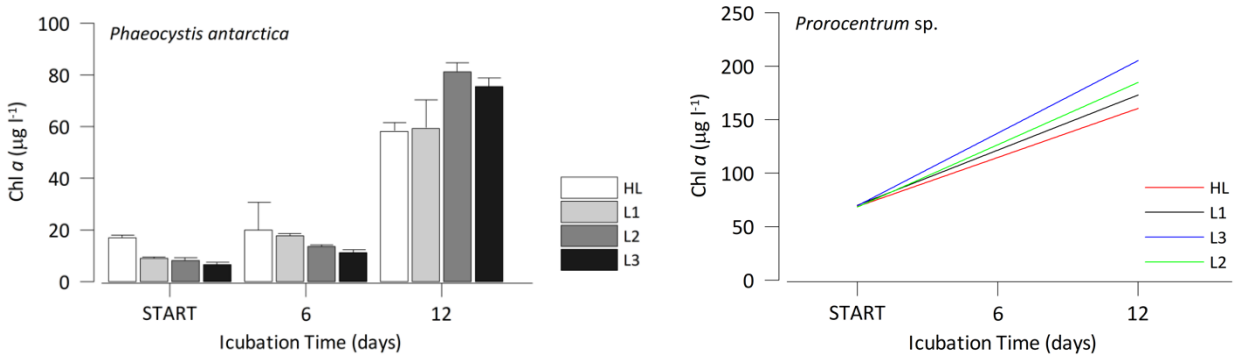

a **b**

Figure 22 – Changes in chl a concentrations (**a**) histograms, and b) linear equations for amended treatments over time in the ***Experiment 2 – High Light –Low Light*** in *Prorocentrum* sp. Incubation light (µmol phtons m^{-2} s^{-1}): HL = 110, L1 = 60, L2 = 36, L3 =19.

Prorocentrum sp. exhibited a completely different trend in both Fv/Fm and σPSII temporal variation (Fig. 23). As regard Fv/Fm, a general decrease in the values was observed at time 6 and time 12, along with an inverse correlation with different levels of irradiance (Fig. 23a). In particular, after 6 days, the treatment L3 presented the highest Fv/Fm (0.32±0.01), followed by L2 (0.22±0.01), L1 (0.17±0.02) and HL (0.07±0.01). At day L2, L3 showed the same Fv/Fm of time 6, but there is a significant decrease in values in other treatments, with L1 and L2 close to time 0 (Fig. 23a).

Differently to what observed in *Phaeocystis antarctica* where σPSII generally decreased over the time, *Prorocentrum* sp. exhibited an increase of σPSII in all treatments (Fig. 23b). At day 1, all treatments did not differ sensibly from each other. At time 6, σPSII was similar in L1, L2 and L3 while in HL was lower than the other two. At time 12, the lowest value has been observed in HL (8,722±536) and the highest in L2 (10,399±163).

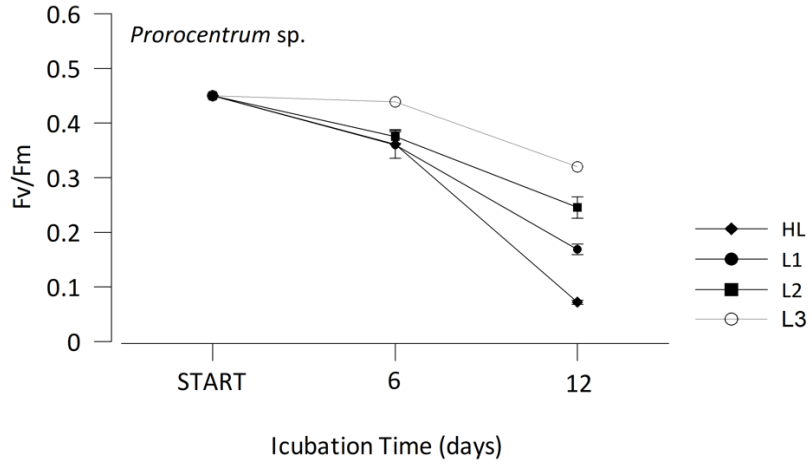

a

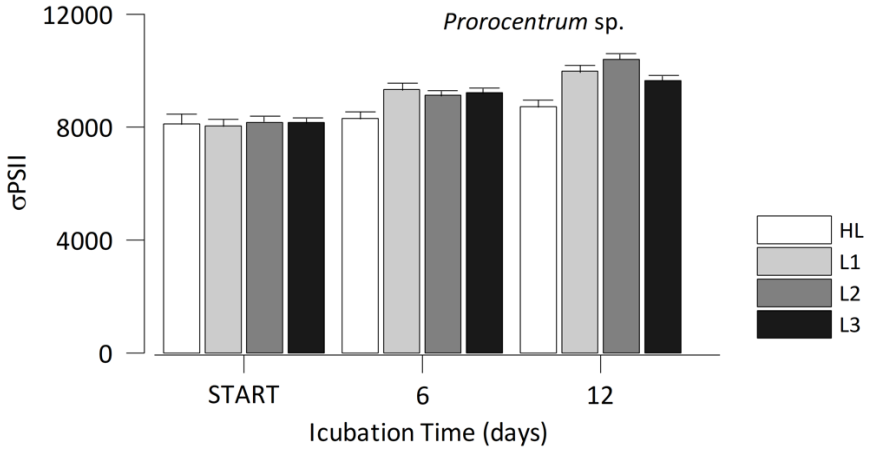

b

Figure 23 - Changes in Fv/Fm and sPSII for amended treatments over time for ***Experiment 2 –High Light-Low Light***. Incubation light (μmol phtons m^{-2} s^{-1}): HL = 110, L1 = 60, L2 = 36, L3 =19.

The identification of phytoplankton functional groups has been made by means of classic chemotaxonomic methods, using marker pigments for the identification of phytoplankton classes. The use of this technique has strongly increased in the past decade, thanks to the software CHEMTAX, a tool that derives the quantitative contributions of phytoplankton taxa with respect to the total chlorophyll pool. Since the pigment:chl a ratios vary according to species, light, nutrients etc. and cannot be known beforehand, the isolation and cultivation of species collected in situ allowed to better define the pigment spectra composition of single species in relation with different environmental conditions, helping to improve the pigment:chl a ratio used for the chemotaxonomic analyses.

Table II shows the ratio pigments: chl a in the two considered species at different levels of irradiance after a 12 days incubation.

Pigment:Chl *a* ratio T14													
	Treatment	Chl c3	Chl c2	Peridinina	Feoforb a	19'BF	19'HF	Violaxantina	Diadinoxantina	Alloxantina	Diatoxantina	ßcarotene	Chl a
P. antarctica	HL	*0.11007*	*0.282*	-	*0.003*	*0.041*	*0.373*	-	*0.026*	-	*0.138*	*0.037*	*1*
	L1	*0.13727*	*0.333*	-	*0.003*	*0.047*	*0.438*	-	*0.025*	-	*0.077*	*0.031*	*1*
	L2	*0.17160*	*0.339*	-	*0.002*	*0.032*	*0.398*	-	*0.024*	-	*0.041*	*0.024*	*1*
	L3	*0.19228*	*0.367*	-	*0.003*	*0.045*	*0.438*	-	*0.026*	-	*0.018*	*0.016*	*1*
	Treamtent	Chl c3	Chl c2	Peridinina	Feoforb a	19'BF	19'HF	Violaxantina	Diadinoxantina	Simil Alloxantin	Diatoxantina	ßcarotene	Chl a
Prorocentrum	HL	-	*0.203*	*1.049*	-	-	-	*0.016*	*0.374*	*0.009*	*0.044*	*0.025*	*1*
	L1	-	*0.213*	*1.140*	-	-	-	*0.017*	*0.394*	*0.010*	*0.035*	*0.028*	*1*
	L2	-	*0.220*	*1.120*	-	-	-	*0.020*	*0.360*	*0.006*	*0.022*	*0.027*	*1*
	L3	-	*0.215*	*1.037*	-	-	-	*0.022*	*0.282*	*0.000*	*0.011*	*0.025*	*1*

Table II - Pigments:chl a ratio in *Prorocentrum* sp. and *Phaeocystis antarctica* at time 12 under different light irradiances.

Results from High-Light, Low-Light experiment clearly show differences between *P. antarctica* and *Prorocentrum* sp. at time 12 in terms of molecules involved in the photo-protection. As regard the percentage ratio of photoprotective pigments, expressed as DT/(DD+DT) *100 (Table III), at time 12 values in *Prorocentum sp*. were 10.87 (HL), 8.31 (L1), 5.75 (L2) and (3.68) L3, while in *P. antarctica* were 84 (HL), 75.7 (L1), 61.90 (L2) and 41.8 (L3).

Day	Treatment	*P. antarctica*	*Prorocentrum* sp.
0	**Start**	65.03	0.00
2	**HL**	71.84	6.06
	L1	70.96	6.85
	L2	70.96	4.21
	L3	64.86	0.00
12	**HL**	84.02	10.82
	L1	75.76	8.31
	L2	61.94	5.75
	L3	41.82	3.68

Table III - Changes in % DT/(DD+DT) for amended treatments over time for ***Experiment 2 – High Light-Low Light***. Incubation light (µmol phtons m^{-2} s^{-1}): HL = 110, L1 = 60, L2 = 36, L3 =19.

As regards the ratio DT:chl a, in *P. antarctica* it ranged from 0.14 (HL) to 0.01 (L3) while in *Prorocentrum* sp. values ranged from a maximum of 0.04 (L1) to 0.01 (L3) displaying less variability. Beyond that, *Prorocentrum* sp. exhibits increasing (although weak) values of the ratio simil-Violaxanthin:chl a at high light irradiance, reaching a maximum of 0.011 in L1, while undetectable quantities of the pigment have been observed at L3.

DISCUSSION AND CONCLUSIONS

The Ross Sea is one of the most studied areas of Antarctica. Geographical factors and related logistic constraints have largely contributed to shape the history and sectorial development of Antarctic research. Since the onset of organized scientific projects, ecology of this area has been approached under the influence of interests mainly focused on understanding of the trophic structure and dynamics of food webs. As a consequence, phytoplankton has occupied, and still does, the centre of Antarctic waters ecology. A rich literature has been produced and some paradigms have emerged, such as the mentioned classical food web articulation. Meanwhile, important information is being made available for improving and strengthening our knowledge on the dynamics of phytoplankton communities, particularly regarding the influence of the different typologies of the coast and of the contributions of adjoining ice systems.

The information gathered during this thesis has confirmed some fundamental points on which is based the present paradigm on the role of the primary component in structuring the Antarctic food web. At same time, new ecological evidence emerges from the research performed *in situ* (see attached papers in appendix: Mangoni *et al*., 2019; Rivaro *et al*., 2019; Mangoni *et al*., 2017) and on phytoplankton species isolated and cultured in laboratory under manipulative conditions.

In particular, the qualitative and quantitative ranges and timing of phytoplankton communities have been further defined, with respect to its structural and functional composition: temporal and spatial dynamics of total biomass, its functional groups and photosynthetic efficiency. This representation is valid for the different environmental contexts considered: the two Ross Sea polynyas, coastal areas, and coastal waters of Marie Byrd Land, and confirms the role of micronutrients in driving the processes of primary production, in accordance to the interpretative approach of the recent literature.

The phytoplankton community structures have been investigated through a chemotaxonomic approach, using diagnostic pigment as markers of functional groups, and appeared to be mainly dominated by diatoms in the Ross Sea while, over a much larger spatial scale and for coastal waters of Marie Byrd Land, it was dominated by *P. antarctica.* In this latter case, the massive freshwater input in coastal water of Marie Byrd Land, especially near Saunders Coast, fueled phytoplankton blooms that reached concentrations more than 45µg/L. On the contrary, strong spatial and temporal variability have emerged comparing the results of different sub-system analyzed in the Ross Sea. Areas 1 and 2 were strongly dominated by diatoms, and the clear coupling between water column characteristics and the chlorophyll a distribution in Area 1 was not observed in Area 2. This suggested different dynamics acting in the polynya of Terra Nova Bay (Area 1), where the mean

integrated value of chl a concentration reached127 mg chl a m^2, compared to the coastal system of the Area 2 where the mean integrated value of chl a concentration was only 74 mg chl a m^2.

The big polynya of the Ross Sea (Area 3a, b) which is considered dominated by *P. antarctica* especially during spring in presence of a deeper mixed layer, exhibited high concentrations of biomass during summer and higher percentage of diatoms in presence of deeper UML. Furthermore, rapid changes observed after 2 days in the water column properties in this area, highlight the high temporal variability in such an open system. The mean value of concentration of integrated chl a reached 104 mg chl a m^2 in Area 3a, and in 132 mg chl a m^2 in Area 3b, contradicting the HNLC nature reported for this area during the summer (e.g. Saggiomo *et al.*, 2002; Mangoni *et al.*, 2004; Arrigo *et al.*, 1998). Moreover, all these aspects echo studies conducted by Mangoni *et al.* (2017, 2019) on the distribution of biomass and main functional groups in the Ross Sea in relation to the stratification of the water column.

However, in the northern area (Area 4) of the Ross Sea, higher percentages of dinoflagellates have been found in association with lowest mean integrated values of biomass reported in the cruise (39 mg chl a m^2), and in some station they exceeded 40% of the biomass. Dinoflagellates of the Ross Sea have been considered by many authors in both spring and summer and including mixotrophic forms (Gast *et al*., 2018), but information on dinoflagellates in this area is limited as they are considered to have a minor impact on the Antarctic food web and biogeochemistry (Phan-Tan *et al.*, 2018, Stoecker *et al*. 1995; DiTullio and Smith, 1996). In addition, a bloom of loricate choanoflagellates was recorded in the same period (summer 2017) in the Ross Sea polynya, representing the 42–55% of the total plankton community (see the attached paper in appendix: Escalera *et al.*, 2019). These composition aspects of the community, could shed light on the role of the planktonic mixotrophic and heterotrophic compartment in the Antarctic food web, also in relation with changes recently reported within phytoplankton communities in the Ross Sea (Mangoni *et al.*, 2019; Kaufman *et al.*, 2017). An important information derived from the culture of *P. antarctica* kept in starving conditions for micronutrients was suggested by a marked change in color of the cultures which turned to a light brown color. A subsequent chemotaxonomic analyses revealed the presence of a dinoflagellate strictly associated with colonial *Phaeocystis antarctica* on the base of the high concentration of peridinin in the pigmentary spectra. By means of cultures kept in stressing conditions, the dinoflagellate species was isolated and utilized to form monospecific cultures, which have provided the material for further molecular analyses that confirmed the character of a not yet identified species of *Prorocentrum.* Moreover, the pigment marker of *Prorocentrum*, in addition with the high concentrations of peridinin, was also accompanied by a distinct peak of a secondary pigment associated to diadinoxanthin. Further

investigation will allow to evaluate if this pigmentary characteristic represents a further identification tool of the species.

Thus, considering the high percentage of dinoflagellates found in Area 4, particular attention was payed to the experiment on the relationship between *Prorocentrum* sp. and *P. antarctica* in both mixed and monospecific cultures. Results from ANEMIA experiment suggest a different effect of vitamin B_{12} and iron limitation on *P. antarctica* and *Prorocentrum*. As regard *Prorocentrum* sp., the lowest Fv/Fm observed at time 12 in absence of vitamin B_{12}, together with the highest value of σ_{PSII} and Chl *a* concentration, suggest that the species most probably requires exogenous source of B_{12}, as already documented for other species of dinoflagellates (Cruz-Lòpez and Maske H., 2016; Tang et al., 2010). On the other hand, the lowest Fv/Fm observed in *Phaeocystis antarctica* in presence of iron limitation, along with strong differences in terms of Chl *a* between treatments, shows that this species is more sensible to iron limitation. A relevant point to consider is that *P. antarctica* has been reported to have a lower iron limitation threshold than some diatoms species (*Chaetocheros* sp.) of the Ross Sea and, at increased iron nutrition (> 120 pM Fe) a shift toward a prevalence of the colonial form was observed implying a role for iron as a trigger for colony formation (Bender *et al.*, 2018).

The role of vitamin B_{12} in these processes has been published by Nef *et al.*, (2019). The analyses of results derived from the mixed culture through the interpolation of Fv/Fm, σPSII, and chl a values with the peridinin:Hex ratio, clearly shown that *Prorocentrum* sp. takes over *P. antarctica* in presence of iron limitation. Data from High Light-Low Light experiment furthermore demonstrated that the two species respond differently to changes in irradiance intensity. While *P. antarctrica* seems able to regulate the functional optical cross-section of PSII in relation to different level of irradiances, maintaining higher (and similar) Fv/Fm values at different light intensity, *Prorocentrum* sp. showed a completely different response, displaying low capabilities to efficiently photosynthesize at high irradiance. This data is also supported by the presence of a simil-Violaxanthin pigment found in *Prorocentrum* sp. under high irradiance. Haptophytes and dinoflagellates, in fact, belongs to a group of species that present a secondary pigment involved in the xanthophyll cycle characterized by the Viola cycle under prolonged high light stress (Lohr and Wilhem, 2001).

Many studies have demonstrated the capability of *P. antarctica* to growth well at low irradiance, and the dominance of this species in presence of a deep mixed layer or weak stratification has in part been correlated with its photosynthetic ability (Arrigo et al., 1999; Moisan and Mitchell, 1999; Kropuenske et al., 2009; Smith et al., 2014) . The photosynthetic activity at low irradiance however requires higher dFe availability (Sedwich et al., 2006) and the high sinking

rate of mucilaginous *P. antarctica* colonies, together with the poorly digestible mucus and low grazing pressure, allow an intense export of carbon to the bottom of the ocean.

Since the data reported in the present study have been collected in environments characterized by low dFe concentration and weak stratification, and since *Prorocentrum sp.* has been isolated from mucilage colonies of *P. antarctica,* considering the tendency of dinoflagellates to feed on external organic sources we are inclined to consider that our results opens new perspectives in approaching the study of the phytoplankton communities of the Ross Sea, particularly at the light of the current climate changes.

Concluding remark

In addition to the results presented in the Discussion section, some aspects of more general importance have emerged by our activity in Antarctica, which deserve to be remarked.

The Ross Sea phytoplankton communities have so far being considered as driven by the seasonal dynamics of the polynya, producing the picture of what is considered as the classical Antarctic food web.

In fact, in addition to polynya sub-areas, others sub-systems are present, which drive alternative pathways for the primary production mechanisms, such as those originated by continental ice run-off contributing to the micronutrient compartment.

This rises the still recurrent problem of adapting sampling to spatial scales insufficient to reveal the real features of the system. Our results show a richer picture of production mechanisms, thanks to adequate scales covering the coupling between water and the different coastal features or with the open waters of the Southern Ocean.

The association of a newly identified dinoflagellate with *Phaeocystis antarctica* points to the necessity of looking to the dinoflagellate component of phytoplankton communities as a significant contributor of heterotrophic pathways to autotrophic primary production processes.

Acknowledgments

First and foremost, I would like to thank my family - especially my parents and sisters - to whom I dedicate this incredible achievement. This was neither foreseeable nor expected and I am honoured and grateful to be able to realize this dream.

I am particularly thankful to my tutor, Prof. Olga Mangoni, for her encouragement, teaching and for having believed in me. She has helped me to cultivate the opportunity to navigate and grow professionally in the world of marine ecology.

My sincerest gratitude I extend to Prof. Gian Carlo Carrada, for many lessons learned, his great humanity and patience. He has taught me to look at the world through the eyes of an ecologist.

I would like to express my deep and special thanks to Jack (Giacomo) DiTullio, with whom I crossed the earth pole-to-pole in six months. I admire and appreciate his kindness, wisdom, and great sincerity.

I would like to express my earnest and heartfelt gratitude to Anna, for every moment spent together, for her devotion and affection - even when separated by thousands of miles or spending innumerable hours in the laboratory and realizing this great accolade.

Furthermore, I would like to highlight my earnest appreciation of those who shared intimate and important moments with me: my childhood friends; my wonderful band-mates, Donnaluna; to everyone that has taught me something and has helped me to reach this point.

To the students at the laboratory who over the years have contributed to this thesis, I want to recognize you and reiterate my thanks for making this possible.

To Maria Saggiomo, my co-tutor, and the whole SZN research team; Prof. Enzo Saggiomo; Augusto Passarelli, for his teachings, his intuition and his sensitivity, and; Francesca Margiotta, who first taught me laboratory techniques. Thank you all very much for all of your help.

To anyone whom I have unintentionally not mentioned, whom are happy to share this incredible moment with me - my sincerest thanks to you all.

Last, but not the least, I would like to thank Mr. Lord Mundy for his contribution to the translation of this page, at midnight.

REFERENCES

Alderkamp A.-C., Kulk G., Buma A.G.J., Visser R.J.W., Van Dijken G.L., Mills M.M. & Arrigo K.R. (2012). The effect of iron limitation on the photophysiology of *Phaeocystis Antarctica* (Prymnesiophyceae) and *Fragilariopsis cylindrus* (Bacillariophyceae) under dynamic irradiance. Journal of Phycology, 48(1): 45.

Arrigo K R. and McClain C.R. (1994). Spring phytoplankton production in the western Ross Sea. Science, 266: 261–63.

Arrigo K.R., Worthen D.L., Schnell A., Lizotte M.P. (1998). Primary production in Southern Ocean waters. Journal of Geophysical Research, 103 (15): 587-600.

Arrigo K.R., Robinson D.H., Worthen D.L., Dunbar R.B., DiTullio G.R., van Woert M., Lizotte M.P. (1999). Phytoplankton community structure and the drawdown of nutrients and CO_2 in the Southern Ocean. Science, 283: 365–367.

Arrigo K.R., DiTullio G.R., Dunbar R.B., Robinson D.H., vanWoert M., Worthen D.L, Lizotte M.P. (2000). Phytoplankton taxonomic variability in nutrient utilization and primary production in the Ross Sea. Journal of Geophysical Research, 105: 8827–8846.

Arrigo K.R. and van Dijken G.L. (2004). Annual cycles of sea ice and phytoplankton near Cape Bathurst, south-eastern Beaufort Sea, Canadian Arctic. Geophysical Research Letters 31, L08304.

Arrigo K.R., van Dijken G.L, Bushinsky S. (2008a). Primary production in the Southern Ocean, 1997–2006. Journal of Geophysical Research, 113: C08004.

Arrigo KR, van Dijken GL, Long M. 2008b. Coastal Southern Ocean: a strong anthropogenic CO_2 sink. Geophysical Research Letters, 35: L21602.

Arrigo K.R., Mills M.M., Kropuenske L.R., Van Dijken G.L., Alderkamp A.-C. and Robinson D.H. (2010). Photophysiology in two major Southern Ocean taxa: photosynthesis and growth of *Phaeocystis antarctica* and *Fragilariopsis cylindrus* under different irradiance levels. Integr. Compar. Biol. 50: 950– 66.

Bates N.R., Hansell D.A., Carlson C.A. and Gordon L.I. (1998), Distribution of CO_2 species, estimates of net community production, and air-sea CO_2 exchange in the Ross Sea polynya, J. Geophys. Res., 10 3(C2): 2883– 2896.

Bender S.J., Moran D.M., McIlvin M.R., Zheng H., McCrow J.P., Badger J., DiTullio G.R., Allen A.E, Saito, M.A. (2018). Colony formation in *Phaeocystis antarctica*: connecting molecular mechanisms with iron biogeochemistry. Biogeosciences, 15: 4923-4942.

Bertrand E.M., Saito M.A., Rose J.M., Riesselman C.R., Lohan M.C., Noble A.E., Lee P.A., DiTullio G.R. (2007). Vitamin B_{12} and iron co-limitation of phytoplankton growth in the Ross Sea. Limnology and Oceanography, 52: 1079-1093.

Bertrand E.M., Saito M.A., Lee P.A., Dunbar R.B., Sedwick P.N., DiTullio G.R. (2011). Iron limitation of a springtime bacterial and phytoplankton community in the Ross Sea: Implications for Vitamin B_{12} nutrition. Frontiers in Microbiology, 2: 1–12.

Bertrand E.M., Saito M.A., Jeon Y.J., Neilan B.A. (2011b) Vitamin B12 biosynthesis gene diversity in the Ross Sea: The identification of a new group of putative polar B12 biosynthesizers. Environ Microbiol., 13(5):1285–1298.

Bertrand E.M., Allen A.E., Dupont C.L., Norden-Krichmar T.M., Bai J., Valas R.E, Saito M.A. (2012). Cobalamin acquisition protein from diatoms- Proceedings of the National Academy of Sciences, 109 (26) E1762-E1771.

Bertrand E.M., McCrow J.P., Moustafa A., Zheng H., McQuaid J.B., Delmont T.O., Post A.F., Sipler R.E., Spackeen J.L., Xu K., Bronk D.A., Hutchins D.A., Allen A.E. (2015). Interactive colimitation at the sea ice edge. Proceedings of the National Academy of Sciences, 112 (32) 9938-9943.

Boyd P.W., LaRoche J., Gall M., Frew R., and McKay R.M. (1999). Role of iron, light, and silicate in controlling algal biomass in subantarctic waters SE of New Zealand, J. Geophy. Res., 104, 13,391–13,404.

Boyd P.W., Watson A.J., Law C.S., Abraham E.R., Trull T., Murdoch R., Bakker D.C., Bowie A.R., Buesseler K.O., Chang H., Charette M., Croot P., Downing K., Frew R., Gall M., Hadfield M., Hall J., Harvey M., Jameson G., LaRoche J., Liddicoat M., Ling R., Maldonado M.T., McKay R.M., Nodder S., Pickmere S., Pridmore R., Rintoul S., Safi K., Sutton P., Strzepek R., Tanneberger K., Turner S., Waite A., Zeldis J. (2000). A mesoscale phytoplankton bloom in the polar Southern Ocean stimulated by iron fertilisation of waters. Nature, 407: 695–702.

Boyd P.W. (2002). Environmental factors controlling phytoplankton processes in the Southern Ocean. J. Phycol., 38: 844–61.

Doyle J.J. and Doyle J.L. (1990). Isolation of plant DNA from fresh tissue. Focus, 12: 13-15.

Bracegirdle T.J., Connolley W.M., Turner J. (2008). Antarctic climate change over the twenty first century. J. Geophys. Res., 113:D03103.

Brunet C. and Mangoni O. (2010). Determinazione quali-quantitativa dei pigmenti fitoplanctonici mediante HPLC, [in:] Metodologie di studio del Plancton marino, G. Socal, I. Buttino, M. Cabrini, O. Mangoni, A. Penna, C. Totti, (eds), ISPRA: 56, 379-385.

Brunet C., Johnsen G., Lavaud J., and Roy S. (2011). Pigments and photoacclimation processes. In: Roy S., Llewellyn C., Egeland E., and Johnsen G. (Eds.), *Phytoplankton Pigments: Characterization, Chemotaxonomy and Applications in Oceanography* (Cambridge Environmental Chemistry Series, pp. 445-471). Cambridge: Cambridge University Press. doi:10.1017/CBO9780511732263.017.

Budillon G., Castagno P., Aliani S., Spezie G., Padman L. (2011). Thermohaline variability and Antarctic bottom water formation at the Ross Sea shelf break. Deep-Sea Research Part I, 1002–1018.

Caron D.A., Dennett M.R., Lonsdale D.J., Moran D.M, Shalapyonok L. (2000). Micro-zooplankton herbivory in Microzooplankton herbivory in the Ross Sea, Antarctica. Deep-Sea Res II, 47: 3249–3272.

Carrada G.C., Mangoni O., Russo G.F., Saggiomo V. (2000). Phytoplankton size-fractionated biomasses in the Ross Sea. Spatial and temporal evolution during the austral spring. [in:] Ross Sea Ecology, Italian Antarctic expeditions (1987-1995). F.M. Faranda, L. Guglielmo, A. Ianora, (eds), Springer Berlin: 205-216.

Caron D.A., Dennett M.R., Lonsdale D.J., Moran D.M., Shalapyonok L. (2000). Micro-zooplankton herbivory in the Ross Sea, Antarctica. Deep-Sea Res. II, 47: 3249–72.

Comiso J.C., Kwok R., Martin S. and Gordon A.L. (2011). Variability and trends in sea ice extent and ice production in the Ross Sea. Journal of Geophysical Research. 116: C4.

Constable A.J., Melbourne-Thomas J., Corney S.P., Arrigo K.R., Barbraud C., Barnes D.K., Bindoff N.L., Boyd P.W., Brandt A., Costa D.P., Davidson A.T., Ducklow H.W., Emmerson L., Fukuchi

M., Gutt J., Hindell M.A., Hofmann E.E., Hosie G.W., Iida T., Jacob S., Johnston N.M., Kawaguchi S., Kokubun N., Koubbi P., Lea M.A., Makhado A., Massom R.A., Meiners K., Meredith M.P., Murphy E.J., Nicol S., Reid K., Richerson K., Riddle M.J., Rintoul S.R., Smith W.O. Jr, Southwell C., Stark J.S., Sumner M., Swadling K.M., Takahashi K.T., Trathan P.N., Welsford D.C., Weimerskirch H., Westwood K.J., Wienecke B.C., Wolf-Gladrow D., Wright S.W., Xavier J.C., Ziegler P. (2014). Climate change and Southern Ocean ecosystems I: how changes in physical habitats directly affect marine biota. Global Change Biology, 20: 3004-3025.

Croft M.T., Lawrence A.D., Raux-Deery E., Warren M.J., Smith A.G. (2005). Algae acquire vitamin B_{12} through a symbiotic relationship with bacteria. Nature, 438: 90–93.

Cruz-López R. and Maske H. (2016). The Vitamin B1 and B12 required by the marine dinoflagellate *Lingulodinium polyedrum* can be provided by its associated bacterial community in culture. Frontiers in Microbiology, 10.3389/fmicb.2016.00560, 7, (2016).

Cullen J. and Davis R.F. (2003). The Blank Can Make A big Difference In oceanographic measurements. Limnology and Oceanography Bulletin, 12 (2). doi.org/10.1002/lob.200312229

Delmont T.O., Hammar K.M., Ducklow H.W. et al. (2014). *Phaeocystis antarctica* blooms strongly influence bacterial community structures in the Amundsen Sea polynya. Front Microbiol., 5: 1–13.

Demers S., Roy S., Gagnon R., Vignault C. (1991). Rapid light-induced changes in cell fluorescence and in xanthophyll-cycle pigments of *Alexandrium excavatum* (Dinophyceae) and *Thalassiosira pseudonana* (Bacillariophyceae)—a photoprotection. Mar. Ecol. Prog. Ser., 76: 185–193.

Dennett M.R., Mathot S., Caron D.A., Smith W.O. Jr, Lonsdale D. (2001). Abundance and distribution of phototrophic and heterotrophic nano- and microplankton in the southern Ross Sea. Deep-Sea Res. II, 48: 4019–38.

Diffey B.L. (1991). Solar ultraviolet radiation effects on biological systems.Phys. Med. B, 36: 299–328.

DiTullio G.R. and Smith W.O. Jr (1996). Spatial patterns in phytoplankton biomass and pigment distributions in the Ross Sea. Journal of Geophysical Research, 101: 18467–18477.

DiTullio G.R., Grebmeier J., Arrigo K.R., Lizotte M.P., Robinson D.H., et al. (2000). Rapid and early export of Phaeocystis antarctica blooms in the Ross Sea, Antarctica. Nature, 404: 595–98.

DiTullio G.R., Grebmeier J., Arrigo K.R., Lizotte M.P., Robinson D.H., Leventer A., Barry J.P, VanWoert M.L. and Dunbar R.B. (2000). Rapid and early export of *Phaeocystis antarctica* blooms in the Ross Sea, Antarctica. Nature, 404: 595-598.

Ducklow H.W., Carlson C.A., Church M., Kirchman D.L., Smith D. and Steward G. (2001). The seasonal development of the bacterioplankton bloom in the Ross Sea, Antarctica, 1994–1997. Deep Sea Res. II, 48: 4199–4221.

Dunbar, R.B., Arrigo, K.R., DiTullio, G.R., Leventer, A., Lizotte, M.P., Van Woert, M.L., Robinson, D.H., 2003. Non-Redfield production and export of marine organic matter: a recurrent part of the annual cycle in the Ross Sea, Antarctica. In: DiTullio, G.R., Dunbar, R.B. (Ed.), Biogeochemistry of the Ross Sea. Ant Res Ser, 78. American Geophysical Union, Washington, DC 79–196.

El-Sayed SZ, Biggs DC, Holm-Hansen O. (1983). Phytoplankton standing crop, primary productivity, and near-surface nitrogenous nutrient fields in the Ross Sea, Antarctica. Deep-Sea Res. 30:871–80

EI-Sayed S.Z. (1987) Biological productivity of Antarctic waters: present paradoxes and emerging paradigms. In: El-Sayed SZ, Tomo AP (eds) Antarctic aquatic biology BIOMASS Sci Ser SCAR, Cambridge, pp 1–21.

Elliott DT, Tang KW, Shields AR. 2009. Mesozooplankton beneath the summer sea ice in McMurdo Sound, Antarctica: abundance, species composition, and DMSP content. Polar Biol. 32:113–22.

Escalera L., Mangoni O., Bolinesi F., Saggiomo M. (2019). Austral Summer Bloom of Loricate Choanoflagellates in the Central Ross Sea Polynya. Journal of Eukaryotic Microbiology. https://doi.org/10.1111/jeu.12720.

Fabiano M and Pusceddu A. (1998). Total and hydrolizable particulate organic matter (carbohydrates, proteins and lipids) at a coastal station in Terra Nova Bay (Ross Sea, Antarctica). Polar Biology.,19:125-132

Falkowski P.G. and Raven J.A. (2007). Aquatic Photosynthesis. Princeton University Press, p. 512

Ferreyra G.A., Schloss I., Demers S., Neale P.J. (1994). Phytoplankton responses to natural ultraviolet irradiance during early spring in the Weddell-Scotia Confluence: An experimental approach. Antarctic Journal United States, 29: 268–270.

Garcia N.S, Sedwick P.N., DiTullio G.R. (2009). Influence of irradiance and iron on the growth of colonial *Phaeocystis antarctica*: implications for seasonal bloom dynamics in the Ross Sea, Antarctica. Aquatic Microbial Ecology, 57: 203–220.

Gast R.J, Scott F.A. and Sanders W.R. (2018) Mixotrophic Activity and Diversity of Antarctic Marine Protists In Austral Summer et al., Front. Mar. Sci., 02 February 2018 doi.org/10.3389/fmars.2018.00013

Geibert W., Assmy P., Bakker D.C.E., Hanfland C., Hoppema M., Pichevin L.E., Schröder M., Schwarz J.N., Stimac I., Usbeck R. and Webb A. (2010). High productivity in an ice melting hot spot at the eastern boundary of the Weddell Gyre, Global Biogeochemical Cycles, 24 (3). GB3007, 01.09.2010.

Geider R.J. and Roche J. (1994). The role of iron in phytoplankton photosynthesis, and the potential for iron limitation of primary productivity in the sea. Photosynthesis Research, 39: 275-301.

Gerringa L.J.A., Alderkamp A.C., Laan P., Thuróczy C.-E., De Baar H.J.W., Mills M.M., van Dijken G.L., van Haren H., Arrigo K.R. (2012). Iron from melting glaciers fuels the phytoplankton blooms in Amundsen Sea (Southern Ocean): Iron biogeochemistry. Deep-Sea Research Part-II, 71(76): 16-31.

Garrison DL, Jeffries MO, Gibson A, Coale SL, Neenan D,Fritsen C, Okolodkov YB, Gowing MM (2003) Development of sea ice microbial communities during autumn iceformation in the Ross Sea. Mar Ecol Prog Ser 259:1–15

Gibson JAE, Garrick RC. Burton HR, McTaggart AR (1990) Dimethylsulfide and the alga Phaeocystis poucheti in Antarctic coastal waters. Mar Biol 104:339-346

Guillard R.R.L. (1995). Culture methods. In: Hallegraeff G.M., Anderson D.M. and Cembella A.D. [Eds.] Manual on Harmful Marine Microalgae. IOC Manual and guides No. 33, UNESCO, New York, pp. 45– 62.

Häder D.P., Helbling E.W., Williamson C.E., Worrest R.C. Effects of UV radiation on aquatic ecosystems and interactions with climate change. Photochem. Photobiol. Sci. (2011);10:242–260. doi: 10.1039/c0pp90036b

Hatta M., Measures C.I., Lam P.J., Ohnemus D.C., Auro M.E., Grand M.M., et al., (2017). The relative roles of modified circumpolar deep water and benthic sources in supplying iron to the recurrent phytoplankton blooms above Pennell and Mawson Banks, Ross Sea, Antarctica. Journal of Marine Systems, 166: 61-72.

Haberman L.K., Quetin B.L., Ross M.R. (2003). Diet of the Antarctic krill (*Euphausia superba* Dana): I. Comparisons of grazing on *Phaeocystis Antarctica* (Karsten) and *Thalassiosira antarctica* (Comber). Journal of Experimental Marine Biology and Ecology, 283 (1-1): 79-95.

Holm-Hansen O., Lorenzen C.J., Holmes R.W., Strickland J.D.H. (1965). Fluorometric determination of chlorophyll, Journal du Conseil/Conseil Permanent International pour l'Exploration de la Mer, 30: 3-15.

Hales T. and Takahashi, T. (2004). High-resolution biogeochemical investigation of the Ross Sea, Antarctica, during the AESOPS (U. S. JGOFS) Program global biogeochemical cycles, vol. 18, GB3006. https://doi.org/10.1029/2003GB002165.

Jacobs S. (2004). Bottom water production and its links with the thermohaline circulation. Antarctic Science, 16: 427–437.

Karentz D., Cleaver J.E., Mitchell D.L. (1991). Cell survival characteristics and molecular responses of Antarcticphytoplankton to Ultraviolet-B radiation. J. Phycol., 27: 326–341.

Koch F., Marcoval M.A., Caterina Panzeca C., Bruland K.W., Sañudo-Wilhelmy S.A., Gobler C.J. (2011). The effect of vitamin B12on phytoplankton growth and community structure in the Gulf of Alaska Florian. Limnol. Oceanogr., 56(3): 1023–1034.

Kohut J.T., Kustka A.B., Hiscock M., Lam P.J., Measures C., Milligan A., et al. (2017). Mesoscale variability of the summer bloom over the northern Ross Sea shelf: A tale of two banks. Journal of Marine Systems, 166: 50-60.

Kropuenske L.R., Mills M.M., van Dijken G.L., Bailey S., Robinson D.H., et al. (2009). Photophysiology in two major Southern Ocean phytoplankton taxa: photoprotection in Phaeocystis antarctica and Fragilariopsis cylindrus. Limnol. Oceanogr. 54:1176–96

Levasseur M., Gosselin M., Michaus S. A new source of Dimethylsulfide (DMS) for the arctic atmosphere: ice diatoms (1994). Marine Biology 121:381-387

Lee P.A., Bertrand E.M., Saito M.A., DiTullio G.R. (2007). Influence of vitamin B12 availability on oceanic dimethylsulfide and dimethylsulfoniopropionate. Environmental Chemistry, doi: 10.1071/EN15043.

Lonsdale D. J., Caron D.A., Dennett M.R., Schaffner R. (2000). Predation by Oithona spp. on protozooplankton in the Ross Sea, Antarctica. Deep Sea Research Part II - Topical Studies in Oceanography, 47(15): 3273-3283.

Lohr, M., Wilhelm, C. (2001) Xanthophyll synthesis in diatoms: quantification of putative intermediates and comparison of pigment conversion kinetics with rate constants derived from a model. Planta 212: 382-391.

Mackey M.D., Mackey D.J., Higgins H.W., Wright S.W. (1996). CHEMTAX-a program for estimating class abundances from chemical markers: application to HPLC measurements of phytoplankton. Marine Ecology Progress Series, 144: 265-283.

Mangoni O., Modigh M., Conversano F., Carrada G.C., Saggiomo V. (2004). Effects of summer ice coverage on phytoplankton assemblages in the Ross Sea, Antarctica. Deep-Sea Research Part I, 51(11): 1601-1617.

Mangoni O., Saggiomo M., Modigh M., Catalano G., Zingone A. and Saggiomo V. (2009). The role of platelet ice microalgae in seeding phytoplankton blooms in Terra Nova Bay (Ross Sea, Antarctica): a mesocosm experiment. Polar Biology, 3 (32): 311-323.

Mangoni O., Saggiomo V., Bolinesi F., Margiotta F., Budillon G., Cotroneo Y., Misic C., Paola Rivaro P., Saggiomo M. (2017). Phytoplankton blooms during austral summer in the Ross Sea, Antarctica: driving factors and trophic implications. PLoS ONE,10.1371/journal.pone.0176033.

Mangoni O., Saggiomo M., Bolinesi F., Castellano M., Povero P., Saggiomo V., DiTullio G.R. (2019) *Phaeocystis antarctica* unusual summer bloom in stratified Antarctic coastal waters (Terra Nova Bay, Ross Sea). Marine Environmental Research, 151. 104733.

Marchant H.J., Davidson A.T., Kelly G.J. (1991). UV-B protecting compounds in the marine alga *Phaeocystis pouchetii* from Antarctica. Mar. Biol. 109: 391–395.

Marinov I., Gnanadesikan A., Toggweiler, J.R., Sarmiento J. (2006). The Southern Ocean biogeochemical divide. Nature, 441: 964-7.

Martin J.H., Gordon R.M., Fitzwater S.E. (1990). Iron deficiency limits phytoplankton growth in Antarctic waters. Global Biogeochemical Cycles, 4(1): 5-12.

Mathot S-, Smith W.O. Jr, Carlson C.A., Garrison D.L. (2000). Estimate of *Phaeocystis* sp. carbon biomass: methodological problems related to the mucilaginous nature of the colonial matrix. J. Phycol. 36:1049–56

Mauzerall D., Greenbaum N.L. (1989). The absolute size of a photosynthetic unit. Biochim Biophys Acta, 974: 119-14.

Maxwell K., Johnson G.N. (2000) Chlorophyll fluorescence – a practical guide. Journal of Experimental Botany, 51: 659–668

Meyer A.A., Tackx M., Daro N. (2000) Xanthophyll cycling in *Phaeocystis globosa* and *Thalassiosira* sp.: a possible mechanism for species succession Journal of Sea Research 43 373–384.

Mills M.M., Kropuenske L. R., van Dijken G.L., Alderkamp A.-C., Berg G.M. (2010). Photophysiology in two southern ocean phytoplankton taxa:photosynthesis ofphaeocystis antarctica(prymnesiophyceae) andfragilariopsis cylindrus(bacillariophyceae) under simulated mixed-layer irradiance. J. Phycol., 46: 1114–1127

Misic C., Covazzi Harriague A., Mangoni O., Cotroneo Y., Aulicino G., Castagno P. (2017). Different responses of the trophic features of particulate organic matter to summer constraints in the Ross Sea. Journal of Marine Systems, 166: 132-143.

Moisan, T., and B. Mitchell (1999), Photophysiological acclimation of Phaeocystis antarctica Karsten under light limitation, Limnology and Oceanography, pp.247-258.

Montes-Hugo M., Doney S.C., Ducklow H.W., Fraser W., Martinson D., et al. (2009). Recent changes in phytoplankton communities associated with rapid regional climate change along the Western Antarctic Peninsula. Science, 323:1470–73

Moore C.M., Mills M.M., Arrigo K.R., Berman-Frank I., Bopp L., Boyd P.W., Galbraith E.D., Geider R.J., Guieu C., Jaccard S.L., Jickells T.D., La Roche J., Lenton T.M., Mahowald N.M., Marañón E., Marinov I., Moore J.K., Nakatsuka T., Oschlies A., M.A. Saito, Thingstad T.F., Tsuda A. and Ulloa O. (2013). Processes and patterns of oceanic nutrient limitation. Nature Geoscience, 6: 701-710.

Neale PJ, Sobrino C, Gargett AE. (2012). Vertical mixing and the effects of solar radiation on photosystem II electron transport by phytoplankton in the Ross Sea polynya. Deep-Sea Res. II 63:118–32.

Nef C., Jung S., Mairet F., Kaas R., Dominique Grizeau D. and Garnier M. (2019). How haptophytes microalgae mitigate vitamin B12 limitation. Sci Rep., 9, 8417.

Orsi A.H., Wiederwohl C.L. (2009). A recount of Ross Sea waters. Deep-Sea Res. II 56:778–95.

Phan-Tan L., Nguyen-Ngoc L., Smith W. and Doan H. (2018). A new dinoflagellate species, *Protoperidinium smithii* H. Doan-Nhu, L. Phan-Tan et L. Nguyen-Ngoc sp. nov., and an emended description of *Protoperidinium defectum* (Balech 1965) Balech 1974 from the Ross Sea, Antarctica. Polar Biology, 41:983–992.

Parkhill J.P., Maillet G., and Cullen J.J. (2001). Fluorescence-based maximal quantum yield for PSII as a diagnostic of nutrient stress. Journal of Phycology, 17: 517–529.

Peloquin J.A. and Smith W.O. Jr (2007). Phytoplankton blooms in the Ross Sea, Antarctica: interannual variability in magnitude, temporal patterns, and composition. Journal of Geophysical Research, 112: C08013.

Rivaro P., Ianni C., Langone L., Ori C., Aulicino G., Cotroneo Y., Saggiomo M., Mangoni O. (2017). Physical and biological forcing on the mesoscale variability of the carbonate system in the Ross Sea (Antarctica) during the summer season 2014. Journal of Marine Systems, 166: 144-158.

Rivaro P., Ardini F., Grotti M., Aulicino G., Cotroneo Y., Fusco G., Mangoni O., Bolinesi F., Saggiomo M., Celussi M. (2018). Mesoscale variability related to iron speciation in a coastal Ross Sea area (Antarctica) during summer 2014. Chemstry and Ecology, 35 (1-2): 1-19.

Saggiomo V., Carrada G.C., Mangoni O., Ribera d'Alcalà M., Russo A. (1998). Spatial and temporal variability of size-fractionated biomass and primary production in the Ross Sea (Antarctica) during austral spring and summer. Journal of Marine Systems, 17:115-127.

Saggiomo V., Carrada G.C., Mangoni O., Marino D., Ribera d'Alcalà M. (2000). Physiological and ecological aspects of primary production in the Ross Sea. In: Ross Sea Ecology, Italian Antarctic expeditions (1987-1995). F.M. Faranda, L. Guglielmo, A. Ianora, (eds), Springer Berlin: 247–258.

Saggiomo V., Catalano G., Mangoni O., Budillon G., Carrada G.C. (2002). Primary production processes in ice-free waters of the Ross Sea (Antarctica) during the austral summer 1996. Deep-Sea Research Part II, 49: 1787–801.

Saino N. and Guglielmo L. (2000). ROSSMZE expedition: distribution and biomass of bird and mammals in the western Ross Sea. [in:] Ross Sea Ecology, Italian Antarctic expeditions (1987-1995). F.M. Faranda, L. Guglielmo, A. Ianora, (eds), Springer Berlin: 469-478.

Schoemanna V., Becquevorta S., Stefelsb J., Rousseaua V., Lancelotte C. (2005). *Phaeocystis* blooms in the global ocean and their controlling mechanisms: a review. Journal of Sea Research, 53: 43–66.

Schreiber U., Klughammer C. and Kolbowski J. (2012). Assessment of wavelength-dependent parameters of photosynthetic electron transport with a new type of multi-color PAM chlorophyll fluorometer. Photosynth Res., 113: 127–144.

Sedwick P.N. and DiTullio G.R. (1997). Regulation of algal blooms in Antarctic shelf waters by the release of iron from melting sea ice. Geophysical Research Letter, 24: 2515–2518.

Sedwick P.N., DiTullio G.R., Mackey D.J. (2000). Iron and manganese in the Ross Sea, Antarctica: seasonal iron limitation in Antarctic shelf waters. J. Geophys. Res. 105:11321–36

Sedwick PN, Garcia NS, Riseman SF, Marsay CM, DiTullio GR (2006) Evidence for high iron requirements of colonial *Phaeocystis antarctica* at low irradiance Biogeochemistry, 83:83–97 DOI 10.1007/s10533-007-9081-7

Sedwick P.N., Garcia N.S., Riseman S.F., DiTullio G.R. (2007). Evidence for high iron requirements for colonial *Phaeocystis antarctica* at low irradiance. Biogeochemistry 83(1-2): 83–97.

Sedwick P.N., Marsay C.M., Sohst B.M., Aguilar-Islas A.M., Lohan M.C., Long M.C., Arrigo K.R., Dunbar R.B., Saito M.A., Smith W.O. and DiTullio G.R. (2011). Early season depletion of dissolved iron in the Ross Sea polynya: Implications for iron dynamics on the Antarctic continental shelf. Journal of Geophysical Research-Oceans, 116: C12.

Shields A.R. and Smith W.O. Jr (2009). Size-fractionated photosynthesis/irradiance relationships during *Phaeocystis antarctica*-dominated blooms in the Ross Sea, Antarctica. Journal of Plankton Research, 31 (7): 701–712.

Smith W.O. Jr and Nelson D.M. (1985). Phytoplankton bloom produced by a receding ice edge in the Ross Sea: spatial coherence with the density field Science, 227: 163–166.

Smith W.O. Jr and Gordon L.I. (1997). Hyperproductivity of the Ross Sea (Antarctica) polynya during austral spring. Geophysical Research Letters, 24: 233–236.

Smith WO Jr, Marra J, Hiscock MR, Barber RT. (2000). The seasonal cycle of phytoplankton biomass and primary productivity in the Ross Sea, Antarctica. Deep-Sea Res, II 47:3119–40.

Smith WO Jr, Asper V. (2001). The influence of phytoplankton assemblage composition on biogeochemical characteristics and cycles in the southern Ross Sea, Antarctica. Deep-Sea Res. I 48:137–61

Smith, W., Jr., M. Dinniman, J. Klinck, and E. Hoffmann (2003), Biogeochemical climatologies in the Ross Sea, Antarctica: Seasonal patterns of nutrients and biomass, Deep Sea Res., Part II, 50, 3083 – 3101.

Smith W.O Jr, Shields A.R., Peloquin J.A., Catalano G., Tozzi S, Dinniman M.S., et al. (2006). Interannual variations in nutrients, net community production, and biogeochemical cycles in the Ross Sea. Deep-Sea Res II, 53: 815-833.

Smith W.O. Jr, Ainley D.G., Cattaneo-Vietti R. (2007). Trophic interactions within the Ross Sea continental shelf ecosystem. Philos. Trans. R. Soc. B, 362: 95–111.

Smith W.O. Jr, Tozzi S., DiTullio G.R., Dinnimand M., Mangoni O., Modigh M., Saggiomo V. (2010). Phytoplankton photosynthetic pigments in the Ross Sea: Patterns and relationships among functional groups. Journal of Marine Systems, 82: 177-185.

Smith W.O. Jr, Asper V., Tozzi S., Liu X., Stammerjohn S.E. (2011a). Continuous fluorescence measurements in the Ross Sea, Antarctica: scales of variability. Prog. Oceanogr. 88: 28–45.

Smith WO Jr, Shields AR, Dreyer JC, Peloquin JA, Asper V. 2011b. Interannual variability in vertical export in the Ross Sea: magnitude, composition, and environmental correlates. Deep-Sea Res. I 58:147–59

Smith W.O. Jr and Jones R.M. (2014). Vertical mixing, critical depths, and phytoplankton growth in the Ross Sea. ICES Journal of Marine Science, 72(6): 1952-1960.

Smith W.O. Jr, Ainley D.G., Arrigo K.R., Dinniman M.S. (2014). The Oceanography and Ecology of the Ross Sea. Annual Review of Marine Science, 6: 469-87.

Stammerjohn S.E., Martinson D.G., Smith R.C., Yuan X., Rind D. (2008). Trends in Antarctic annual sea ice retreat and advance and their relation to El Ni ˜ no–Southern Oscillation and Southern Annular Mode variability. J. Geophys. Res. 113:C03S90.

Stammerjohn S.E., Massom R., Rind D., Martinson D.G. (2012). Regions of rapid sea ice change: an interhemispheric seasonal comparison. Geophys. Res. Lett. 39: L0650.

Swift D.G and Guillard R.R.L. (1977). Diatoms as tools for assay of total B12 activity and cyanocobalamin activity in sea water. J. Mar. Res., 35: 309–320.

Stoecker DK, Putt M, Moisan T (1995) Nano- and microplankton dynamics during the spring *Phaeocystis sp*. bloom in McMurdo Sound, Antarctica. J Mar Biol Assoc UK 75: 815–832

Strzepek R.F., Maldonado M.T., Hunter K.A., Frew R.D., Boyd P.W. (2011). Adaptive strategies by Southern Ocean phytoplankton to lessen iron limitation: Uptake of organically complexed iron and reduced cellular iron requirements. Limnology and Oceanography, 56(6): 1983–2002.

Tagliabue A. and Arrigo K.R. (2003). Anomalously low zooplankton abundance in the Ross Sea: an alternative explanation. Limnology and Oceanography, 48: 686–99.

Tang K.W., Smith Jr., W.O., Elliot D.T., Schields A.R. (2008). Colony size of *Phaeocystis antarctica* (Prymnesiophyceae) as influenced by zooplankton grazers. Journal of Phycology, 44: 1372–137.

Tang Y.Z., Koch F., and Gobler C.J. (2010). Most harmful algae are vitamin B1 and B12 auxotrophs. Proc. Natl. Acad. Sci. USA 107: 20756–2076.

Taylor M.H., Losch M. and Bracher A. (2013). On the drivers of phytoplankton blooms in the Antarctic marginal ice zone: A modeling approach. Journal of Geophysical Research Oceans, 118(1): 63-75.

Turner J., Barrand N.E., Bracegirdle T.J. et al. (2013). Antarctic climate change and the environment: an update. Polar Record, 50: 237–259.

Vidussi F., Claustre H., Bustillos-Guzman J., Cailliau C., Marty J.C. (1996). Determination of chlorophylls and carotenoids of marine phytoplankton: separation of chlorophyll a from divinylchlorophyll a and zeaxanthin from lutein. J Plankton Res., 18 (12): 2377-2382.

Vernet M., Brody E.A., Holm-Hansen O., Mitchell B.G. (1994). The response of Antarctic phytoplankton toultraviolet radiation: Absorption, photosynthesis, and taxonomic composition. Antarct. Res. Ser., 62,143–158.

Wakeman K.C.,Yamaguchi A., Horiguchi T. (2018). Molecular phylogeny and morphology of *Haplozoon ezoense* n. sp. (Dinophyceae): a parasitic dinoflagellate with ultrastructural evidence of remnant non-photosynthetic plastids. Protist. 169: 333-350.

Wang S. and Moore J.K. (2011). Incorporating *Phaeocystis* into a Southern Ocean ecosystem model. Journal of Geophysical Research, 116: C01019. doi:10.1029/2009jc005817.

Wu, J., and E. A. Boyle (1998). Determination of iron in seawater by high resolution isotope dilution inductively coupled plasma mass spectrometry after Mg(OH)2 co-precipitation, Anal. Chim. Acta, 367, 183–191.

Wright S.W., Thomas D.P., Marchant H.J., Higgins H.W., Mackey M.D., Mackey D.J. (1996). Analysis of phytoplankton of the Australian sector of the Southern Ocean: comparisons of microscopy and size frequency data with interpretations of pigment HPLC data using the 'CHEMTAX' matrix factorisation program. Marine Ecology Progress Series, 144: 285-298.

Xavier J.C., Brandt A., Ropert-Coudert Y., Badhe R., Gutt J., Havermans C., Jones C., Costa E.S, Karin Lochte K., Schloss I.R., Mahlon C. Kennicutt II M.C. and Sutherland W.J. (2016). Future Challenges in Southern Ocean Ecology Research. Frontiers in Marine, Science, doi.org/10.3389/fmars.2016.00094.

Marine Environmental Research 151 (2019) 104733

Contents lists available at ScienceDirect

Marine Environmental Research

journal homepage: www.elsevier.com/locate/marenvrev

Phaeocystis antarctica unusual summer bloom in stratified antarctic coastal waters (Terra Nova Bay, Ross Sea)

Olga Mangoni[a,b], Maria Saggiomo[c,*], Francesco Bolinesi[a], Michela Castellano[d], Paolo Povero[d], Vincenzo Saggiomo[c], Giacomo R. DiTullio[e]

[a] Dipartimento di Biologia, Università degli Studi di Napoli Federico II, Complesso di Monte Sant'Angelo, via Cinthia 21, Naples 80126, Italy
[b] CoNISMa, Piazzale Flaminio 9, Rome 00196, Italy
[c] Stazione Zoologica Anton Dohrn, Villa Comunale I, Naples 80122, Italy
[d] Dipartimento di Scienze della Terra, dell'Ambiente e della Vita, Università degli Studi di Genova, Corso Europa 26, Genoa 16132, Italy
[e] Hollings Marine Laboratory, College of Charleston, 331 Fort Johnson Rd, Charleston, SC 29412, USA

ARTICLE INFO

Keywords:
Phytoplankton
Biomarker pigments
Climate change

ABSTRACT

This study focuses on the potential explanations for a *Phaeocystis antarctica* summer bloom occurred in stratified waters of Terra Nova Bay (TNB) - which is part of the Antarctic Special Protected Area (n.161) in the Ross Sea - trough a multi-parameter correlative approach. Many previous studies have highlighted that water column stratification typically favors diatom dominance compared to the colonial haptophyte *P. antarctica,* in the Ross Sea, and this correlation has often been used to explain the historic dominance of diatoms in TNB.

To explore the spatial and temporal progression of *P. antarctica* bloom in coastal waters, four stations were sampled three times each between December 31, 2009 and January 13, 2010.

Taxonomic and pigment composition of phytoplankton communities, macro-nutrient concentrations and various different indices, all indicated the relative dominance of *P. antarctica*. Cell abundances revealed that *P. antarctica* contributed 79% of total cell counts in the upper 25 m and 93% in the lower photic zone. Similarly, a strong correlation was observed between Chl-a and the Hex:Fuco pigment ratio, corroborating the microscopic analyses. Recent studies have shown that iron can trigger colonial *P. antarctica* blooms. Based on the Hex:Chl-c_3 proxy for iron limitation in *P. antarctica*, we hypothesize that anomalously higher iron fluxes were responsible for the unusual bloom of colonial *P. antarctica* observed in TNB.

1. Introduction

Coastal Antarctic pelagic food webs are primarily based on two main photoautotrophic communities comprising: diatoms and haptophytes (e.g. *Phaeocystis antarctica*) (DiTullio and Smith, 1996; Alderkamp et al., 2012; Smith et al., 2014; Mangoni et al., 2017). The relative dominance of diatoms and haptophytes varies on different temporal and spatial scales and thereby can have major implications on trophodynamics and CO_2 drawdown processes in the Ross Sea (Sweeney et al., 2000; Arrigo et al., 1999, 2002; Saggiomo et al., 2000; Schoemann et al., 2005; Peloquin and Smith, 2007; Rivaro et al., 2017; Mangoni et al., 2018). *P. antarctica* populations can exist as both solitary cells (3–4 μm in size) and palmelloides colonies (> 2 mm) that can differ by several orders of magnitude in size (Mathot et al., 2000; Schoemann et al., 2005). Grazing rates on *Phaeocystis* appear to be low due to the large size of colonies (Caron et al., 2000; Lonsdale et al., 2000; Elliott et al., 2009; Tang et al., 2008), so that diatom blooms may represent a critical ecological link between primary production and higher trophic levels in the Ross Sea.

Mixed layer depth (MLD) has been correlated to phytoplankton community structure, with diatoms and *Phaeocystis* populations dominating under shallower and deeper MLD conditions, respectively (DiTullio and Smith, 1996; Arrigo et al., 2000; Mathot et al., 2000; Arrigo and van Dijken, 2004; Arrigo et al., 2010; Mills et al., 2010). According to the accepted current paradigm, water column stratification favors diatom dominance under high light conditions due to their physiological superiority in photoprotection and their high tolerance to photoinhibition compared to *P. antarctica* populations (Saggiomo et al., 2002; Kropuenske et al., 2009; Mangoni et al., 2009; Arrigo et al., 2010; Mills et al., 2010). In addition, water column iron bioavailability is critical for sustaining high diatom relative growth rates in high macronutrient regions such as the Ross Sea (Martin et al., 1990). As a result,

* Corresponding author.
E-mail address: m.saggio@szn.it (M. Saggiomo).

https://doi.org/10.1016/j.marenvres.2019.05.012
Received 29 March 2019; Received in revised form 17 May 2019; Accepted 18 May 2019
Available online 20 July 2019
0141-1136/ © 2019 Published by Elsevier Ltd.

diatoms typically dominate in iron enriched stratified waters like marginal ice zones (Smith and Nelson, 1985; Garrison et al., 2003; Mangoni et al., 2004; Wang et al., 2014), or near melting pack ice (Sedwick and DiTullio, 1997; Saggiomo et al., 2002). In contrast, the competitive advantage of *P. antarctica* over diatoms is thought to be due to their lower iron half-saturation constants for growth, potential to luxuriously store iron within the colonies, as well as their ability to efficiently photosynthesize under relatively low or fluctuating light levels due to vertical mixing of the water column (Schoemann et al., 2005; Sedwick et al., 2007; Garcia et al., 2009; Alderkamp et al., 2012). Recent studies have implicated high iron conditions in triggering colony formation in *P. antarctica* (e.g, Bender et al., 2018). Previous work also showed that *P. antarctica* can dominate in stratified waters when iron and light levels are high (Feng et al., 2010). Although photophysiological processes are no doubt important for sustaining diatom blooms in stratified surface waters of the Ross Sea, an increasing number of studies have revealed that diatom growth can also be co-limited by Vitamin B_{12} and iron, especially during the austral summer (Bertrand et al., 2007, 2011). In contrast, *P. antarctica* populations are not as susceptible as diatoms to co-limitation by Vitamin B_{12}, presumably due to the consortium of Vitamin B_{12}-producing bacteria housed within the colonial matrix (Bertrand et al., 2007; Delmont et al., 2015).

Although diatoms and *Phaeocystis* populations typically coexist throughout the Ross Sea (Garrison et al., 2005) each taxon can form nearly monospecific blooms that can leave distinct biogeochemical signatures in the water column. For example, per unit phosphorus, *Phaeocystis* populations can assimilate nearly twice the carbon and nitrogen of diatoms (Arrigo et al., 1999; Dunbar et al., 2003; Hales and Takahashi, 2004).

In the open Ross Sea, chlorophyll-a concentrations within blooms of *P. antarctica* can exceed 15 mg m^{-3} (Smith et al., 1996; Smith and Gordon, 1997; Arrigo et al., 1999; Smith and Asper, 2001), and 65%–85% of the austral spring production as well as 36%–45% of the annual production (Smith et al., 2006). After the seasonal decline of colonial *P. antarctica* in the central Ross Sea, phytoplankton communities are typically dominated by diverse populations of diatoms and flagellated single-celled *Phaeocystis*, which tend to dominate in summer (Garrison et al., 2003; Smith et al., 2014). In 2006, a European Long Term Ecological Research (LTER) site was initiated near the Italian station (Mario Zucchelli) in TNB (http://www.lteritalia.it/?q=macrositi/it17-stazioni-di-ricerca-antartide). Both LTER data as well as previous Italian expeditions to TNB (from 1987 to 1995) all document that the phytoplankton blooms during summer consist primarily of diatoms (Saggiomo et al., 1998, 2000; Innamorati et al., 2000; Nuccio et al., 2000). Understanding the dynamics controlling the influence of bottom-up factors on phytoplankton species composition in Antarctic coastal waters as well as the open Southern Ocean, represents an important research area given the impact of biogeochemical cycling in the Southern Ocean on climate change processes (Boyd and Doney, 2003; Boyd et al., 2008).

In order to contribute ecological information to the Italian LTER program in TNB, four stations were occupied during the austral summer of 2009–2010. We determined various hydrographic and biological parameters to assess the relationship between the water column structure, nutrient and biochemical concentrations with the phytoplankton community.

To shed light on this topic, here we document the occurrence of an anomalous *P. antarctica* bloom occurred in the coastal area of Terra Nova Bay (Ross Sea) during the austral summer 2009–2010 and provide potential explanations using a multi-parameter correlation approach.

2. Materials and methods

Sampling was conducted in the coastal TNB area during austral summer 2009–2010 as part of the "LTER-Marine Observatory of Antarctic Specially Protected Area – Terra Nova Bay (MOA-TNB) Project", funded by the Italian National Program for Antarctic Research (PNRA, 2009/A1.13). Physical-chemical features of the water column at these LTER stations, together with phytoplankton biomass measurements, have been recorded since 1989 as a component of various oceanographic expeditions funded by PNRA (Innamorati et al., 1991; Nuccio et al., 2000; Misic et al., 2006, Povero et al., 2006, 2012). The phytoplankton community was investigated at three LTER coastal stations, identified as: (1) Portofino (PTF), (2) Santa Maria Novella (SMN), and (3) Faraglioni (FAR). An additional station, Santa Lucia (SLC), was also sampled and is located near the marginal ice zone of Tethys Bay, (Fig. 1). The depths of the four coastal stations varied with the shallowest being FAR (100 m) and the deepest SMN (500 m). The other two stations (SLC and PTF) had a depth of approximately 200 m. The areal extent of the sampling area was ≈30 Km^2.

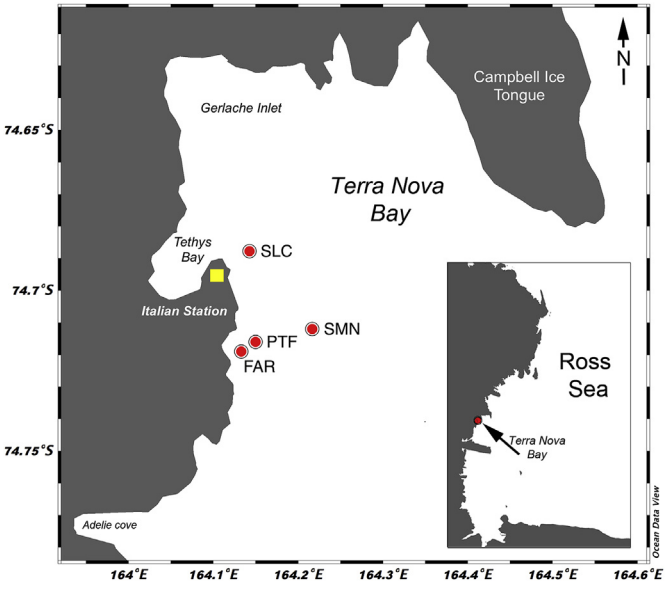

Fig. 1. Map of the sampling sites during the 2009–10 austral summer in Terra Nova Bay (Antarctica) (ASPA n°161). Faraglioni (FAR), Portofino (PTF), Santa Maria Novella (SMN) and Santa Lucia (SLC) stations were sampled three times each.

The stations FAR, PTF, SMN and SLC were sampled three times each between December 31, 2009 and January 13, 2010 with the 3 sampling time periods designated as T1, T2 and T3 (Table 1).

Vertical profiles of temperature and salinity were acquired using an Idronaut 304 CTD. Water samples were collected by 5-L Niskin bottles in order to determine various physical and biological parameters including: inorganic nutrient concentrations, total chlorophyll *a* biomass (Chl-a), HPLC accessory pigment concentrations, phytoplankton cell concentrations via microscopy, elemental and biochemical analyses of particulate organic matter. Meteorological data (air temperature, velocity of wind) and solar irradiance were reported from 25 December to the end of the research activities. Wind speed, air temperature and daily average of photosynthetically active radiation (PAR) date were obtained from 'Meteo Climatological Observatory at the Italian Station (Mario Zucchelli Station, MZS) of PNRA (http://www.climantartide.it).

2.1. Pigment analyses

Four liters of seawater were drawn from the Niskin bottles and, after careful mixing, sub samples were aliquoted for the analysis of total and fractionated Chl-a concentrations, and for the analysis of accessory pigments to determine the phytoplankton community. For the analysis of total Chl-a, 500 ml of sea water were filtered from each depth through Whatman GF/F filters (25-mm diameter). Size-fractionated

Table 1
Hydrographic measurements made during the 2009–10 austral season in Terra Nova Bay (Antarctica). Station sampling sites and (time period of sampling) are denoted for each of the variables. Sea surface temperature (SST) and sea surface salinity (SSS) were used to calculate sea surface density (σ_t). Water column stability (E) in the upper 40 m was calculated according to the method of Knauss and Garfield (2017). The daily average values of surface wind speed, atmospheric temperature and irradiance were tabulated.

Station name	Lat. S	Long. W	Bottom depth (m)	Date	Sampling periods	SST (°C)	SSS	σ_t (kg m^{-3})	Water Column Stability (E) ($10^{-8} m^{-1}$)	Wind speed (m sec^{-1})	Air Temp (°C)	Light (E m^{-2} d^{-1})
PTF	74°42.1	164°09	200	31-Dec	T1	0.87	33.90	26.61	1711	4	−0,81	44
				05-Jan	T2	−0.08	34.05	26.79	1157	12	−0,46	53
				09-Jan	T3	0.30	33.91	26.65	1203	4	0,08	53
SLC			200	01-Jan	T1	0.26	33.62	26.98	2210	2	−1.70	19
	74°41.16	164°07.94		06-Jan	T2	−0.38	33.77	27.13	1718	13	−2.34	27
				11-Jan	T3	0.00	34.11	27.39	1026	5	−0.06	52
FAR			100	02-Jan	T1	0.38	33.69	27.03	2140	3	0.12	38
	74°42.7	164°13		06-Jan	T2	0.03	34.34	27.57	537	13	−2.34	27
				10-Jan	T3	0.91	33.16	26.57	2923	8	0.95	51
SMC	74°43	164°13	500	03-Jan	T1	0.78	33.72	27.03	2035	12	1.24	53
				08-Jan	T2	0.03	33.92	27.23	1214	4	−1.37	39
				13-Jan	T3	1.05	33.53	26.86	2323	5	−0.51	49

Chl-a sea water samples were filtered through polycarbonate Nuclepore polycarbonate membranes (2 μm pore size), and a Nitex mesh (20 μm). The filtrate from each was then collected on Whatman GF/F filters thereby resulting in a < 2 μm and a < 20 μm fraction, respectively (see Mangoni et al. (2004) and Jeffrey et al. (2005) for additional details). The analyses of size-fractionated Chl-a and phaeopigments (Phaeo) were carried out according to Holm-Hansen et al. (1965) using a Spex Fluoromax spectrofluorometer. The instrument was calibrated and checked daily with a Chl-a standard solution (*Anacystis nidulans*, Sigma). In order to determine accessory pigments using high performance liquid chromatography (HPLC), 2 L of seawater were filtered onto Whatman GF/F filters (47 mm diameter) and stored at −80 °C until onshore pigment analysis was performed. HPLC pigment separations were made on an Agilent 1100 HPLC according to the method outlined in Vidussi el al. (1996) as modified by Brunet and Mangoni (2010). The system was equipped with an HP 1050 photodiode array detector and a HP 1046 A fluorescence detector for the determination of chlorophyll degradation products. Calibration of the instruments was carried out using 20 different pigment standards provided by the International Agency for ^{14}C Determination, VKI Water Quality Institute, Copenhagen, Denmark. Three major marker pigments were used to identify the contribution of the major phytoplankton taxa: fucoxanthin (Fuco) as predominantly diagnostic for diatoms and 19'-hexanoyloxyfucoxanthin (Hex) and Chlorophyll-c_3 (Chl-c_3) for *Phaeocystis antarctica* (DiTullio et al., 2003, 2007; van Leeuwe et al., 2014). In addition, we used phaeophorbide *a* (PhaeoB *a*) as a grazing marker as reported by Barlow et al. (1993).

2.2. Cell counts

For microscopic analysis of phytoplankton cell densities, 500 ml water samples were collected and preserved with formaldehyde (4% final concentration). Cell counts were performed with an inverted light microscope (Zeiss Axiophot) according to the Utermöhl method (Utermöhl, 1958).

2.3. Nutrient analyses and silicate to nitrate ratios

Water samples for the determination of inorganic nutrient [NO_2^-, NO_3^-, NH_4^+, PO_4^{3-}, $Si(OH)_4$] concentrations were filtered and collected in 20 ml vials, and immediately stored at −20 °C until analysis. The analyses were performed using a FlowSys Systea autoanalyzer, following the procedures described by Hansen and Grasshoff (1983). The ambient Si/N ratio was used as proxy to identity the possible effect of phytoplankton community composition on the water column chemistry in TNB. In fact silicate and nitrate concentrations in the deep waters of the Ross Sea are approximately 76 μM and 32 μM, respectively, yielding a silicate to nitrate (Si/N) ratio of ~2.5 (Gordon et al., 2000). Changes in the ambient Si/N ratio can reflect both physiological changes in diatom nutrient uptake (e.g. iron limitation) as well as changes due to phytoplankton species composition. For example, under high iron and macronutrient replete conditions, the Si/N assimilation ratio in diatoms is ~1 (Brzezinski, 1985). Under low iron conditions, diatom Si/N uptake ratios are elevated to values > 2 (Hutchins and Bruland, 1998; Takeda, 1998).

2.4. Elemental and biochemical analyses of particulate organic matter

Aliquots of 500–2000 ml of seawater were filtered depending upon the particular biochemical parameter. Water samples were filtered onto combusted Whatman GF/F filters for analyses of particulate organic carbon (POC), particulate organic nitrogen (PON), particulate carbohydrates (CHO) and particulate proteins (PRT). POC/PON analyses were carried out after exposing filters to HCl fumes for 24 h to remove the inorganic carbon fraction (Hedges and Stern, 1984). Cycloexanone 2,4-dinitrophenyl hydrazone was used as the calibration standard. Analyses were performed on an elemental analyser (Model 1100 CHN; Carlo Erba). CHO analyses were carried out following the phenol-sulphuric acid colorimetric method (Dubois et al., 1956). Absorbances were measured at 490 nm. Solutions of D(+)glucose were used as the calibration standard. The PRT assay was based on the reaction between protein amino acids and the copper sulphate-Folin Ciocalteu reagent (Hartree, 1972). Protein absorbance was measured at 650 nm using bovine serum albumin as the calibration standard. Both CHO and PRT analyses were performed using a Jasco V530 spectrophotometer.

2.5. Statistical analysis

Relationships between depth, Hex:Chl-c_3 ratio, Hex:Fuco ratio, PO_4, $Si(OH)_4$, NO_3, Chl-a, temperature and salinity were investigated through Spearman correlation matrix. To investigate the relationships among environmental variables and biological features, a multivariate approach based on principal component analysis (PCA) was carried out using the XLSTAT 2017 software.

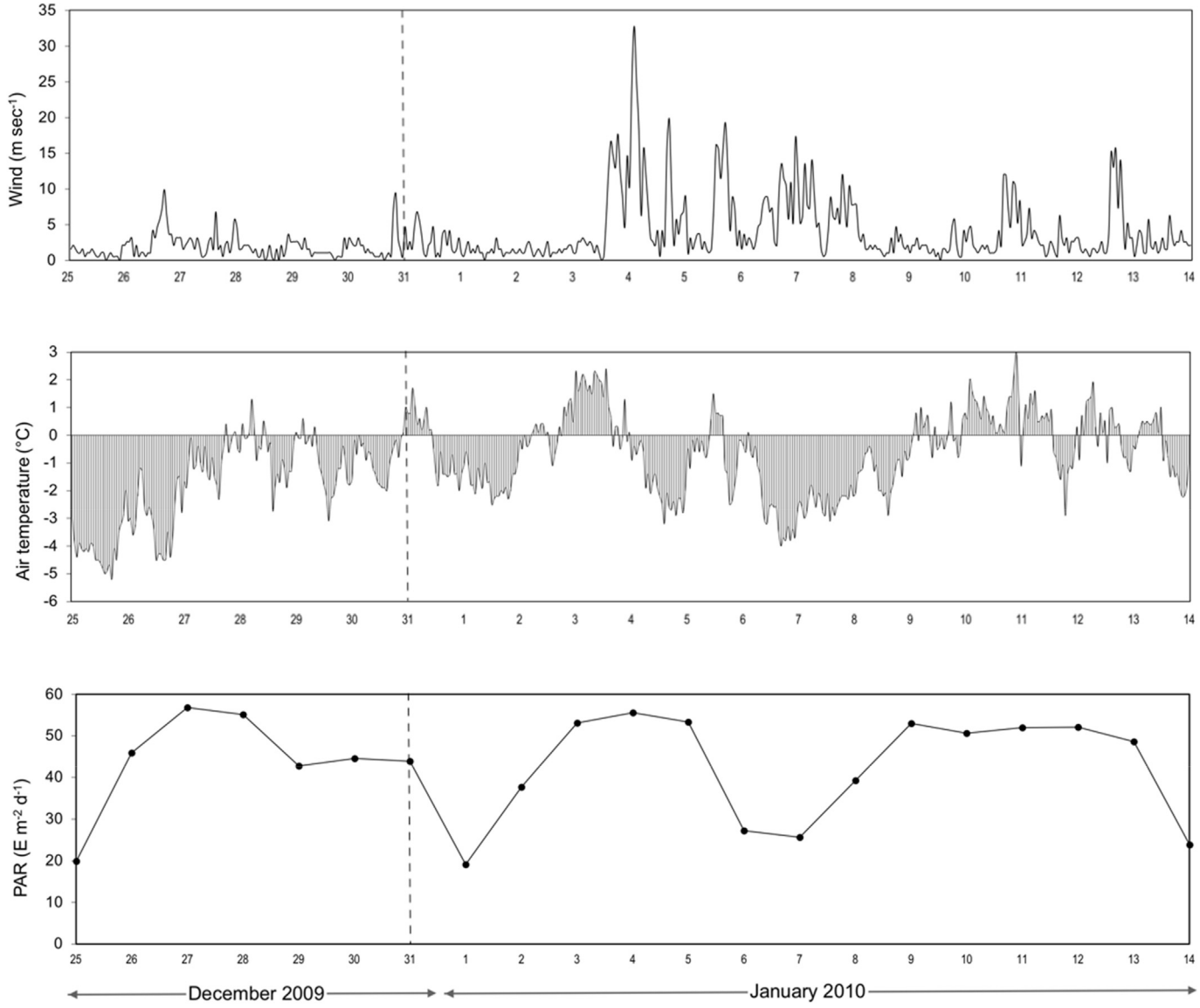

Fig. 2. Meteorological data from December 25, 2009 to January 13, 2010 in Terra Nova Bay (Antarctica). Wind speed (m sec^{-1}), air temperature (°C) and daily average of photosynthetically active radiation (PAR) (E m^{-2} d^{-1}) were measured.

3. Results

3.1. Environmental parameters and hydrography

Atmospheric air temperatures were generally warmer (from -1 °C to +1 °C) during the week before the first sampling time point (T1) between December 31 and January 3 compared to the second sampling time period (T2) during the presence of a wind event (Jan 04 to Jan 08) when air temperatures decreased to approximately −2.5 °C (Fig. 2).

Following the wind event, air temperatures gradually increased during the T3 sampling period (Jan 09 to Jan 13) to above zero. Relatively low wind velocities ($< 5.14\,m\,s^{-1}$) were recorded for the week leading up to the T1 sampling time point with sustained winds of $10\,m\,s^{-1}$ with gusts of 20–30 $m\,s^{-1}$ occurring during the three day T2 sampling period between Jan 05 and Jan 08 (Fig. 2). The wind event during the T2 sampling period decreased the upper water column stratification as evidenced by vertical profiles of density (Fig. 3). The MLD at all stations was < 10 m (using a conservative $\Delta\sigma_t = 0.125$ criterion). For example, the MLD at Station FAR was calculated to be 4 m, 10 m, and 3 m during the T1, T2 and T3 sampling periods. Daily integrated irradiance levels were generally higher during the T1 and T3 sampling periods and were lower during the low pressure disturbance occurring within the T2 sampling period (Fig. 2).

3.2. Water column stratification and stability

The average water column stability index (E) observed in the upper 40 m of the water column at the 4 sampling stations during T1 was relatively high ($E = 2024 \times 10^{-8}\,m^{-1}$) compared to average values observed during the vertical mixing event that occurred during T2 (e.g. $1157 \times 10^{-8}\,m^{-1}$) and the subsequent re-stratification period occurring during T3 ($18{,}69 \times 10^{-8}\,m^{-1}$: Table 1). The breakdown in vertical stratification of the water column during T2 is also evident from the σ_t vertical profiles, especially at the FAR station where the lowest ($537 \times 10^{-8}\,m^{-1}$) value of water column stability was observed (Table 1 and Fig. 3). But even at this station the MLD only increased to 10 m during the T2 period.

3.3. Nutrient concentrations and N/P, Si/N ratios

Macro-nutrient concentrations in the photic zone were generally non-limiting with integral average nitrate concentrations > 10 μM in

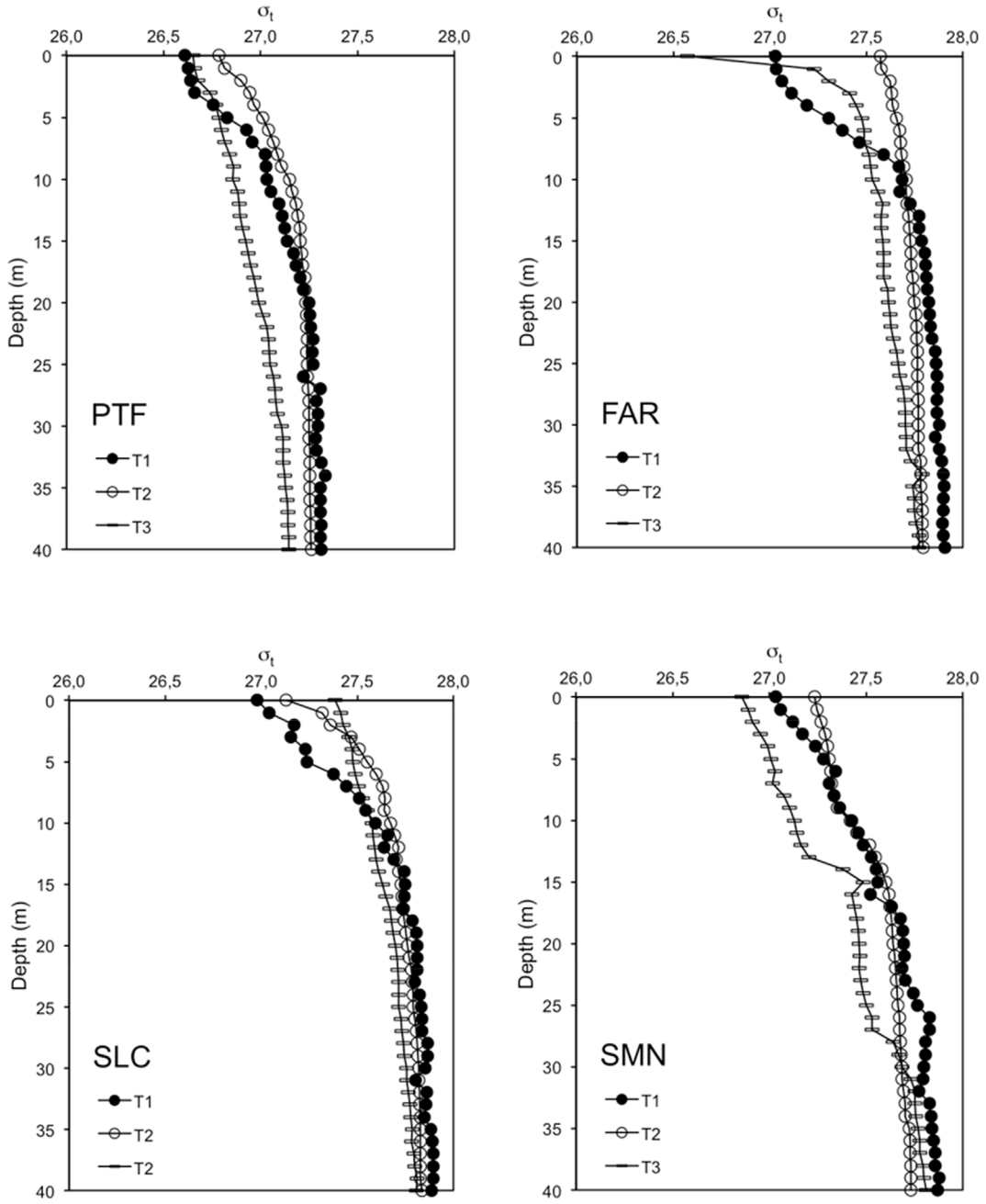

Fig. 3. σ_t profiles at four stations during the 2009–2010 austral season in Terra Nova Bay (Antarctica). The stations PTF, FAR, SLC and SMN were sampled three times each and the sampling periods are indicated as T1, T2 and T3.

the upper 25 m throughout the 3 sampling periods (Table 2). During the course of the sampling period the nitrate to phosphate (N/P) in-situ ratio was approximately 15.7 for all depths and stations sampled (Fig. 4).

The Si/N ratios recorded in TNB were approximately 2.5 at depth and ranged from 3 to 15 in most of the samples collected in the upper 25 m at all 4 stations (Fig. 5). The largest temporal deviation from the hypothetical 1:1 Si/N line was observed in the upper 10 m during the T1 sampling period before the wind event (i.e. during T2).

3.4. Phytoplankton biomass, POC and PON concentrations

Phytoplankton biomass was estimated using spectrofluorometric Chl-a concentrations (Fig. 6) and particulate organic carbon (POC) and nitrogen (PON) (Table 2).

In general, the Chl-a vertical profiles at specific sampling time points were similar at all stations (Fig. 6). Chl-a concentrations were maximal in near surface waters (ca. 10 m) at all stations and ranged from ~6 to 8 mg Chl-a m^{-3} during the T1 sampling period (Fig. 6). During the T2 sampling period, enhanced vertical mixing resulted in lower Chl-a concentrations in the upper layer (< 25 m) relative to deeper waters (e.g. 50–120 m; Fig. 6).

For example, the integral average Chl-a concentration in the upper layer (< 25 m) during T1, T2 and T3 represented 71%, 54% and 36%, respectively, of the total water column integral average at all 4 stations (Tables 2 and 4). Total integrated Chl-a values (averaged for all 4 stations) in the layer 0–80 m revealed the same temporal trend with the highest Chl-a values measured during T1 (275 ± 57 mg m^{-2}) and decreasing values at T2 (258 ± 20 mg m^{-2}) and T3 (176 ± 29 mg m^{-2}) (Table 4). Generally, the micro size-class (> 20 μm) dominated the

Table 2
Nutrient, total Chl-a, size fraction Chl-a [micro- (> 20 μm), nano-(20-2 μm), pico-(< 2 μm)], PON, POC, CHO, PRT concentrations and Phaeo/Chl-a ratios at four stations during the 2009–10 austral season in Terra Nova Bay (Antarctica). Means were integrated along the upper 25 m of the water column (A) and below 25 m (B) during the sampling periods (T1, T2 and T3).

A

Station name	Sampling periods	NH_4^+ (μM)	$NO_3^- + NO_2^-$ (μM)	PO_4^{3-} (μM)	$Si(OH)_4$ (μM)	Chl-a (mg m^{-3})	Micro-(%)	Nano-(%)	Pico-(%)	Pheo/ Chl-a	PON (mg m^{-3})	POC (mg m^{-3})	CHO (mg m^{-3})	PRT (mg m^{-3})
PTF	T1	0.91	10.71	1.06	65.14	3.88	68.7	14.4	16.8	0.45	133	780	352	636
	T2	0.34	18.95	1.98	64.09	3.49	86.7	3.1	10.0	0.44	81	587	287	437
	T3	0.45	12.47	1.25	62.68	1.64	43.6	31.1	25.1	0.42	65	173	173	367
SLC	T1	1.32	9.88	1.59	60.16	3.93	69.8	20.9	9.1	0.49	131	912	562	703
	T2	0.77	13.93	1.32	65.69	3.02	71.6	13.0	15.3	0.50	100	632	321	526
	T3	0.88	13.07	1.32	66.83	1.33	39.1	33.1	27.7	0.52	51	316	130	299
FAR	T1	0.43	11.32	1.61	60.90	3.78	70.0	22.3	7.6	0.47	129	604	281	516
	T2	0.33	18.57	1.91	63.99	3.93	81.8	7.8	10.2	0.43	79	473	253	465
	T3	0.50	11.74	1.28	66.01	1.47	46.4	26.9	26.1	0.44	57	341	151	314
SMC	T1	0.39	10.48	1.24	64.29	3,54	75.5	16.1	8.3	0.40	90	572	380	550
	T2	0.08	16.23	1.61	58.62	2.10	60.9	22.8	16.1	0.41	73	569	282	447
	T3	0.25	9.86	1.06	60.28	0.42	28.3	38.9	32.6	0.72	37	328	231	116

B

Station name	Sampling periods	NH_4^+ (μM)	$NO_3^- + NO_2^-$ (μM)	PO_4^{3-} (μM)	$Si(OH)_4$ (μM)	Chl-a (mg m^{-3})	Micro-(%)	Nano-(%)	Pico-(%)	Pheo/ Chl-a	PON (mg m^{-3})	POC (mg m^{-3})	CHO (mg m^{-3})	PRT (mg m^{-3})
PTF	T1	0.73	27.30	2.06	72.61	2.14	79.7	8.9	11.2	0.50	26	209	109	129
	T2	0.14	24.57	2.19	67.34	2.46	83.0	8.1	8.7	0.46	64	390	158	311
	T3	0.90	24.78	2.07	72.65	2.22	66.9	20.3	12.7	0.48	56	403	252	357
SLC	T1	0.31	26.87	2.26	66.40	2.11	76.5	15.3	8.1	0.51	39	303	159	213
	T2	0.47	22.52	1.83	62.74	2.81	84.1	9.6	6.2	0.49	64	444	257	371
	T3	1.08	27.11	2.26	74.28	2.03	69.9	9.4	20.6	0.61	39	257	143	204
FAR	T1	0.19	28.56	2.23	67.26	0.85	72.8	19.0	8.1	0.50	23	141	88	88
	T2	0.56	24.07	2.07	67.35	2.68	82.1	6.8	10.9	0.52	40	296	134	268
	T3	0.66	28.21	2.43	75.78	2.21	80.5	10.9	8.5	0.51	43	319	119	221
SMC	T1	0.21	29.35	2.28	72.43	1.14	61.5	24.1	14.3	0.62	20	146	39	110
	T2	0.31	23.08	2.03	65.17	2.67	75.3	17.3	7.2	0.49	44	347	195	332
	T3	0.96	25.60	2.10	71.46	2.22	75.1	11.1	13.7	0.56	44	310	341	179

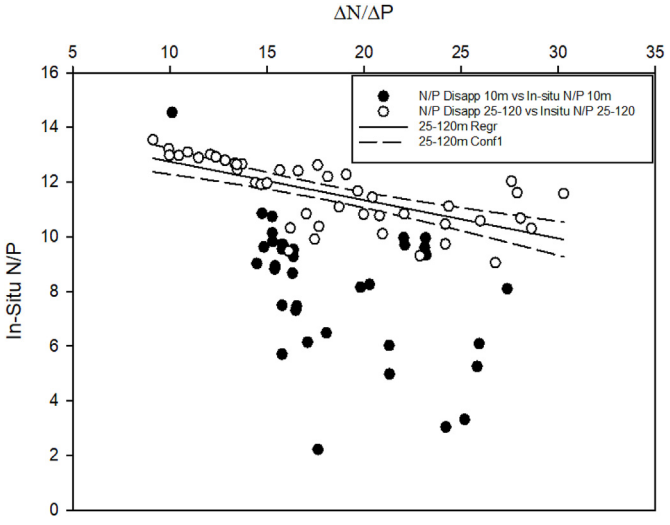

Fig. 4. Correlation between N/P ratio and ΔN/ΔP ratio.

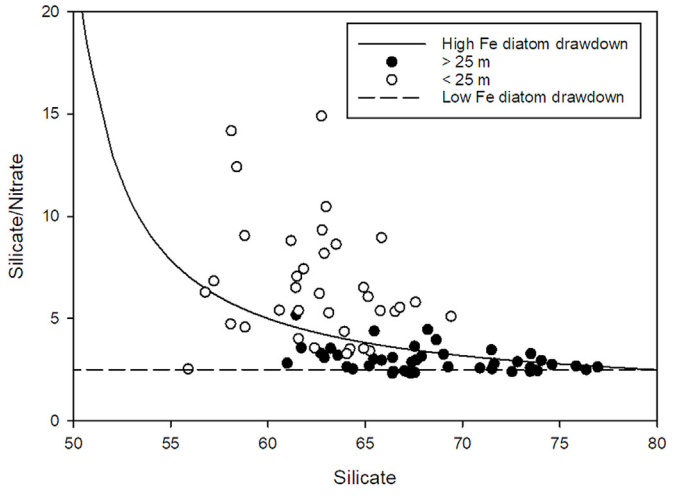

Fig. 5. Variation of the ambient silicate/nitrate ratio *vs* silicate concentration during the 2009–2010 austral season in Terra Nova Bay (Antarctica). Si/N ratios were determined in the upper water column (< 25 m depth, open symbols) and below 25 m (solid symbols). The hypothetical Si/N drawdown ratio by diatoms under iron replete (solid line) and iron deplete (dashed line) conditions are also shown and assume a Si/N assimilation ratio by diatoms of 1 and 2.5, respectively.

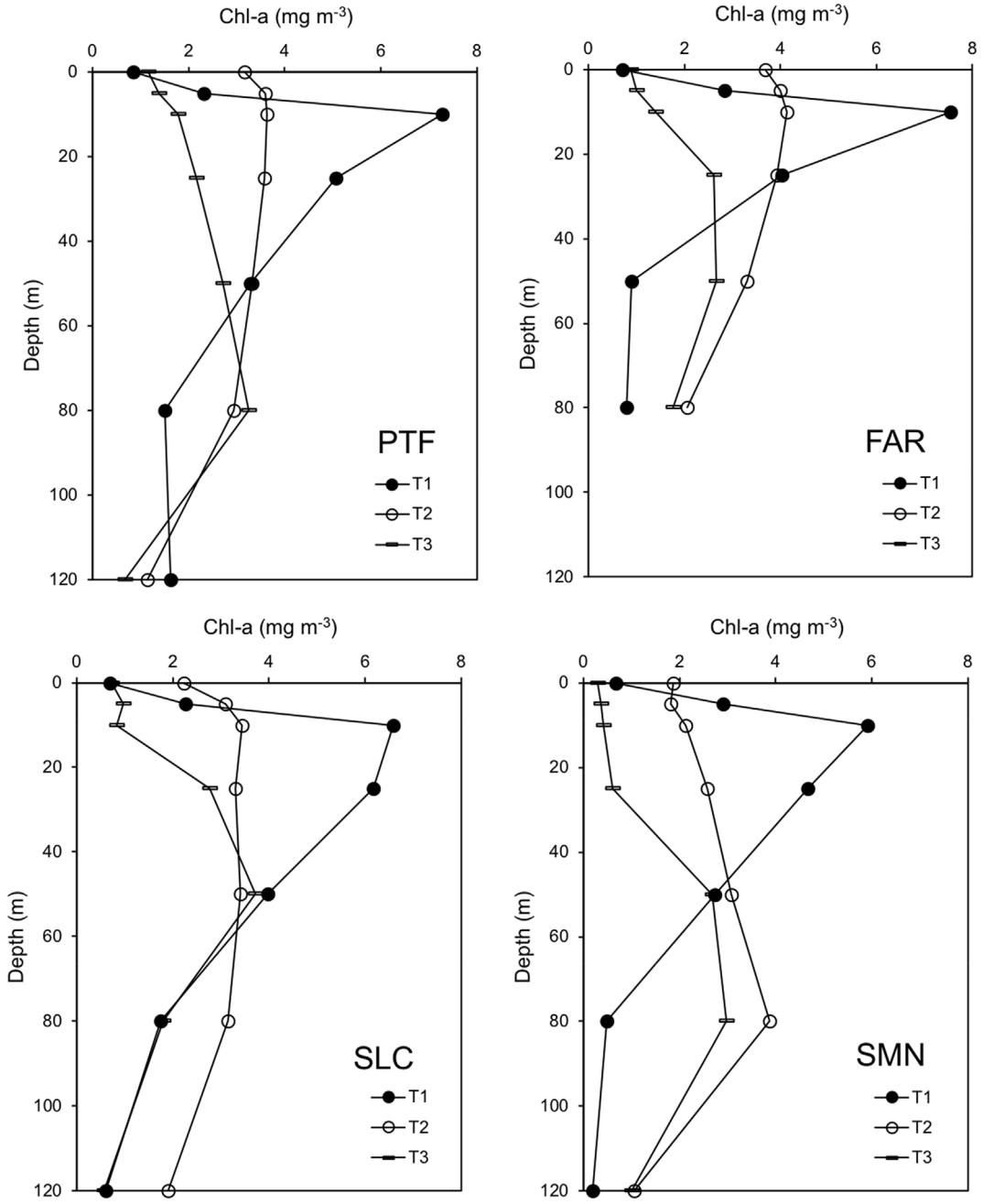

Fig. 6. Chl-a profiles at four stations during the 2009–2010 austral season in Terra Nova Bay (Antarctica). The stations PTF, FAR, SLC and SMN were sampled three times each and the sampling periods are indicated as T1, T2 and T3.

entire area reaching a maximum of 84% at station SLC 2 (below 25 m) and a minimum of 29% at station SMN 3 (upper 25 m). In the upper 25 m of water column the percentage of micro decreased from T1 to T3, while below 25 m we observed a relative increase at SMN and FAR with values exceeding 70%. Lower Phaeo/Chl-a ratios and phaephorbide concentrations were measured in the water column throughout the three sampling periods (Table 2).

Vertical profiles of POC and PON were similar to total Chl-a profiles (Figs. S1 and S2). For instance, the highest POC levels were also measured in surface waters (< 10 m) at all stations during the T1 sampling period. Similar to the Chl-a trend, the integrated water column (to 80 m) average POC value (for all 4 stations) was highest at T1 (39.1 ± 13.6 gC m^{-2}) and lowest at T3 (30.1 ± 4.0 gC m^{-2}; Table 4). PON integrated values followed the same trend as POC with the highest values measured at T1 (6.2 ± 1.4 gN m^{-2}) and the lowest at T3 (4.7 ± 0.6 gN m^{-2}). The integrated POC:Chl-a ratio at T1 and T2 time were 180 and 200 respectively, with a maximun of 288 at T3 when we found a strong differences between the upper (0–25 m) and deeper layer (410 and 166). The integrated protein:carbohydrate (PRT:CHO) ratio ranged from 1.5 (T1) to 1.8 (T3) with slightly higher values in the upper layer of the water column during T1 and T2.

Phytoplankton composition was assessed using microscopic cell counts and HPLC pigment composition (Table 3, Fig. 7).

As is typical of the Ross Sea polynya, the TNB phytoplankton assemblages was dominated by diatoms and the colonial haptophyte, *Phaeocystis antarctica.* In terms of cell abundances, the *P. antarctica* population dominated the community assemblage throughout the sampling periods at all stations (Table 3). In fact, colonial *P. antarctica* cells comprised an average of 79 ± 14% of the total phytoplankton cell abundance in the upper 10 m and approximately 93 ± 5% in deeper

Table 3
Percentage contribution of diatoms, *Phaeocystis antarctica* and other flagellates to phytoplankton community at four stations during the 2009–10 austral season in Terra Nova Bay (Antarctica). Cell counts were made at 0, 10, 50 and 80 m during the sampling periods (T1, T2 and T3).

Station name	Sampling periods	Station depth (m)	Diatoms	*P. antartica*	Other flagellates	Station name	Sampling periods	Depth (m)	Diatoms	*P. antartica*	Other flagellates
PTF	T1	0	41.5	57.1	1.4	**FAR**	T1	0	6.7	92.2	1.1
	T2	0	5.2	93.3	1.5		T2	0	6.9	92.8	0.3
	T3	0	48.0	48.4	3.6		T3	0	20.5	78.4	1.1
	T1	10	12.5	85.6	1.9		T1	10	2.1	97.6	0.3
	T2	10	6.2	92.1	1.7		T2	10	5.8	94.1	0.1
	T3	10	14.3	73.7	12.0		T3	10	19.9	74.7	5.4
	T1	50	5.2	91.9	3.0		T1	50	8.5	91.5	0.0
	T2	50	4.8	93.7	1.5		T2	50	-	-	-
	T3	50	18.1	80.3	1.6		T3	50	0.6	99.4	0.0
	T1	80	10.4	89.0	0.6		T1	80	0.0	100	0.0
	T2	80	5.3	92.8	1.8		T2	80	4.0	95.8	0.2
	T3	80	2.3	97.5	0.2		T3	80	13.0	87.0	0.0
Station name	Sampling periods	Station depth (m)	Diatoms	*P. antartica*	Other flagellates	Station name	Sampling periods	Depth (m)	Diatoms	*P. antartica*	Other flagellates
SLC	T1	0	20.0	80.0	0.0	**SMC**	T1	0	17.0	78.4	4.6
	T2	0	6.5	81.0	12.5		T2	0	28.9	67.9	3.2
	T3	0	27.0	70.9	2.1		T3	0	34.0	64.2	1.8
	T1	10	1.0	98.3	0.8		T1	10	10.2	88.8	1.0
	T2	10	2.9	95.1	2.0		T2	10	32.8	64.6	2.6
	T3	10	22.3	74.2	3.4		T3	10	40.0	57.9	2.1
	T1	50	1.0	99.0	0.0		T1	50	6.5	92.5	1.0
	T2	50	7.2	91.3	1.5		T2	50	10.5	89.3	0.3
	T3	50	1.6	98.0	0.4		T3	50	3.5	95.2	1.3
	T1	80	2.4	97.3	0.3		T1	80	3.5	95.7	0.8
	T2	80	2.9	87.0	0.1		T2	80	8.3	91.0	0.7
	T3	80	4.1	95.9	0.0		T3	80	6.8	93.1	0.1

Table 4
Chl-a, PON, POC, CHO and PRT concentrations at four stations during the 2009–10 austral season in Terra Nova Bay (Antarctica). Values are the means integrated throughout the water column (0–80 m) for the sampling periods (T1, T2 and T3).

Station name	Sampling periods	Chl-a (mg m^{-2})	PON (mg m^{-2})	POC (mg m^{-2})	CHO (mg m^{-2})	PRT (mg m^{-2})
PTF	T1	301	5510	36834	20863	29322
	T2	269	6678	42682	20926	32427
	T3	194	5488	35279	21433	30596
SLC	T1	338	8267	58801	35160	45450
	T2	262	6989	45898	26403	38611
	T3	200	4460	27206	14772	24080
FAR	T1	208	5878	28779	15537	22246
	T2	271	4820	30451	15449	28590
	T3	173	4183	26723	11234	21968
SMC	T1	251	5172	31908	16186	27794
	T2	229	5188	39914	19615	32942
	T3	137	4080	31023	28781	14949

waters (50–80 m; Table 3). Relative diatom populations (i.e. % total) were more prevalent in the upper 10 m of the water column compared to 50–80 m. In addition, enhanced vertical mixing from the wind event during the early T2 sampling period caused an increase of 4–10 fold (at SLC) in the % diatom abundance in the upper 10 m during the T3 time period relative to T2 (Table 3). The diatom community composition at all stations and times was dominated by four species that represented approximately 88 ± 5% of the total diatom cell abundance with *Fragilariopsis cylindrus* dominating the diatom biomass.

The diagnostic photosynthetic pigments fucoxanthin (Fuco) and 19'hexanoyloxyfucoxanthin (Hex) that reflective of diatoms and *P. antarctica* dominance were reported (Fig. 7). The highest Hex:Fuco ratios (ca. 3 to 4) were generally found in the upper 10 m during the T1 period with lower ratios (i.e. < 1) observed during T3 (Fig. 7). Moreover, the Hex:Chl-c_3 ratio can be used as diagnostic of *P. antarctica* populations because these pigment markers are not typically present in diatoms of the Ross Sea (DiTullio et al., 2003). In addition, pigment ratios such as Hex:Fuco and Hex:Chl-c_3, can be influenced by environmental variables such as iron concentrations (DiTullio et al., 2007; van Leeuwe and Stefels, 2007). During T1 sampling, the Hex:Chl-c_3 ratios (4–6) were 2–3 fold higher in the upper 10 m compared to ratios (~2) measured in the lower photic zone (Fig. 8). Similarly, Hex:Chl-c_3 ratios were higher in the upper 25 m compared to the lower zone, except for the T3 sampling at the SMN station where low values were also observed near the surface (Fig. 8). In the upper 25 m, the Hex:Chl-c_3 ratios decreased during the T2 sampling period at 3 of the 4 stations.

3.5. Principale component analysis

A multivariate approach based on principal component analysis (PCA) was carried out to investigate the relationships among environmental variables (e.g. temperature, salinity, nutrients) and biological features including phytoplankton biomass and pigments ratio (e.g. Chl-a, Hex:Fuco, Hex:Chl-c_3). The first two principal components (F1 and F2) explained 79.7% of the total variance, with F1 and F2 accounting for 46% and 34.7% respectively (Fig. 9).

The F1 component mainly explained the environmental variability, while F2 the biological one. The $Si(OH)_4$ and NO_3^- concentrations

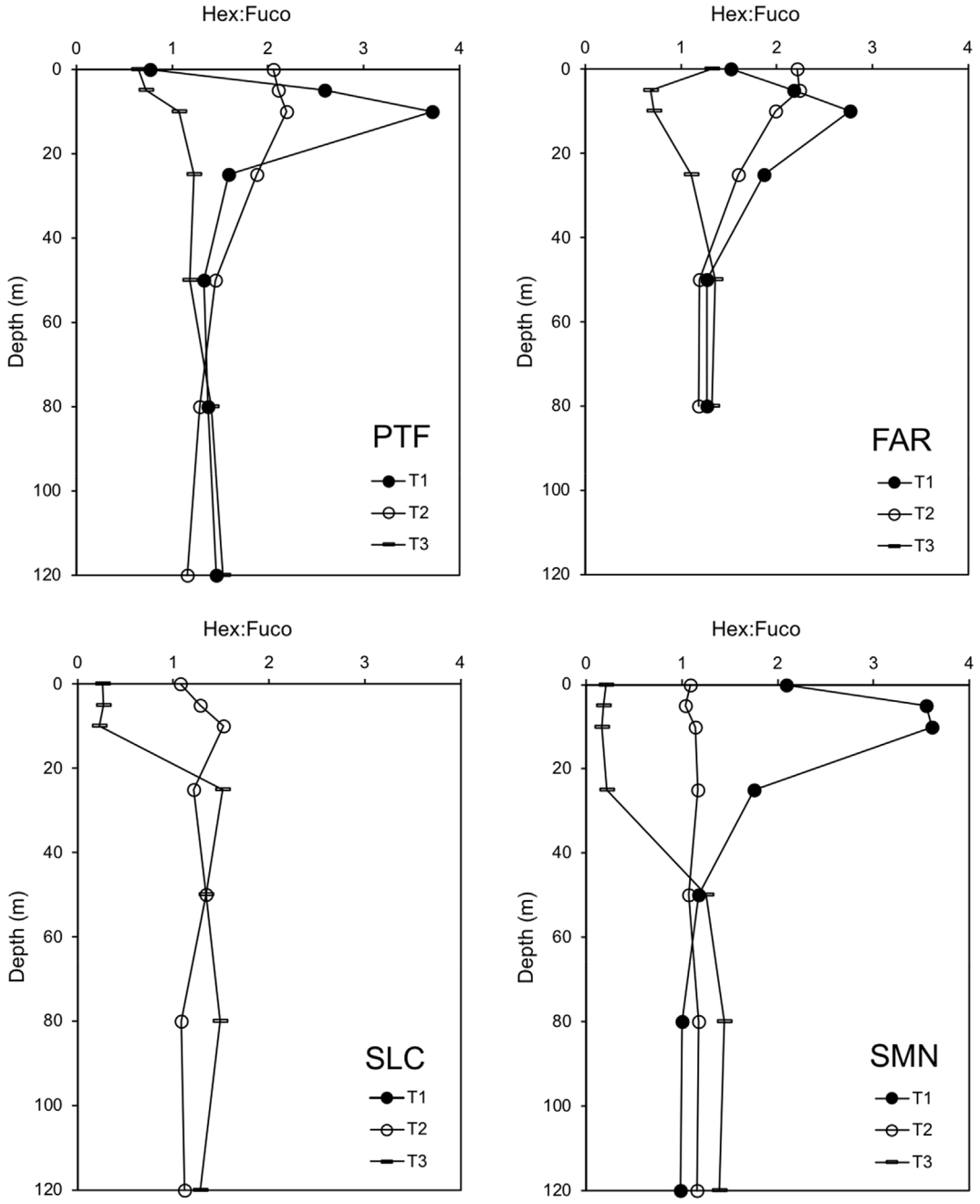

Fig. 7. Hex:Fuco ratio profiles at four stations during the 2009–2010 austral season in Terra Nova Bay (Antarctica). The stations PTF, FAR, SLC and SMN were sampled three times each and the sampling periods were indicated as T1, T2 and T3.

were positively correlated with salinity and depth along the negative F1 axis, while the Hex:Chl-c_3 ratio was directly correlated with temperature along the positive F1 axis. In the Ross Sea, high Hex:Fuco ratios are typically indicative of a community composition that is dominated by the presence of *P. antarctica*. Hex:Fuco ratios were significantly correlated with total phytoplankton biomass (Chl-a) as revealed by the Spearman correlation index and the correlation was also shown along the positive F2 axis of the PCA analysis (Table 5, Fig. 9).

The observations in the first quadrant of the PCA were represented by shallow water samples (i.e. 5–10 m) collected between December 31, 2009 and January 6, 2010. The second quadrant was characterized by the presence of samples collected between January 08 to 11 in the first 25 m of the water column, in which temperature and the Hex:Chl-c_3 ratio were strongly correlated (Fig. 9). Other observations between the third and fourth quadrants show high correlations of high nutrient concentrations and high salinity associated with increasing depth (Fig. 9). An inverse correlation was observed between the higher salinity and nutrient concentrations in deeper waters and the higher temperature and Hex:Chl-c_3 ratios in surface waters (Table 5, Fig. 9).

4. Discussion

During the austral summer 2009–2010, an intense phytoplankton bloom was observed in the surface stratified waters of coastal TNB region. Several lines of evidence, ranging from microscopic cell counts, chemotaxonomic pigment ratios, macronutrient ratio indices (e.g. Si/NO_3), revealed the dominance of *Phaeocystis antarctica* populations in the upper (< 25 m) water column.

Typically, diatom populations have been observed to dominate in stratified Antarctic coastal waters, in marginal sea ice zones, and near

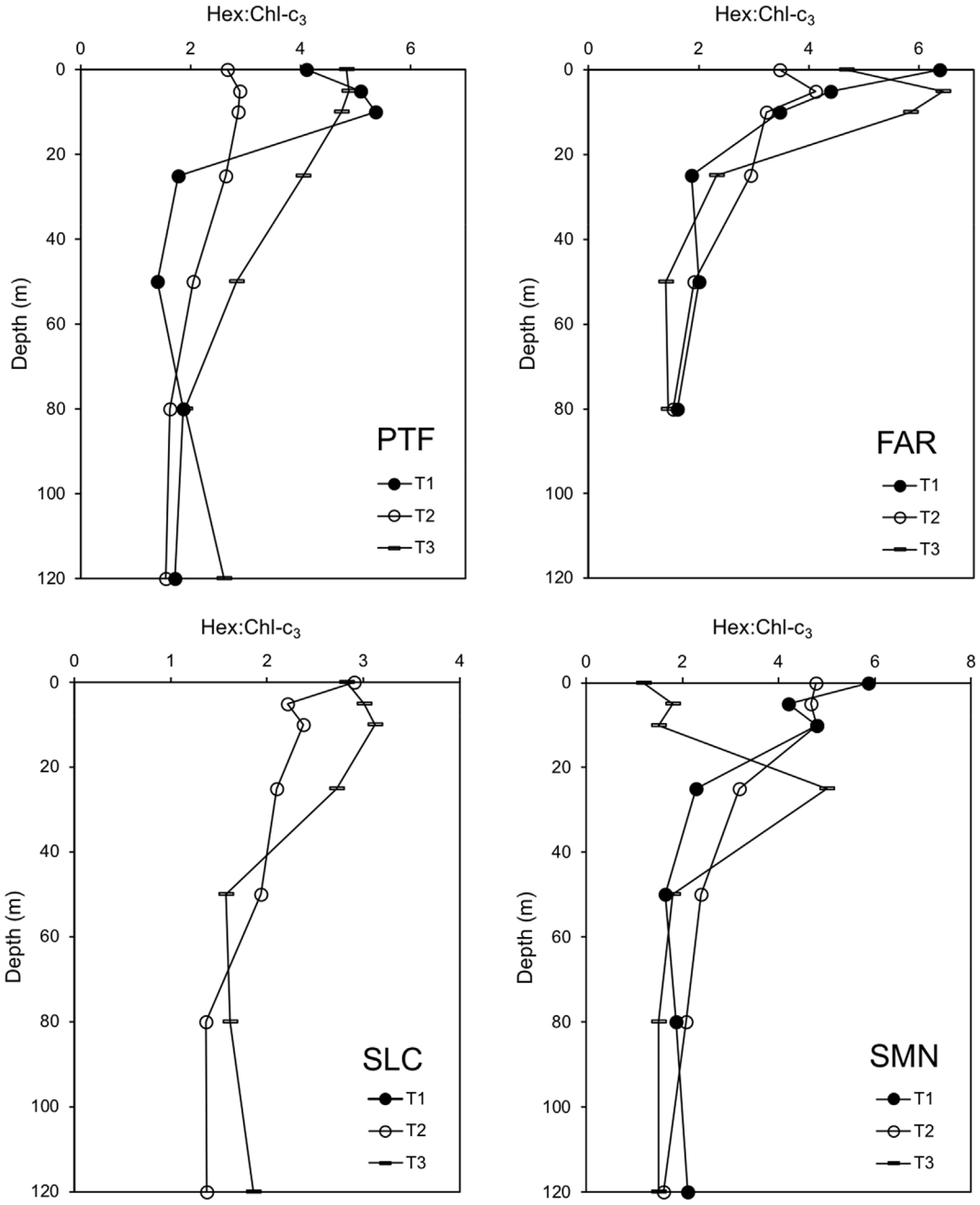

Fig. 8. Hex:Chl-c_3 profiles at four stations during the 2009–2010 austral season in Terra Nova Bay (Antarctica). The stations PTF, FAR, SLC and SMN were sampled three times each and the sampling periods are indicated as T1, T2 and T3.

melting pack ice under presumably relatively high iron and macronutrient concentrations (Smith and Nelson, 1985; Sedwick and DiTullio, 1997; Saggiomo et al., 2002). Since the mid-1980's, diatoms have dominated algal blooms in stratified water columns of the western Ross Sea and especially within TNB (Innamorati et al., 1991; DiTullio and Smith, 1996; Nuccio et al., 2000; Arrigo et al., 2000). Several studies have suggested that the photo-physiological superiority of diatoms relative to *P. antarctica* in stratified waters was due to their ability in photoprotection processes as well as their high tolerance to photoinhibition via heat dissipation (e.g. xanthophyll cycle) (Ryan-Keogh et al., 2017; Kropuenske et al., 2009; Mills et al., 2010; Arrigo et al., 2010; Alderkamp et al., 2012). In contrast, the ability of *P. antarctica* to dominate over diatoms in well-mixed water columns is related to their dynamic range in the photophysiological parameters α and β (the initial slope and inhibitory portion of the productivity *vs* irradiance curve), respectively (Mills et al., 2010). In addition, a lower iron half-saturation constant for growth relative to diatoms has been reported (Garcia et al., 2009).

Measurement of cell abundances via microscopy (Utermöhl method) in this study revealed that *P. antarctica* constituted an average of 79% (14,187,997 cells L^{-1}) of the total cell counts in the upper 10 m of the water column and 93% (14,497,473 cells L^{-1}) in the lower zone (50–80 m) during the 3 sampling periods (Table 3). Visual observations of the colonial *P. antarctica* bloom in surface waters were also noted by the clogging of plankton and fish nets (Figs. S3 and S4).

The N/P disappearance ratio was non-Redfieldian and led to higher N/P ratios (23.5 ± 7.5) in the upper 10 m compared to those measured (15.6) in the lower photic zone (i.e. > 25 m), presumably reflective of the dominance of *P. antarctica* populations in the upper 10 m (Fig. 4; Arrigo et al., 1999; Dunbar et al., 2003).

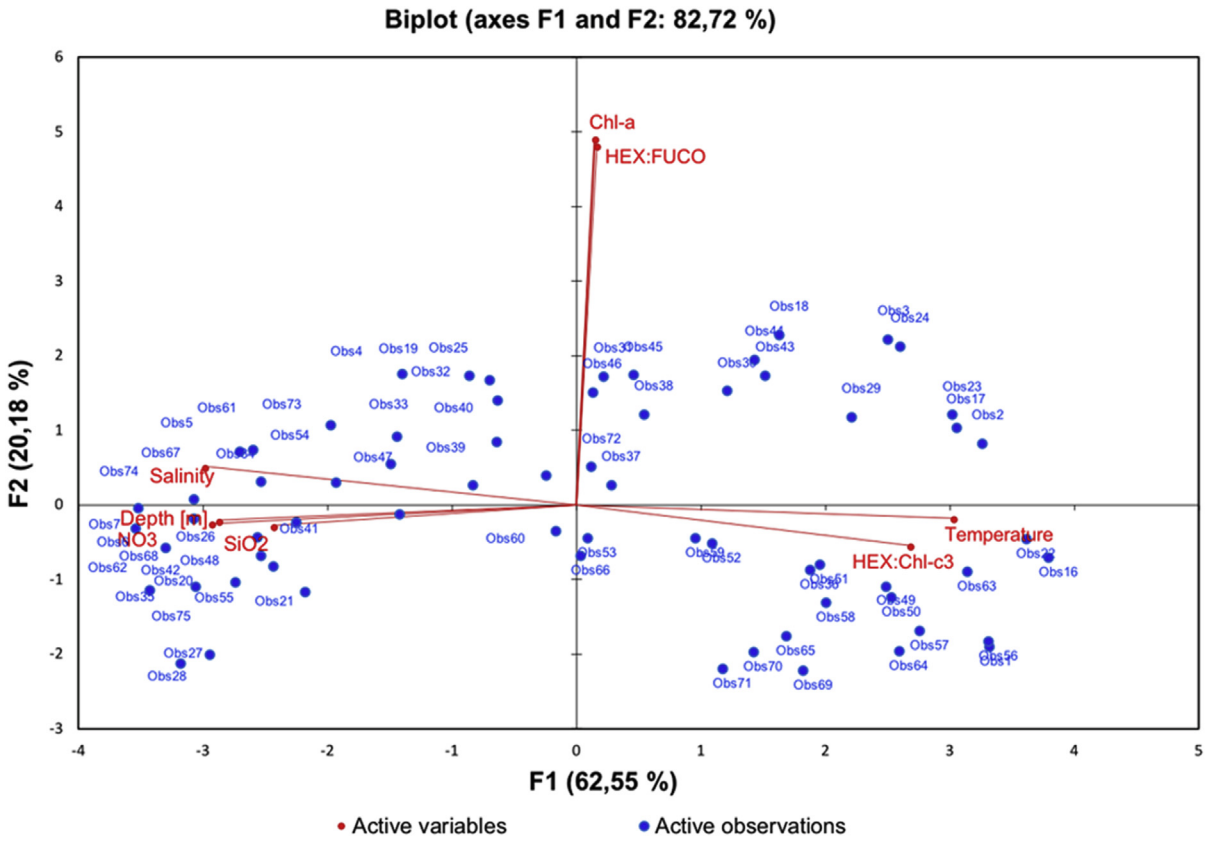

Observation	Obs1	Obs2	Obs3	Obs4	Obs5	Obs6	Obs7	Obs8	Obs9	Obs10
Station	PTF 1	PTF 1	PTF 1	PTF 1	PTF 1	PTF 1	PTF 1	FAR 1	FAR 1	FAR 1
Depth (m)	0	5	10	25	50	80	120	0	5	10
Observation	Obs11	Obs12	Obs13	Obs14	Obs15	Obs16	Obs17	Obs18	Obs19	Obs20
Station	FAR 1	FAR 1	FAR 1	SMN 1	SMN 1	SMN 1	SMN 1	SMN 1	SMN 1	SMN 1
Depth (m)	25	50	80	0	5	10	25	50	80	120
Observation	Obs21	Obs22	Obs23	Obs24	Obs25	Obs26	Obs27	Obs28	Obs29	Obs30
Station	PTF 2	PTF 2	PTF 2	PTF 2	PTF 2	PTF 2	PTF 2	SLC 2	SLC 2	SLC 2
Depth (m)	0	5	10	25	50	80	120	0	5	10
Observation	Obs31	Obs32	Obs33	Obs34	Obs35	Obs36	Obs37	Obs38	Obs39	Obs40
Station	SLC 2	SLC 2	SLC 2	SLC 2	FAR 2	FAR 2	FAR 2	FAR 2	FAR 2	FAR 2
Depth (m)	25	50	80	120	0	5	10	25	50	80
Observation	Obs41	Obs42	Obs43	Obs44	Obs45	Obs46	Obs47	Obs48	Obs49	Obs50
Station	SMN 2	SMN 2	SMN 2	SMN 2	SMN 2	SMN 2	SMN 2	PTF 3	PTF 3	PTF 3
Depth (m)	0	5	10	25	50	80	120	0	5	10
Observation	Obs51	Obs52	Obs53	Obs54	Obs55	Obs56	Obs57	Obs58	Obs59	Obs60
Station	PTF 3	PTF 3	PTF 3	PTF 3	FAR 3	FAR 3	FAR 3	FAR 3	FAR 3	FAR 3
Depth (m)	25	50	80	120	0	5	10	25	50	80
Observation	Obs60	Obs61	Obs62	Obs63	Obs64	Obs65	Obs66	Obs67		
Station	FAR 3	SLC 3	SLC 3	SLC 3	SLC 3	SLC 3	SLC 3	SLC 3		
Depth (m)	80	0	5	10	25	50	80	120		

Fig. 9. Results of principal component analysis (PCA). The multivariate approach was applied to environmental (temperature, salinity, nutrients) and biological variables (Chl-a, Hex:Fuco, Hex:Chl-c_3). The table reported the correspondence from observations with station and sample depth.

Integrated Chl-a values ranged from 275 ± 20 mg Chl-a m^{-2} during T1 to 176 ± 29 mg Chl-a m^{-2} at T3 (Table 4). The decrease of Chl-a concentrations, integrated over the water column (0–80 m), from T1 to T3, was not probably due to zooplankton grazing on the colonial *P. antarctica* as relatively constant levels of Phaeo:Chl-a ratio and pheophorbide concentrations were measured throughout the three sampling periods (Table 2). Accordingly, previous studies have also indicated that colonial blooms of *P. antarctica* are not effectively grazed in the Ross Sea (Caron et al., 2000; Lonsdale et al., 2000). For example, *Euphausia superba,* the primary prey for a multitude of predators in Antarctic waters, can graze small colonies of *P. antarctica* but not larger colonies or single cells (Haberman et al., 2003). As observed for Chl-a, POC and PON concentrations integrated over the water column increased over time (Table 4). Altogether these results suggest that factors other than only grazing, including hydrographic processes such as particle advection or export (DiTullio et al., 2003) were most likely responsible for the observed biomass decrease over time.

To better understand the phytoplankton dynamics, we investigated

Table 5
Spearman correlation matrix showing the relationship among physical, chemical and biological variables. Values in bold are significant p < 0,05.

Variables	Depth [m]	Hex:Chl-c_3	Hex:Fuco	PO_4	$Si(OH)_4$	NO_3	Chl-a	Temperature	Salinity
Depth [m]	**1**	**−0.728**	−0.121	**0.800**	**0.667**	**0.851**	−0.080	**−0.906**	**0.854**
Hex:Chl-c_3	**−0.728**	**1**	0.102	**−0.723**	**−0.616**	**−0.782**	−0.141	**0.810**	**−0.797**
Hex:Fuco	−0.121	0.102	**1**	0.054	−0.067	−0.091	**0.571**	0.036	0.011
PO_4	**0.800**	**−0.723**	0.054	**1**	**0.605**	**0.930**	0.026	**−0.894**	**0.867**
$Si(OH)_4$	**0.667**	**−0.616**	−0.067	**0.605**	**1**	**0.655**	−0.126	**−0.701**	**0.683**
NO_3	**0.851**	**−0.782**	−0.091	**0.930**	**0.655**	**1**	−0.062	**−0.945**	**0.903**
Chl-a	−0.080	−0.141	**0.571**	0.026	−0.126	−0.062	**1**	0.013	0.081
Temperature	**−0.906**	**0.810**	0.036	**−0.894**	**−0.701**	**−0.945**	0.013	**1**	**−0.946**
Salinity	**0.854**	**−0.797**	0.011	**0.867**	**0.683**	**0.903**	0.081	**−0.946**	**1**

two proxies associated with iron limited growth in the western Ross Sea: Si/NO_3 and Hex:Chl-c_3 ratios. The Hex:Chl-c_3 ratio can be a useful diagnostic proxy to determine the iron physiological status of *P. antarctica* in the Ross Sea (DiTullio et al., 2003). Laboratory studies on *P. antarctica* have shown that Hex:Chl-c_3 ratios were inversely correlated with iron physiological status, such that under conditions of severe iron limitation the Hex:Chl-c_3 ratios (5–6) were approximately two-fold higher relative to the Hex:Chl-c_3 ratios (2–3) observed under iron replete growth conditions (DiTullio et al., 2007; van Leeuwe and Stefels, 2007). Hex:Chl-c_3 ratios were significantly correlated with depth as determined by the Spearman correlation index (Table 5). For example, high Hex:Chl-c_3 ratios (e.g. 4 to 6) were observed in the upper 10 m of the water column, where colonial *P. antarctica* populations dominated the community structure under relatively high stratification conditions as observed during T1 (c.f. Figs. 3 and 8). Lower Hex:Chl-c_3 ratios (e.g. 2–3) were observed in the deeper layer of the water column (i.e. > 25 m) suggesting that iron concentrations were relatively higher compared to the upper 25 m. A previous study measured a shallow ferricline depth (~50 m) in TNB (Station NX10; Sedwick et al., 2011) during summer 2005–2006. Hence, the wind event that occurred during T2 resulted in a deepening of the MLD relative to T1 (Table 1) and was associated with lower Hex:Chl-c_3 ratios, especially in the upper 25 m as vertical mixing presumably re-supplied iron back into the upper 25 m (Figs. 3 and 8). Furthermore, the high Si/NO_3 ratios observed in the upper 25 m (Fig. 5) can not simply reflect the uptake of silicate due to diatoms growing under Fe-sufficient conditions, explaining the dominance of *P. antarctica* in the upper 10 m. We have assumed that nitrate is the major provider of nitrogen to the phytoplankton community, and that relatively low denitrification rates occur in TNB as previously determined in the Ross Sea polynya (Gordon et al., 2000), caused enhanced vertical mixing rates and an increase in MLD that presumably replenished nutrient concentrations in the upper zone (Fig. 5).

The colonial *P. antarctica* blooms can develop under both iron-deplete and iron replete growth conditions in the Ross Sea (Feng et al., 2010; Sedwick et al., 2011; Bender et al., 2018). The presence of low turbulence and presumably elevated nutrients at the beginning of the sampling period could have favored palmelloid stage of *Phaeocystis* as suggested by Smayda and Reynolds (2001). The ability of the colonial matrix of *P. antarctica* to sequester iron could be an important advantage in competing with diatoms during episodic iron delivery events (Schoemann et al., 2005). Various mechanisms have been suggested to identify the mechanisms of iron re-supply during summer in Antarctic coastal systems that can play a pivotal role in the development and maintenance of phytoplankton blooms (Sedwick et al., 2011). These processes, for TNB, include sea ice melt, glacial melt and lateral advection from the Victoria Land coast, from the Antarctic coastal current, sediment iron re-suspension, upwelling of circumpolar deep water onto the shelf, and mesoscale eddies (Sedwick and DiTullio, 1997; Sedwick et al., 2011; McGillicuddy et al., 2015; Marsay et al., 2017; Kohut et al., 2017; Rivaro et al., 2019).

Based on the lower Hex:Chl-c_3 ratio during the T2 sampling period, we hypothesized that wind-induced vertical mixing resupplied iron to surface waters and was instrumental in re-fueling the *P. antarctica* bloom and favoring it at the expenses of diatoms. Relatively lower Hex:Chl-c_3 ratios were observed in the lower water column and suggest that iron levels were relatively high compared to those in the upper 10 m (Fig. 8). The higher Hex:Chl-c_3 ratios in the upper water column during T1 may simply reflect the consumption of iron by the high biomass of *P. antarctica* colonies. The ability of *P. antarctica* cells to continue growing even as the bloom depletes the iron available in surface waters can be another mechanism favoring their dominance over diatoms due to their lower iron half-saturation constant for growth relative to diatoms (Garcia et al., 2009).

In addition to iron limitation, evidence for the co-limitation of iron and Vitamin B_{12} on phytoplankton growth has been observed in the Ross Sea (Bertrand et al., 2007, 2011). Since only certain bacterial species in polar waters have the ability to synthesize Vitamin B_{12}, the possibility exists that a mutualistic symbiosis can develop between certain bacterial groups that produce Vitamin B_{12} (e.g., SAR 92, *Oceanospirillaceaea* spp. and *Cryomorphaceae* spp.) and colonial *P. antarctica* cells as was recently shown in the Amundsen Sea (Bertrand et al., 2015; Delmont et al., 2015). The addition of iron alone has been shown to stimulate the growth of *P. antarctica* cells while the addition of both iron and Vitamin B_{12} stimulated diatoms in the Ross Sea (Bertrand et al., 2007). Hence, it is conceivable that the diatom community in TNB were co-limited by iron and Vitamin B_{12} (e.g. Bertrand et al., 2007). Although our data do not allow us to fully demonstrate the mechanisms underlying the anomalous *P. antarctica* bloom, we hypothesize that changes in the supply of Vitamin B_{12} in TNB, perhaps due to a shift in the bacterial community composition could explain this result. This change in Vitamin B_{12} availability would preferentially favor the growth of *P. antarctica* colonies over diatoms by allowing *P. antarctica* cells to sequester both iron and B_{12} inside the colonies and away from diatoms, thereby conferring *P. antarctica* with a competitive edge. Further studies measuring iron and Vitamin B_{12} concentrations in TNB are needed to test this hypothesis.

Even after several decades of study, spatial and temporal uncoupling of diatom and *Phaeocystis* blooms obscures our understanding of bloom dynamics in the Ross Sea (DiTullio and Smith, 1996; Smith et al., 2000). Our data do not allow us to identify the mechanism underlying the anomalous *P. antarctica* bloom. Understanding the dynamics controlling the influence of bottom-up factors such as iron and Vitamin B_{12} on phytoplankton species composition in Antarctic coastal waters, as well as the open Southern Ocean, continues to represent an important research area, given the impact of biogeochemical cycling in the Southern Ocean on climate change processes (Boyd and Doney, 2003).

The austral summer blooms in the western Ross Sea are responsible for carbon export to deeper waters (Arrigo et al., 2000) and changes in the phytoplankton community structure can have a strong impact on the carbon flux and biogeochemical properties of the water column. The colonial haptophyte *Phaeocystis antarctica* bloom that developed in TNB under a stably stratified water column with a shallow MLD during summer 2009–2010, does not conform to our current understanding

regarding climatological bloom dynamics in TNB. Changes in the delivery of iron and/or Vitamin B_{12} are the most likely factors impacting the change in the phytoplankton community composition in TNB.

Acknowledgments

This study was carried out within the framework of the Italian National Program for Antarctic Research (PNRA, 2009/A1.13), which provided financial and logistic support. We thank the officers, crew, and technical personnel on board of the M/V Malippo for their support during the seagoing operations. The authors are grateful to Augusto Passarelli for nutrient analyses made in Italy. Our special thanks to Prof Gian Carlo Carrada for his valuable criticism on this work and to anonymous referees for their suggestions.

Appendix A. Supplementary data

Supplementary data to this article can be found online at https://doi.org/10.1016/j.marenvres.2019.05.012.

References

Alderkamp, A.C., Kulk, G., Buma, A.G.J., Visser, R.J.W., Van Dijken, G.L., Mills, M.M., Arrigo, K.R., 2012. The effect of iron limitation on the photophysiology of *Phaeocystis antarctica* (Prymnesiophyceae) and *Fragilariopsis cylindrus* (Bacillariophyceae) under dynamic irradiance. J. Phycol. 48 (1), 45–59. https://doi.org/10.1111/j.1529-8817.2011.01098.x.

Arrigo, K.R., Robinson, D.H., Worthen, D.L., Dunbar, R.B., DiTullio, G.R., van Woert, M., Lizotte, M.P., 1999. Phytoplankton community structure and the drawdown of nutrients and CO_2 in the Southern Ocean. Science 283, 365–367. https://doi.org/10.1126/science.283.5400.365.

Arrigo, K.R., DiTullio, G.R., Dunbar, R.B., Robinson, D.H., VanWoert, M., Worthen, D.L., Lizotte, M.P., 2000. Phytoplankton taxonomic variability in nutrient utilization and primary production in the Ross Sea. J. Geophys. Res. 105, 8827–8846. https://doi.org/10.1029/1998JC000289.

Arrigo, K.R., van Dijken, G.L., 2004. Annual cycles of sea ice and phytoplankton near Cape Bathurst, southeastern Beaufort Sea, Canadian Arctic. Geophys. Res. Lett. 31, L08304. https://doi.org/10.1029/2003GL018978.

Arrigo, K.R., Dunbar, R.B., Lizotte, M.P., Robinson, D.H., 2002. Taxon-specific differences in C/P and N/P drawdown for phytoplankton in the Ross Sea, Antarctica. Geophys. Res. Lett. 29, 1938. https://doi.org/10.1029/2002GL015277.

Arrigo, K.R., Mills, M.M., Kropuenske, L.R., van Dijken, G.L., Alderkamp, A.-C., Robinson, D.H., 2010. Photophysiology in two major Southern Ocean phytoplankton taxa: photosynthesis and growth of *Phaeocystis antarctica* and *Fragilariopsis cylindrus* under different irradiance levels. Integr. Comp. Biol. 1–17. https://doi.org/10.4319/lo.2009.54.4.1176.

Barlow, R.G., Mantoura, R.F.C., Gough, M.A., Fileman, T.W., 1993. Phaeopigment distribution during the 1990 spring bloom in the north eastern Atlantic. Deep-Sea Res. II 40, 2229–2242. https://doi.org/10.1016/0967-0637(93)90101-8.

Bender, S.J., Moran, D.M., McIlvin, M.R., Zheng, H., McCrow, J.P., Badger, J., DiTullio, G.R., Allen, A.E., Saito, M.A., 2018. Colony formation in *Phaeocystis antarctica*: connecting molecular mechanisms with iron biogeochemistry. Biogeosciences 15, 4923–4942. https://doi.org/10.5194/bg-15-4923-2018.

Bertrand, E.M., Saito, M.A., Rose, J.M., Riesselman, C.R., Lohan, M.C., Noble, A.E., Lee, P.A., DiTullio, G.R., 2007. Vitamin B_{12} and iron colimitation of phytoplankton growth in the Ross Sea. Limnol. Oceanogr. 52 (3), 1079–1093. https://doi.org/10.4319/lo.2007.52.3.1079.

Bertrand, E.M., Saito, M.A., Lee, P.A., Dunbar, R.B., Sedwick, P.N., DiTullio, G.R., 2011. Iron limitation of a springtime bacterial and phytoplankton community in the Ross Sea: implications for Vitamin B_{12} nutrition. Front. Microbiol. 2, 1–12. https://doi.org/10.3389/fmicb.2011.00160.

Bertrand, E.M., McCrow, J.P., Moustafa, A., Zheng, H., Mcquaid, J., Delmont, T., Post, A.F., Sipler, R.E., Spackeen, J.L., Xu, K., Bronk, D.A., Hutchins, D.A., Allen, A.E., 2015. Phytoplankton-bacterial interactions mediate micronutrient colimitation at the coastal Antarctic sea ice edge. Proc. Natl. Acad. Sci. 112, 9938–9943. https://doi.org/10.1073/pnas.1501615112.

Boyd, P.W., Doney, S.C., 2003. The impact of climate change and feedback processes on the ocean carbon cycle. In: Fasham, M.J.R. (Ed.), Ocean Biogeochemistry. The Role of the Ocean Carbon Cycle in Global Change. Springer, pp. 156–193 The IGBP Series.

Boyd, P.W., Doney, S.C., Strzepek, R., Dusenberry, J., Lindsay, K., Fung, I., 2008. Climate-mediated changes to mixed-layer properties in the Southern Ocean: assessing the phytoplankton response. Biogeosciences 5, 847–864. https://doi.org/10.5194/bg-5-847-2008.

Brunet, C., Mangoni, O., 2010. Determinazione quali-quantitativa dei pigmenti fitoplanctonici mediante HPLC. In: In: Socal, G., Buttino, I., Cabrini, M., Mangoni, O., Penna, A., Totti, C. (Eds.), Metodologie di studio del Plancton marino, vol. 56. ISPRA, pp. 379–385.

Brzezinski, M.A., 1985. The Si:C:N ratio of the marine diatoms: interspecific variability and the effect of some environmental variables. J. Phycol. 21, 347–357. https://doi.org/10.1111/j.0022-3646.1985.00347.x.

Caron, D.A., Dennett, M.R., Lonsdale, D.J., Moran, D.M., Shalapyonok, L., 2000. Microzooplankton herbivory in the Ross Sea, Antarctica. Deep-Sea Res. Part II 47, 3249–3272.

Delmont, T.O., Eren, A.M., Vineis, J.H., Post, A.F., 2015. Genome reconstructions indicate the partitioning of ecological functions inside a phytoplankton bloom in the Amundsen Sea. Antarctic 5, 1090. https://doi.org/10.3389/fmicb.2015.01090.

DiTullio, G.R., Smith Jr., W.O., 1996. Spatial patterns in phytoplankton biomass and pigment distributions in the Ross Sea. J. Geophys. Res. 101, 18467–18477. https://doi.org/10.1029/96JC00034.

DiTullio, G.R., Geesey, M.E., Leventer, A.R., Lizotte, M.P., 2003. Algal pigment ratios in the Ross Sea: implications for CHEMTAX analysis of Southern Ocean data. In: Di Tullio, G.R., Dunbar, R.B. (Eds.), Biogeochemistry of the Ross Sea. Antarctic Research Series 78. American Geophysical Union, Washington DC, USA, pp. 279–293.

DiTullio, G.R., Garcia, N., Riseman, S.F., Sedwick, P.N., 2007. Effects of iron concentration on pigment composition in *Phaeocystis antarctica* grown at low irradiance. Biogeochemistry 83, 71–81. https://doi.org/10.1007/s10533-007-9080-8.

Dubois, M., Gilles, K.A., Hamilton, J.K., Rebers, P.A., Smith, F., 1956. Colorimetric method for determination of sugars and related substances. Anal. Chem. 39, 350–356. https://doi.org/10.1021/ac60111a017.

Dunbar, R.B., Arrigo, K.R., DiTullio, G.R., Leventer, A., Lizotte, M.P., Van Woert, M.L., Robinson, D.H., 2003. Non-Redfield production and export of marine organic matter: a recurrent part of the annual cycle in the Ross Sea, Antarctica. In: DiTullio, G.R., Dunbar, R.B. (Eds.), Biogeochemistry of the Ross Sea. Ant Res Ser, 78. American Geophysical Union, Washington, DC, pp. 79–196.

Elliott, D.T., Tang, K.W., Shields, A.R., 2009. Mesozooplankton beneath the summer sea ice in McMurdo Sound, Antarctica: abundance, species composition, and DMSP content. Polar Biol. 32, 113–122. https://doi.org/10.1007/s00300-008-0511-3.

Feng, Y., Hare, C.E., Rose, J.M., Handy, S.M., DiTullio, G.R., Lee, P.A., Smith Jr., W.O., Peloquin, J., Tozzi, S., Sun, J., Zhang, Y., Dunbar, R.B., Long, M.C., Sohst, B., Lohan, M., Hutchins, D.A., 2010. Interactive effects of iron, irradiance and CO_2 on Ross Sea phytoplankton. Deep-Sea Res. Part I 57, 368–383. https://doi.org/10.1016/j.dsr.2009.10.013.

Garcia, N.S., Sedwick, P.N., DiTullio, G.R., 2009. Influence of irradiance and iron on the growth of colonial *Phaeocystis antarctica*: implications for seasonal bloom dynamics in the Ross Sea, Antarctica. Aquat. Microb. Ecol. 57, 203–220. https://doi.org/10.3354/ame01334.

Garrison, D.L., Gibson, A., Kunze, H., Gowing, M.M., Vickers, C.L., Mathot, S., Bayre, R.C., 2003. The Ross Sea polynya Project: diatom- and phaeocystis-dominated phytoplankton assemblages in the Ross Sea, Antarctica, 1994 and 1995. In: DiTullio, G.R., Dunbar, R.B. (Eds.), Biogeochemistry of the Ross Sea. American Geophysical Union, Washington, DC, pp. 53–76.

Garrison, D.L., Gibson, A., Coale, S.L., Gowing, M.M., Okolodkov, Y.B., Fritsen, C.H., Jeffries, M.O., 2005. Sea-ice Microbial Communities in the Ross Sea: Autumn and Summer Biota Marine Ecology Progress Series, vol. 300. pp. 39–52. https://doi.org/10.3354/meps300039.

Gordon, L.I., Codispoti, L.A., Jennings, J.C., Morrison, J.M., Millero, F.J., Sweeney, C., 2000. Seasonal evolution of hydrographic properties in the Ross Sea, Antarctica, 1996-1997. Deep-Sea Res. Part II 47, 3095–3117. https://doi.org/10.1016/S0967-0645(00)00060-6.

Haberman, L.K., Quetin, B.L., Ross, M.R., 2003. Diet of the antarctic krill (*Euphausia superba* dana): I. Comparisons of grazing on *Phaeocystis Antarctica* (karsten) and *Thalassiosira antarctica* (comber). J. Exp. Mar. Biol. Ecol. 283 (1–1), 79–95. https://doi.org/10.1016/S0022-0981(02)00466-5.

Hales, T., Takahashi, T., 2004. High-resolution biogeochemical investigation of the Ross Sea, Antarctica, during the AESOPS (U. S. JGOFS) Program. Glob. Biogeochem. Cycles 18, GB3006. https://doi.org/10.1029/2003GB002165.

Hansen, H.P., Grasshoff, K., 1983. Automated chemical analysis. In: Grasshoff, K., Ehrardt, M., Kremlin, K. (Eds.), Methods of Seawater Analysis. Chemie, Weinheim, pp. 347–379.

Hartree, E.F., 1972. Determination of proteins: a modification of the Lowry method that gives a linear photometric response. Anal. Biochem. 48, 422–427. https://doi.org/10.1016/0003-2697(72)90094-2.

Hedges, J.I., Stern, J.H., 1984. Carbon and nitrogen determination of carbonate-containing solids. Limnol. Oceanogr. 29, 657–663. https://doi.org/10.4319/lo.1984.29.3.0657.

Holm-Hansen, O., Lorenzen, C.J., Holmes, R.W., Strickland, J.D.H., 1965. Fluorometric determination of chlorophyll. J. Conseil - Conseil Perm. Int. Explor. Mer 30, 3–15.

Hutchins, D.A., Bruland, K.W., 1998. Iron-limited diatom growth and Si/N uptake ratios in a coastal upwelling regime. Nature 393, 561–564. https://doi.org/10.1038/31203.

Innamorati, M., Lazzara, L., Mori, G., Saggiomo, V., 1991. Phytoplankton ecology. In: National Scientific Commission for Antarctica, vol. 1. Data Rep Part, Genova, pp. 141–252 Oceanographic Campaign 1989-90.

Innamorati, M., Mori, G., Massi, L., Lazzara, L., Nuccio, C., 2000. Phytoplankton biomass related to environmental factors in the Ross Sea. In: Faranda, F.M., Guglielmo, L., Ianora, A. (Eds.), Ross Sea Ecology Italian Antarctic Expeditions (1987–1995). Springer, Berlin, pp. 259–273.

Jeffrey, S., Mantoura, R., Wright, S. (Eds.), 2005. Phytoplankton Pigments in Oceanography. Guidelines to Modern Methods. Monographs on Oceanographic Methodology, second ed. UNESCO, Paris, pp. 661.

Knauss, J.A., Garfield, N., 2017. Introduction to Physical Oceanography. Waveland Press, Inc. long Grove, I.L, pp. 310.

Kohut, J.T., Kustka, A.B., Hiscock, M., Lam, P.J., Measures, C., Milligan, A., et al., 2017. Mesoscale variability of the summer bloom over the northern Ross Sea shelf: a tale of two banks. J. Mar. Syst. 166, 50–60. https://doi.org/10.1016/j.jmarsys.2016.10.010.

Kropuenske, L.R., Mills, M.M., Van dijken, G.L., Baileyd, S., Robinson, D.H., Welschmeyer, N.A., Arrigo, K.R., 2009. Photophysiology in two major Southern Ocean phytoplankton taxa: photoprotection in *Phaeocystis antarctica* and *Fragilariopsis cylindrus*. Limnol. Oceanogr. 54, 1176–1196. https://doi.org/10.1093/icb/icq021.

Lonsdale, D.J., Caron, D.A., Dennett, M.R., SchaVner, R., 2000. Predation by *oithona* spp. on protozooplankton in the Ross Sea, Antarctica. Deep-Sea Res. Part II 47, 3273–3283. https://doi.org/10.1016/S0967-0645(00)00068-0.

Mangoni, O., Modigh, M., Conversano, F., Carrada, G.C., Saggiomo, V., 2004. Effects of summer ice coverage on phytoplankton assemblages in the Ross Sea, Antarctica. Deep-Sea Res. Part I 51 (11), 1601–1617. https://doi.org/10.1016/j.dsr.2004.07.006.

Mangoni, O., Saggiomo, M., Modigh, M., Catalano, G., Zingone, A., Saggiomo, V., 2009. The role of platelet ice microalgae in seeding phytoplankton blooms in Terra Nova Bay (Ross Sea, Antarctica): a mesocosm experiment. Polar Biol. 3 (32), 311–323. https://doi.org/10.1007/s00300-008-0507-z.

Mangoni, O., Saggiomo, V., Bolinesi, F., Margiotta, F., Budillon, G., Cotroneo, Y., Misic, C., Rivaro, P., Saggiomo, M., 2017. Phytoplankton Blooms during Austral Summer in the Ross Sea, Antarctica: Driving Factors and Trophic Implications PLoS ONE. https://doi.org/10.1371/journal.pone.0176033.

Mangoni, O., Saggiomo, V., Bolinesi, F., Saggiomo, M., 2018. A review of past and present summer primary production processes in the Ross Sea in relation to changing ecosystems. Ecol. Quest. 29 (3), 75–85. https://doi.org/10.12775/EQ.2018.024.

Marsay, C., Barrett, P.M., McGillicuddy, D.J., Sedwick, P., 2017. Distributions, sources and transformations of dissolved and particulate iron on the Ross Sea continental shelf during summer. J. Geophys. Res.: Oceans 122 (8), 6371–6393. https://doi.org/10.1002/2017JC013068.

Martin, J.H., Gordon, R.M., Fitzwater, S.E., 1990. Iron deficiency limits phytoplankton growth in Antarctic waters. Glob. Biogeochem. Cycles 4 (1), 5–12. https://doi.org/10.1029/GB004i001p00005.

Mathot, S., Smith, W.O., Carlson Jr., C.A., Garrison, D.L., Gowing, M.M., Vickers, C.L., 2000. Carbon partitioning within *Phaeocystis antarctica* (prymnesiophyceae) colonies in the Ross Sea, Antarctica. J. Phycol. 36, 1049–1056. https://doi.org/10.1046/j.1529-8817.2000.99078.x.

McGillicuddy, D.J., Sedwick, P.N., Dinniman, M.S., Arrigo, K.R., Bibby, T.S., Greenan, B.J.W., Hofmann, E.E., Klinck, J.M., Smith Jr., W.O., Mack, S.L., Marsay, C.M., Sohst, B.M., van Dijken, G.L., 2015. Iron supply and demand in an Antarctic shelf ecosystem. Geophys. Res. Lett. 42 (19), 8088–8097. https://doi.org/10.1002/2015GL065727.

Mills, M.M., Kropuenske, L.R., van Dijken, G.L., Alderkamp, A.-C., Berg, G.M., Robinson, D.H., Welschmeyer, N.A., Arrigo, K.R., 2010. Photophysiology in two Southern Ocean phytoplankton taxa: photosynthesis of *Phaeocystis antarctica* (Prymnesiophyceae) and *Fragilariopsis cylindrus* (Bacillariophyceae) under simulated mixed-layer irradiance. J. Phycol. 46, 1114–1127. https://doi.org/10.1111/j.1529-8817.2010.00923.x.

Misic, C., Castellano, M., Ruggieri, N., Povero, P., 2006. Dissolved organic matter characterisation and temporal trends in Terra Nova Bay (Ross Sea, Antarctica). Estuarine. Coast Shelf Sci. 70, 405–414.

Nuccio, C., Innamorati, M., Lazzara, L., Mori, G., Massi, L., 2000. Spatial and temporal distribution of phytoplankton assemblages in the Ross Sea. In: Faranda, F.M., Guglielmo, L., Ianora, A. (Eds.), Ross Sea Ecology, Italian Antarctic Expeditions (1987–1995). Springer, Berlin, pp. 231–245.

Peloquin, J.A., Smith Jr., W.O., 2007. Phytoplankton blooms in the Ross Sea, Antarctica: interannual variability in magnitude, temporal patterns, and composition. J. Geophys. Res. 112, C08013. https://doi.org/10.1029/2006JC003816.

Povero, P., Castellano, M., Ruggieri, N., Monticelli, L., Saggiomo, V., Chiantore, M., Guidetti, M., Cattaneo-Vietti, R., 2006. Water column features and their relationship with sediments and benthic communities along the Victoria Land coast (Ross Sea, summer 2004). Antarct. Sci. 18 (4), 603–613.

Povero, P., Cattaneo-Vietti, R., Chiantore, M.C., Castellano, M., Mangoni, O., Saggiomo, V., Schiaparelli, S., Vacchi, M., 2012. Baia Terra Nova (BTN). In: Aracne (Ed.), La rete italiana per la ricerca ecologica a lungo termine (LTER-Italia): situazione e prospettive dopo un quinquennio di attività (2006-2011). A cura di Bertoni R. Pubblicazione CNR, 978-88-548-4661-6, pp. 222–226.

Rivaro, P., Ianni, C., Langone, L., Ori, C., Aulicino, G., Cotroneo, Y., Saggiomo, M., Mangoni, O., 2017. Physical and biological forcing on the mesoscale variability of the carbonate system in the Ross Sea (Antarctica) during the summer season 2014. J. Mar. Syst. 166, 144–158. https://doi.org/10.1016/j.jmarsys.2015.11.002.

Rivaro, P., Ardini, F., Grotti, M., Aulicino, G., Cotroneo, Y., Mangoni, O., Bolinesi, F., Saggiomo, M., Celussi, M., 2019. Mesoscale variability related to iron speciation in a coastal Ross Sea area (Antarctica) during summer 2014. Chem. Ecol. 35 (1), 1–19. https://doi.org/10.1080/02757540.2018.1531987.

Ryan-Keogh, T.J., DeLizo, M.L., Smith Jr., W.O., Sedwick, N.P., McGillicuddy Jr., D.J., Moore, M., Bibby, T.S., 2017. Temporal progression of photosynthetic-strategy in phytoplankton in the Ross Sea, Antarctica. J. Mar. Syst. 166, 87–96. https://doi.org/10.1016/j.jmarsys.2016.08.014.

Saggiomo, V., Carrada, G.C., Mangoni, O., Ribera d'Alcalà, M., Russo, A., 1998. Spatial and temporal variability of size-fractionated biomass and primary production in the Ross Sea (Antarctica) during austral spring and summer. J. Mar. Syst. 17, 115–127. https://doi.org/10.1016/S0924-7963(98)00033-5.

Saggiomo, V., Carrada, G.C., Mangoni, O., Marino, D., Ribera d'Alcalà, M., 2000. Physiological and ecological aspects of primary production in the Ross Sea. In: Faranda, F.M., Guglielmo, L., Ianora, A. (Eds.), Ross Sea Ecology, Italian Antarctic Expeditions (1987–1995). Springer, Berlin, pp. 247–258.

Saggiomo, V., Catalano, G., Mangoni, O., Budillon, G., Carrada, G.C., 2002. Primary production processes in ice-free waters of the Ross Sea (Antarctica) during the austral summer 1996. Deep-Sea Res. Part II 49, 1787–1801.

Schoemann, V., Becquevort, S., Stefels, J., Rousseau, V., Lancelot, C., 2005. *Phaeocystis* blooms in the global ocean and their controlling mechanisms: a review. J. Sea Res. 53, 43–66. https://doi.org/10.1016/j.seares.2004.01.008.

Sedwick, P.N., DiTullio, G.R., 1997. Regulation of algal blooms in Antarctic shelf waters by the release of iron from melting sea ice. Geophys. Res. Lett. 24 (20), 2515–2518. https://doi.org/10.1029/97GL02596.

Sedwick, P.N., Garcia, N.S., Riseman, S.F., DiTullio, G.R., 2007. Evidence for high iron requirements for colonial *Phaeocystis antarctica* at low irradiance. Biogeochemistry 83 (1–2), 83–97. https://doi.org/10.1007/s10533-007-9081-7.

Sedwick, P.N., Marsay, C.M., Sohst, B.M., Aguilar Islas, A.M., Lohan, M.C., Long, M.C., Arrigo, K.R., Dunbar, R.B., Saito, M.A., Smith, W.O., DiTullio, G.R., 2011. Early season depletion of dissolved iron in the Ross Sea polynya: implications for iron dynamics on the Antarctic continental shelf. J. Geophys. Res. 116 C12019. https://doi.org/10.1029/2010JC006553.

Smayda, T.J., Reynolds, C.S., 2001. Community assembly in marine phytoplankton: application of recent models to harmful dinoflagellate blooms. J. Plankton Res. 23, 447–461.

Smith Jr., W.O., Asper, V.A., 2001. The influence of phytoplankton assemblage composition on biogeochemical characteristics and cycles in the southern Ross Sea, Antarctica. Deep-Sea Res. I 48, 137–161. https://doi.10.1016/S0967-0637(00)00045-5.

Smith Jr., W.O., Gordon, I.L., 1997. Hyperproductivity of the Ross Sea (Antarctica) polynya during austral spring. Geophys. Res. Lett. 24 (3), 233–236. https://doi.org/10.1029/96GL03926.

Smith Jr., W.O., Nelson, D.M., 1985. Phytoplankton bloom produced by a receding ice edge in the Ross Sea: spatial coherence with the density field. Science 227, 163–166. https://doi.org/10.1126/science.227.4683.163.

Smith Jr., W.O., Nelson, D.M., DiTullio, G.R., Leventer, A.R., 1996. Temporal and spatial patterns in the Ross Sea: phytoplankton biomass, elemental composition, productivity and growth rates. J. Geophys. Res. 101, 18455–18466. https://doi.org/10.1029/96JC01304.

Smith Jr., W.O., Marra, J., Hisckock, R.,M., Barber, T.R., 2000. The seasonal cycle of phytoplankton biomass and primary productivity in the Ross Sea, Antarctica. Deep Sea Res. Part II Top. Stud. Oceanogr. 47, 15–16. https://doi.org/10.1016/S0967-0645(00)00061-8.

Smith Jr., W.O., Shields, A.R., Peloquin, J.A., Catalano, G., Tozzi, S., Dinniman, M.S., Asper, V.A., 2006. Biogeochemical budgets in the Ross Sea: variations among years. Deep-Sea Res. Part II 53, 815–833.

Smith Jr., W.O., Ainley, D.G., Arrigo, K.R., Dinniman, M.S., 2014. The oceanography and ecology of the Ross Sea. The Annu. Rev. Mar. Sci. 6, 469–487. https://doi.org/10.1146/annurev-marine-010213-135114.

Sweeney, C., Smith Jr., W.O., Hales, B., Bidigare, R.R., Carlson, C.A., Codispoti, L.A., Gordon, L.I., Hansell, D.A., Millero, F.J., Park, M.-O., Takahashi, T., 2000. Nutrient and carbon removal ratios and fluxes in the Ross Sea, Antarctica. Deep-Sea Res. Part II 47, 3395–3421. https://doi.org/10.1016/S0967-0645(00)00073-4.

Takeda, S., 1998. Influence of iron availability on nutrient consumption ratios of diatoms in oceanic waters. Nature 393, 774–777. https://doi.org/10.1038/31674.

Tang, K.W., Smith Jr., W.O., Elliot, D.T., Schields, A.R., 2008. Colony size of *Phaeocystis antarctica* (Prymnesiophyceae) as influenced by zooplankton grazers. J. Phycol. 44, 1372–1378. https://doi.org/10.1111/j.1529-8817.2008.00595.x.

Utermöhl, H., 1958. Zur vervollkommnung der quantitativen phytoplankton-methodik. Mittl. Int. Ver. Theoretische Angew. Limnol. 9, 1–38.

van Leeuwe, M.A., Stefels, J., 2007. Photosynthetic responses in *Phaeocystis antarctica* towards varying light and iron conditions. Biogeochemistry 83, 61–70. https://doi.org/10.1007/s10533-007-9083-5.

van Leeuwe, M., Visser, R.J.W., Stefels, J., 2014. The pigment composition of *Phaeocystis antarctica* (Haptophyceae) under various conditions of light, temperature, salinity and iron. J. Phycol. 50 (6), 1070–1080. https://doi.org/10.1111/jpy.12238.

Vidussi, F., Claustre, H., Bustillos-Guzman, J., Cailliau, C., Marty, J.C., 1996. Determination of chlorophylls and carotenoids of marine phytoplankton: separation of chlorophyll a from divinylchlorophyll a and zeaxanthin from lutein. J. Plankton Res. 18 (12), 2377–2382. https://doi.org/10.1093/plankt/18.12.2377.

Wang, S., Bailey, D., Lindsay, K., Moore, J.K., Holland, M., 2014. Impact of sea ice on the marine iron cycle and phytoplankton productivity. Biogeosciences 11, 4713–4731. https://doi.org/10.5194/bg-11-4713-2014.

Chemistry and Ecology

ISSN: 0275-7540 (Print) 1029-0370 (Online) Journal homepage: https://www.tandfonline.com/loi/gche20

Mesoscale variability related to iron speciation in a coastal Ross Sea area (Antarctica) during summer 2014

Paola Rivaro, Francisco Ardini, Marco Grotti, Giuseppe Aulicino, Yuri Cotroneo, Giannetta Fusco, Olga Mangoni, Francesco Bolinesi, Maria Saggiomo & Mauro Celussi

To cite this article: Paola Rivaro, Francisco Ardini, Marco Grotti, Giuseppe Aulicino, Yuri Cotroneo, Giannetta Fusco, Olga Mangoni, Francesco Bolinesi, Maria Saggiomo & Mauro Celussi (2019) Mesoscale variability related to iron speciation in a coastal Ross Sea area (Antarctica) during summer 2014, Chemistry and Ecology, 35:1, 1-19, DOI: 10.1080/02757540.2018.1531987

To link to this article: https://doi.org/10.1080/02757540.2018.1531987

Published online: 11 Oct 2018.

Submit your article to this journal

Article views: 73

View related articles

View Crossmark data

Full Terms & Conditions of access and use can be found at
https://www.tandfonline.com/action/journalInformation?journalCode=gche20

CHEMISTRY AND ECOLOGY
2019, VOL. 35, NO. 1, 1–19
https://doi.org/10.1080/02757540.2018.1531987

Taylor & Francis
Taylor & Francis Group

RESEARCH ARTICLE

Check for updates

Mesoscale variability related to iron speciation in a coastal Ross Sea area (Antarctica) during summer 2014

Paola Rivaro [a], Francisco Ardini [a], Marco Grotti [a], Giuseppe Aulicino [b,f], Yuri Cotroneo [b], Giannetta Fusco [b], Olga Mangoni [c], Francesco Bolinesi[c], Maria Saggiomo[d] and Mauro Celussi [e]

[a]Department of Chemistry and Industrial Chemistry, University of Genoa, Genoa, Italy; [b]Department of Science and Technology, Parthenope University of Naples, Naples, Italy; [c]Department of Biology, University of Napoli Federico II, Naples, Italy; [d]Stazione Zoologica Anton Dohrn, Naples, Italy; [e]OGS (Istituto Nazionale di Oceanografia e Geofisica Sperimentale), Oceanography Division, Trieste, Italy; [f]Department of Life and Environmental Sciences, Marche Polytechnic University, Ancona, Italy

ABSTRACT

Dissolved iron (Fe) distribution and speciation was determined in water samples (0–200 m) collected in a coastal area near Terra Nova Bay during the austral summer of 2014. Nutrients, dissolved oxygen, chlorophyll-a, phytoplankton composition and prokaryotic biomass distribution were investigated in combination with measurements of the physical properties of the water columns and its dynamics. The dFe value was above the limiting growth concentration, ranging from 0.52 to 4.51 nM, and it showed a spatial variability with a horizontal length scale of about 10 km, according to the variability of the water column physical properties and to iron sources. The organic ligands (L) maintained the concentrations of dFe at levels much higher than the inorganic solubility of Fe, keeping it available for phytoplankton and the log K'_{FeL} values found (from 22.1 to 23.6) highlighted the presence of complexes of differing stabilities.

ARTICLE HISTORY
Received 17 May 2018
Final Version Received
1 October 2018

KEYWORDS
Ross Sea; mesoscale; dissolved iron; iron speciation; biological activity; Antarctica

1. Introduction

Iron (Fe) is the most important trace metal in the ocean, being involved in several metabolic pathways, including biosynthesis of chlorophyll, transport of electrons through the photosynthetic and respiratory transport chains and nitrate assimilation by phytoplankton [1,2]. In the Southern Ocean, which is strongly characterised by mesoscale activity [3,4] and intense interactions between sea surface and atmosphere [5–7], iron supply influences phytoplankton biomass and species composition, as well as primary productivity in both high and low nitrate surface waters [8,9]. The quantum yield (F_v/F_m) of phytoplankton is Fe-driven and low values should be indicators of Fe stress [10,11]. Moreover, Fe is also used over the whole water column by microbial communities which are responsible for the degradation and remineralisation of sinking organic matter [12]. Fe is present in

CONTACT Paola Rivaro rivaro@chimica.unige.it Department of Chemistry and Industrial Chemistry, University of Genoa, Via Dodecaneso 31, Genoa 16146, Italy

© 2018 Informa UK Limited, trading as Taylor & Francis Group

seawater in different physical (particulate, colloidal, dissolved) and chemical (inorganic and organic complexes) forms. It has been recognised that Fe bioavailability is influenced by the chemical forms, biogeochemical cycling and the different uptake strategies of the phytoplankton and bacterioplankton communities [13]. Despite the dissolved Fe (dFe) concentrations in the ocean being extremely low, they are higher than might be calculated on the basis of the solubility of ferric hydroxide in seawater at pH 8.1 and 25°C due to the ability of iron to form organic complexes [14]. Oceanographic research has shown that more than 99% of the dFe in the ocean is bound to organic ligands [15]. It is now widely recognised that, in high-nutrient low-chlorophyll (HNLC) regions, the algal growth is limited, not only by a general lack of Fe, but also by the bioavailability of organically bound Fe [16–19]. The Ross Sea accounts for almost 30% of the total Southern Ocean annual production [20]. Significant inter-annual variability in phytoplankton biomass has been observed and substantial rates of primary production (>1 g C m^{-2} d^{-1}) are often associated in the shelf area with polynyas, fronts and marginal ice zones [21–24]. Field observations and model simulations indicate four potential sources of dFe to the Ross Sea surface waters: Circumpolar Deep Water (CDW) intruding from the shelf edge, sediments on shallow banks and nearshore areas, melting sea ice around the perimeter of the polynya and glacial meltwater from the Ross Ice Shelf (RIS) [25]. Fe availability and its influence on phytoplankton structure and nutrient cycling has been extensively studied in the Ross Sea [26–31]. Fe limitation has been reported in offshore waters north of the continental shelf, but evidence suggests that Fe limitation is important in the highly productive shelf area too [32–34]. Our understanding of the distribution and speciation of dFe in the Ross Sea has been improved significantly in the past two decades; however, there have only been a few studies on their mesoscale variability. To fill this lack, the Ross Sea Mesoscale Experiment (RoME) was designed to investigate the short temporal and small spatial scales (i.e. mesoscale with an horizontal resolution of few km) variability of biogeochemical properties of the upper 200 m layers in the Ross Sea and to study their interaction with mesoscale currents, fronts and eddies that can facilitate the supply of dFe to the surface waters.

RoME used a combination of remote sensing and high-resolution ship measurements during a cruise in the austral summer 2013–14, as a part of the Italian National Program of Research in Antarctica (PNRA, Programma Nazionale di Ricerca in Antartide). Remote sensing supported both the determination of the iron sampling strategy and the deployment of 43 complete casts, with a horizontal resolution of 5–10 km. Near-real-time satellite images of the study area were sent twice a day to the research vessel in order to design the sampling strategy. The sampling activity was performed in three different areas of the Ross Sea, named RoME 1, 2 and 3. The aim of the present paper is to characterise the mesoscale iron speciation in the RoME 2 site, a coastal area next to the recurrent winter Terra Nova Bay polynya. This polynya plays a major role in shaping the sea ice and ocean dynamics of this region [35,36] and is characterised by high biological primary production which favours atmospheric carbon sequestration into the ocean [38]. Additionally, previous papers showed the presence of significant chemical and biological mesoscale variability in the RoME 2 area, mainly connected to the different water mass properties observed and to the presence of a thermohaline front associated to changes in the current pattern [11,37,38].

2. Materials and methods

2.1. Sampling strategy and water sampling

The data were collected aboard the R.V. Italica, as part of RoME 2 area from 26 to 28 January 2014. The RoME 2 study area has an extension of ca. 35 × 30 km and was monitored through 12 complete multi-parameter casts. The position of the CTD stations (Figure 1) was chosen on the basis of the available MODIS (Moderate Resolution Imaging Spectroradiometer) Aqua and Terra satellites level-2 products relative to the previous 12/24 hours. Sea surface temperature (SST) and chlorophyll-a concentration (Chl-a) maps at 1 km resolution were generated, analysed and transmitted to the ship to allow sampling of both high and low chlorophyll and temperature regions. Full depth hydrographic casts, current measurement and water sampling were carried out using a SBE 9/11 Plus CTD, with dual temperature and conductivity sensors, coupled with a SBE 32 plastic coated carousel sampler, on which twenty-four 12-L Niskin bottles and a couple of Acoustic Doppler Current Profiler (ADCP) were mounted. The properties of the ocean deep layers will not be treated in this paper, because the objectives of the RoME Project were focused on the upper 200 m of the water column.

During RoME 2, a total of 12 casts was realised and in each cast, 5–7 depths (2–200 m, chosen according to the fluorescence profiles) were sampled for dissolved oxygen, nutrients, phytoplankton pigments and total prokaryote biomass determination. At selected stations (Figure 1 and Table 1), seawater samples for iron analysis were collected by a 20-L teflon-lined GO-FLO bottle (General Oceanics Inc.) which was deployed on a kevlar 6 mm diameter line and closed using a PVC messenger. Seawater was transferred in acid-cleaned (see Section 2.2.1) 2-L low-density polyethylene (LDPE) bottles and immediately treated as reported below (see Section 2.2.2).

2.2. Analytical procedures

2.2.1. Cleaning procedures for iron analysis

All the materials coming into contact with the samples were extensively acid-cleaned and the final cleaning conditions were checked by inductively coupled plasma mass spectrometry (ICP-MS). In particular, 2-L LDPE bottles for seawater collection (Nalgene, Rochester, NY, USA) and the polycarbonate (PC) filtration apparatus (Sartorius, Goettingen, Germany) were cleaned as follows: (1) 1% (v/v) tracepur® HNO_3 (Merck, Darmstadt, Germany) for 2–3 days; (2) rinsing 3 times with ultrapure water (Milli-Q from Merck-Millipore); (3) 0.1% (v/v) suprapur® HNO_3 (Merck) for 2–3 days; (4) rinsing 3 times with ultrapure water. The 0.4-µm PC filters membranes (HTTP04700 Isopore™ by Millipore) and the 200-mL polypropylene (PP) bottles (VWR International, Radnor, PA, USA) used for the collection and storage of filtered samples were cleaned with the same procedure, but using two-times lower acid concentration and suprapur® grade quality acid for both steps (1) and (3). PC 85-mL centrifuge tubes (Nalgene) for the co-precipitation procedure (Section 2.2.2) were acid-cleaned following the five-step procedure reported in [45]. PP 50-mL and 15-mL graduated tubes (VWR International) for iron speciation analysis were cleaned using 0.1% (v/v) HNO_3 (TraceSelect® Ultra from Sigma-Aldrich) and thoroughly rinsed with ultrapure water.

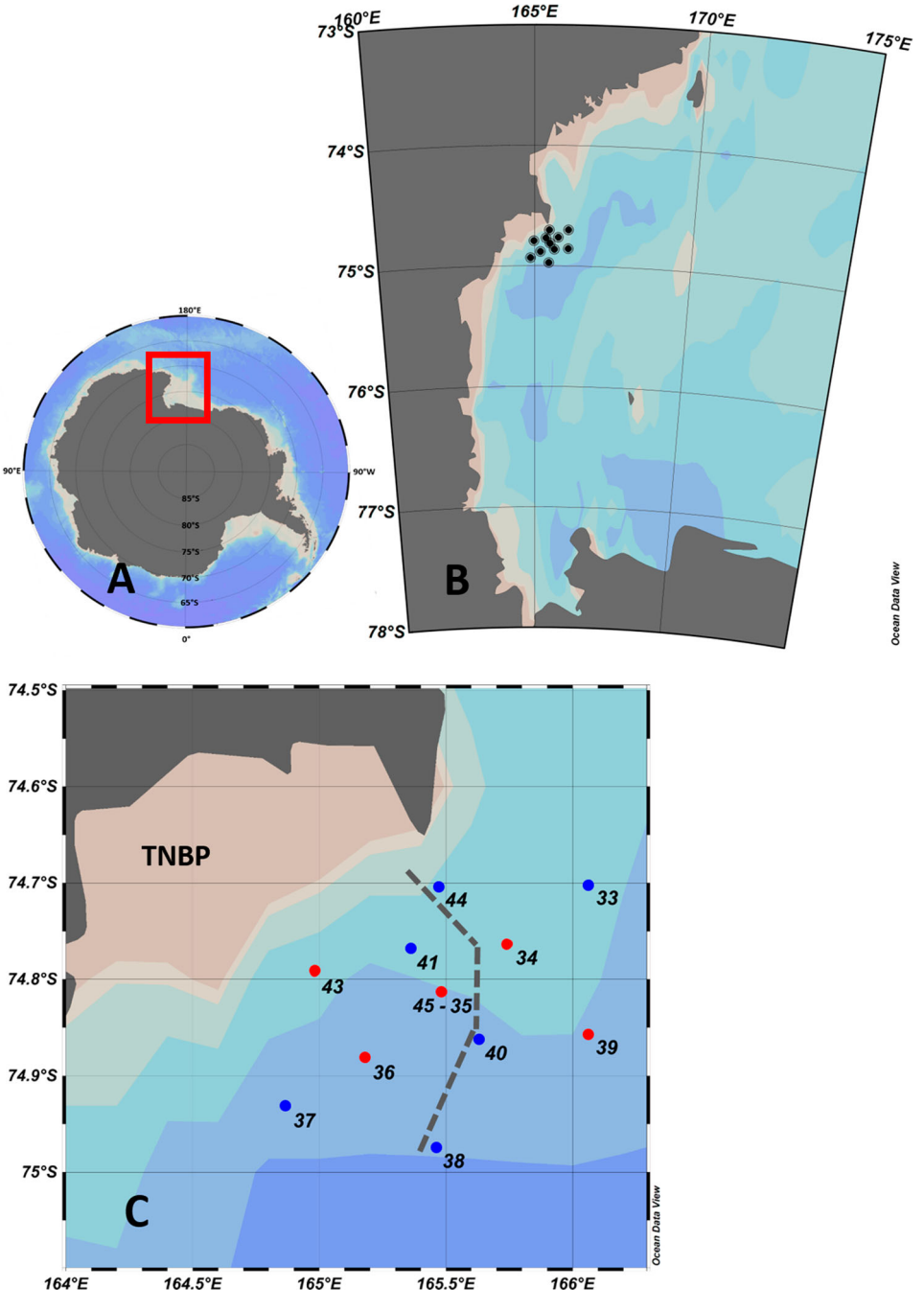

Figure 1. Map of the study site RoME 2 in the Ross Sea. (A) the Ross Sea inside the Southern Ocean; (B) the sampled area inside the Ross Sea; (C) the sampled stations: the red dots show the stations sampled for iron and the dashed grey line the position of the front (colour online).

Table 1. Sampling stations and collected samples for iron determination.

Station	Latitude (S)	Longitude (E)	Bottom depth (m)	Sampling date	Sampled depths (m)
34	−74.772	165.739	719	26/01/2014	10, 30, 60
36	−74.891	165.193	818	27/01/2014	10, 20, 160
39	−74.860	166.073	1080	27/01/2014	20, 50, 200
43	−74.799	164.990	775	27/01/2014	20, 40, 200
45	−74.826	165.486	702	28/01/2014	10, 25, 200

2.2.2. Total dissolved iron

Seawater samples were filtered through 0.4 µm pore-size PC membranes, collected in 200-mL PP bottles and stored at −20°C until analysis.

The total dissolved Fe was determined by ICP-MS after a metal pre-concentration procedure through co-precipitation with $Mg(OH)_2$ [39], based on a previous work by Wu and Boyle [40]. In brief, under a laminar flow work area, aliquots of seawater samples were acidified (pH 1.8) at least 24 h before analysis. Then, 50.0 g of sample were transferred into an acid-cleaned 85-mL PC centrifuge tube (Nalgene) and 500 µL of concentrated NH_4OH (Trace Select® Ultra from Sigma-Aldrich) were added. After 1.5 min, the tube was quickly shaken and left to stand for 3 min. The sample was centrifuged (3000 rpm, 3 min) and most of the supernatant discarded. Then, the centrifugation was repeated and the remaining solution removed. The resulting precipitate was dissolved in 5 mL of 1% (v/v) HNO_3 (Trace Select® Ultra from Sigma-Aldrich) and the solution analysed by ICP-MS equipped with a dynamic reaction cell (DRC). The ICP-MS system used was a Perkin Elmer-Sciex (Concord, Ontario, Canada) Elan DRC II, equipped with PFA-ST micronebulizer (Elemental Scientific, Omaha, NE, USA) and a 20-mL inner volume Cinnabar spray chamber (Glass Expansion, Melbourne, Australia). Platinum sampler and skimmer cones were used. The operating conditions (Table 2) were optimised according to Tanner et al. [41]. The monitored ions were $^{54}Fe^+$ and $^{52}Cr^+$ and the latter was used to correct the isobaric interference due to $^{54}Cr^+$ by means of the following equation: $I(^{54}Fe) = I(54) - 0.028226\ I(^{52}Cr)$. Since the seawater samples have similar composition, calibration was performed by the 'addition calibration' technique [42], a simplification of the standard

Table 2. ICP-MS operating parameters.

Parameter	Value
RF power	1500 W
Plasma gas flow rate	14.5 L min^{-1}
Auxiliary gas flow rate	1.65 L min^{-1}
Nebulizer gas flow rate	1.00 L min^{-1}[a]
Sample uptake rate	100 µL min^{-1}
Lens voltage	6 V[a]
Reaction cell rod offset	−1 V
Quadrupole rod offset	−8 V
RF amplitude	150 V
Axial field voltage	300 V
Cell path voltage	−28 V
Mathieu stability parameters	$a = 0$ $q = 0.57$
Reaction gas flow rate (NH_3)	0.9 mL min^{-1}
Dwell time	100 ms
Sweeps	50
Replicates	10

[a]Optimised daily.

'addition' method, in which the slope obtained for a single representative sample is used for the calibration of the other samples. For each calibration curve, four additions were performed in the 0–6 µg L^{-1} concentration range. The correlation coefficients were higher than 0.999. The procedural blank was 0.15 ± 0.06 nM (mean ± SD, $n = 10$), providing a limit of detection ($3 \times SD_{blank}$) of 0.18 nM. The accuracy of the analytical method was confirmed by replicated analyses of the seawater reference materials SAFe D1 (found concentration: 0.81 ± 0.10 nM, $n = 8$; consensus concentration: ~0.65 ± 0.10 nM) and SAFe D2 (found concentration: 0.99 ± 0.09 nM, $n = 12$; consensus concentration: 0.92 ± 0.03 nM).

2.2.3. Organic complexation of Fe: sample treatment, voltammetric procedure and calculations

Iron speciation was determined by adsorptive cathodic stripping voltammetry (AdCSV) with ligand competition against 2,3-dihydroxynaphtalene (DHN) [43,44].

Under a laminar flow work area, the samples were thawed at ambient temperature and homogenised before transferring 50-mL aliquots into 50-mL PP graduated tubes (VWR International). Then, 250 µL of 0.1 mM methanolic solution of DHN (Sigma-Aldrich) were added and the samples were mixed to obtain a final concentration of 0.5 µM DHN. Incremental additions of Fe(III) standard solution were added to eight 15-mL PP graduated tubes and a 6-mL aliquot of the sample/ligand solution prepared above was pipetted into each tube. The concentrations of Fe(III) additions were selected according to the total Fe concentration of each sample, with approximately four increments in the competition region and four increments where the ligands are saturated. The samples were then left to equilibrate overnight (15 h) in the dark (to prevent the slow oxidation of DHN).

Voltammetric measurements were performed using the 757 VA Computrace system by Metrohm (Herisau, Switzerland), equipped with a mercury drop electrode, Ag/AgCl reference electrode and glassy carbon counter-electrode. The working electrode was filled with 99.999% mercury (Sigma-Aldrich), and the 3M KCl (Sigma-Aldrich) filling solution of the reference electrode was cleaned by MnO_2 co-precipitation [43]. The equilibrated solutions were sequentially (starting from the lowest concentration) transferred into the Teflon® voltammetric cell; then, after addition of 300 µL of bromate/3-[4-(2-hydroxyethyl)-1-piperazinyl]propanesulfonic acid (HEPPS) buffer/oxidant solution (0.4 M potassium bromate/0.1 M HEPPS/0.05 M ammonium hydroxide, all from Sigma-Aldrich) to obtain a pH of 8.0, they were analysed by AdCSV, according to the following method [43]: N_2 purge for 300 s; adsorption potential: −0.1 V; adsorption time: 90 s; rotating speed: 2400 rpm; equilibration time: 8 s; voltage scan: from −0.3 to −0.8 V; scan type: sampled-DC (potential step: 4 mV; frequency: 10 Hz). Four replicate measurements were performed for each aliquot. The voltammetric cell was not rinsed during the titration to keep the cell conditioned. After each sample was analysed, the cell was soaked overnight in 0.5% (v/v) HNO_3 and then thoroughly rinsed with ultrapure water and pre-conditioned before use.

Calculation of the iron speciation parameters was performed by using the following equation [45,46]:

$$\frac{[Fe_{labile}]}{[FeL]} = \frac{[Fe_{labile}]}{L} + \frac{\alpha'_{Fe} + \alpha'_{FeDHN}}{L \cdot K'_{FeL}} \quad (1)$$

where [Fe_{labile}] (labile Fe) in each aliquot was computed by the ratio of the measured peak height to the instrumental sensitivity, while [FeL] (organically bound Fe) was obtained as the difference between the total Fe concentration and labile Fe. The sensitivity was iteratively calculated according to Turoczy and Sherwood [47], and the obtained values were in good agreement (within 10%) with those computed by using the non-linear fitting model by Gerringa et al. [48].

A plot of [Fe_{labile}]/[FeL] as a function of [Fe_{labile}] allowed the determination of L (ligand concentration) and K'_{FeL} (conditional stability constant, here expressed with respect to Fe^{3+}), which were used to calculate the side reaction coefficient of Fe^{3+} and the ligands (α'_{FeL}). The side reaction coefficient for inorganic complexation $\alpha'_{Fe} = 10^{10}$ was obtained from Hudson et al. [49], while $\alpha'_{FeDHN} = 6.4 \times 10^{12}$ was calculated by Laglera et al. [44] and used also to calculate the Fe', i.e. Fe not bound to organic ligands. Finally, L' (concentration of ligands not bound to Fe) was computed as a difference between L and dFe [50].

The method is characterised by great sensitivity, low limits of detection and short analysis time [43]. On the other hand, as other procedures, it is susceptible to potential interferences by humic substances, which would result in an underestimation of the complexing capacity of the natural ligands, as highlighted by a loss of the curvature of the titration plot [44]. A previous investigation in the same area and season reported concentrations of fulvic acids lower than 0.2 mg L^{-1}, while humic acids were not found [51]. In addition, curved titration plots were always obtained (e.g. Figure 2), suggesting a negligible interference of these substances, although humic complexation cannot be completely ruled out.

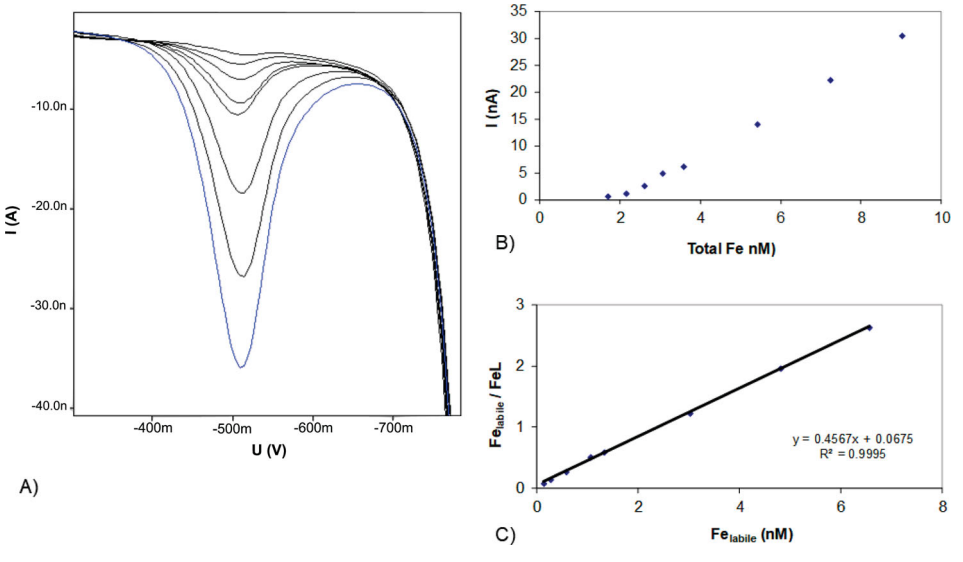

Figure 2. Speciation analysis of seawater sampled in Station 55 at 60 m. (A) Voltammetric scans for the titration with iron; (B) peak height as a function of the total iron concentration; (C) data linearisation with Fe_{labile}/FeL as a function of Fe_{labile}.

2.2.4. Dissolved oxygen, nutrients, phytoplankton pigments and total prokaryote biomass

Dissolved oxygen (O_2) was measured by the Winkler method using automated micro-titrations [52] with a potentiometric detection of the end point using a Metrohm 719 titroprocessor. The measurement precision was ±0.05 mg L^{-1}.

Subsamples for the determination of nutrients (NO_3^-, NO_2^-, NH_4^+, $Si(OH)_4$ and PO_4^{3-}) were collected from the Niskin bottles, filtered through 0.7 µm glass fibre filters (GFF) and stored at −20°C in 100 mL LDPE containers. The samples were analysed using a five-channel continuous flow Technicon® Autoanalyzer II, according to the method described by Hansen and Grasshoff [53], which was adapted to our instrumentation. The accuracy and the precision of the method were checked by Certified Reference Material (CRM) MOOS-3 (Seawater Certified Reference Material for Nutrients; http://www.nrc-cnrc.gc.ca/eng/solutions/advisory/crm/certificates/moos_3.html). Measurement precision was 0.3 µM for NO_3^-+ NO_2^-, 0.01 µM for NO_2^-, 0.07 µM for PO_4^{3-} and 0.30 µM for $Si(OH)_4$. The recoveries fell in the 100–110% range.

Subsamples for the determination of phytoplankton biomass, taxonomic composition and F_v/F_m were collected in the 0–100 m depth layer. For a more detailed description of the methods and of the data see Mangoni et al. [11] and Rivaro et al. [37].

For total prokaryote abundances, samples of 50 mL of seawater were collected directly from the Niskin bottles and fixed with a formaldehyde solution (pre-filtered through a 0.2 µm Acrodisc filter) at 2% final concentration. Aliquots of 3–5 mL were filtered in triplicate onto 0.2 µm black polycarbonate membranes (Whatman). The membranes were then placed on a drop (50 µL) of DAPI (4,6-diamidino-2-phenyl-indole, Sigma-Aldrich, 30 µg mL^{-1} final concentration in an autoclaved 3.7% NaCl solution) and kept in the dark for 15 min [54]. The backs of the filters were then gently dried with a kimwipe tissue, mounted on microscope slides between layers of immersion oil (type A, Cargille) and stored at −20°C. Cells were counted by epifluorescence microscopy (Olympus BX 60 F5) at 1000× magnification under a UV (BP 330–385 nm, BA 420 nm) filter set. A minimum of 300 cells was counted for each membrane in at least 20 randomly selected fields. Prokaryotic biomass was calculated by adopting the 20 fg C $cell^{-1}$ factor [55].

2.3. Ancillary data and data processing

Meltwater percentage in the surface layer (MW%) was calculated from the difference between the salinity measured at the surface (S_{meas}) and at greater depth (S_{deep}, i.e. 200 m) and assuming an average sea ice salinity of 6 [34]:

$$MW\% = 1 - \frac{S_{meas} - 6}{S_{deap} - 6} \cdot 100 \quad (2)$$

All the available CTD profiles were used to determine the depth of the Upper Mixed Layer (UML) through the water column stability (E) analysis. E is proportional to the Brunt-Väisälä buoyancy frequency $N^2(z)$, which represents the strength of the density stratification. The depth at which $N^2(z)$ was estimated to be maximal represents the depth of maximum stability and was selected to represent the UML depth z(UML) [56].

Data processing and statistical analysis were performed using the software RStudio version 0.97.318 (RStudio Inc., Boston, MA, USA). Relationships between all parameters

were evaluated by means of the Pearson's correlation coefficient (r) and the Spearman coefficient (ρ) of rank correlation, after assessing normality of datasets to choose between parametric and non-parametric statistics. The maps were drawn with Ocean Data View software [57].

3. Results

3.1. Environmental conditions and biogeochemical properties

Figure 3 shows the main hydrographic features observed during the RoME 2 experiment. Properties of the water masses and the circulation patterns of the three RoME legs have been already reported and discussed in Mangoni et al. [11], Rivaro et al. [37] and Misic et al. [38]. In RoMe 2, the surface (0-100 m depth) and intermediate layers (100–200 m depth) of the water column were mainly occupied by Antarctic Surface Water (AASW) and High Salinity Shelf Water (HSSW) respectively (Figure 3). AASW is a relatively light surface water characterised by potential temperatures ranging between −1.8°C and +1°C and by salinity values lower than 34.50, while HSSW is characterised by salinity greater than 34.70, potential temperature near freezing point and potential density greater than 27.9 kg m^{-3}[58]. The mean circulation during the RoME 2 experiment was characterised by the presence of a meridionally oriented frontal zone located at about 165.5°E. This front (grey dashed line in Figure 1) has been extensively described in [37] and represents the boundary between two circulation systems characterised by different thermohaline properties and current regime (see Figure 3 and 7 in [37]). In particular, colder and fresher water masses are observed on the western flank of the front and their eastward extension is limited by the front itself. Crossing the front, an increase in both temperature and salinity of the surface layer is evident, with stations located in proximity of the front showing intermediate T and S values between the coastal and open sea stations. Current pattern as depicted by both LADCP and geostrophic current data (not shown) is characterised by eastward current in the coastal stations and prevalently southward currents on the eastern side of the front generating a convergence in correspondence of the front [37].

The water column was well stratified all over the study area, but differences in UML depth and in the strength of the pycnocline were observed [11]. Almost all stations were above the O_2 saturation level (102–115%) in the upper 20 m (Figure 4, panel A). Nutrient concentrations were generally high, with the lowest values in surface and subsurface layers and they were not fully depleted (Figure 4, panels B, C and D). The N:P ratio (calculated from the slope of $NO_3^- + NO_2^-$ plotted against PO_4^{3-}) of 17.0 was consistent with the phytoplankton taxonomic composition data that highlighted the concurrence of diatoms and *P. antarctica* [11,37]. The Si:NO_3 ratio was about 1 suggesting Fe-replete condition, as proven by the dFe data, similarly to previous investigations in the Ross Sea shelf and coastal areas [17,27,28,34]. The net nutrient utilisation was estimated by subtracting the nutrient concentration measured in the UML from that measured in the Winter Water (WW) layer, assuming that the nutrient values in surface water at the beginning of the growing season are similar to those in WW, which are not affected by meltwater dilution or biological uptake [59]. In this study, the concentration of nutrients measured at the depth below the UML, at the top of the WW layer depth z(L), is considered as the reference value for WW (Table 3).

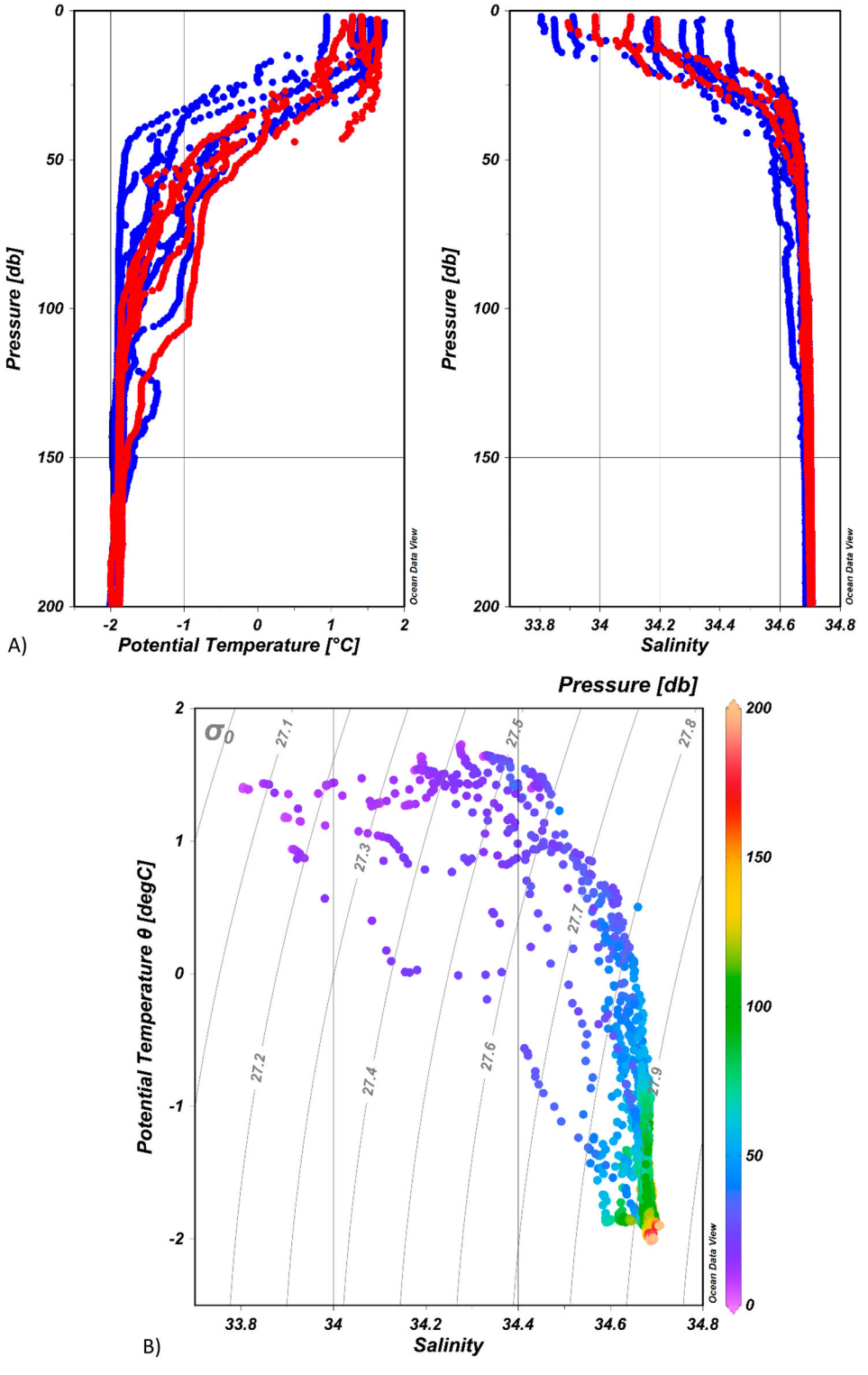

Figure 3. (A) Potential temperature (ITS-90) and salinity (practical) profiles of RoME 2 stations. Red dots show the stations sampled for iron. (B) θ/S diagram colour coded with depth (colour online).

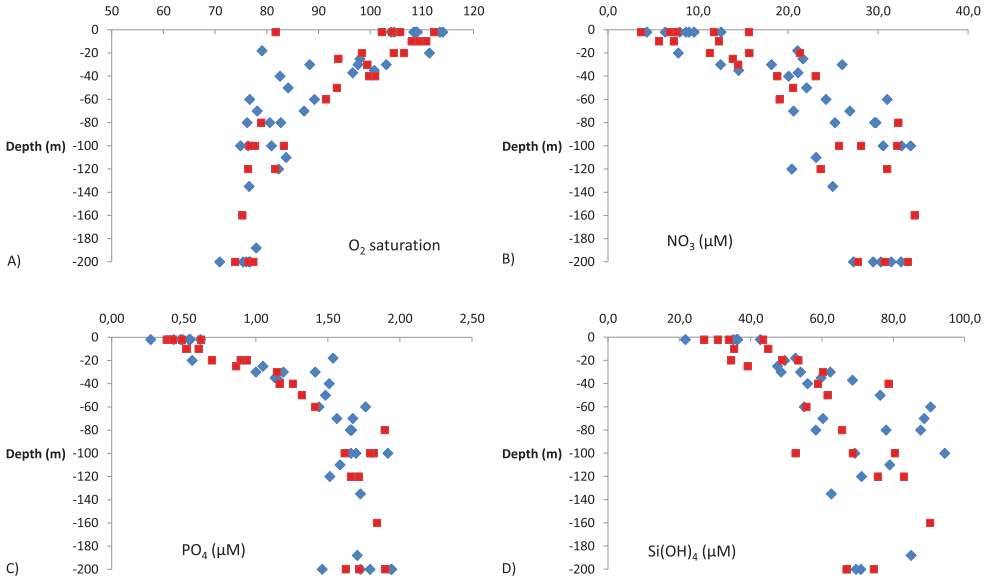

Figure 4. Depth profiles of: (A) dissolved oxygen saturation percentage; (B) nitrate; (C) phosphate and (D) silicate area. Squares show the stations sampled for iron, diamonds refer to the other sampled stations.

The calculated net nutrient utilisation ranges for nitrate, silicic acid and phosphate (ΔNO_3^-, $\Delta Si(OH)_4$ and ΔPO_4^{3-}) were 4.6–13.6, 3.6–24.1 and 0.26–0.82 µM, respectively (Table 3). The highest ΔNO_3^-, which corresponds to the highest ΔPO_4^{3-}, was measured in station 43. The net nutrient utilisation values were in the range of the reported values for the Ross Sea shelf area [59].

Prokaryotic biomass values in the upper 70 m did not display any depth-related trend and ranged between 11.30 (± 0.45) and 14.41 (± 1.06) µg C L^{-1}. Lower values were found between 160 and 200 m, being on average 1.31 ± 0.17 µg C L^{-1}. A highly significant correlation with Chl-a (Spearman's $\rho = 0.65$; $p < .001$; $n = 32$) was found.

Data on phytoplankton biomass, taxonomic composition and F_v/F_m collected in the framework of the RoME project have been already published [11,37,38]. As concerns RoME 2 area, Chl-a maxima were measured from 20 to 40 m depth, but high Chl-a values were also found at greater depth in some stations (up to 2.48 µg L^{-1} at 100 m at station 45). Diatoms, which were observed with empty frustules and in a senescent status, constituted the dominance of the phytoplankton in the upper layer, whereas *Phaeocystis antarctica* in the colonial form dominated in the deep layers. With regards to the photochemical efficiency of

Table 3. Values of strength (Ez(UML)) and depth of the maximum stability (z(UML) of the upper mixed layer, top of the Winter Water depth (z(L)), meltwater percentage (MW%) and calculated nutrient removal (ΔNO_3^-, $\Delta Si(OH)_4$, ΔPO_4^{3-}).

Station	Ez(UML) (m^{-1} * 1000)	z(UML) (m)	z(L) (m)	MW (%)	ΔNO_3^- (µM)	ΔPO_4^{3-} (µM)	$\Delta Si(OH)_4$ (µM)
34	55	32	66	2.09	6.93	0.49	3.57
36	59	16	54	2.51	5.46	0.47	19.3
39	87	25	71	1.23	6.73	0.50	7.59
43	44	26	75	2.83	13.4	0.82	16.8
45	40	18	60	1.80	6.14	0.48	12.1

photosystem II of phytoplankton, the values of F_v/F_m were lower in the presence of diatoms-dominated waters compared with *P. antarctica*-dominated waters.

3.2. Total dissolved iron and iron speciation

Total dissolved iron (dFe) and speciation data are presented in Table 4. The dFe concentration ranged from 0.52 to 4.51 nM, L from 1.4 to 8.0 nM and Fe' from 0.2 to 3.5 pM. The dFe concentrations are comparable with values reported for Antarctic coastal waters [29,34,60–63], and significantly higher than those found in open waters [26]. More than 99% of dFe in our samples was bound to organic ligands, similarly to other seawater analysis carried out in the Southern Ocean [64]. The L values exceeded dFe in all the samples and, as a consequence, L' varied from 0.12 to 2.11 nM. A significant positive correlation was observed between L and dFe (Spearman's $\rho = 0.96$, $p < .001$, $n = 13$). The L/dFe ratio is used to evaluate the saturation level of dissolved organic ligands in the marine environment [65]. When it is close to 1 the ligands are relatively saturated, whereas a higher ratio suggests that the ligands are still available to buffer additional Fe input. The L/dFe varied between 1.07 and 2.82; similar values have been already reported by Boye et al. [17] for Southern Ocean and by Thuróczy et al. [65] for Amundsen Sea shelf waters.

The conditional stability constant (log K'_{FeL}) varied over one order of magnitude, ranging from 22.1 to 23.6; these values are consistent with those reported for the strongest ligands found in the Southern Ocean [48,64,66].

The side reaction coefficient of iron complexation by the natural ligands (log α'_{FeL}) ranged between 13.3 and 14.6, with an average of 14.0 ± 0.5 ($n = 13$).

4. Discussion

The water column properties in the Ross Sea exhibit high levels of spatial and temporal variability and seem to be also linked to larger scales patterns [5,67]. Unfortunately, due to the difficulty in obtaining high-frequency observations, the effect of the mesoscale physical processes on biological and chemical distributions is poorly known, but is still likely to be significant [67]. For this reason, the sampling strategy of the RoME cruise was designed on the basis of real-time satellite data, with the aim of examining selected

Table 4. Iron speciation data.

Station	Depth (m)	dFe (nM)	L (nM)	*SD*	log K'_{FeL}	*SD*	L' (nM)	L/dFe	Fe' (pM)	FeL (%)	log α'_{FeL}
34	10	2.10	4.2	0.1	22.5	0.2	2.11	2.00	0.3	100.0	14.1
	30	1.19	1.7	0.1	22.5	0.1	0.48	1.41	0.8	99.9	13.7
	60	1.95	2.8	0.1	22.8	0.1	0.83	1.43	0.4	100.0	14.2
36	10	0.57	1.4	0.1	22.3	0.1	0.81	2.42	0.3	99.9	13.5
	160	1.80	1.9	0.1	23.3	0.4	0.12	1.07	0.7	100.0	14.6
39	20	1.80	2.5	0.1	22.7	0.1	0.73	1.41	0.5	100.0	14.1
	50	1.21	1.9	0.1	22.7	0.1	0.65	1.54	0.4	100.0	13.9
	200	4.51	5.0	0.1	22.8	0.1	0.48	1.11	1.5	100.0	14.5
43	20	0.65	1.8	0.1	22.2	0.1	1.18	2.82	0.4	99.9	13.4
	40	0.52	1.5	0.1	22.1	0.1	0.99	2.91	0.4	99.9	13.3
	200	3.19	5.0	0.1	22.6	0.1	1.76	1.55	0.4	100.0	14.3
45	10	1.97	–	–	–	–	–	–	–	–	–
	25	1.82	2.0	0.1	23.6	0.6	0.19	1.10	0.2	100.0	14.9
	200	3.29	3.7	0.1	22.3	0.1	0.44	1.13	3.5	99.9	13.9

mesoscale features in detail and to study the biogeochemical processes associated to them. In this framework, the spatial coverage of the RoME 2 area was of ca. 35 × 30 km and was monitored through 12 complete multi-parameter casts and a set of near real-time satellite images.

A thermohaline front was the main physical feature of the area (cf. Figure 1), with the surface layer characterised by a temperature and salinity gradient between the coastal and the easternmost and open ocean station. Fresh and cold water, possibly influenced by both sea or glacier ice melting and then driven offshore by eastwards currents, was observed at stations 41, 43, 44 sampled near Cape Washington and inner bay [11,37,38].

The higher dFe concentration found in the RoME 2 area in the subsurface waters compared with offshore waters (Figure 5, panel G) reflects the iron input either from land [29] or from ice melting, similar to the observations made by Sedwick et al. [28] at stations sampled at the edge of the receding annual pack ice. The iron cycle is closely related to the dynamics of sea ice that acts as a reservoir for iron during winter, releasing it to the surface ocean in spring and summer [68]. The area experienced ice-free conditions starting from early December [11,37]. The melting produced a strong water column stratification highly favourable for iron recycling, through the enrichment of Fe for surface waters and retarding the loss of Fe to deeper waters. Dissolved Fe concentrations were relatively low near the surface in correspondence of the highest MW% (Figure 5, panel C, stations 36 and 43). This apparent contradiction can be explained taking into account the role of the UML stratification in favouring the phytoplankton growth (Figure 5, panels A, B and D). In fact, a reduction in the dFe may be associated with an increase in algal biomass as the iron is taken up. The melting of the sea ice, besides stratifying the water column, supported the phytoplankton growth, as the negative correlation found between dFe and fluorescence (Spearman's $\rho = -.60$, $p < .05$, $n = 14$) together with the O_2 values above the saturation level, the nutrient utilisation and the Chl-a concentrations confirmed (Figure 5, panels E

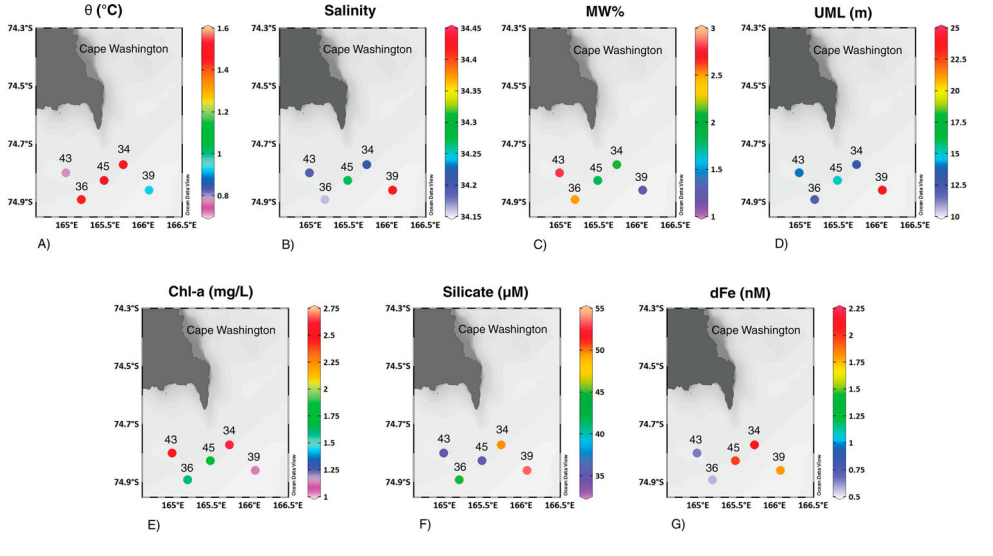

Figure 5. Subsurface distribution of: (A) potential temperature (θ); (B) salinity; (C) meltwater percentage (MW%); (D) upper mixed layer (UML) depth; (E) chlorophyll-a (Chl-a); (F) silicate ($Si(OH)_4$); (G) total dissolved iron (dFe).

and F). Changes in PS II efficiency are assumed to reflect the 'photosynthetic health' of the phytoplankton and to be affected mainly by cellular acclimations to changing abiotic conditions (including nutrient availability, especially N and Fe) [10,69]. However, from the Si: NO_3 ratio in the upper layer, that suggested Fe-replete condition, we conclude that the reduced F_v/F_m detected at the surface was not due to Fe limitation. The correlation between dFe and L (Spearman's $\rho = 0.96$, $p < .001$, $n = 13$) demonstrated that organic ligands maintained the concentrations of dFe at levels much higher than the inorganic solubility of Fe, keeping it available for phytoplankton [14]. Ligand distribution did not co-vary with Chl-a, but it negatively and significantly co-varied with prokaryotic biomass (Pearson's $r = -0.62$, $p < .05$, $n = 11$) suggesting a role of microbial activities in determining L distribution. However, it should be noted that the variations in ligand concentrations in the surface layer are the result of a balance between production and breakdown processes, including photo-chemical reactions, which can obscure a possible relationship between L and the biomass parameters [70,71]. In oceanic waters, iron-complexing ligands comprise a wide range of organic species, including humic substances, siderophores and biological degradation/extraction products (e.g. exopolymeric substances and saccharides), characterised by different production and loss pathways, functions and reactivity [14]. According to their binding affinities for iron, the ligands can be divided into different classes: L_1 includes stronger ligands, with log $K'_{FeL} = 22$-23 or higher, while L_2- to L_4- types gather weaker ligands, with log $K'_{FeL} = 20$-22 or lower [64]. Siderophores usually fall in the first group, although a photoactive siderophore belonging to the L_2 class has been reported, while exopolymeric and humic substances belong to the L_1–L_2 and L_2–L_3 classes, respectively. Finally, saccharides have a weak affinity for iron (L_3–L_4 classes), but can compete with the L_1 class for iron binding when occurring at a relatively high concentration [72]. The log K'_{FeL} values found in the RoME 2 area (22.1–23.6) highlighted the presence of complexes of differing stabilities, which could not be differentiated with the applied method, thus masking possible trends with depth, or distance, from shore [14,17]. The published data for the Southern Ocean, in which L_1 and L_2 ligands could be distinguished [64,66], reported log $K'_{L1} = 22.3$–23.6 and log $K'_{L2} = 21$–22 Therefore, our data would indicate the presence of L_1-type ligands. On the other hand, the values found in the surface waters of the fresher coastal stations 36 and 43 (22.2–22.3) are also consistent with data obtained for the iron complexes in under-ice seawater (21.2-22.1), attributed to exopolymeric substances [73]. Below the UML (where log K'_{FeL} values ranged from 22.1 to 23.3), *P. antarctica* was observed in a colonial form and in good physiological status [11]. The mucilaginous matrix that encapsulates the cells is composed of polysaccharides, with a high carbohydrate content, embedding floating of particulate organic matter and dissolved organic matter [74]. We can speculate that the mucilage, besides providing ecological niches for microbial heterotrophs [75], can play the role as a Fe binding ligand, although their Fe binding strength is relatively lower than what we found. Therefore, in this way, it could sustain the bloom of *P. antarctica*.

5. Conclusions

The distribution of dFe and iron speciation in the upper 200 m layers of the water column was investigated in a coastal area of the Ross Sea during the austral summer 2014. Our results document substantial spatial heterogeneity and complexity in iron distribution

and speciation at a horizontal length scale of about 10 km, emphasising the importance of mesoscale physical events, such as front, to regional biogeochemistry. Nutrients and iron were above any limiting growth concentration reported for the Ross Sea during summer. The high dFe concentration is the result of different sources, such as the melting of the sea ice or the delivering from the landmasses. The organic ligands maintained the concentrations of dFe at levels much higher than the inorganic solubility of Fe, keeping it available for phytoplankton. Moreover, the log K'_{FeL} values found highlighted the presence of complexes of differing stabilities, suggesting both autotrophic and heterotrophic contribution to the iron speciation. Further mesoscale measurements of the iron speciation in the Ross Sea will provide insights into the iron sources and on the mechanisms controlling the bioavailable species, thus helping the interpretation of data on iron biogeochemical cycle on a large scale. This will be of particular importance considering, for example, the effects of climate change on iron sources (such as the sea ice) and on the physical characteristics of surface waters. For instance, the lengthening of the ice season observed in summer in the Ross Sea, thought to supply iron to surface waters, could induce a considerable increase in phytoplankton biomass which may have a powerful impact on the trophic structure of the entire ecosystem.

Acknowledgments

The help of the officers and the crew on the R.V. Italica is kindly acknowledged. The authors are grateful to Gabriele Capodaglio for providing them with the GO-FLO sampler and to Giuseppe Arena, Federico Angelini and Leonardo Langone for their help during the sampling. The authors thank Elena Soddu for her assistance with the iron measurements, Eugen Behrens and Ivano Vascotto for helping with the prokaryote counts. We are grateful to anonymous referees for their suggestions.

Disclosure statement

No potential conflict of interest was reported by the authors.

Funding

This study was conducted in the framework of the project 'Ross Sea Mesoscale Experiment (RoME)' funded by the Italian National Program for Antarctic Research [PNRA, 2013/AN2.04].

Notes on contributors

Paola Rivaro is an associate professor in Chemical Oceanography and Environmental Analytical Chemistry at the Department of Chemistry and Industrial Chemistry in Genoa (Italy). She holds a PhD in Marine Environmental Sciences in Parma-Genoa Universities.

Francisco Ardini is a researcher in Analytical Chemistry at the Department of Chemistry and Industrial Chemistry in Genoa (Italy). He earned a PhD in Chemical Sciences and Technologies at the University of Genoa in 2012.

Marco Grotti is an associate professor in Analytical Chemistry at the Department of Chemistry and Industrial Chemistry in Genoa (Italy). He holds a PhD in Chemistry at Genoa University.

Giuseppe Aulicino received the environmental sciences degree from the University 'Parthenope' in Napoli, Italy, in 2007 and the PhD degree in 'Polar Sciences' from the University of Siena, Siena, Italy, in 2011. Since 2012, he has been a Postdoctoral Research Fellow with the University 'Parthenope' in Napoli and then with the Marche Polytechnic University.

Yuri Cotroneo is a researcher at the Department of Science and Technologies (DiST) of the University 'Parthenope' of Naples (Italy), and since 2018 he is a lecturer in Oceanography and Meteorology. He earned a master's degree in 'Environmental Sciences' at University 'Parthenope' of Naples (Italy) in 2003 and then a doctorate in 'Polar Sciences' at the University of Siena (Italy) in 2009.

Giannetta Fusco earned the Laurea degree in nautical sciences, major in physical oceanography, in 1996 at the University 'Parthenope' in Napoli, Italy. She is currently with the University 'Parthenope' – Department of Science and Technologies (DiST), where she became an Assistant Professor in 2005 and Lecturer in Polar Oceanography since 2007. From 2008 to 2013 she was Lecturer in Meteorology and Oceanography. From 2013 to present she is Lecturer in Climatology.

Olga Mangoni is an associate Professor in Ecology at the 'Federico II' University in Naples (Italy). She earned a science degree in 'Natural Sciences' at the 'Federico II' University in Naples (Italy) and then a PhD in 'Environmental Sciences' at the University of Messina (Italy).

Francesco Bolinesi is a PhD student at the Biology Department of University of Naples, Federico II, Neaples (Italy), with expertise in Limnology, Marine Biology and Ecology.

Maria Saggiomo is a Technologist at the 'Stazione Zoologica Anthon Dhorn' in Naples (Italy). She earned a science degree in 'Natural Sciences' at the 'Federico II' University in Naples (Italy) in 2003 and then a PhD in 'Environmental Sciences' at the University of Messina (Italy) in 2007.

Mauro Celussi is a researcher at the Istituto Nazionale di Oceanografia e Geofisica Sperimentale, Trieste, Italy. He holds a PhD in Polar Sciences at the Siena University. He performed research activity in Marine Microbial Ecology.

ORCID

Paola Rivaro http://orcid.org/0000-0001-5412-7371
Francisco Ardini http://orcid.org/0000-0003-0094-9227
Marco Grotti http://orcid.org/0000-0001-6956-5761
Giuseppe Aulicino http://orcid.org/0000-0001-6406-8715
Yuri Cotroneo http://orcid.org/0000-0002-0099-0142
Giannetta Fusco http://orcid.org/0000-0003-1769-2456
Olga Mangoni http://orcid.org/0000-0001-7789-0820
Mauro Celussi http://orcid.org/0000-0002-5660-6832

References

[1] Morel FMM, Price NM. The biogeochemical cycles of trace metals in the oceans. Science. 2003;300:944–947.
[2] Behrenfeld MJ, Milligan AJ. Photophysiological expressions of iron stress in phytoplankton. Annu Rev Mar Sci. 2013;5:217–246.
[3] Cotroneo Y, Budillon G, Fusco G, et al. Cold core eddies and fronts of the antarctic circumpolar current south of New Zealand from in situ and satellite data. J Geophys Res Oceans. 2013;118:2653–2666.
[4] Buongiorno Nardelli B, Guinehut S, Verbrugge N, et al. Southern Ocean mixed-layer seasonal and interannual variations from combined satellite and In situ data. J Geophys Res Oceans. 2017;122:10042–10060.
[5] Cerrone D, Fusco G, Cotroneo Y, et al. The antarctic circumpolar wave: its presence and inter-decadal changes during the last 142 years. J Clim. 2017;30:6371–6389.
[6] Cerrone D, Fusco G, Simmonds I, et al. Dominant covarying climate signals in the Southern Ocean and antarctic Sea Ice influence during the last three decades. J Clim. 2017;30:3055–3072.
[7] Fusco G, Cotroneo Y, Aulicino G. Different behaviours of the ross and weddell seas surface heat fluxes in the period 1972–2015. Climate. 2018;6:17.

[8] Sosik HM, Olson RJ. Phytoplankton and iron limitation of photosynthetic efficiency in the Southern Ocean during late summer. Deep Sea Res Part Oceanogr Res Pap. 2002;49:1195–1216.
[9] Arrigo KR, Worthen DL, Robinson DH. A coupled ocean-ecosystem model of the Ross Sea: 2. Iron regulation of phytoplankton taxonomic variability and primary production. J Geophys Res Oceans. 2003;108:3231.
[10] Hiscock MR, Lance VP, Apprill AM, et al. Photosynthetic maximum quantum yield increases are an essential component of the Southern Ocean phytoplankton response to iron. Proc Natl Acad Sci USA. 2008;105:4775–4780.
[11] Mangoni O, Saggiomo V, Bolinesi F, et al. Phytoplankton blooms during austral summer in the Ross Sea, Antarctica: Driving factors and trophic implications. PLOS ONE. 2017;12:e0176033.
[12] Tortell PD, Maldonado MT, Granger J, et al. Marine bacteria and biogeochemical cycling of iron in the oceans. FEMS Microbiol Ecol. 1999;29:1–11.
[13] Hassler CS, Schoemann V. Bioavailability of organically bound Fe to model phytoplankton of the Southern Ocean. Biogeosciences. 2009;6:2281–2296.
[14] Gledhill M, Buck KN. The organic complexation of iron in the marine environment: a review. Front Microbiol. 2012;3:69.
[15] Rue EL, Bruland KW. Complexation of iron(III) by natural organic-ligands in the Central North Pacific as determined by a new competitive ligand equilibration adsorptive cathodic stripping voltammetric method. Mar Chem. 1995;50:117–138.
[16] Hutchins DA, Witter AE, Butler A, et al. Competition among marine phytoplankton for different chelated iron species. Nature. 1999;400:858–861.
[17] Boye M, van den Berg CMG, de Jong JTM, et al. Organic complexation of iron in the Southern Ocean. Deep Sea Res Part Oceanogr Res Pap. 2001;48:1477–1497.
[18] Maldonado MT, Strzepek RF, Sander S, et al. Acquisition of iron bound to strong organic complexes, with different Fe binding groups and photochemical reactivities, by plankton communities in Fe-limited subantarctic waters. Glob Biogeochem Cycles. 2005;19:GB4S23.
[19] Hassler CS, Schoemann V, Boye M, et al. Iron bioavailability in the Southern Ocean. In: Gibson RN, Atkinson RJA, Gordon JDM, et al., editor. Oceanography and marine biology. Boca Raton (FL): CRC Press; 2012. p. 1–64.
[20] Smith WO, Jr, Ainley DG, Arrigo KR, et al. The oceanography and ecology of the Ross Sea. Annu Rev Mar Sci. 2014;6:469–487.
[21] Saggiomo V, Carrada GC, Mangoni O, et al. Spatial and temporal variability of size-fractionated biomass and primary production in the Ross Sea (Antarctica) during austral spring and summer. J Mar Syst. 1998;17:115–127.
[22] Saggiomo V, Catalano G, Mangoni O, et al. Primary production processes in ice-free waters of the Ross Sea (Antarctica) during the austral summer 1996. Deep Sea Res Part II Top Stud Oceanogr. 2002;49:1787–1801.
[23] Catalano G, Budillon G, La Ferla R, et al. The Ross Sea. In: Liu K-K, Atkinson L, Quiñones R, et al., editors. Carbon and nutrient fluxes in continental margins: a global synthesis. Berlin: Springer-Verlag; 2010. p. 303–318.
[24] Smith WO, Jr, Dinniman MS, Tozzi S, et al. Phytoplankton photosynthetic pigments in the Ross Sea: patterns and relationships among functional groups. J Mar Syst. 2010;82:177–185.
[25] McGillicuddy DJ, Sedwick PN, Dinniman MS, et al. Iron supply and demand in an Antarctic shelf ecosystem. Geophys Res Lett. 2015;42:8088–8097.
[26] Gerringa LJA, Laan P, van Dijken GL, et al. Sources of iron in the Ross Sea Polynya in early summer. Mar Chem. 2015;177:447–459.
[27] Fitzwater SE, Johnson KS, Gordon RM, et al. Trace metal concentrations in the Ross Sea and their relationship with nutrients and phytoplankton growth. Deep Sea Res Part II Top Stud Oceanogr. 2000;47:3159–3179.
[28] Sedwick PN, DiTullio GR, Mackey DJ. Iron and manganese in the Ross Sea, Antarctica: seasonal iron limitation in Antarctic shelf waters. J Geophys Res Oceans. 2000;105:11321–11336.
[29] Grotti M, Soggia F, Abelmoschi ML, et al. Temporal distribution of trace metals in Antarctic coastal waters. Mar Chem. 2001;76:189–209.

[30] Coale KH, Michael Gordon R, Wang X. The distribution and behavior of dissolved and particulate iron and zinc in the Ross Sea and Antarctic circumpolar current along 170°W. Deep Sea Res Part Oceanogr Res Pap. 2005;52:295–318.
[31] Feng Y, Hare CE, Rose JM, et al. Interactive effects of iron, irradiance and CO2 on Ross Sea phytoplankton. Deep Sea Res Part Oceanogr Res Pap. 2010;57:368–383.
[32] Coale KH, Wang X, Tanner SJ, et al. Phytoplankton growth and biological response to iron and zinc addition in the Ross Sea and Antarctic Circumpolar Current along 170°W. Deep Sea Res Part II Top Stud Oceanogr. 2003;50:635–653.
[33] Arrigo KR. Physical control of primary productivity in arctic and Antarctic polynyas. In: Smith WOJr, Barber DG, editors. Polynyas: Windows to the World. Amsterdam: Elsevier; 2007. p. 223–238.
[34] Rivaro P, Abelmoschi ML, Grotti M, et al. Combined effects of hydrographic structure and iron and copper availability on the phytoplankton growth in Terra Nova Bay Polynya (Ross Sea. Antarctica) Deep-Sea Res Part Oceanogr Res Pap. 2012;62:97–110.
[35] Sansiviero M, Morales Maqueda MÁ, Fusco G, et al. Modelling sea ice formation in the Terra Nova Bay polynya. J Mar Syst. 2017;166:4–25.
[36] Aulicino G, Sansiviero M, Paul S, et al. A New approach for monitoring the terra nova Bay polynya through MODIS Ice surface temperature imagery and Its validation during 2010 and 2011 winter seasons. Remote Sens. 2018;10:366.
[37] Rivaro P, Ianni C, Langone L, et al. Physical and biological forcing of mesoscale variability in the carbonate system of the Ross Sea (Antarctica) during summer 2014. J Mar Syst. 2017;166:144–158.
[38] Misic C, Covazzi Harriague A, Mangoni O, et al. Effects of physical constraints on the lability of POM during summer in the Ross Sea. J Mar Syst. 2017;166:132–143.
[39] Grotti M, Soggia F, Ardini F, et al. Determination of sub-nanomolar levels of iron in sea-water using reaction cell inductively coupled plasma mass spectrometry after $Mg(OH)_2$ coprecipitation. J Anal At Spectrom. 2009;24:522–527.
[40] Wu JF, Boyle EA. Determination of iron in seawater by high-resolution isotope dilution inductively coupled plasma mass spectrometry after $Mg(OH)_2$ coprecipitation. Anal Chim Acta. 1998;367:183–191.
[41] Tanner SD, Baranov VI, Vollkopf U. A dynamic reaction cell for inductively coupled plasma mass spectrometry (ICP-DRC-MS) – Part III. Optimization and analytical performance. J Anal At Spectrom. 2000;15:1261–1269.
[42] Vieira MA, Welz B, Curtius AJ. Determination of arsenic in sediments, coal and fly ash slurries after ultrasonic treatment by hydride generation atomic absorption spectrometry and trapping in an iridium-treated graphite tube. Spectrochim Acta Part B-At Spectrosc. 2002;57:2057–2067.
[43] van den Berg CMG. Chemical speciation of iron in seawater by cathodic stripping voltammetry with dihydroxynaphthalene. Anal Chem. 2006;78:156–163.
[44] Laglera LM, Battaglia G. Van den Berg CMG. Effect of humic substances on the iron speciation in natural waters by CLE/CSV. Mar Chem. 2011;127:134–143.
[45] Ružić I. Theoretical aspects of the direct titration of natural waters and its information yield for trace metal speciation. Anal Chim Acta. 1982;140:99–113.
[46] Van Den Berg CMG. Determination of copper complexation with natural organic ligands in seawater by equilibration with MnO_2 I. Theory Mar Chem. 1982;11:307–322.
[47] Turoczy NJ, Sherwood JE. Modification of the van den Berg/Ruzic method for the investigation of complexation parameters of natural waters. Anal Chim Acta. 1997;354:15–21.
[48] Gerringa LJA, Rijkenberg MJA, Thuróczy C-E, et al. A critical look at the calculation of the binding characteristics and concentration of iron complexing ligands in seawater with suggested improvements. Environ Chem. 2014;11:114–136.
[49] Hudson RJM, Covault DT, Morel FMM. Investigations of iron coordination and redox reactions in seawater using ^{59}Fe radiometry and ion-pair solvent extraction of amphiphilic iron complexes. Mar Chem. 1992;38:209–235.
[50] Thuróczy CE, Gerringa LJA, Klunder MB, et al. Observation of consistent trends in the organic complexation of dissolved iron in the Atlantic sector of the Southern Ocean. Deep Sea Res Part II Top Stud Oceanogr. 2011;58:2695–2706.

[51] Calace N, Casagrande A, Mirante S, et al. Distribution of humic substances dissolved and particulated in water column in Ross Sea, Antarctica. Microchem J. 2010;96:218–224.
[52] Grasshoff K. Determination of oxygen. In: Grasshoff K, Ehrhardt M, Kremling K, editor. Methods Seawater Analysis. Weinheim: Verlag Chemie; 1983. p. 61–72.
[53] Hansen HP, Grasshoff K. Automated chemical analysis. In: Grasshoff K, Ehrhardt M, Kremling K, editor. Methods Seawater Analysis. Weinheim: Verlag Chemie; 1983. p. 347–370.
[54] Celussi M, Malfatti F, Franzo A, et al. Ocean acidification effect on prokaryotic metabolism tested in two diverse trophic regimes in the Mediterranean Sea. Estuar Coast Shelf Sci. 2017;186:125–138.
[55] Lee S, Fuhrman JA. Relationships between biovolume and biomass of naturally derived marine bacterioplankton. Appl Environ Microbiol. 1987;53:1298–1303.
[56] Wunsch C. Modern observational physical oceanography: understanding the global ocean. Princeton (NJ): Princeton University Press; 2015.
[57] Schlitzerp R. Ocean data view [Internet]. 2015. Available from: http://odv.awi.de/.
[58] Budillon G, Pacciaroni M, Cozzi S, et al. An optimum multiparameter mixing analysis of the shelf waters in the Ross Sea. Antarct Sci. 2003;15:105–118.
[59] Massolo S, Messa R, Rivaro P, et al. Annual and spatial variations of chemical and physical properties in the Ross Sea surface waters (Antarctica). Cont Shelf Res. 2009;29:2333–2344.
[60] Martin JH, Gordon RM, Fitzwater SE. Iron in Antarctic waters. Nature. 1990;345:156–158.
[61] Rivaro P, Ianni C, Massolo S, et al. Distribution of dissolved labile and particulate iron and copper in Terra Nova Bay polynya (Ross Sea, Antarctica) surface waters in relation to nutrients and phytoplankton growth. Cont Shelf Res. 2011;31:879–889.
[62] Annett AL, Skiba M, Henley SF, et al. Comparative roles of upwelling and glacial iron sources in Ryder Bay, coastal western Antarctic Peninsula. Mar Chem. 2015;176:21–33.
[63] Quéroué F, Sarthou G, Planquette HF, et al. High variability in dissolved iron concentrations in the vicinity of the Kerguelen Islands (Southern Ocean). Biogeosciences. 2015;12:3869–3883.
[64] Ibisanmi E, Sander SG, Boyd PW, et al. Vertical distributions of iron-(III) complexing ligands in the Southern Ocean. Deep Sea Res Part II Top Stud Oceanogr. 2011;58:2113–2125.
[65] Thuróczy C-E, Alderkamp A-C, Laan P, et al. Key role of organic complexation of iron in sustaining phytoplankton blooms in the Pine Island and Amundsen Polynyas (Southern Ocean). Deep Sea Res Part II Top Stud Oceanogr. 2012; 71–76:49–60.
[66] Nolting RF, Gerringa LJA, Swagerman MJW, et al. Fe (III) speciation in the high nutrient, low chlorophyll Pacific region of the Southern Ocean. Mar Chem. 1998;62:335–352.
[67] McGillicuddy DJ, Budillon G, Kustka A. Mesoscale and high-frequency variability in the Ross Sea (Antarctica): an introduction to the special issue. J Mar Syst. 2017;166:1–3.
[68] Wang S, Bailey D, Lindsay K, et al. Impact of sea ice on the marine iron cycle and phytoplankton productivity. Biogeosciences. 2014;11:4713–4731.
[69] Parkhill JP, Maillet G, Cullen JJ. Fluorescence-based maximal quantum yield for PSII as a diagnostic of nutrient stress. J Phycol. 2001;37:517–529.
[70] Croot PL, Andersson K, Öztürk M, et al. The distribution and speciation of iron along 6°E in the Southern Ocean. Deep Sea Res Part II Top Stud Oceanogr. 2004;51:2857–2879.
[71] Gerringa LJA, Blain S, Laan P, et al. Fe-binding dissolved organic ligands near the kerguelen Archipelago in the Southern Ocean (Indian sector). Deep Sea Res Part II Top Stud Oceanogr. 2008;55:606–621.
[72] Hassler CS, van den Berg VD, Boyd PW. Toward a regional classification to provide a more inclusive examination of the ocean biogeochemistry of iron-binding ligands. Front Mar Sci. 2017;4:19.
[73] Lannuzel D, Grotti M, Abelmoschi ML, et al. Organic ligands control the concentrations of dissolved iron in Antarctic sea ice. Mar Chem. 2015;174:120–130.
[74] Del Negro P, Crevatin E, Larato C, et al. Mucilage microcosms. Sci Total Environ. 2005;353:258–269.
[75] Delmont TO, Hammar KM, Ducklow HW, et al. Phaeocystis antarctica blooms strongly influence bacterial community structures in the Amundsen Sea polynya. Front Microbiol. 2014;5:646.

The Journal of Eukaryotic Microbiology

ISOP Published by the International Society of Protistologists

Journal of Eukaryotic Microbiology ISSN 1066-5234

SHORT COMMUNICATION

Austral Summer Bloom of Loricate Choanoflagellates in the Central Ross Sea Polynya

Laura Escalera[a], Olga Mangoni[b,c], Francesco Bolinesi[a,b] & Maria Saggiomo[a]

a Research Infrastructures for Marine Biological Resources, Stazione Zoologica Anton Dohrn, Naples 80121, Italy
b Department of Biology, Università degli Studi di Napoli Federico II, Complesso Universitario di Monte Sant'Angelo, Naples 80126, Italy
c CoNISMa, Piazzale Flaminio 9, Rome 00196, Italy

Keywords
Acanthoecidae; Antarctica; colonies; food web.

Correspondence
L. Escalera, Research Infrastructures for Marine Biological Resources, Stazione Zoologica Anton Dohrn, Villa Comunale Naples 80121, Italy
Telephone number: (+39)0815833240; FAX number: (+39)0815833360; e-mail: laura.escalera@szn.it

Received: 4 September 2018; revised 8 February 2019; accepted February 10, 2019.
Early View publication 9 March, 2019

doi:10.1111/jeu.12720

ABSTRACT

A bloom of loricate choanoflagellates was recorded for the first time in the Ross Sea polynya during the austral summer 2017. Both individual cells and uncommon large-size colonies (200 μm length) represent the 42–55% of the total plankton community (i.e. specimens from 5 to 150 μm length). Choanoflagellates serve as a link between low and mid trophic levels since they prey on bacteria and in turn are ingested by zooplankton. This twofold role and the unusual abundance recorded in the Antarctic ecosystem may have relevant but still unknown effects on food web structure and dynamics in that area.

THE aim of this study was to provide insights into the diversity of choanoflagellates and abundance in the Ross Sea, particularly during an unusual bloom recorded in austral summer 2017. Acanthoecid choanoflagellates are small bacteriophagous cells surrounded by a delicate siliceous armour (lorica). They are common within Antarctic and Artic plankton communities (Buck and Garrison 1983; Chen 1994; Fritsen et al. 2001; Marchant et al. 1987) but we have found no data available about the choanoflagellate concentrations in the western area of the Ross Sea.

MATERIALS AND METHODS

Plankton samples were collected in January 2017 as part of an oceanographic cruise in the western Ross Sea within the framework of the Plankton biodiversity and functioning of the Ross Sea Ecosystems in a changing southern oceans (P-ROSE) project. The 500 ml water samples were collected using Niskin bottles. Four depths from surface to 60 m at the 28 stations (Fig. S1), with two of the stations (15 and 57) sampled twice, were collected based on the vertical fluorescence profiles of chlorophyll *a*. Samples for taxonomic analysis, of specimens from 5 to 150 μm length, were preserved in 4% $CaCO_3$ buffered formalin solution. Depending on cell concentrations, 3–10 ml of sample was settled in Utermöhl- type chambers (Lund et al. 1958; Utermöhl 1931) for 24–48 h respectively. Cell counts were performed at 400X magnification using a Zeiss Ax10 Observerz.1 inverted light microscope equipped with an AxioCam MRc5 (Carl Zeiss Microscopy GmbH, Jena, Germany) image capture system. Up to four transects with an area of 0.78 mm^2 each of the settling chamber, were examined to reach at least 200 cells per sample which is considered statistically valid.

RESULTS AND DISCUSSION

During January 2017, five species of loricate choanoflagellates (Fig. 1) were identified: *Bicosta spinifera* (Fig. 1A), *Calliacantha* sp. (Fig. 1B), *Parvicorbicula socialis* (Fig. 1C, D), *Diaphanoeca multiannulata* (Fig. 1E, F) and *Crinolina aperta* (Fig. 1G–I). In agreement with the description by Throndsen (1970) for *B. spinifera*, two longitudinal costae that run slightly spiral at the cell body level were visible on

© 2019 International Society of Protistologists

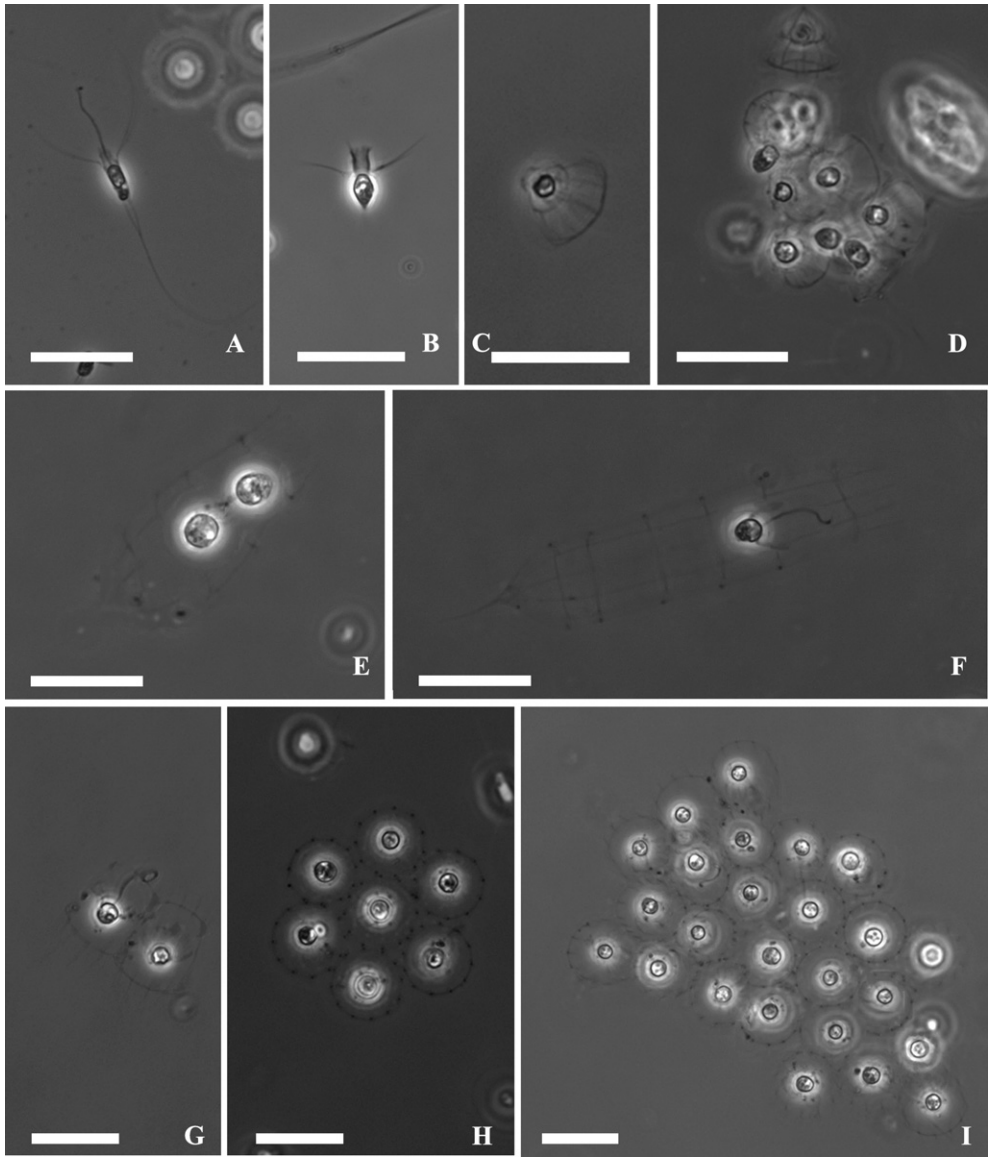

Figure 1 Acanthoecid choanoflagellates of the Ross Sea. **A.** *Bicosta spinifera*. **B.** *Calliacantha* sp. **C** and **D.** *Parvicorbicula socialis* single cell (C) and in colonial form (D). **E** and **F.** *Diaphanoeca multiannulata* with a recently divided daughter cell inside the parental lorica (E). **G–I.** *Crinolina aperta* in pairs (G) or in colonies (H and I). Cells of *C. aperta* colonies remained attached by longitudinal costae (G and H). Scale bar = 20 μm.

the outer surface of the cell and continued as spines. The absence of transverse costa was observed in some organisms (Fig. 1A). Specimens belonging to the genus *Calliantha* had a conical shaped lorica and the lorica chamber delimited, at the anterior part of the cell body, by a transverse costa (Leadbeater 1978). Those features were observed in some of our cells (Fig. 1B). *Parvicorbicula socialis* was distinct by the formation of colonies (Fig. 1D), a conical basket lorica (Fig. 1C) in which the cell body was located, two circular transverse costae with marked differences in diameter and approximately 10 longitudinal costae, all of which were present. *Diaphanoeca multiannulata* (Buck 1981) was described to possess 4–5 transverse circular costae and barrel-shaped siliceous lorica (Fig. 1E). Few years later, Thomsen et al. (1990) highlighted that lorica dimensions of *D. multiannulata* were highly variable together with length and number of transverse and longitudinal costae and strips. The most frequently observed specimens had morphological characteristics reported in the original description (Buck 1981). Very few longer (~80 μm) specimens with a straight outline and seven transverse costae (Fig. 1F), similar to fig. 43 in Thomsen et al. (1990) were also observed within samples. Finally, the open lorica, the number of longitudinal costae (11–12), the length of their posterior projections and the slight differences in diameter of the two transverse costae that confers them an almost cylindrical shape, led us to identify those specimens as *C. aperta* (Fig. 1G–I) and not as

© 2019 International Society of Protistologists

C. isefjordensis, a quite similar species of the same genus. All the species mentioned above, except for *P. socialis*, possessed characteristic posterior "tails" or projections that are thought to be indicators of the presence of ice (Manton et al. 1975). Although our sampling area is an ice-free zone (polynya), ice floes can retain choanoflagellates (Fritsen et al. 2001) and may transport them to other areas.

Loricate choanoflagellates were the most abundant group within the plankton community with peak concentrations above 10^6 cells/liter reached in a transect that included stations from 43 to 48 (75°18.8′S–76°36′S, 168°53.2′E–177°59.8′E). Maxima densities (above 3.5×10^6 cells/liter) were observed at the end of January at stations 44 (45 m) and 48 (42 m). These abundances contributed 55% and 42% respectively of the total plankton abundance. Within the choanoflagellate group, *P. socialis* contributed 44% and 35.6%, whereas *C. aperta* reached the 45.8% and 54.5% respectively. *Diaphanoeca multiannulata* and *Calliantha* spp. appeared at < 10% and *B. spinifera* was undetectable within those samples. Previous studies reported maximal choanoflagellates concentrations of 2×10^6 cells/liter at the ice edge zone (Buck and Garrison 1983) and 2.7×10^5 cell/liter at 31 m (Buck and Garrison 1988) in the Weddell Sea. Abundances of 10^5 and 2.1×10^6 cell/liter have been reported in the freeboard sea ice of the eastern zone and in the sea ice area of the Ross Sea respectively (Fritsen et al. 2001; Garrison et al. 2005). Dennett et al. (2001) observed high average biomass (65%) of heterotrophic nanoplanktoners during autumn in the southeastern part of the Ross Sea, where choanoflagellates dominated but the numerical contribution to the total biomass was not indicated. Thus, the cell concentrations of loricate choanoflagellates observed in this study are the highest reported in the Antarctic Ocean so far. Moreover, because these observations, were made along a transect and across the water column in the central Ross Sea polynya, they add new information about the biogeographical distribution of the loricate choanoflagellates in a poorly studied area (see fig. 9.12. in Leadbeater 2015).

The choanoflagellate bloom observed in this study was characterized by the presence of *P. socialis* (Fig. 1E, F) and *C. aperta* colonies (Fig. 1G–I), that reached ~200 μm length and 100 μm width in the latter species. The formation of colonies in some choanoflagellates has been suggested to be a consequence of extremely calm weather conditions during which the daughter cell completes the formation of the lorica close to the parental cell and the new lorica remains attached to it by the longitudinal costae of the foremost costal rings (Thomsen 1976). Colonies formed by *P. socialis* have been described as a mat formed by clusters of four cells (Braarud 1935; Manton et al. 1976) or spherical with clusters of six cells (Pavillard 1917). The former authors suggested that globular colonies were unnaturally formed as a consequence of the weak contact between cells after sample fixation and handling. However, Thomsen (1976) reported that spherical colonies were the result of the physical contact between cells with different diameters of the transverse costal rings. Conversely, we observed *C. aperta* specimens with a quite straight outline of the siliceous lorica that formed almost flat colonies with up to 25 cells in which one cell was contacted to six surrounding cells that resulted in a zigzag pattern (Fig. 1G–I). Thus, the cell disposition in *C. aperta* (Fig. 1H, I) coincided with those for *P. socialis* drawn by Pavillard (1917). The arrangement of cells within the colony (one cell surrounded by six) and the different outlines of the lorica, conical, in *P. socialis* (Fig. 1C, D), and cylindrical, in *C. aperta* (Fig. 1G–I), are in agreement with Pavillard (1917) and Thomsen (1976). Previous studies described *C. aperta* colonies (Buck and Garrison 1983; Marchant et al. 1987) but the cell pattern in Fig. 1H, I is shown in this work for the first time.

Choanoflagellates play an important ecological role in the transfer of carbon and energy from surface to deep water communities and from lower to higher trophic levels (Vincent 2004). Studies on natural samples and cultures indicated that their diet includes bacteria and particulate organic matter (Buck and Garrison 1988). At the same time, choanoflagellates are potential preys of zooplankton, such as the Antarctic krill (Tanoue and Hara 1986). Thus, the concentrations reached and the formation of such large colonies suggests that choanoflagellates may play a pivotal role by connecting primary producers and higher trophic levels in the Antarctic pelagic food web. Our observations support the recent trend of changes in the plankton succession that are potentially restructuring trophic relationships in the Antarctic food web (Mangoni et al. 2017; Rivaro et al. 2017).

ACKNOWLEDGMENTS

This study was carried out in the framework of the activities of the Italian National Program for Antarctic Research (P-ROSE Project, PNRA, 2016/A3.06) which provided logistic support. We thank the officers, crew and technical personnel on board the R/V Italica, G. Zazo for his help during the cruise and F. Iamunno for technical support. Our special thanks to V. Saggiomo for his valuable criticism of this work.

LITERATURE CITED

Braarud, T. 1935. The "Ost" expedition to the Denmark Strait 1929. II The Phytoplankton and its conditions of growth. *Hvalråd. Skr.*, 10:1–173.

Buck, K. R. 1981. A study of choanoflagellates (Acanthoecidae) from the Weddell Sea, including a description of *Diaphanoeca multiannulata* n. sp. *J. Protozool.*, 28:47–54.

Buck, K. R. & Garrison, D. L. 1983. Protists from the ice-edge region of the Weddell Sea. *Deep-Sea Res. Pt I*, 30:1261–1277.

Buck, K. R. & Garrison, D. L. 1988. Distribution and abundance of choanoflagellates (Acanthoecidae) across the ice-edge zone in the Weddell Sea, Antarctica. *Mar. Biol.*, 98:263–269.

Chen, B. 1994. Distribution and abundance of choanoflagellates in Great-Wall Bay, King George Island, Antarctica in austral summer. *Proc. NIPR Symp. Polar Biol.*, 7:32–42.

Dennett, M. R., Mathot, S., Caron, D. A., Smith, W. O. & Lonsdale, D. J. 2001. Abundance and distribution of phototrophic

© 2019 International Society of Protistologists

and heterotrophic nano- and microplankton in the southern Ross Sea. *Deep-Sea Res. Pt II*, 48:4019–4037.
Fritsen, C. H., Coale, S. L., Neenan, D. R., Gibson, A. H. & Garrison, D. L. 2001. Biomass, production and microhabitat characteristics near the freeboard of ice floes in the Ross Sea, Antarctica, during the austral summer. *Ann. Glaciol.*, 33:280–286.
Garrison, D. L., Gibson, A., Coale, S. L., Gowing, M. M., Okolodkov, Y., Fritsen, C. H. & Jeffries, M. O. 2005. Sea-ice microbial communities in the Ross Sea: autumn and summer biota. *Mar. Ecol. Prog. Ser.*, 300:39–52.
Leadbeater, B. S. C. 1978. Renaming of *Salpingoeca sensu* Grøntved. *J. Mar. Biol. Assoc. U.K.*, 58:511–515.
Leadbeater, B. S. C. 2015. Choanoflagellate ecology. *In:* Leadbeater, B. S. C. (ed.), The Choanoflagellates: Evolution, Biology and Ecology. Cambridge University Press, Cambridge. 9:202–240.
Lund, J. W. G., Kipling, C. & Le Cren, E. D. 1958. The inverted microscope method of estimating algal numbers and the statistical basis of estimations by counting. *Hydrobiologia*, 11:143–170.
Mangoni, O., Saggiomo, V., Bolinesi, F., Margiotta, F., Budillon, G., Cotroneo, Y., Misic, C., Rivaro, P. & Saggiomo, M. 2017. Phytoplankton blooms during austral summer in the Ross Sea, Antarctica: driving factors and trophic implications. *PLoS ONE*, 12:e0176033. https://doi.org/0176010.0171371/journal.pone.0176033.
Manton, I., Sutherland, J. & Leadbeater, B. S. C. 1976. Further observations on the fine structure of marine collared flagellates (Choanoflagellata) from arctic Canada and west Greenland: species of *Parvicorbicula* and *Pleurasiga*. *Can. J. Bot.*, 54:1932–1955.
Manton, I., Sutherland, J. & Thomsen, H. A. 1975. Four new species of choanoflagellates from Arctic Canada. *Proc. R. Soc. Lond. B Biol. Sci.*, 189:15–27.
Marchant, H., Van den Hoff, J. & Burton, H. 1987. Loricate choanoflagellates from Ellis Fjord, Antarctica including the description of *Acanthocorbis tintinnabulum* sp. nov. *Proc. NIPR Symp. Polar Biol.*, 1:10–22.
Pavillard, M. J. 1917. Protistes nouveaux ou peu connus du plancton mediterraneen. *C. R. Hebd. Seanc. Acad. Sci.*, 164:92–928.
Rivaro, P., Ianni, C., Langone, L., Ori, C., Aulicino, G., Cotroneo, Y., Saggiomo, M. & Mangoni, O. 2017. Physical and biological forcing of mesoscale variability in the carbonate system of the Ross Sea (Antarctica) during summer 2014. *J. Mar. Syst.*, 166:144–158.
Tanoue, E. & Hara, S. 1986. Ecological implications of fecal pellets produced by the Antarctic krill *Euphausia superba* in the Antarctic Ocean. *Mar. Biol.*, 91:359–369.
Thomsen, H. A. 1976. Studies on marine choanoflagellates. II. Fine structural observations on some silicified choanoflagellates from the Isefjord (Denmark), including the description of two new species. *Norw. J. Bot.*, 23:33–51.
Thomsen, H. A., Buck, K. R., Coale, S. L., Garrison, D. L. & Gowing, M. M. 1990. Loricate choanoflagellates (Acanthoecidae, Choanoflagellida) from the Weddell Sea, Antarctica. *Zool. Scr.*, 19:367–387.
Throndsen, J. 1970. *Salpingoeca spinifera* sp. nov., a new planktonic species of the Craspedophyceae recorded in the Arctic. *Br. Phycol. J.*, 5:87–89.
Utermöhl, v. H. 1931. Neue Wege in der quantitativen Erfassung des Planktons (mit besondere Beriicksichtigung des Ultraplanktons). *Verh. Int. Ver. Theor. Angew. Limnol.*, 5:567–595.
Vincent, W. F. 2004. Microbial ecosystems of Antarctica. Cambridge University Press, Cambridge. p. 320.

SUPPORTING INFORMATION

Additional supporting information may be found online in the Supporting Information section at the end of the article.

Figure S1. Map of the sampling stations in the central Ross Sea polynya (Antarctica). Note that stations 15 and 57 were sampling twice.

© 2019 International Society of Protistologists

Ecological Questions 29 (2018) 3: 75–85 http://dx.doi.org/10.12775/EQ.2018.024

A review of past and present summer primary production processes in the Ross Sea in relation to changing ecosystems

Olga Mangoni[1*], Vincenzo Saggiomo[2], Francesco Bolinesi[1], Laura Escalera[2], Maria Saggiomo[2]

[1] Department of Biology, University of Naples "Federico II", Naples, Italy
[2] Stazione Zoologica Anton Dohrn, Naples, Italy
e-mail: olga.mangoni@unina.it

Received 1 July 2018 / Accepted 09 September 2018

Abstract: We analyse primary production processes during austral summer 1996 and 2001 in different environmental conditions such as ice-free waters and extensive ice-covered areas. Spatio-temporal distribution of phytoplankton biomass and functional groups along with photosynthetic parameters are presented. Production *vs* irradiance (P*vs*E) experiments were performed using ^{14}C incubations at several stations and three or four different depths to define the eco-physiology of phytoplankton communities.
The results of the oceanographic campaign conducted in ice-free waters of the Ross Sea (summer 1996) emphasize that these ecosystems are characterized by high nutrient low chlorophyll (HNLC) conditions due to limiting factors (eg. Fe). Conversely, the results of the oceanographic cruise in extensively packice-covered areas (summer 2001) indicate that the average phytoplankton biomass (estimated from Chl*a*) was about three times the values recorded in ice-free conditions, but the primary production was relatively lower. In fact, *in situ* primary production and P*vs*E experiments over few days show that high primary production values occurred in most of the area, but only within the first five meters of the water column and the melting pack ice. Notwithstanding some high values of phytoplankton biomass during the 2001 campaign, water column stability, similar irradiance levels along the water column, photosynthetic capacity was suppressed in deeper layers, indicating a low carrying capacity of the pelagic ecosystem due to iron limitation, as shown by low values of the photo-chemical efficiency of photosystem II (PSII), variable fluorescence and maximal fluorescence ratio (Fv/Fm). In contrast with a very high variability in phytoplankton biomass at several temporal and spatial scales, photosynthetic parameters (P^B_{max}, α, E_k) varied within narrow ranges.

Relevant changes in phytoplankton abundance and species composition are reported in this study although the environmental factors that drive these changes in primary production processes and prevalence of principal functional groups of phytoplankton communities compared to the past (1996 and 2001) are still unknown. The effect of these changes on the carrying capacity of Ross Sea ecosystems, carbon export and the potentially new asset of the food web will need to be determined.

Key words: Phytoplankton functional groups, photosynthetic parameters, global change, Southern Ocean.

1. Introduction

The Ross Sea is a globally important site of sea ice production in two permanent polynias (Tamura et al., 2008; Ohshima et al., 2016) and bottom water formation (Jacobs, 2004; Budillon et al., 2011). Rates of primary production can be very high, often exceeding 2 gCm^{-2} d^{-1} (Smith & Gordon, 1997; Saggiomo et al., 1998; Arrigo et al., 1999, 2000), which makes the Ross Sea the most productive sector of the Southern Ocean on an annual basis (Arrigo et al., 1998). In this region, large phytoplankton blooms can trigger significant biological sequestration of atmospheric

CO_2 via the formation and export of particulate organic carbon to the deep waters where the Antarctic bottom water (AABW) moves northwards (Arrigo et al., 2008).

In spring, impressive phytoplankton blooms are observed at landfast-ice and platelet-ice (Guglielmo et al., 2004; Saggiomo M et al., 2017) and at ice melting in offshore areas (Carrada et al., 2000; Saggiomo et al., 2000). Large numbers of organisms at different trophic levels (krill, birds, seals, whales) convey along the ice margins (Saino & Guglielmo, 2000). The production of meltwater was related to the generation of a stratified surface layer and to the release of micronutrients and epontic algae into the water which can increase primary production within marginal ice zones (MIZ) (Smith & Nelson, 1985, Arrigo et al., 1998; Mangoni et al., 2004; Geibert et al., 2010; Taylor et al., 2013). During the austral summer, a sharp drop in primary production is observed after pack ice dispersal due to two major processes: the deepening of the upper mixed layer and iron limitation (Sedwick et al., 2011; Alderkamp et al., 2012; Smith & Jones, 2014). These processes may also explain why offshore ecosystems during austral summer showed high nutrient low chlorophyll (HNLC) conditions in ice-free areas (Saggiomo et al., 1998, 2002; Peloquin & Smith, 2007; Wang & Moore, 2011).

Phytoplankton species composition and physiology are likely to influence carbon (C) export to depth (DiTullio et al., 2000). Blooms of diatoms (such as *Fragilariopsis cylindrus*) have historically dominated production in open waters of the western Ross Sea during summer, whereas blooms of haptophytes (*Phaeocystis antarctica*) have been found to dominate the larger Ross Sea polynya during spring and early summer (DiTullio & Smith, 1996; Arrigo et al., 1999). These two taxa coexist throughout the Ross Sea (Smith et al., 2014), although each taxon can form nearly monospecific blooms that leave distinctive biogeochemical imprints (DiTullio et al., 2000; Smith et al., 2010; Mangoni et al., 2017).

In the latest 10 years, relevant changes in the abundance and species composition of phytoplankton in offshore waters of the Ross Sea have been recorded during austral summer in prolonged ice cover conditions (Mangoni et al., 2004; Smith et al., 2006) as well as in ice-free waters (Kohut et al., 2017; Mangoni et al. 2017) Such phenomenon could have a major impact on both C export and trophic structure of the Ross Sea ecosystem.

The aim of this study is to assess the seasonal limiting factors and the carrying capacity of the Ross Sea in different environmental ecosystems for ice-free waters during austral summer 1996 and in anomalous ice-covered systems during austral summer 2001. The effect of the anomalous ice coverage in 2001 on phytoplankton assemblages is reported in Mangoni et al. (2004). In this study, data about primary production processes which have never been published before are analysed. We compare the 2001 data about ice-covered areas with those collected in ice-free waters in 1996 (Saggiomo et al., 2002) and discuss the implications of prolonged ice coverage on the primary production processes. Different environmental conditions during austral summer in 1996 and 2001 are discussed in light of the recent changes in phytoplankton abundance and species composition in the Ross Sea ecosystems.

2. Materials and methods

Study areas. During the oceanographic cruise in 1996, 38 hydrological stations were sampled in different ecological contexts (Fig. 1) (Saggiomo et al., 2002). Primary production was measured at 28 stations and P*vs*E experiments were performed at 18 stations at 3 or 4 depths. The cruise in 2001 was conducted on the R.V. Italica from 11 January to 19 February within the frame of the XVI Italian Antarctic Research Expedition. The sampling plan included 30 stations (Fig. 2), P*vs*E measurements were performed in order to obtain photosynthetic parameters to study the eco-physiology of phytoplankton communities. Three stations located in the southwestern part of the Ross Sea were replicated over time.

Phytoplankton biomass. In both years, for determination of total phytoplankton biomass, 500ml of seawater were filtered onto 25 mm Whatman GF/F filters. Spectrofluorometric analyses of Chlorophyll-a (Chl*a*) and phaeopigments (Phaeo) were made using a Spex Fluoromax

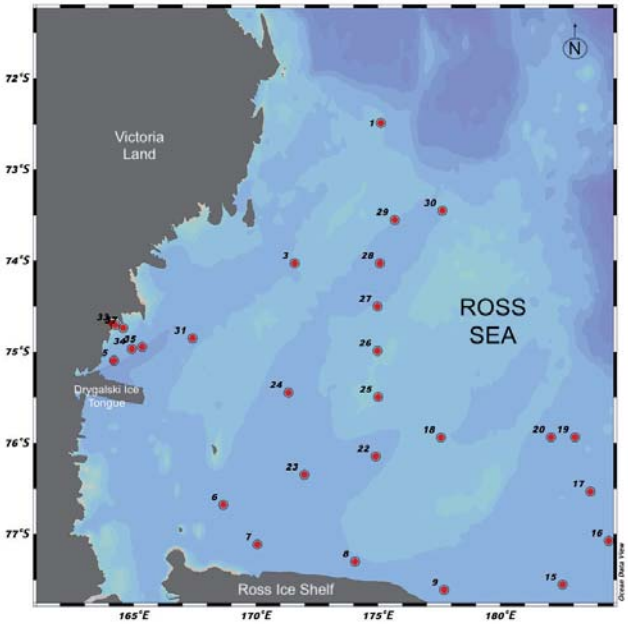

Figure 1. Sampling stations in the ice-free waters of the Ross Sea (Antarctica) during summer 1996.

spectrofluorometer (Holm-Hansen et al., 1965). The instrument was checked daily with a solution of Chl*a* from *Anacystis nidulans* (Sigma).

Phytoplankton functional groups. In 2001, HPLC analyses were performed at 4–7 depths at 41 hydrological stations (Fig. 2). Five litres of water were filtered onto 47mm Whatman GF/F filters. HPLC analyses were performed using a Hewlett-Packard HPLC (mod. 1100) according to protocol by Mantoura & Llewellyn (1983) and modified by Brunet & Mangoni (2010). For more details see Mangoni et al. (2004). The concentrations of pigments were used to estimate the contribution of the main functional groups to the total Chl*a* using a matrix factorisation software (CHEMTAX) (Mackey et al., 1996; Wrigth et al., 2010).

Primary production. Primary production measurements were performed at *in situ* simulated conditions. Samples collected at the optical depths were incubated in light and dark polycarbonate (Nalgene) 450-ml bottles with 1 ml (740 KBq) of $NaH^{14}CO_3$ for 4-6 hours in running surface sea water. The different light intensities were obtained using electroformed nickel screens (Veco Int. Co., USA). After incubation, samples were filtered on Whatman GF/F filters. Filters after acidification were processed as reported in the next paragraph.

Photosynthetic parameters. P*vs*E measurements were performed at 3 or 4 depths in 30 stations during 2001 and in 18 stations during 1966 in order to obtain photosynthetic parameters of phytoplankton community (Babin et al., 1994). At each depth, which was selected according to both irradiance and hydrographic structure, sub-samples of water (50 ml) were collected in 12 culture flasks and inoculated with 740 KBq of $NaH^{14}CO_3$. Incubations were carried out for one hour in an artificial light gradient incubator (Osram HQI-T 250W/D lamp), cooled by circulating surface (-6 m depth) seawater. In order to determine dark fixation, one sub-sample from each sample was placed in the dark inside the incubator, with 4 drops of seawater saturated with DCMU solution (Legendre et al., 1983). The irradiance was measured in each incubation bottle using a 4π sensor QLS-101 (Biospherical Instruments). After incubation, samples passed through a Whatman GF/F filter. Filtration was carried out as fast as possible in dim light and vacuum was <0.2 atm for all filtration procedures. Filters were acidified with 200 µl of HCL 0.1 N and after adding 10 ml of Aquasol II scintillation cocktail, they were read within 24 hours from filtration with a Beckman LS 1801 liquid scintillator.

P*vs*E data were derived from the model by Platt et al. (1980):

$$P^B(E) = P^B_S\ [1- \exp\ (-\alpha E/\ P^B_S)]\exp\ (-\beta E/\ P^B_S)$$

where P^B_S is the potential light-saturated Chl-specific rate of photosynthesis in absence of photoinhibition (mgC(mgChla^{-1} h^{-1}), α is the initial slope of P*vs*E curves mgC(mgChl$a)^{-1}$ h^{-1} (µmol photon m^{-2} s^{-1}) $^{-1}$ and β is the index of photoinhibition (same units as α) and E is the irradiance (µmol photon m^{-2} s^{-1}).

The photochemical efficiency of PSII was monitored as the ratio of variable to maximal fluorescence: F_v/F_m (where F_v is the difference between maximal (F_{max}) and initial fluorescence (F_o) determined using a Fast Repetition Rate Flurometry) (FRRF).

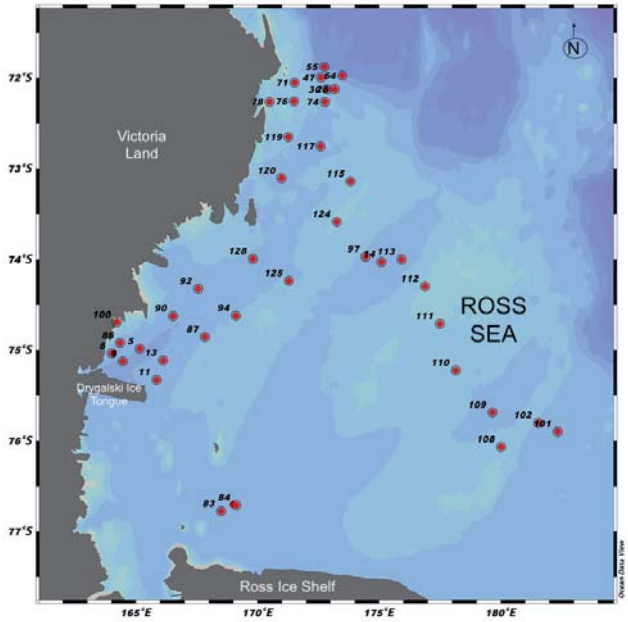

Figure 2. Sampling stations in ice-covered waters of the Ross Sea (Antarctica) during summer 2001.

3. Results and Discussion

Sea ice has strong impacts on ocean biogeochemical cycles and marine ecosystems (Sedwick & DiTullio, 1997; Ducklow et al., 2012; Wang et al., 2014). Phytoplankton blooms are often observed in the MIZ, where there is recent melting of sea ice (Fitch & Moore, 2007; Mangoni et al., 2004). The sea ice represents the most climate change-sensitive ecosystem, while there are strong interannual variations in ice extent and concentration and large regional variations (Oza et al., 2011; Kurtz & Markus, 2012; Parkinson & Cavalieri, 2012; Arrigo et al., 2015; Comiso et al., 2017). During the past few decades from satellite records were reveal the off-shore waters of the Ross Sea essentially free from ice in austral summer (Comiso et al., 2011; Turner & Comiso, 2017).

Saggiomo and co-workers (2002) report that in off-shore waters and the coastal area of Terra Nova Bay (TNB) the integrated phytoplankton biomass varied between 15 and 102 mg Chl*a* m^{-2} and ranged from 41 to 226 mg Chl*a* m^{-2} in the 0-100 m layer, respectively (Fig. 3A). Primary production in off-shore waters varied between 124 and 638 mg C m^{-2} d^{-1} and ranged between 620 and 2411 mg C m^{-2} d^{-1} during a typical late summer bloom at TNB. The mean photosynthetic parameters (P^B_{max}, α, E_k) varied within a limited range of values (Table 1). Phytoplankton communities were characterized by the prevalence of diatoms. These results emphasize that off-shore waters of the Ross Sea were HNLC during the austral summer and then were affected by limiting factors (e.g. Fe) as also reported by several authors (e.g. Bertrand et al., 2007; Feng et al., 2010).

The extensive ice coverage observed in off-shore waters of the Ross sea in 2001 appeared quite anomalous. Based on the data collected in this cruise, our group reported a considerable spatial variability of the phytoplankton biomass, with high concentrations along the southern and eastern ice edges and in the coastal area of TNB (Mangoni et al., 2004). Phytoplankton biomass concentrations, ranging between 25 and 215 mg m^{-2} Chl*a* in off-shore waters and from 181 to 237 mg m^{-2} Chl*a* in TNB during late summer blooms (Fig. 3B), were higher all over the Ross Sea in 2001 than in 1996 (Mangoni et al., 2004; Saggiomo et al., 2002). Diatoms dominated phytoplankton populations across the entire Ross Sea in both years. Fucoxanthin determined using HPLC analyses was by far the dominant pigment, with Fuco/Chl*a* being generally > 0.5. The results of CHEMTAX analyses for summer 2001 showed that diatoms were the major contributors to the biomass in the 0-100 m layer (Fig. 4A); they accounted for more than 50% of the phytoplankton community in the entire Ross Sea. On the contrary, the percentage of haptophytes was generally low (Fig. 4B). In both campaigns, macro nutrients were never limiting (Saggiomo et al., 2002; Mangoni et al., 2004).

PvsE experiments (24 stations in 1996, 30 stations in 2001 at 3-4 depths) showed similar photoacclimation index (E_k) and photosynthetic capacity (Table 1). The P^B_{max} values recorded in 2001 were in sharp contrast with the considerably higher biomass concentrations in the extensive MIZ areas.

Table 1. Mean, maximum, minimum and standard deviation of photosynthetic parameters determined during the austral summer 1996 and 2001 in the Ross Sea (Antarctica).

	P^B_{max}	α	β	E_m	E_k
1996					
MEAN	1.27	0.073	0.00045	120	23
MIN	0.72	0.024	0.00002	49	3
MAX	2.83	0.132	0.00220	211	55
STD	0.39	0.088	0.00048	32	8
2001					
MEAN	1.34	0.0487	0.00106	136	31
MIN	0.38	0.0082	0.00005	47	8
MAX	3.95	0.1391	0.00521	267	58
STD	0.66	0.0272	0.00091	52	12

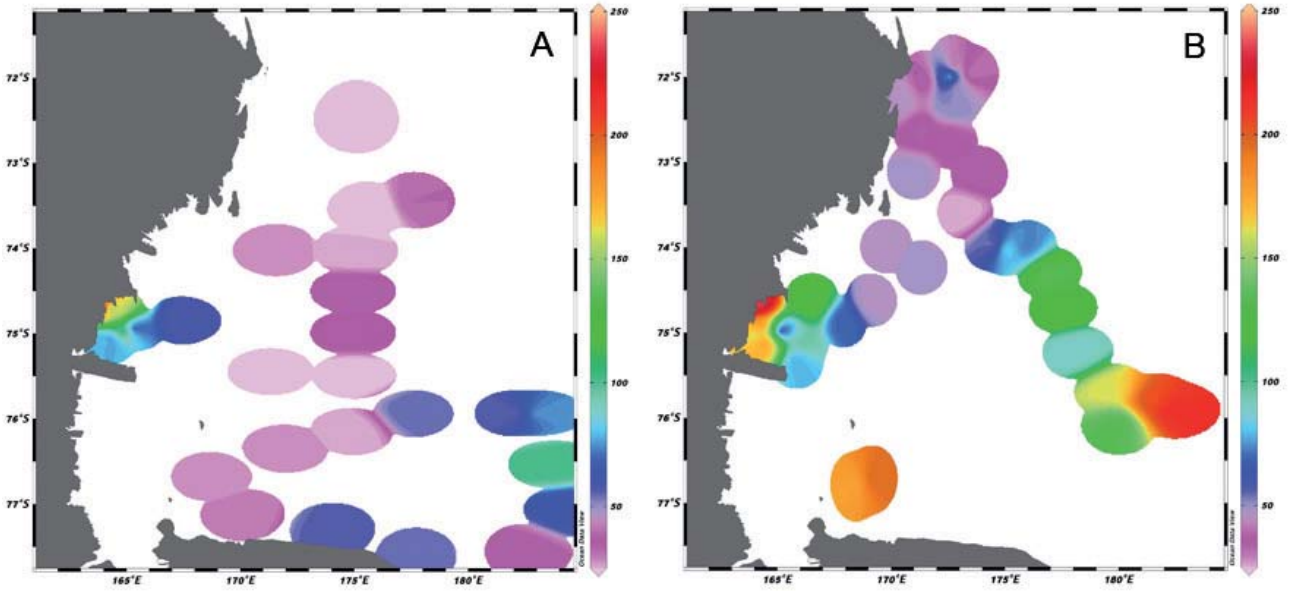

Figure 3. Spatial distribution of integrated total biomass (Chl*a* mg m^{-2}) in the 0-100 m layer during summer 1996 (A) and 2001 (B)

The variability in P^B_{max} across all stations and depths showed high variability in 2001 (Fig. 5). The difference in variations in P^B_{max} values between two different years may be related to the relatively deep mixed layer in ice-free waters during 1996 (Fig. 3 in Saggiomo et al., 2002) and, as a result of ice melting, the presence of a shallow upper mixed layer (UML) and a strong stratification in 2001 (Fig. 3 in Mangoni et al., 2004). Spatial distribution of mean values of P^B_{max} showed similar trend in offshore water above and below the UML; maximum values were recorded in the UML of the Terra Nova Bay polynya (Fig. 6).

The southwestern area is reported as one of the most productive areas in the Ross Sea and this area was furthermore a MIZ in 2001. Replicate sampling over three days showed an increment of phytoplankton biomass coupled with a decrease of primary production in the subsurface

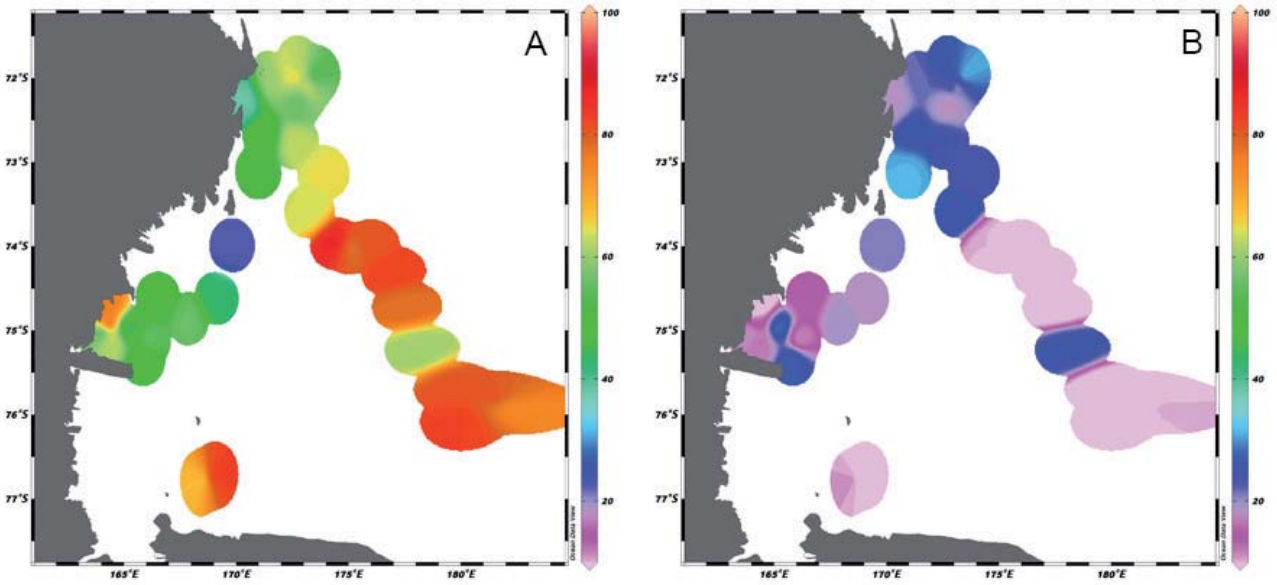

Figure 4. Spatial distribution of the mean percentage contribution of diatoms (A) and haptophytes (B) to phytoplankton community during summer 2001 in the layer 0-100 m

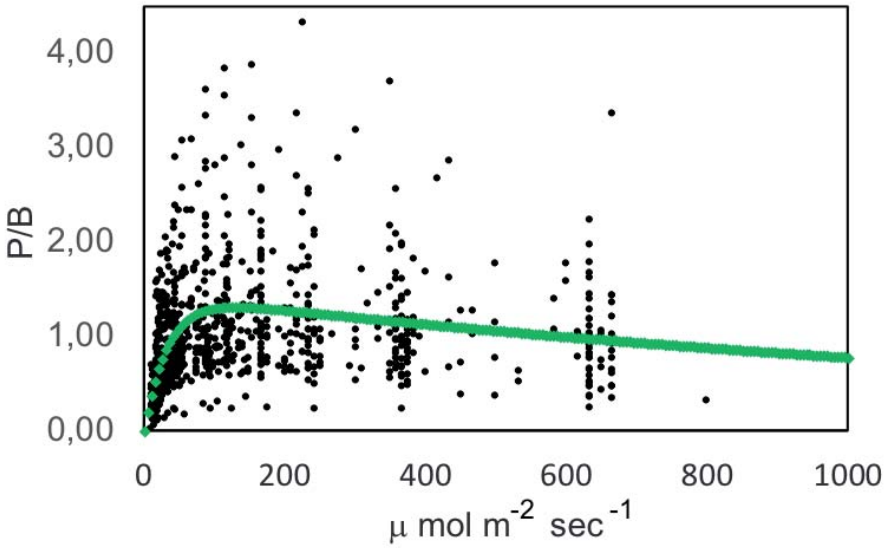

Figure 5. P*vs*E curves determined at 4 depths of all stations sampled in summer 2001

layers (Fig. 7). P*vs*E experiments conducted at two days interval showed similar values at surface in the first experiment (P^B_{max} 1.42 at surface and 1.38 mgC(mgChl*a*)$^{-1}$h^{-1} at 10 m depth) and a sharp decline of P^B_{max} 0.46 mgC(mgChl*a*)$^{-1}$h^{-1} two days later at 10m depth (Fig. 8). Macronutrient concentrations did not change. Unfortunately, micronutrient measurements were not performed but photosynthetic performance F_v/F_m was well below 0.3 in the upper layer of the off-shore MIZ areas (Fig. 7), which indicates iron limitation (Parkhill et al., 2001). In fact, high F_v/F_m values (0.45-0.65) are in the optimal range reported for the Ross Sea, which suggests the onset of a phytoplankton bloom, not affected by limiting factors (Fragoso & Smith, 2012; Mangoni et al., 2017). High photosynthetic performance ($F_v/F_m > 0.3$) and the highest integrated primary production values were recorded in the coastal area of TNB, where iron limitation does not occur.

In the northern area, the ratio between primary production and Chl*a* (PP/Chl*a*) was similar in both years, resulting in primary production values 2.5 times higher than

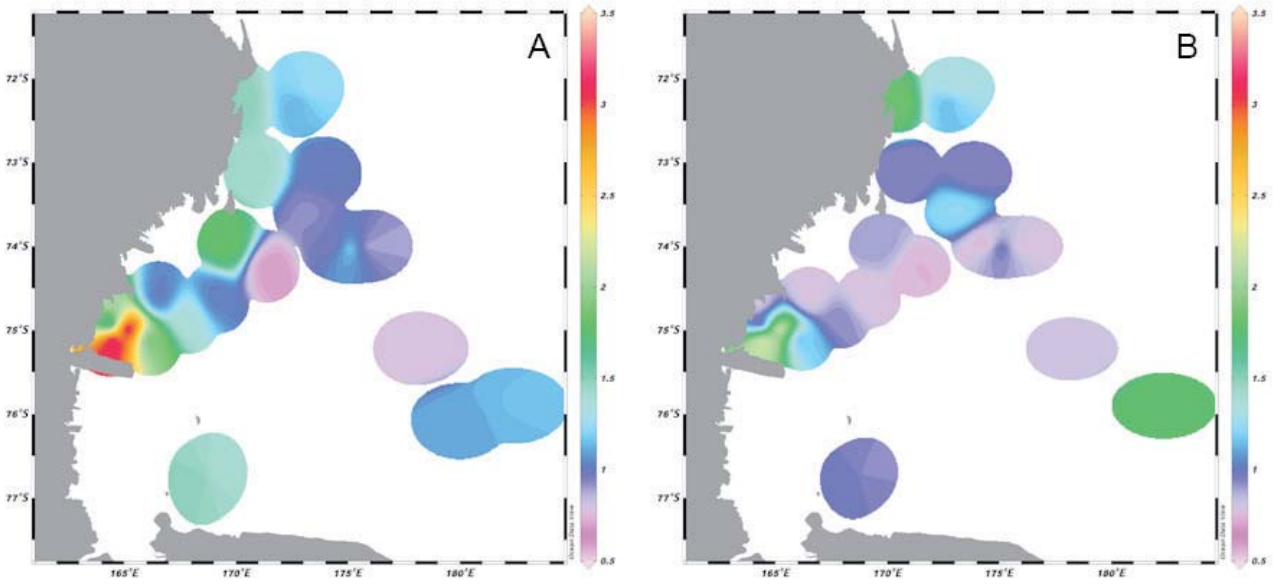

Figure 6. Spatial distribution of mean values of P^B_{max} above (A) and below (B) the UML in summer 2001

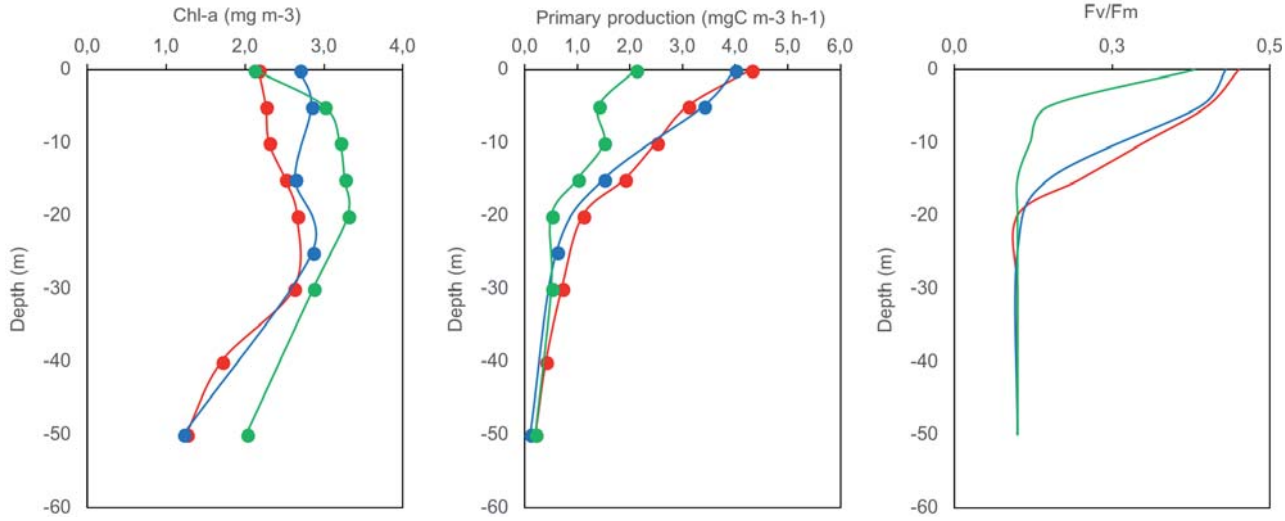

Figure 7. Replicate vertical profiles of Chl*a*, primary production and F_v/F_m in the southwestern Ross Sea area during summer 2001 (Jan. 30, Jan. 31, Feb. 1)

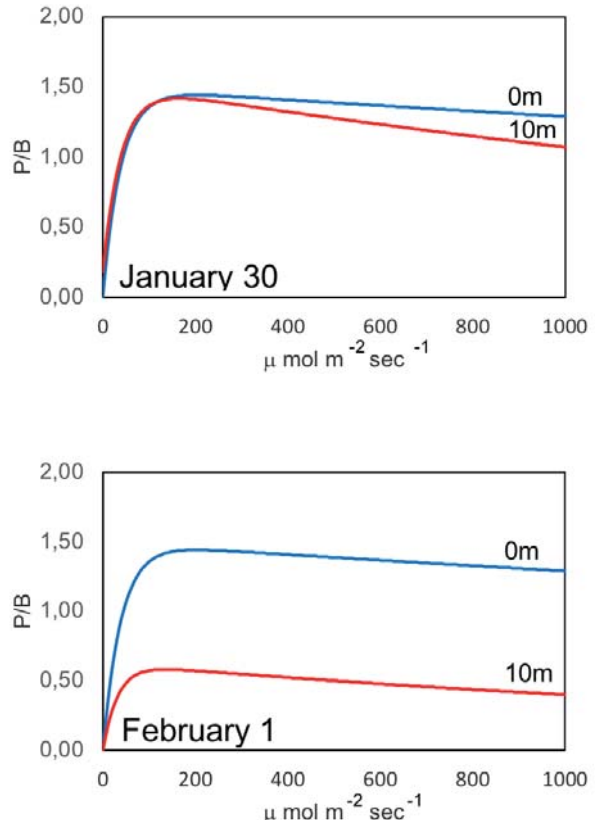

Figure 8. Replicate PvsE experiments at two depths (0 and 10m) in the southwestern Ross Sea area during summer 2001

those recorded in 1996 (Table 2). In all other areas, the PP/Chl*a* ratio was lower in 2001 and minimum growth capacity was recorded in the southwestern ice edge area. Only minor differences were observed in the coastal area, that indicates non-limiting conditions.

Table 2. Mean values of integrated primary production (mgC m^{-2} d^{-1}) of different areas in the Ross Sea during austral summer 1996 and 2001.

	North	Southwest	Southeast	Coastal water (BTN)
Summer 1996	188	200	600	1410
Summer 2001	479	707	1100	1562

The data collected during austral summer 1996 and 2001 in different environmental conditions (ice-free and ice-covered waters) emphasize that the off-shore waters of the Ross Sea represent the classic ecological Antarctic paradox with limiting factors such as micronutrients. The magnitude, extent and timing of phytoplankton blooms are likely affected by the timing of sea ice disappearance, prevailing wind speed and wave action. In contrast with this scenario, in the latest 10 years relevant changes in the abundance of phytoplankton in off-shore waters of the Ross Sea have been verified during austral summer in ice-free waters (Hatta et al., 20017; Kohut et al., 2017).

To identify the mechanisms that modulate phytoplankton blooms and the consequent fate of organic materials produced by the blooms during austral summer in the Ross Sea, an oceanographic cruise was conducted in 2014 (Mangoni et al., 2017; Misic et al., 2017; Rivaro et al., 2017). Mangoni and co-workers (2017) reported that the distribution of the main functional groups showed significant incongruities with the past. Diatoms (in different physiological status) were the dominant taxon. The high percentage of diatoms appears to be independent from the thickness of the UML. In our opinion, it is relevant that the presence of large diatoms in a wide UML contradicts the classic paradigm of Antarctic diatom accumulation in highly stratified waters (Smith & Nelson, 1985, Arrigo et al., 1998). In addition, *P. antarctica* colonial bloom occurs in an area and in a season that are usually characterized by the prevalence of diatoms. The considerable phytoplankton biomass observed, in agreement with the recent literature (e.g. Kohut et al., 2017), suggests relevant alterations in the Ross Sea summer productivity. Moreover, our findings show an uncoupled increase in large diatoms and primary consumers independent from the phase of the bloom. The low Pheapigment/Chl*a* ratios and the presence of senescent (instead of grazed) phytoplankton cells suggest the presence of a relatively scarce trophic efficiency. The considerable increases in phytoplankton biomass and large size structure (micro-fraction accounting for 75% of the total biomass on average, independent from the functional groups) suggest that the Ross Sea could now be extremely productive in summer (Mangoni et al., 2017). The phytoplankton features in summer 2014 were more similar to typical spring conditions, as characterized by the dominance of micro-phytoplankton fractions along the ice edge, which sustains the energy transfer through the Antarctic short trophic chain "diatoms-euphausiids- whales" (Xavier et al., 2016).

The comparison between conditions observed during summer 2014 and those reported for previous years reveals considerably different ecological assets that may result from current climate changes. Yet the magnitude and nature of changes remain unclear (Massom & Stammerjohn, 2010; Constable et al., 2014; Ainley et al., 2015; Turner et al., 2015). It is unclear what are the environmental factors that drive these extraordinary changes in primary production processes during austral summer and the prevalence of

different functional groups. Probably, a modification of the Ross Sea hydrography is having a key role in reducing the limiting factors and as a consequence in modifying the primary production processes. Hatta and co-workers (2017) suggested that these changes are driven by modifications of the circumpolar deep water circulation and variations of the benthic sources which supply iron to the system.

Recent information coming from the sampling cruise carried out during austral summer 2017 by our group highlights an extraordinary increase of flagellates in the composition of phytoplankton communities but the factors that drove changes in the functional groups are unclear. Other studies reported that the cobalamin (vitamin B_{12}) and iron availability can simultaneously increase the percentage of diatoms, suggesting that vitamin B_{12} may help govern rates of primary production as well as phytoplankton species composition (Croft et al., 2005; Betrand et al., 2007; 2015).

4. Conclusions

Antarctic marine ecosystems have been changing, in response to increasing ocean temperatures and changes in the extent and seasonality of sea ice. The magnitude and direction of these changes vary between regions around Antarctica that could see populations of the same species changing differently in diverse regions. The analysis of our data and the recent literature clearly show that some paradigms of functioning in polar ecosystems must necessarily be reviewed in light of new knowledge. The changes that are occurring in polar environments impose different approaches, a new era of study and their global function not only in terms of climate regulations but also in terms of resources and acquisitions of new knowledge. The dynamics of sea ice will probably not change drastically in the coming years and we will see even more interannual variability and different responses of the biotic communities. Climate change effects (Fe?) on algal community structure and carbon and nutrient cycles are difficult to predict, due to the need for multivariate approaches to address synergistic and antagonistic interactions.

There is no new set-up of the ecological dynamics of the polar systems, but the need to increase the studies on these areas that play a key role in the future asset of the planet. Some of the open questions are listed below:

- Could the present ecological asset of the Ross Sea during austral summer affect not only the Ross Sea itself, but probably the entire Southern Ocean ecology, and consequently have an impact at a global scale?
- Could recurrent blooms of un-grazed *Phaeocystis antartica* during austral spring and summer play an important role in driving CO_2 drawdown?
- Could the imbalance between phytoplankton standing stocks and primary consumers, independently from the phase of the bloom, dramatically alter the fate of the summer primary production and the C export in the Ross Sea?
- Could the changes in the phytoplankton composition to determine a new asset of the food web in the Ross Sea?

References

Ainley D.G., Ballard G., Jones R.M., Jongsomjit D., Pierce S.D., Smith W.O. & Veloz S., 2015, Trophic cascades in the western Ross Sea, Antarctica: revisited, Marine Ecology Progress Series, 534: 1-16.

Alderkamp A.-C., Kulk G., Buma A.G.J., Visser R.J.W., Van Dijken G.L., Mills M.M. & Arrigo K.R., 2012, The effect of iron limitation on the photophysiology of *Phaeocystis antarctica* (Prymnesiophyceae) and *Fragilariopsis cylindrus* (Bacillariophyceae) under dynamic irradiance, Journal of Phycology, 48(1): 45.

Arrigo K.R., Worthen D.L., Schnell A., Lizotte M.P., 1998, Primary production in Southern Ocean waters, Journal of Geophysical Research, 103 (15): 587-600.

Arrigo K.R., Robinson D.H., Worthen D.L., Dunbar R.B., DiTullio G.R., van Woert M., Lizotte M.P., 1999, Phytoplankton community structure and the drawdown of nutrients and CO_2 in the Southern Ocean, Science, 283: 365-367.

Arrigo K.R., DiTullio G.R., Dunbar R.B., Robinson D.H., VanWoert M., Worthen D.L, Lizotte M.P., 2000, Phytoplankton taxonomic variability in nutrient utilization and primary production in the Ross Sea, Journal of Geophysical Research, 105: 8827-8846.

Arrigo K.R., Van Dijken G., Long M., 2008, Coastal Southern Ocean: A strong anthropogenic CO_2 sink, Geophysical Research Letters, 35: L21602. doi: 10.1029/2008GL035624.

Arrigo K.R., van Dijken G.L., Strong A.L., 2015, Environmental controls of marine productivity hot spots around Antarctica, Journal of Geophysical Research Oceans, 120(8): 5545-5565.

Babin M., Morel A., Gagnon R., 1994, An incubator designed for extensive and sensitive measurements of phytoplankton photosynthetic parameters, Limnology and Oceanography, 39: 694-702.

Bertrand E.M., Saito M.A., Rose J.M., Riesselman C.R., Lohan M.C., Noble A.E., Lee P.A., DiTullio G.R., 2007, Vitamin B_{12} and iron co-limitation of phytoplankton growth in the Ross Sea, Limnology and Oceanography, 52: 1079-1093.

Brunet C. & Mangoni O., 2010, Determinazione quali-quantitativa dei pigmenti fitoplanctonici mediante HPLC, [in:] Metodologie di studio del Plancton mari-

no, G. Socal, I. Buttino, M. Cabrini, O. Mangoni, A. Penna, C. Totti, (eds), ISPRA: 56, 379-385.

Budillon G., Castagno P., Aliani S., Spezie G., Padman L., 2011, Thermohaline variability and Antarctic bottom water formation at the Ross Sea shelf break, Deep-Sea Research Part I, 1002-1018.

Carrada G.C., Mangoni O., Russo G.F., Saggiomo V., 2000, Phytoplankton size-fractionated biomasses in the Ross Sea. Spatial and temporal evolution during the austral spring. [in:] Ross Sea Ecology, Italian Antarctic expeditions (1987-1995). F.M. Faranda, L. Guglielmo, A. Ianora, (eds), Springer Berlin: 205-216.

Comiso J.C., Kwok R., Martin S. & Gordon A.L., 2011, Variability and trends in sea ice extent and ice production in the Ross Sea. Journal of Geophysical Research, 166: C4.

Comiso J.C, Gersten R.A, Stock L.V., Turner J., Perez G.J. & Cho K., 2017, Positive Trend in the Antarctic Sea Ice Cover and Associated Changes in Surface Temperature, American Meteorological Society, 30(6): 2151-2267.

Constable A.J., Melbourne-Thomas J., Corney S.P., Arrigo K.R., Barbraud C., Barnes D.K., Bindoff N.L., Boyd P.W., Brandt A., Costa D.P., Davidson A.T., Ducklow H.W., Emmerson L., Fukuchi M., Gutt J., Hindell M.A., Hofmann E.E., Hosie G.W., Iida T., Jacob S., Johnston N.M., Kawaguchi S., Kokubun N., Koubbi P., Lea M.A., Makhado A., Massom R.A., Meiners K., Meredith M.P., Murphy E.J., Nicol S., Reid K., Richerson K., Riddle M.J., Rintoul S.R., Smith W.O. Jr, Southwell C., Stark J.S., Sumner M., Swadling K.M., Takahashi K.T., Trathan P.N., Welsford D.C., Weimerskirch H., Westwood K.J., Wienecke B.C., Wolf-Gladrow D., Wright S.W., Xavier J.C., Ziegler P., 2014, Climate change and Southern Ocean ecosystems I: how changes in physical habitats directly affect marine biota, Global Change Biology, 20: 3004-3025.

Croft M.T., Lawrence A.D., Raux-Deery E., Warren M.J., Smith A.G., 2005, Algae acquire vitamin B_{12} through a symbiotic relationship with bacteria, Nature, 438: 90-93.

DiTullio G.R. & Smith W.O. Jr, 1996, Spatial patterns in phytoplankton biomass and pigment distributions in the Ross Sea, Journal of Geophysical Research, 101: 18467-18477.

DiTullio G.R., Grebmeier J., Arrigo K.R., Lizotte M.P., Robinson D.H., Leventer A., Barry J.P, VanWoert M.L. & Dunbar R.B., 2000, Rapid and early export of *Phaeocystis antarctica* blooms in the Ross Sea, Antarctica, Nature, 404: 595-598.

Ducklow H.W., Schofield O., Vernet M., Stammerjohn S., & Erickson M., 2012, Multiscale control of bacterial production by phytoplankton dynamics and sea ice along the western Antarctic Peninsula: A regional and decadal investigation, Journal of Marine Systems, 99: 26-39.

Feng Y., Hare C.E., Rose J.M., Handy S.M., DiTullio G.R., Lee P.A., Smith W.O. Jr, Peloquin J., Tozzi S., Sun J., Zhang Y., Dunbar R.B., Long M.C., Sohst B., Lohan M., Hutchins D.A., 2010, Interactive effects of iron, irradiance and CO_2 on Ross Sea phytoplankton, Deep-Sea Research Part I, 57: 368-383.

Fragoso G.M. & Smith W.O., 2012, Influence of hydrography on phytoplankton distribution in the Amundsen and Ross Seas, Antarctica, Journal of Marine Systems, 89(1): 19-29.

Fitch D.T. & Moore J.K., 2007, Wind speed influence on phytoplankton bloom dynamics in the Southern Ocean marginal ice zone, Journal of Geophysical Research Oceans, 112: C08006, doi:10.1029/2006jc004061.

Geibert W., Assmy P., Bakker D.C.E., Hanfland C., Hoppema M., Pichevin L.E., Schröder M., Schwarz J.N., Stimac I., Usbeck R. & Webb A., 2010, High productivity in an ice melting hot spot at the eastern boundary of the Weddell Gyre, Global Biogeochemical Cycles, 24 (3). GB3007, 01.09.2010.

Guglielmo L., Carrada G.C., Catalano G., Cozzi S., Dell'Anno A., Fabiano M., Granata A., Lazzara L., Lorenzelli R., Manganaro A., Mangoni O., Misic C., Modigh M., Pusceddu A., Saggiomo V., 2004, Biogeochemistry and algal communities in the annual sea ice at Terra Nova Bay (Ross Sea, Antarctica), Chemistry and Ecology, 20 (1): 43-55.

Hatta M., Measures C.I., Lam P.J., Ohnemus D.C., Auro M.E., Grand M.M., et al., 2017, The relative roles of modified circumpolar deep water and benthic sources in supplying iron to the recurrent phytoplankton blooms above Pennell and Mawson Banks, Ross Sea, Antarctica, Journal of Marine Systems, 166: 61-72.

Holm-Hansen O., Lorenzen C.J., Holmes R.W., Strickland J.D.H., 1965, Fluorometric determination of chlorophyll, Journal du Conseil/Conseil Permanent International pour l'Exploration de la Mer, 30: 3-15.

Jacobs S., 2004, Bottom water production and its links with the thermohaline circulation, Antarctic Science, 16: 427-437.

Kohut J.T., Kustka A.B., Hiscock M., Lam P.J., Measures C., Milligan A, et al., 2017, Mesoscale variability of the summer bloom over the northern Ross Sea shelf: A tale of two banks, Journal of Marine Systems, 166: 50-60.

Kurtz N.T. & Markus T, 2012, Satellite observations of Antarctic sea ice thickness and volume, Journal of Geophysical Research Oceans, 117: C08025, doi:10.1029/2012jc008141.

Legendre L., Demers S., Yentsch C.M., Yentsch C.S., 1983, The ^{14}C method: patterns ofdark CO_2 fixation and DCMU correction to replace the dark bottle, Limnology and Oceanography, 28: 996-1003.

Mackey M.D., Mackey D.J., Higgins H.W., Wright S.W., 1996, CHEMTAX-a program for estimating class abundances from chemical markers: application to HPLC measurements of phytoplankton, Marine Ecology Progress Series, 144: 265-283.

Mangoni O., Modigh M., Conversano F., Carrada G.C. & Saggiomo V., 2004, Effects of summer ice coverage on phytoplankton assemblages in the Ross Sea, Antarctica, Deep-Sea Research Part I, 51(11): 1601-1617.

Mangoni O., Saggiomo V., Bolinesi F., Margiotta F., Budillon G., Cotroneo Y., Misic C., Paola Rivaro P., Saggiomo M., 2017, Phytoplankton blooms during austral summer in the Ross Sea, Antarctica: driving factors and trophic implications, PLoS ONE,10.1371/journal.pone.0176033.

Mantoura R.F.C. & Llewellyn C.A., 1983, The rapid determination of algal chlorophyll and carotenoid pigments and their breakdown products in natural waters by reverse-phase high-performance liquid chromatography, Analytica Chimica Acta, 151: 297-314.

Massom R.A. & Stammerjohn S.E., 2010, Antarctic sea ice change and variability – Physical and ecological implications, Polar Science, 4(2): 149-186.

Misic C., Covazzi Harriague A., Mangoni O., Cotroneo Y., Aulicino G., Castagno P., 2017, Different responses of the trophic features of particulate organic matter to summer constraints in the Ross Sea, Journal of Marine Systems, 166: 132-143.

Ohshima K.I., Nihashi S. & Iwamoto K., 2016, Global view of sea-ice production in polynyas and its linkage to dense/bottom water formation, Geoscience Letter, 3:13. doi: 10.1186/s40562-016-0045-4.

Oza S.R., Singh R.K.K., Srivastava A., Dash M.K., Das I.M.L. & Vyas N.K., 2011, Inter-annual variations observed in spring and summer Antarctic sea ice extent in recent decade, Mausam, 62: 633-640.

Parkhill J.P., Maillet G., & Cullen J.J., 2001, Fluorescence-based maximal quantum yield for PSII as a diagnostic of nutrient stress, Journal of Phycology, 17: 517-529.

Parkinson C.L. & Cavalieri D.J., 2012, Antarctic sea ice variability and trends 1979-2010, Cryosphere, 6: 871-880.

Peloquin J.A. & Smith W.O. Jr, 2007, Phytoplankton blooms in the Ross Sea, Antarctica: interannual variability in magnitude, temporal patterns, and composition, Journal of Geophysical Research, 112: C08013. doi: 10.1029/2006JC003816.

Platt T., Gallegos C.L., Harrison W.G., 1980, Photoinhibition of photosynthesis in natural assemblages of marine phytoplankton, Journal of Marine Research, 38: 687-701.

Rivaro P., Ianni C., Langone L., Ori C., Aulicino G., Cotroneo Y., et al., 2017, Physical and biological forcing on the mesoscale variability of the carbonate system in the Ross Sea (Antarctica) during the summer season 2014, Journal of Marine Systems, 166: 144-158.

Saggiomo V., Carrada G.C., Mangoni O., Ribera d'Alcalà M., Russo A., 1998, Spatial and temporal variability of size-fractionated biomass and primary production in the Ross Sea (Antarctica) during austral spring and summer, Journal of Marine Systems, 17:115-127.

Saggiomo V., Carrada G.C., Mangoni O., Marino D., Ribera d'Alcalà M., 2000, Physiological and ecological aspects of primary production in the Ross Sea, [in:] Ross Sea Ecology, Italian Antarctic expeditions (1987-1995). F.M. Faranda, L. Guglielmo, A. Ianora, (eds), Springer Berlin: 247-258.

Saggiomo V., Catalano G., Mangoni O., Budillon G., Carrada G.C., 2002, Primary production processes in ice-free waters of the Ross Sea (Antarctica) during the austral summer 1996, Deep-Sea Research Part II, 49: 1787-801.

Saggiomo M., Poulin M., Mangoni O., Lazzara L., De Stefano M., Sarno D., et al., 2017, Spring-time dynamics of diatom communities in landfast and underlying platelet ice in Terra Nova Bay, Ross Sea, Antarctica, Journal of Marine Systems, 166: 26-36.

Saino N. & Guglielmo L., 2000, ROSSMZE expedition: distribution and biomass of bird and mammals in the western Ross Sea. [in:] Ross Sea Ecology, Italian Antarctic expeditions (1987-1995). F.M. Faranda, L. Guglielmo, A. Ianora, (eds), Springer Berlin: 469-478.

Sedwick P.N. & DiTullio G. R., 1997, Regulation of algal blooms in Antarctic shelf waters by the release of iron from melting sea ice, Geophysical Research Letter, 24: 2515-2518.

Sedwick P.N., Marsay C.M., Sohst B.M., Aguilar-Islas A.M., Lohan M.C., Long M.C., Arrigo K.R., Dunbar R.B., Saito M.A., Smith W.O. & DiTullio G.R., 2011, Early season depletion of dissolved iron in the Ross Sea polynya: Implications for iron dynamics on the Antarctic continental shelf, Journal of Geophysical Research-Oceans, 116: C12.

Smith W.O. Jr & Nelson D.M., 1985, Phytoplankton bloom produced by a receding ice edge in the Ross Sea: spatial coherence with the density field, Science, 227: 163-166.

Smith W.O. Jr & Gordon L.I., 1997, Hyperproductivity of the Ross Sea (Antarctica) polynya during austral spring, Geophysical Research Letters, 24: 233-236.

Smith W.O Jr, Shields A.R., Peloquin J.A., Catalano G., Tozzi S, Dinniman M.S., et al., 2006, Interannual variations in nutrients, net community production, and biogeochemical cycles in the Ross Sea, Deep-Sea Res II, 53: 815-833.

Smith W.O. Jr, Tozzi S., DiTullio G.R., Dinnimand M., Mangoni O., Modigh M., Saggiomo V., 2010, Phytoplankton photosynthetic pigments in the Ross Sea: Pat-

terns and relationships among functional groups, Journal of Marine Systems, 82: 177-185.

Smith W.O. Jr & Jones R.M., 2014, Vertical mixing, critical depths, and phytoplankton growth in the Ross Sea, ICES Journal of Marine Science, 72(6): 1952-1960. doi: 10.1093/icesjms/fsu234.

Smith W.O. Jr, Ainley D.G., Arrigo K.R., Dinniman M.S., 2014; The Oceanography and Ecology of the Ross Sea, Annual Review of Marine Science, 6: 469-87.

Tamura T., Ohshima K.I., Nihashi S., 2008, Mapping of sea ice production for Antarctic coastal polynyas, Geophysical Research Letter, 35: L07606

Taylor M.H., Losch M. & Bracher A., 2013, On the drivers of phytoplankton blooms in the Antarctic marginal ice zone: A modeling approach, Journal of Geophysical Research Oceans, 118(1): 63-75.

Turner J.J., Hosking S., Bracegirdle T.J., Marshall G.J., Phillips T., 2015, Recent changes in Antarctic Sea Ice, Philosophical Transactions of the Royal Society A Mathematical, Physical and Engineering, 373: 20140163, doi:10.1098/rsta.2014.0163.

Turner J. & Comiso J., 2017, Solve Antarctica's sea-ice puzzle, Nature, 547: 275-277.

Wang S. & Moore J.K., 2011, Incorporating *Phaeocystis* into a Southern Ocean ecosystem model, Journal of Geophysical Research, 116: C01019. doi:10.1029/2009jc005817.

Wang S., Bailey D., Lindsay K., Moore J. K. & Holland M., 2014, Impact of sea ice on the marine iron cycle and phytoplankton productivity, Biogeosciences, 11: 4713-4731.

Wright S.W., van den Enden R.L., Pearce I., Davidson A.T., Scott F.J., Westwood K.J. 2010, Phytoplankton community structure and stocks in the Southern Ocean (30-80°E) determined by CHEMTAX analysis determined by HPLC pigment signatures, Deep-Sea Research Part II, 57: 758-778.

Xavier J.C., Brandt A., Ropert-Coudert Y., Badhe R., Gutt J., Havermans C., Jones C., Costa E.S, Karin Lochte K., Schloss I.R., Mahlon C. Kennicutt II M.C. & Sutherland W.J., 2016, Future Challenges in Southern Ocean Ecology Research, Frontiers in Marine, Science, doi. org/10.3389/fmars.2016.00094.

PLOS ONE

RESEARCH ARTICLE

Phytoplankton blooms during austral summer in the Ross Sea, Antarctica: Driving factors and trophic implications

Olga Mangoni[1]*, Vincenzo Saggiomo[2], Francesco Bolinesi[1], Francesca Margiotta[2], Giorgio Budillon[3], Yuri Cotroneo[3], Cristina Misic[4], Paola Rivaro[5], Maria Saggiomo[2]

1 Dipartimento di Biologia, Università degli Studi di Napoli Federico II, Naples, Italy, **2** Stazione Zoologica Anton Dohrn, Naples, Italy, **3** Dipartimento di Scienze e Tecnologie, Università degli Studi di Napoli Parthenope, Naples, Italy, **4** Dipartimento di Scienze della Terra, dell'Ambiente e della Vita, Università degli Studi di Genova, Genoa, Italy, **5** Dipartimento di Chimica e Chimica Industriale Università degli Studi di Genova, Genoa, Italy

* olga.mangoni@unina.it

Check for updates

OPEN ACCESS

Citation: Mangoni O, Saggiomo V, Bolinesi F, Margiotta F, Budillon G, Cotroneo Y, et al. (2017) Phytoplankton blooms during austral summer in the Ross Sea, Antarctica: Driving factors and trophic implications. PLoS ONE 12(4): e0176033. https://doi.org/10.1371/journal.pone.0176033

Editor: Syuhei Ban, University of Shiga Prefecture, JAPAN

Received: January 6, 2017

Accepted: April 4, 2017

Published: April 21, 2017

Copyright: © 2017 Mangoni et al. This is an open access article distributed under the terms of the Creative Commons Attribution License, which permits unrestricted use, distribution, and reproduction in any medium, provided the original author and source are credited.

Data Availability Statement: All relevant data are within the paper and its Supporting Information files.

Funding: This work was carried in the framework of the Project Ross Sea Mesoscale Experiments (RoME) funded by the Italian National Program for Antarctic Research (PNRA, 2013/AN2.04).

Competing interests: The authors have declared that no competing interests exist.

Abstract

During the austral summer of 2014, an oceanographic cruise was conducted in the Ross Sea in the framework of the RoME (Ross Sea Mesoscale Experiment) Project. Forty-three hydrological stations were sampled within three different areas: the northern Ross Sea (RoME 1), Terra Nova Bay (RoME 2), and the southern Ross Sea (RoME 3). The ecological and photophysiological characteristics of the phytoplankton were investigated (i.e., size structure, functional groups, PSII maximum quantum efficiency, photoprotective pigments), as related to hydrographic and chemical features. The aim was to identify the mechanisms that modulate phytoplankton blooms, and consequently, the fate of organic materials produced by the blooms. The observed biomass standing stocks were very high (e.g., integrated chlorophyll-a up to 371 mg m^{-2} in the top 100 m). Large differences in phytoplankton community composition, relative contribution of functional groups and photosynthetic parameters were observed among the three subsystems. The diatoms (in different physiological status) were the dominant taxa in RoME 1 and RoME 3; in RoME 1, a post-bloom phase was identified, whereas in RoME 3, an active phytoplankton bloom occurred. In RoME 2, diatoms co-occurred with *Phaeocystis antarctica*, but were vertically segregated by the upper mixed layer, with senescent diatoms dominating in the upper layer, and *P. antarctica* blooming in the deeper layer. The dominance of the phytoplankton micro-fraction over the whole area and the high Chl-a suggested the prevalence of non-grazed large cells, independent of the distribution of the two functional groups. These data emphasise the occurrence of significant temporal changes in the phytoplankton biomass in the Ross Sea during austral summer. The mechanisms that drive such changes and the fate of the carbon production are probably related to the variations in the limiting factors induced by the concurrent hydrological modifications to the Ross Sea, and they remain to be fully clarified. The comparison of conditions observed during summer 2014 and those reported for previous years reveal considerably different ecological assets that might be the result of current

climate change. This suggests that further changes can be expected in the future, even at larger oceanic scales.

Introduction

Global temperatures have risen by >1˚C over the last few decades [1], and more than 75% of the heat excess has been stored in the Southern Ocean [2]. Investigations on climate change are focused intensely on this area due to a combination of biological and physical processes, although the magnitude and direction of the changes differ on a regional scale [3, 4].

These spatially heterogeneous changes will have differential effects on phytoplankton composition, productivity, and carbon sequestration, through alterations to ambient temperature, total irradiance, wavelength structure, nutrient availability, and trophodynamics [5–7]. However, our understanding of the environmental controls on phytoplankton growth and standing stocks is still incomplete, and to date, current variations that affect the pelagic food web remain mostly unknown [8, 9]. Therefore, these topics are included in the list of the 80 priority scientific questions for future Antarctic research, as identified by the 1st Scientific Committee on Antarctic Research, Antarctic and Southern Ocean Science Horizon Scan [10, 11].

The Ross Sea is the most productive sector of the Southern Ocean, and thus it has a strong impact on marine biogeochemical cycles and air-sea heat and CO_2 fluxes on a global scale [5] [12, 13]. The phytoplankton of the Ross Sea are alternatively dominated by two functional groups, diatoms and Haptophytes (e.g., *Phaeocystis antarctica*), which are typically separated both in space and time [14, 15]. The relative abundances of diatoms and *P. antarctica* have key roles in shaping the food web, and can impair the absorption and export of carbon to the bottom of the Ross Sea [16–19]. Diatoms usually comprise 90% of the phytoplankton along the western continental shelf and in the Terra Nova Bay polynya, where the stratification of the melting ice of the surface waters results in relatively shallow mixed layers (≤20 m) [20, 21]. In contrast, in December, *P. antarctica* in mucilaginous colonies comprises 95% of the phytoplankton in the Ross Sea polynya in the deep mixed layer (40–60 m). During this time frame, the colonies are largely ungrazed and exported to the deep ocean [17, 22]. In summer, *P. antarctica* abundance is low, and it can occur in colonies or as single cells; the latter form can directly enter the microbial food web [23, 24]. However, the spatial and temporal mosaic of phytoplankton dynamics in the Ross Sea is more complex, as there are significant inter-annual variations [25–27]. Nevertheless, *P. antarctica*- and diatom-dominated waters derive from a combination of multiple physical-chemical factors, which include macro-nutrients, micro-nutrients and CO_2 concentrations, as well as the sea surface temperature [28–32]. Among these, the timing and supply of Fe input can affect the phytoplankton composition, due to the potentially distinct Fe requirements of *P. antarctica* and diatoms [33–36].

At the community level, the maximum quantum yield (F_v/F_m) and electron transfer rate of photosystem II (PSII) in photosynthesis are widely used as indicators to assess responses of phytoplankton to different levels of environmental stressors, including deficiencies in macro-nutrients and micro-nutrients [37–39]. In this regard, it is commonly stated that a decline in F_v/F_m indicates a compromised photosynthetic performance [40]. Thus, understanding the combined effects of such complex changes on phytoplankton photophysiology, and unveiling the mechanisms responsible for the distribution of these two different functional groups is

crucial, due to the particular biogeochemical and ecological roles that they have within Antarctic marine ecosystems [41, 42].

To shed light on the mechanisms that modulate the distribution of phytoplankton (i.e., in terms of biomass, size classes, functional groups) and their photophysiology, this study investigated three different areas of the Ross Sea during the austral summer of 2014. The phytoplankton community structure, the factors driving the blooms and the trophic implications are discussed here, as related to water mass properties and dynamics of the surface water layer (0–200 m).

Materials and methods

Ethics statement

All samples were obtained during the project "Ross Sea Mesoscale Experiment" (RoME) in the framework of the Italian National Antarctic Program (PNRA, 2013/AN2.04) coordinated by the Ministry of Education, University and Research (MIUR). The permission to collect samples was authorised by the National Environmental Officer of the National Agency for New Technologies, Energy and the Sustainable Economic Development (ENEA) on the base of Environmental Evaluation (Impact) Assessment of the RoME Project, following the "Protocol on Environmental Protection of the Antarctic Treaty", Annex II, art.3.

Study areas and sampling strategy

A multidisciplinary oceanographic cruise in the Ross Sea was conducted on the *R/V Italica* from 16 January to 3 February, 2014, in the framework of the project entitled "Ross Sea Mesoscale Experiment" (RoME).

The sampling strategy was designed on the basis of real-time satellite data, and was aimed at covering three areas that are characterised by different sea surface temperatures and chlorophyll-a (Chl-a) signatures, which appear to be related to the differences in water mass properties and dynamics. Maps from the Moderate Resolution Imaging Spectroradiometer Aqua and Terra satellite level-2 (products for the previous 12/24 h) were used to define the locations of the sampling stations. Sea ice conditions were obtained from the Advanced Microwave Scanning Radiometer-2 satellite maps provided by the University of Bremen (Germany). The sampling activity was then performed in three different areas of the Ross Sea (Fig 1; for list of geographical coordinates of stations see S1 Table). Fig 2 shows the sampling stations within each area, with a map of the upper mixed layer (UML) and Θ/S diagram.

First, the offshore sampling area was named RoME 1 (carried out from 16 to 17 January, 2014) and it was located in the northern section of the Ross Sea, between 74˚S and 75˚S, at approximately 170˚E (Fig 2A). The "L" shape of this leg, which crossed Crary Bank, was designed to identify the location of the thermohaline fronts connected to expected differences in temperature and salinity between the more coastal and offshore water masses.

The second sampling area was named RoME 2 (carried out from 26 to 28 January, 2014) and it was located more coastward, next to the Terra Nova Bay polynya over the Drygalski Ice Tongue (Fig 2D). According to a clear signature in the satellite Chl-a maps and to the bathymetry forcing, it displayed a frontal structure in several oceanographic variables, oriented in the NE/SW direction [45].

Finally, the third sampling area was named RoME 3 (carried out from 31 January to 3 February, 2014), and it was situated in the offshore area of the southern Ross Sea at approximately 76.5˚S, in a position south of Franklin Island and on the margin of the Ross Sea polynya

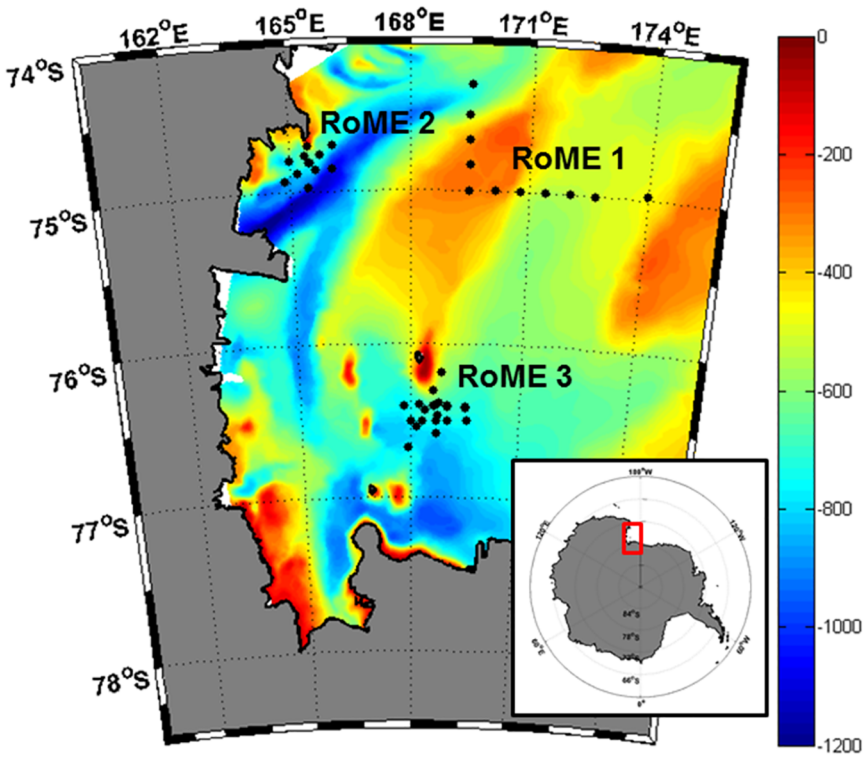

Fig 1. Sampling stations of the RoME Project. The black dots indicate the sampling stations. The bathymetry data of the Ross Sea from [43] under a CC BY license, with permission from [Davey], original copyright [2004–2005].

https://doi.org/10.1371/journal.pone.0176033.g001

(Fig 2G). This site was chosen due to the presence of an isolated mesoscale structure observed in the Chl-a concentration and the surface temperature satellite maps.

A total of 43 stations were sampled: RoME 1, 11 stations; RoME 2, 12 stations; and RoME 3, 20 stations (S1 Table). Continuous data and water samples were collected using a carousel sampler (Sea-Bird Electronics 32) equipped with 24 12-L Niskin bottles, a conductivity–temperature-depth (CTD) instrument (9/11 Plus; Sea-Bird Electronics) with double temperature and conductivity sensors, an oxygen sensor (Sea-Bird Electronics), a fluorometer (Chelsea Aquatracka III) and a programmable sonar altimeter (Datasonics). Furthermore, two lowered acoustic Doppler current profilers were deployed together with the CTD, to obtain current fields every 10 m from the surface to the maximum sampled depth. The water sampling depths (6–7 for each station) were chosen according to the fluorescence profile. Subsamples drawn from each Niskin bottle were collected for analysis of inorganic nutrients, particulate matter and phytoplankton (i.e., biomass, size classes, functional groups, taxonomic composition, photophysiology). Incident irradiance (LI-193SA quantum sensor; Licor) was measured during the whole length of the cruise.

Hydrography, nutrients and particulate organic matter

Full resolution CTD data from the surface to the maximum sampled depth (always $\geq$200 m) were used to describe the main water masses and the water column characteristics during the three RoME legs. For each station, the UML depth was determined as the depth at which the *in-situ* density (σt) changed by 0.05 kg m^{-3} over a 5 m depth interval [45]. The melt-water percentage (MW%) was calculated from the difference between the salinity measured at a

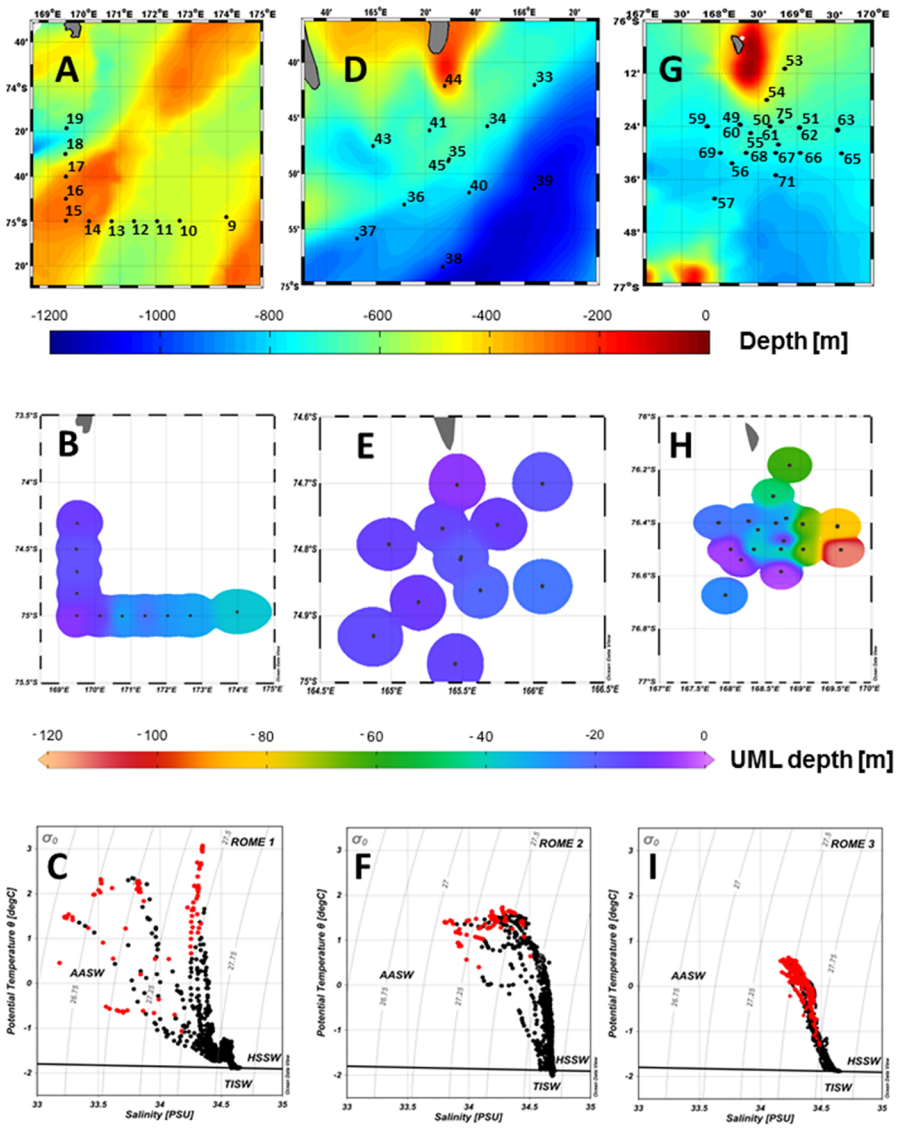

Fig 2. Sampling stations within each area, corresponding map of the upper mixed layer (UML) and the Θ/S diagram. Station maps for the RoME 1, 2 and 3 (A, D, G, respectively). The bathymetry data of the Ross Sea from [43] under a CC BY license, with permission from [Davey], original copyright [2004–2005]. Map of the UML depth (colour scale) for the three areas (B, E, H). The Θ/S diagrams for each leg with indication of data shallower than the UML (red dots) and of the freezing point (C, F, I). UML maps and Θ/S diagrams produced through Ocean Data View software [44].

https://doi.org/10.1371/journal.pone.0176033.g002

given depth (S_{meas}) and the deep salinity (S_{deep}; i.e., at 200 m), assuming a mean sea-ice salinity of 6 [46].

For determination of the nutrients (NO_3^-, NO_2^-, NH_4^+, $Si(OH)_4$, PO_4^{3-}), samples were taken directly from the Niskin bottles, filtered through GF/F filters, stored at –30˚C in 100 mL low-density polyethylene containers, and analysed using a five-channel continuous flow autoanalyser (Technicon Autoanalyser II), according to the method described by [47], which was adapted to the present instrumentation.

Particulate organic carbon (POC) and particulate organic nitrogen (PON) were analysed after acidification with HCl fumes, to remove inorganic carbon [48]. Cyclohexanone 2-4-dinitrophenyl hydrazone was used to calibrate an elemental analyser (Model 1110 CHN; Carlo Erba). The particulate protein and carbohydrate concentrations were determined [49, 50]. Albumin and glucose solutions were used to calibrate the spectrophotometer (Jasco V530).

Phytoplankton pigments, taxonomic composition and photophysiology

Samples for determination of the total phytoplankton biomass and size structure (as micro [>20 μm], nano [2–20 μm], pico [<2 μm] fractions) were collected at 6 or 7 depths, following a protocol of serial filtration [51]. Filters were stored at -80˚C until further analysis. The analyses of Chl-a and phaeopigments (Phaeo-a) were carried out according to [52], with a spectrofluorometer (Varian Eclipse), which was checked daily with a Chl-a standard solution (from *Anacystis nidulans*; Sigma).

For pigment spectra samples, 1 L or 2 L seawater was filtered (GF/F Whatman) and stored at -80˚C for HPLC (1100 Series, Hewlett Packard) analyses [53]. Instrument calibration was carried out with external standard pigments provided by the International Agency for ^{14}C determination-VKI Water Quality Institute. The relationship between spectrofluorimetric Chl-a and HPLC Chl-a for all samples was very close ($p < 0.001$, $y = 1.28\ x + 0.26$, $R^2 = 0.82$, $n = 198$). The concentrations of pigments were used to estimate the contributions of the main functional groups to the total Chl-a using a matrix factorisation programme (CHEMTAX) [54, 55]. The carotenoids participating in the photoregulatory processes through the xanthophyll cycle were analysed [56, 57]. The photo-protective pigment ratio was calculated as the ratio of the sum of diadinoxanthin (Dd) and diatoxanthin (Dt) to Chl-a (Dd+Dt/Chl-a). The de-epoxidation state of the xanthophyll cycle was expressed as the ratio between the Dt and Dd+Dt concentrations (Dt/[Dd+Dt]).

Previous investigations on the interaction between Fe, diatoms and nutrient uptake highlighted a preferential drawdown of silicate under Fe-deplete compared to Fe-replete conditions, which resulted in an increase in the ratio between used silica and fucoxanthin [58]. In the present study, this ratio was computed as the difference between the mean $Si(OH)_4$ concentration at 200 m in each RoME experiment and the corresponding $Si(OH)_4$ concentration at a certain depth divided by the corresponding fucoxanthin concentration (ΔSi/Fuco). The ΔSi/Fuco ratio has been used as a proxy of Fe availability.

Samples for the phytoplankton taxonomic identification were collected at 4 or 5 depths, according to the vertical fluorescence profiles, and preserved in formalin solution (final concentration, 4%), buffered with $CaCO_3$. Cell counts were performed with an inverted light microscope (Zeiss Axiophot), according to the Utermöhl method [59].

At each station (at 4–5 depths), aliquots of 30 mL water samples were rapidly collected from the Niskin bottles to measure the quantum yield. The photochemical efficiency of photosystem PSII was estimated by pulse amplitude fluorescence measurements using a fluorometer (Phyto-PAM; Walz, Effeltrich, Germany), with the PhytoWIN software used for the data elaboration [60]. After each water sample had been left in a dark-adapted environment for 10 min, 3 mL were injected into a quartz cuvette to determine the maximum quantum yield (F_v/F_m) of the photochemical energy conversion in PSII.

Statistical analyses

Descriptive statistics (i.e., box plots, scattergrams, means, minima, maxima, standard deviations), correlation (Spearman) and multivariate (principal component analysis [PCA]) analyses were carried out using the XLSTAT software. PCA based on a correlation matrix was used

to investigate the relationships among the *in-situ* environmental variables (temperature, melt-water fraction, nutrient concentrations) and biological features (F_v/F_m, ΔSi/Fuco, relative contribution of diatoms and Haptophytes) using the complete dataset (all of the selected parameters analysed in the three experiments).

Results

Physical and chemical constraints

During the entire sampling period, weather conditions were characterised by cloudiness, which partially influenced the satellite map availability and reduced the irradiance, with incident light ranging from 17 to 54 mol photons m^{-2} d^{-1}. The means of the incident light during the RoME 1 and RoME 3 samplings were 30 and 28 mol photons m^{-2} d^{-1}, respectively, while the RoME 2 sampling activities were characterised by higher daily irradiance levels, ranging from 27 up to 54 mol photons m^{-2} d^{-1} (on 28 January).

The ice retreat had occurred at different times over these three areas. In particular, the RoME 2 sampling area was free from ice from early December, whereas the northernmost station of RoME 1 and RoME 3 showed ice until early January and late December, respectively [61].

The lowered acoustic Doppler current profiler data and geostrophic velocities calculated from full-depth CTD data (not shown) confirmed that different satellite sea surface temperature and Chl-a patterns were also associated with particular water mass dynamics in each area. During RoME 1, the current data showed weak northward currents for the western stations, and stronger currents on the eastern side of Crary Bank. Here, a frontal structure was also evident, with large temperature and salinity gradients between the eastern and western parts of the leg, corresponding to stations 13 and 14. A thermohaline front was the main feature of the RoME 2 leg too, which was extensively described on the basis of current meter and CTD data [45]. Fresher and colder water masses were confined to the coastal area on the eastern part of the transect from station 33 to 37. Saltier and warmer waters were found in the eastern and deeper section of the leg, corresponding to the Drygalski Ice Tongue. The current meter and CTD data acquired during RoME 3 showed cyclonic circulation associated with the shoaling of temperature and salinity isolines at the centre of the mesoscale structure observed in the satellite data.

The Θ/S diagrams (Fig 2C, 2F and 2I) showed typical Ross Sea water masses as the Antarctic Surface Water (AASW), the High Salinity Shelf Water (HSSW) and the Terra Nova Bay Ice Shelf Water (TISW) [62, 63]. Nonetheless, significant differences in temperature and salinity properties were found mainly in the surface layer during the three legs. To highlight the variability of the UML water masses, this study is thus focused on the upper 200 m, while a complete analysis of the water mass properties along the entire water column can be found in [45, 61].

The intensity of the surface stratification is dependent on the freshwater input, melting sea-ice, and solar heating of the surface water. Consistent with the warmer temperatures and high melt water content at the surface, the water column was stratified, but differences in UML depth were observed (Figs 2B, 2E, 2H and 3). The mean thicknesses of the UML calculated for RoME 1 and RoME 2 were 21 m and 16 m, respectively. In contrast, the RoME 3 area was characterised by deeper UML and showed a mean that was about two-fold higher (48 m) compared to RoME 1 and RoME 2.

During RoME 1 the UML depth differed in space (Fig 2B) and was tightly coupled with the surface salinity distribution. For the eastern section (stations 9–13), which was characterised by longer ice-free conditions and separated from the low salinity coastal waters, the UML was deeper (23–38 m). On the other hand, stations 14 to 19 showed shallower mixed layers, which

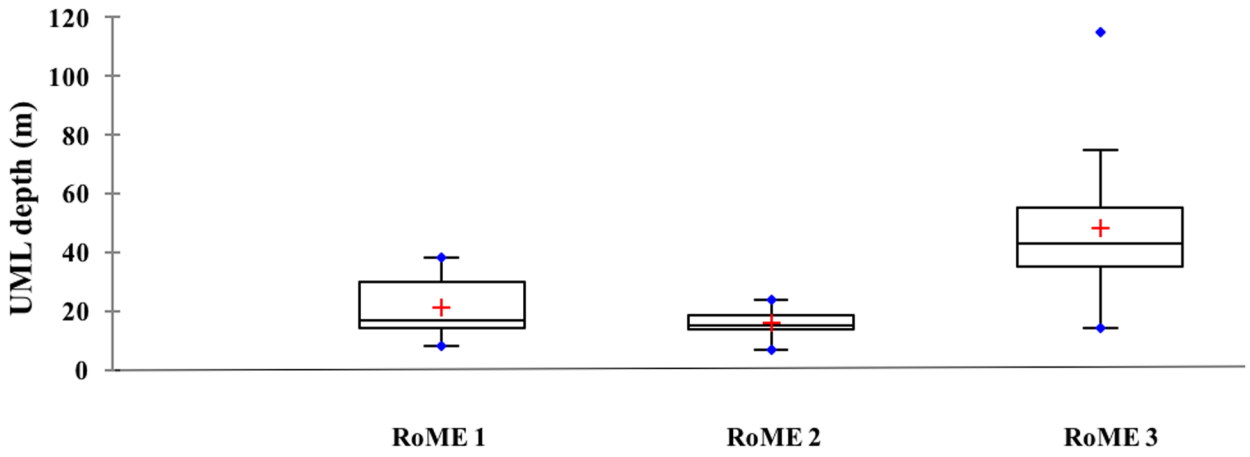

Fig 3. Upper mixed layer (UML) depth (m) in the three areas (boxplot by RoME). The red line shows the median, and the red cross the mean.

https://doi.org/10.1371/journal.pone.0176033.g003

ranged between 8 m and 17 m. For RoME 2, the surface temperature and salinity showed low spatial variability, resulting in homogeneous UML depths, which ranged from 7 m to 24 m (Fig 2E). The RoME 3 was characterised by the presence of AASW and HSSW included in a cyclonic circulation, which was centred at about 168.5˚E 76.45˚S, and was associated to the strongest current intensities of the entire RoME cruise. This circulation pattern implied a shoaling of temperature, salinity and density isolines in the centre of the eddy and, as a consequence, enhanced the water mixing and increased the UML depth on the eddy border [64]. The shallowest UML depth was observed corresponding to the eddy centre, while a progressive deepening of the UML was observed at increasing distance from the centre (Fig 2H), especially in the north-eastern section of the area.

To examine the role of mixing dynamics in shaping the phytoplankton community, all of the data will be discussed by grouping the samples according to their depth. The first group includes all of the data at shallower depths than the UML, while the second group collects all of the data at deeper depths than the UML (Table 1).

In the UML, the temperature was $\geq$0˚C in almost all of the sampling stations (Fig 4). The highest temperatures (up to 3.07˚C) were recorded in the easternmost stations of RoME 2, whereas the lowest temperatures were in RoME 3. Below the UML, the mean temperatures were similar in the three experiments, although RoME 2 showed the highest variability. The fraction of melt-water was highest (up to 4.96%) and mostly variable in the UML of RoME 1 (Fig 4). In the same layer, a progressive decrease of melt-water percentage was observed from RoME 2 (mean, 1.98%) to RoME 3 (1.20%). Below the UML, the percentage of melt-water decreased compared to the surface layers in all of the experiments. The lowest melt-water fraction (0.39%) was recorded during RoME 2. Dissolved inorganic nitrogen (DIN [NO_3^- + NO_2^- + NH_4^+]), PO_4^{3-} and $Si(OH)_4$ were never fully depleted in any of the investigated areas, and their concentrations were generally high and showed the lowest values at the surface, in the UML (Fig 4).

The POM concentrations, on average, were relatively similar for the three areas (Table 1), although slightly higher for RoME 3. Only the particulate carbohydrate concentrations were consistently higher in RoME 2 than in the other two areas. The POM concentrations decreased with depth, generally rather sharply for RoME 1 and RoME 3, with the highest concentrations observed in the UML. For RoME 2, this decrease was relatively smoother, with carbohydrate concentrations sometimes increasing in the 20 m to 50 m layer. The highest POC/PON ratios were in the deeper water layer (100 m), whereas the lowest ones (<6) were in the UML,

Table 1. Mean (±standard deviations), minimum and maximum values, calculated in the upper mixed layer (UML) (A) and below the UML (B) for the three sampled areas.

	RoME 1						RoME 2						RoME 3					
	Mean		*Min*		*Max*		*Mean*		*Min*		*Max*		*Mean*		*Min*		*Max*	
	A	**B**	**A**	**B**	**A**	**B**	**A**	**B**	**A**	**B**	**A**	**B**	**A**	**B**	**A**	**B**	**A**	**B**
Temperature	1.75 (±1)	-1.41 (±0.3)	0.02	-1.86	3.07	-0.19	1.32(±1)	-0.86 (±1)	0.58	-1.91	3.54	1.54	0.35(±0.2)	-0.92 (±0.6)	0.10	-1.71	0.640	-0.01
Salinity	33.99 (±0.4)	34.44 (±0.1)	33.18	34.12	34.35	34.58	34.20 (±0.2)	34.62 (±0.1)	33.80	34.62	34.62	34.70	34.28 (±0.1)	34.45 (±0.1)	34.16	34.32	34.40	34.57
DIN	21.9 (±7)	30.4 (±7)	10.9	16.8	34.8	42.5	14.4 (±6)	27.5 (±5)	6.8	16.7	25.3	36.6	21.1 (±3)	28 (±4)	15.7	19.8	27.0	35.5
PO_4^{3-}	0.93 (±0.5)	1.61 (±0.2)	0.15	1.00	1.78	1.87	0.67 (±0.4)	1.49 (±0.3)	0.27	0.86	1.54	1.92	1.05 (±0.3)	1.67 (±0.4)	0.50	1.09	1.59	1.99
$Si(OH)_4$	36.5 (±14)	61.6 (±16)	6.6	30.8	57.5	84.8	42.3 (±10)	66.5 (±15)	21.7	38.5	59.8	94.4	43.8 (±9)	58,5 (±17)	27.4	22	62.6	89
POC PN	274.4 (±89.7)	46.8 (±22.5)	139.3	23.3	444.2	93.7	208.3 (±23.4)	161.9 (±59.4)	166.4	52.1	233.5	256.0	227.9 (±84.4)	70.2 (±55.5)	45.4	24.6	350.7	198.7
PON	46.1 (±16.4)	6.6 (±3.3)	19.51	3.7	77.6	14.1	35.8 (±4.4)	22.6 (±8.9)	30.0	8.4	43.1	38.2	40.0 (±15.5)	11.6 (±10.9)	7.8	3.0	61.9	38.8
Prot	310.7 (±99.5)	53.0 (±26.6)	164.8	21.1	493.3	101.2	254.0 (±39.3)	162.8 (±72.0)	181.4	43.3	306.7	312.7	281.4 (±107.9)	87.2 (±81.2)	59.0	22.5	459.2	279.4
Carb	102.3 (±43.4)	21.7 (±8.3)	31.7	10.5	176.9	33.3	94.7 (±22.8)	98.2 (±54.7)	58.0	18.4	117.5	203.0	78.0 (±38.0)	20.2 (±13.8)	15.7	6.9	145.8	43.4
POC/Chl-a	209.2 (±119.8)	124.5 (±79.8)	84.0	51.7	495.3	317.1	161.8 ±(46.1)	66.9 (±8.6)	80.9	50.7	232.9	78.2	87.6 (±25.5)	109.7 (±60.3)	57.0	11.4	150.6	235.5
POC/PON	5.7 (±0.3)	6.6 (±1.0)	5.3	5.6	6.1	8.1	5.8 (±0.3	7.0 (±0.8)	5.4	5.9	6.3	8.9	5.8 (±0.5)	6.5 (±1.1)	5.1	5.1	7.5	8.9
Prot/Carb	3.3 (±0.8)	2.5 (±1.0)	2.4	1.3	5.2	4.5	2.8 (±0.5)	1.9 (±0.7)	2.3	1.1	3.6	3.4	3.8 (±0.8)	3.9 (±1.3)	2.5	1.8	5.6	6.5
Chl-a	1.50 (±0.4)	0.64 (±0.5)	0.56	0.07	2.37	1.66	1.86 (±0.8)	2.34 (±0.9)	0.58	0.71	3.54	3.79	2.95 (±1.3)	0.88 (±0.8)	0.51	0.10	4.71	3.06
Phaeo/Chl-a	1.15 (±0.8)	1.42 (1.2)	0.35	0.62	3.87	5.97	0.46 (±0.2)	0.45 (±0.1)	0.29	0.30	1.24	0.62	0.41 (±0.1)	1.04 (±0.9)	0.27	0.29	0.66	3.68
ΔSi/Fuco	49 (±30)	95 (±86)	24	0	140	314	91 (±37)	72 (±55)	40	0	184	196	38 (±20)	87 (±51)	18	6	112	165
Diato	77 (±15)	64 (±15)	50	27	89	84	67 (±16)	38 (±16)	33	15	98	74	93 (±2)	90 (±5)	90	65	99	97
Hapto	12 (±12)	26 (±13)	4	10	37	62	24 (±16)	54 (±16)	1	11	54	84	1 (±1)	3 (±3)	<0.1	0.5	3	11
Micro	68 (±14)	58 (±22)	37	15	87	93	73 (±11)	73 (±13)	51	43	86	85	82 (±12)	70 (±15)	51	50	96	92
Nano	22 (±11)	28 (±15)	7	13	52	68	15 (±9)	8 (±5)	4	0.4	38	22	12 (±12)	22 (±16)	2	3	45	48
Pico	12 (±7)	19 (±13)	2	7	23	45	12 (±4)	20 (±14)	7	6	23	48	7 (±3)	8 (±6)	2	2	14	16
F_v/F_m	0.25 (±0.1)	0.5 (±0.1)	0.15	0.37	0.44	0.65	0.34 (±0.1)	0.41 (±0.1)	0.19	0.22	0.49	0.60	0.58 (±0.1)	0.53 (±0.1)	0.22	0.40	0.64	0.66
Dd+Dt/Ch-a	0.24 (±0.06)	0.11 (±0.05)	0.12	0.06	0.40	0.24	0.11 (±0.06)	0.05 (±0.01)	0.04	0.02	0.24	0.07	0.14 (±0.04)	0.11 (±0.04)	0.1	0.06	0.25	0.23

Physical-chemical data: temperature (˚C), salinity, inorganic nutrients [DIN ([NO_3^- + NO_2^- + NH_4^+), PO_4^{3-}, $Si(OH)_4$] (μM) and POC [particulate organic carbon], PON [particulate organic nitrogen], Prot [protein] and Carb [carbohydrate] (mg m^{-3}), POC/Chl-a, POC/PON, Prot/Carb. Biological and photophysiological variables: Chl-a (mg m^{-3}), Phaeo/Chl-a [Phaeopigments/Chl-a], ΔSi/Fuco [$\Delta Si(OH)_4$/Fucoxanthin], Diato [diatoms] and Hapto [Haptophytes], micro (>20 μm), nano (2–20 μm) and pico (<2 μm) fractions (%), F_v/F_m [maximum quantum yield], Dd+Dt/Ch-a.

https://doi.org/10.1371/journal.pone.0176033.t001

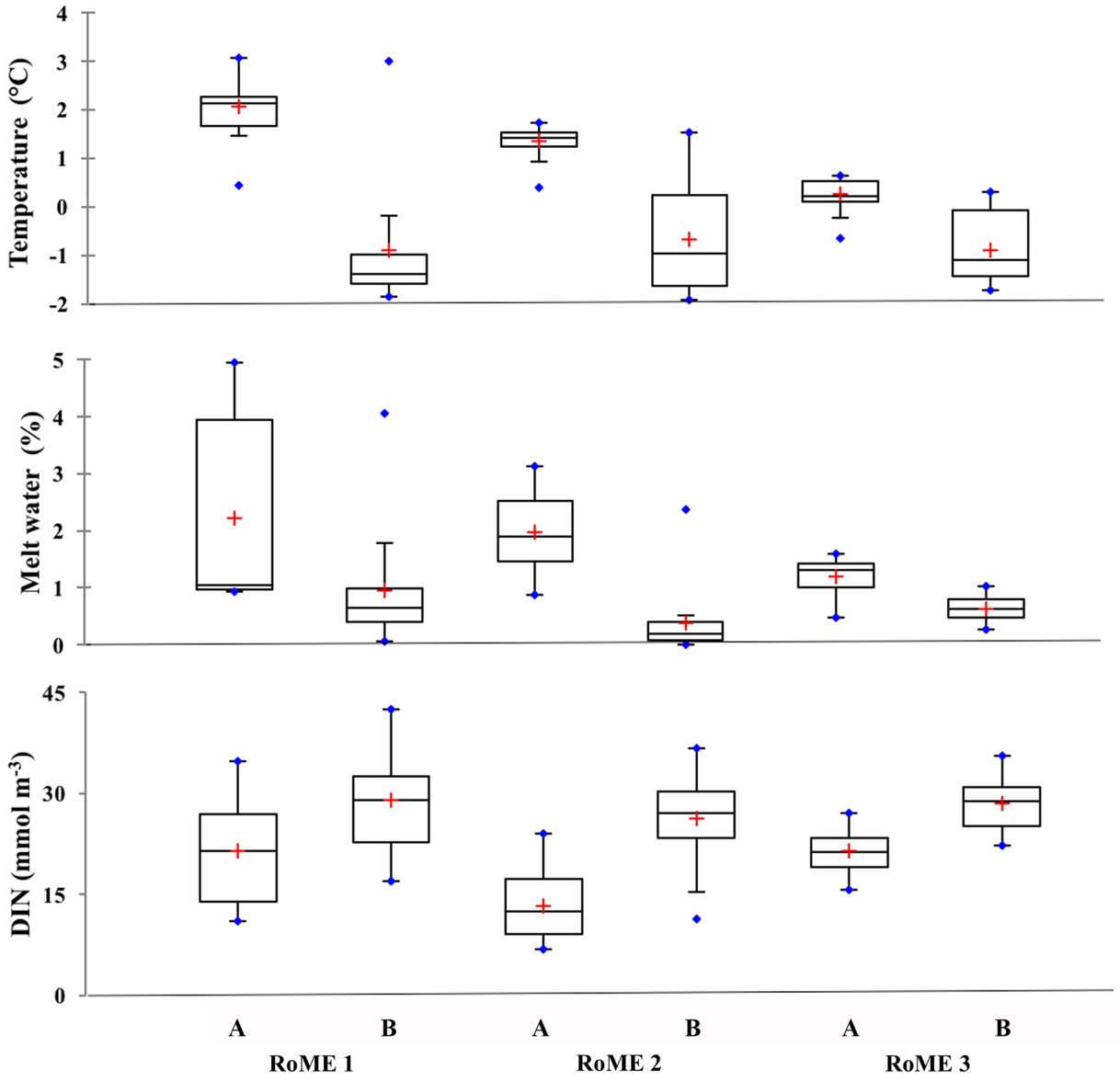

Fig 4. Environmental features in the two investigated layers of each area. Temperature (˚C), melt-water (%) and DIN [dissolved inorganic nitrogen] concentrations (μM). The red cross shows the mean. Samples in the UML (A) and samples below the UML (B).

https://doi.org/10.1371/journal.pone.0176033.g004

especially for RoME 3, where the highest protein/carbohydrate ratios were also seen. The POC/Chl-a ratio was highest in RoME 1 (Table 1). Further details on the POM composition and distribution were reported by [61].

Phytoplankton community structure and photophysiology

The phytoplankton community and physiological characteristics will be discussed as related to the UML dynamics (Fig 5).

Stations were identified as diatom-dominated or Phaeocystis-dominated, based on CHEMTAX [65]. The most abundant pigments for all of the stations were fucoxanthin (mean concentration, 0.31 mg m^{-3}) and 19-hexanoyloxyfucoxanthin (mean concentration, 0.16 mg m^{-3}). All

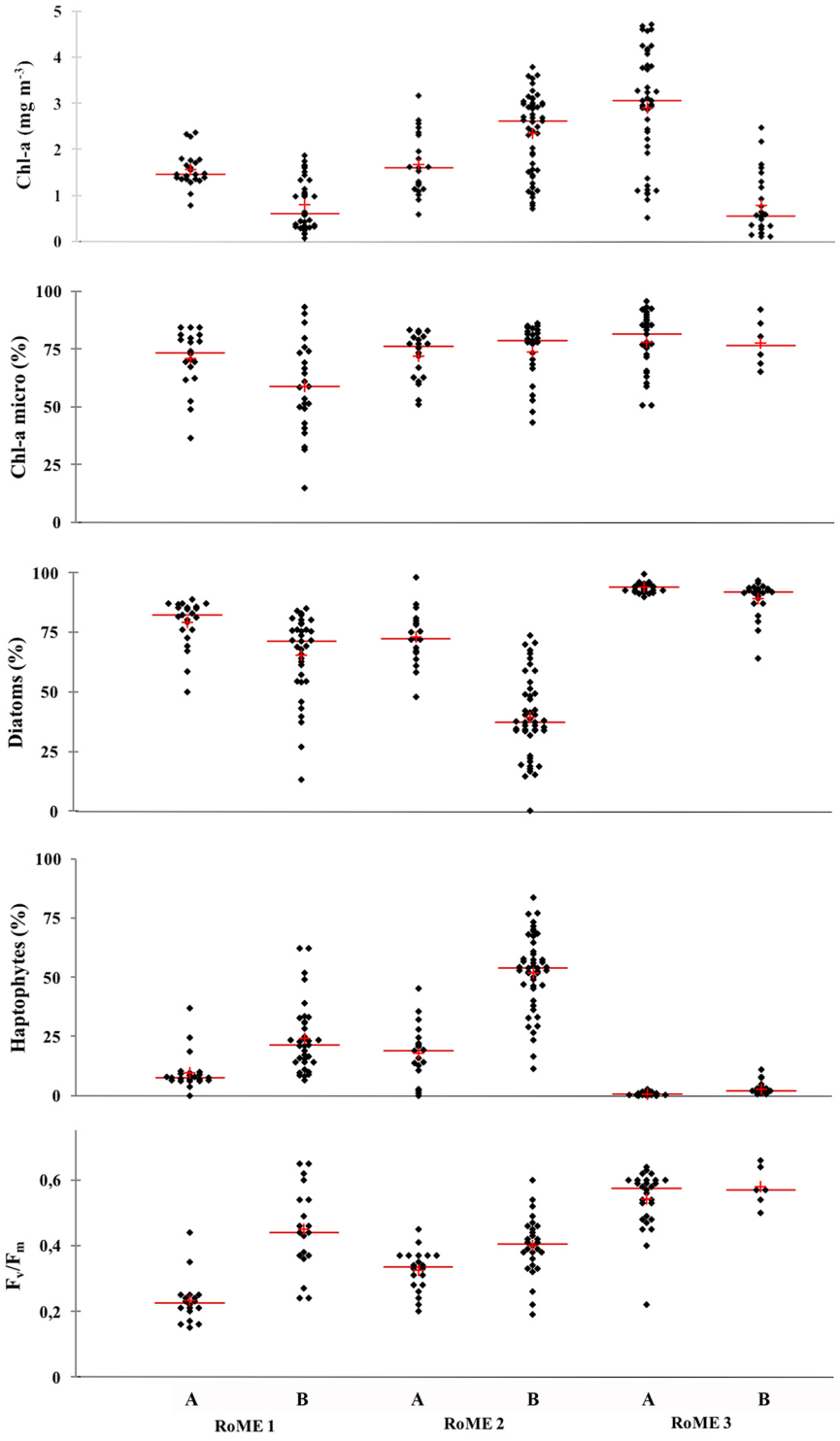

Fig 5. Biological features in the two investigated layers of each area. Total biomass (mg Chl-a m^{-3}), micro (>20 μm) fractions (%), diatoms (%), Haptophytes (%) and F_v/F_m [maximum quantum yield]. The red line is the median and red cross is the mean. Samples in the UML (A) and samples below the ULM (B).

https://doi.org/10.1371/journal.pone.0176033.g005

of the other accessory (non-chlorophyll) pigments (except diadinoxanthin, Dd) were present at <0.03 mg m^{-3}.

In RoME 1, the integrated standing stock of Chl-a in the 0 m to 80 m layer varied from 44 mg m^{-2} to 110 mg m^{-2}. At depths shallower than 20 m to 30 m (in the UML), the Chl-a concentrations ranged from 0.56 mg m^{-3} to 2.37 mg m^{-3}, and decreased below the UML (0.07–1.66 mg m^{-3}) (Fig 5 and Table 1). The analyses of the phytoplankton size fractions showed the dominance of micro-phytoplankton, mainly in the UML (means, 68% and 58%, in the UML and below the UML, respectively), whereas the contributions of the nano (20–2 μm) and pico (<20 μm) fractions were lower (Table 1). Phytoplankton were dominated by diatoms, with means of 77% in the UML and 64% below the UML. *Pseudo-nitzschia* spp. and *Fragilariopsis curta* were the most abundant diatom species, which varied from 50% to 90% and from 45% to 50%, respectively. The majority of the diatoms were found at their lower limits of cell size and in a senescent status. A small contribution of Haptophytes was observed, which was characterised by high variability and small increases (up to 62%) below the UML (Fig 5 and Table 1). In particular, the highest percentages of Haptophytes were recorded at the deepest layer of the northernmost coastal stations (17, 18, 19). In RoME 1, the F_v/F_m measurements were low (mean, 0.25) in the UML, increasing up to a maximum (0.65) below the UML, at about 50 m depth (Fig 5). The vertical distribution of the photoprotective pigments, diadinoxanthin (Dd) +diatoxanthin (Dt) normalised to Chl-a (Dd+Dt/Chl-a), showed the highest values (0.12–0.40) in the UML, while the lowest values were recorded below the UML (0.06–0.24) (Table 1). The ratio of Dt to Dd was relatively higher below the UML.

In RoME 2, the integrated Chl-a concentrations varied from 133 mg m^{-2} to 371 mg m^{-2}, which revealed standing stocks remarkably higher than RoME 1. The vertical profiles of Chl-a showed the presence of sub-surface maxima at 20 m to 40 m depth. The Chl-a concentrations in the UML ranged from 0.58 mg m^{-3} to 3.54 mg m^{-3} (mean, 1.86 mg m^{-3}). Underneath the UML, Chl-a concentrations were highest at station 41 (mean, 2.34 mg m^{-3}; reaching the highest value of 3.79 mg m^{-3}), at 30 m depth. The micro-phytoplankton fraction (>20 μm) was the most abundant, which accounted for 73% of the total biomass in the entire water column (Fig 5). Phytoplankton community were co-dominated by both taxa. In the UML, the phytoplankton was mainly made up of diatoms, with means from 67% to the maximum of 98%. On the contrary, below the UML, the Haptophytes contribution increased to up to 54% of the total biomass. *Fragilariopsis* spp. and *Pseudo-nitzschia* spp. were the most abundant diatom species in the UML, whereas *Phaeocystis antarctica* in colonial forms dominated below the UML. In the stations where the diatoms were observed below the UML, they were all senescent, with empty frustules.

In the UML of RoME 2, the F_v/F_m ratio was low (about 0.34), but slightly increased below the UML (mean, 0.41) (Fig 5). The (Dd+Dt)/Chl-a ratio was highest, but particularly variable (0.04–0.24) in the UML, and almost constant below the UML (about 0.05). The Dt/Dd ratio showed high variability, both in the UML and below the UML.

In RoME 3, the integrated Chl-a varied between 67 mg m^{-2} to 202 mg m^{-2} in the 0 m to 80 m layer, with the highest values occurring for the deepest UML. Chl-a concentrations ranged from 0.51 mg m^{-3} to 4.71 mg m^{-3} in the UML, and were generally <1.00 mg m^{-3} below the UML (Fig 5). In this area, diatoms were the almost exclusive taxa. Similar vertical profiles and low variability patterns were observed for all of the stations, characterised by a mean diatom percentage close to 90%, both in the UML and below the UML (Fig 5). The diatom species observed in RoME 3 were slightly different compared to the two other areas. As well as being dominated by *Pseudo-nitzschia* spp., *Dactyliosolen* spp. was the other most abundant species. Most diatoms were in good condition, with cells dividing, many at their largest size and full of cytoplasm. In some stations, senescent diatoms with empty frustules were also observed, but only below the UML.

The F_v/F_m showed high values at all depths, with a mean of 0.58. The Dd+Dt/Chl-a ratio was higher in the samples in the UML (0.14) compared to those below the UML (0.11). In addition, at the surface layer, the ratio did not show any appreciable variability and also the Dt/(Dt+Dd) ratio was relatively constant within the whole water column.

Relationships between environmental and biological features

A multivariate approach was used to obtain information on the overall functioning of the three investigated areas. PCA based on correlations (Spearman) was used to investigate the relationships among the *in-situ* physical-chemical (temperature, melt-water percentage, nutrient concentrations) and biological (F_v/F_m, ΔSi/Fuco, relative contribution of diatoms and Haptophytes) variables.

The first two principal components (PCs), explained about 70% of the total variance, with the first accounting for 41%, and the second for 27% (Fig 6).

The first PC mainly explained the environmental variability. All the nutrient concentrations were negatively correlated to temperature and melt-water fraction, which thus indicated a dependence of nutrient concentrations from the sea-ice melting processes. The second axis explained the biological variability, where total Chl-a, F_v/F_m and diatoms percentage were negatively correlated to the second axis, while the ΔSi/Fuco ratio (proxy got Fe availability) and the percentage of Haptophytes were positively correlated (Fig 6). The factor plane highlighted that the samples collected during the third experiment (RoME 3) were separated from samples collected during RoME 1 and RoME 2, and were mainly ordered following the biological variables. Samples collected during RoME 1 and 2 showed strong variability related to the physical and chemical variables, with different features mostly related to stratification (samples in the UML disposed in the fourth quarter and those below the UML in the first quarter of the ordination).

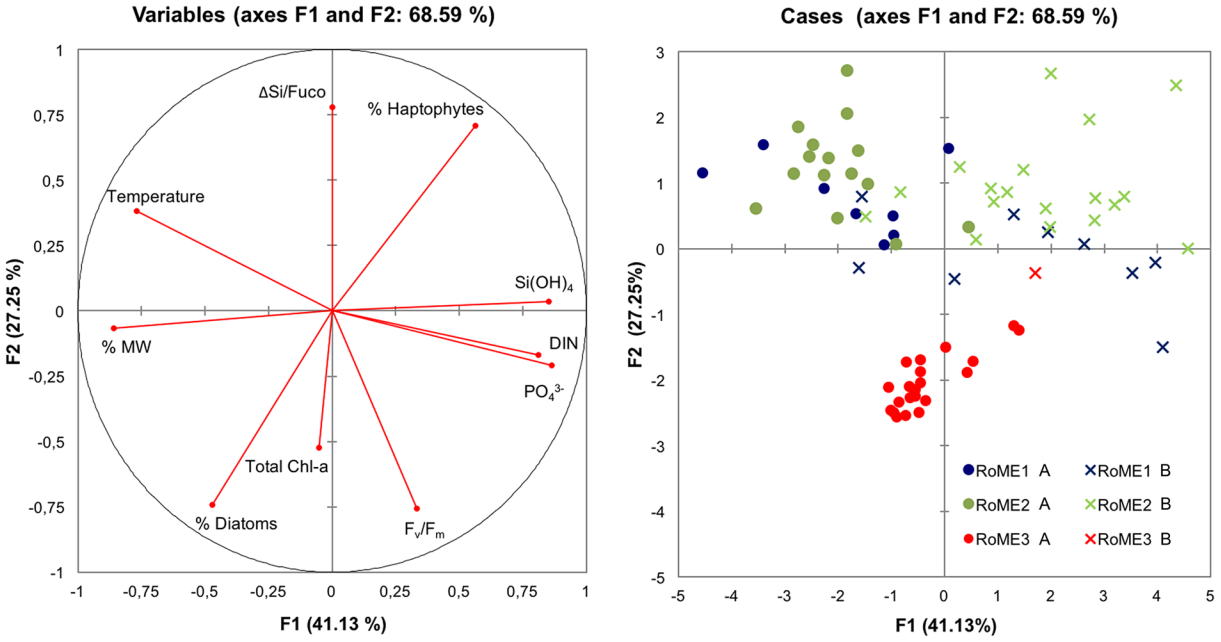

Fig 6. Results of PCA applied to physical, chemical and biological parameters. Parameters included in the analysis: ΔSi/Fuco [$\Delta Si(OH)_4$/Fucoxanthin], Haptophytes (%), $Si(OH)_4$ [silicate], DIN [dissolved inorganic nitrogen ($NO_3^- + NO_2^- + NH_4^+$)], PO_4^{3-} [phosphate], F_v/F_m [maximum quantum yield], Total Chl-a, Diatoms (%), MW [melt-water] (%) and Temperature (˚C). The samples in the UML (full shot-A) and samples below the ULM (cross-B): RoME 1, blu; RoME 2, green; and RoME 3, red.

https://doi.org/10.1371/journal.pone.0176033.g006

Table 2. Correlation matrix (Spearman) among physical, chemical and biological variables.

Variables	F_v/F_m	DIN	PO_4^3	$Si(OH)_4$	ΔSi/Fuco	TChl-a	Temp	MW	Hapto	Diato
F_v/F_m	**1**	**0.296**	**0.370**	0.212	**-0.376**	**0.375**	**-0.605**	-0.218	**-0.305**	**0.354**
DIN	**0.296**	**1**	**0.810**	**0.617**	-0.135	-0.173	**-0.626**	**-0.579**	0.218	-0.187
PO_4^{3-}	**0.370**	**0.810**	**1**	**0.674**	-0.133	-0.100	**-0.669**	**-0.702**	**0.245**	-0.158
$Si(OH)_4$	0.212	**0.617**	**0.674**	**1**	-0.091	-0.083	**-0.534**	**-0.715**	**0.492**	**-0.404**
ΔSi/Fuco	**-0.376**	-0.135	-0.133	-0.091	**1**	**-0.523**	0.180	-0.074	**0.453**	**-0.464**
TChl-a	**0.375**	-0.173	-0.100	-0.083	**-0.523**	**1**	-0.190	-0.004	-0.134	0.123
Temp	**-0.605**	**-0.626**	**-0.669**	**-0.534**	0.180	-0.190	**1**	**0.572**	-0.208	0.110
MW	-0.218	**-0.579**	**-0.702**	**-0.715**	-0.074	-0.004	**0.572**	**1**	**-0.516**	**0.404**
Hapto	**-0.305**	0.218	**0.245**	**0.492**	**0.453**	-0.134	-0.208	**-0.516**	**1**	**-0.920**
Diato	**0.354**	-0.187	-0.158	**-0.404**	**-0.464**	0.123	0.110	**0.404**	**-0.920**	**1**

Significant correlations ($p < 0.05$) are shown in bold face. Variables: F_v/F_m [maximum quantum yield], DIN [dissolved inorganic nitrogen (NO_3^- + NO_2^- + NH_4^+)], PO_4^{3-} [phosphate], $Si(OH)_4$ [silicate], ΔSi/Fuco [Δ$Si(OH)_4$/Fucoxanthin], TChl-a [Total chlorophyll-a], Temp [temperature] MW [melt-water], Hapto [Haptophytes], Diato [diatoms].

https://doi.org/10.1371/journal.pone.0176033.t002

The percentage contributions of Haptophytes and diatoms to total biomass were negatively correlated. The diatoms positively correlated to the quantum yield and the melt-water percentage, and negatively to silicates concentration and to ΔSi/Fuco ratio, whereas opposite correlations were observed for Haptophytes (Table 2).

Correlation analyses among the phytoplankton and POM quantity and composition were also carried out to achieve information on the trophic status of the investigated areas (Table 3). The results suggest a strong dependence of POM attributes on the main phytoplankton functional groups: diatoms were highly correlated with the quantitative features of POM, whereas Haptophytes were mostly correlated with the qualitative characteristics of POM.

Discussion

Ecological and photophysiological features of phytoplankton

During the austral summer of 2014, well-defined peculiarities in the qualitative and quantitative distributions of phytoplankton were observed in the three investigated areas of the Ross Sea, linked to water column dynamics and nutrients (i.e, availability, uptake, cycling). Physiological characteristics and xanthophyll pigments support the observed differences.

Two phytoplankton blooms occurred: the first was in the southernmost sampling stations (RoME 3), while the second was in the Terra Nova Bay polynya area (RoME 2). For RoME 1 (northern part of the Ross Sea), only a post-bloom phase was identified.

In the RoME 1 area, relatively low phytoplankton biomass was measured compared to the other two sub-systems. These results are comparable with other data collected during summer cruises in the Ross Sea in the 1990s, which were characterised by Chl-a concentrations that rarely exceeded 60 mg m^{-2} [66, 67]. Diatoms dominated in the RoME 1 area, as mostly inactive or dead cells. The high POC/Chl-a ratios observed reveal the low contributions of phytoplankton to particulate carbon. These findings are in agreement with the low values of the photosynthetic quantum yield, which indicates phytoplankton stress conditions, probably related to Fe limitation. The quantum yield of phytoplankton of the Southern Ocean is Fe-driven, and low values should be indicators of Fe stress [68]; the F_v/F_m values below 0.40 suggest that Fe is the most relevant limiting factor [38, 69]. Several studies have reported an increase in the total

Table 3. Spearman correlation matrixes between the phytoplankton and the POM features (quantitative: POC, protein and carbohydrate concentrations; qualitative: Protein to carbohydrate ratio, and POC/PON ratio) for the three sampled areas.

	Variable	Correlation with					
		TChl-a	Phaeo	Micro	Pico	Hapto	Diato
RoME 1	POC	***0.76***	**0.60**	**0.66**	-	-	***0.84***
	PON	***0.74***	**0.57**	**0.64**	-	-	***0.82***
	Prot	***0.78***	**0.59**	***0.70***	-	-	***0.86***
	Carb	***0.72***	0.53	**0.67**	-	-	***0.82***
	Prot/Carb	-	-	-	-	-	-
	POC/PON	**-0.61**	-0.45	-	-0.57	-	-0.60
		TChl-a	Phaeo	Micro	Pico	Hapto	Diato
RoME 2	POC	0.43	-	-	***-0.70***	-	**0.71**
	PON	-	-	-	***-0.80***	-	**0.60**
	Prot	-	-	-	***-0.69***	-	**0.70**
	Carb	***0.66***	**0.59**	**0.62**	-	-	0.66
	Prot/Carb	-0.52	**-0.62**	-	-	**-0.58**	-
	POC/PON	0.49	0.55	***0.69***	-0.57	***0.68***	-
		TChl-a	Phaeo	Micro	Pico	Hapto	Diato
RoME 2	POC	***0.92***	***0.86***	***0.76***	0.48	0.38	***0.95***
	PON	***0.92***	***0.85***	***0.77***	-	0.39	***0.94***
	Prot	***0.92***	***0.85***	***0.74***	-	0.38	***0.94***
	Carb	***0.88***	***0.84***	***0.78***	0.57	-	***0.93***
	Prot/Carb	-	-	-	-	-	-
	POC/PON	-	-	-	-	-	-0.43

Underlined numbers: p <0.05, bold numbers: p <0.01, italic-bold numbers: p <0.001, dash: not significant. POC [particulate organic carbon], PON [particulate organic nitrogen], Prot [proteins], Carb [carbohydrates], Prot/Carb, POC/PON, TChl-a [total chlorophyll-a], Phaeo [pheopigments], micro (>20 μm), nano (2–20 μm) and pico (<2 μm) fractions (%), Hapto [Haptophytes], Diato [diatoms].

https://doi.org/10.1371/journal.pone.0176033.t003

pool of xanthophylls—diadinoxanthin (Dd) and diatoxanthin (Dt)—under stress conditions due to Fe deficiency [42] [70–72], even if the xanthophylls pool is traditionally used to couple the phytoplankton acclimations to light and water column dynamics [73, 74]. In the present study, the high values of (Dd+Dt)/Chl-a recorded in RoME 1 in the UML might be a combination of prolonged high light exposure, related to the high stability of the water column, and stress conditions, linked to the end of the bloom. Furthermore, the unusual high Dt/(Dd+Dt) ratio (Table 1) recorded below the UML in RoME 1 might be explained by the strong water column stratification. Recent studies focused on the Southern Ocean highlighted relatively high values of Dt/(Dd+Dt) observed below the mixed layer as result of chlororespiration, which was activated when phytoplankton were exposed to prolonged darkness [39, 75].

Different phytoplankton features were observed in RoME 2, coupled with the shallowest UML. The highest values were found for integrated biomass, which exceeded 300 mg Chl-a m^{-2}, and exceptionally high concentrations were recorded below the UML (up to 3 mg m^{-3} at 100 m). These Chl-a concentrations were higher compared to those reported in the studies conducted before 2000, both in offshore and coastal areas of the Ross Sea [14, 21, 67, 76]. Recent studies focused on the Ross Sea have shown that during summer, phytoplankton biomass escapes from the ecological paradox of high-nutrient low-chlorophyll conditions. For instance, the prolonged ice seasons recorded in 2001 [25] and February 2004 [26] resulted in Chl-a

concentrations greater than 6.0 mg m^{-3} in the southern Ross Sea. In 2011, Chl-a concentrations as high as 15 mg m^{-3} in the UML (about 50 m) were observed in the waters of the Pennell Bank [77, 78]. An intriguing feature for RoME 2 concerns the co-occurrence of diatoms and *P. antarctica*. The two investigated layers showed diverse phytoplankton community in different physiological status, characterised by diatoms in the UML and *P. antarctica* in the layer below the UML. The *P. antarctica* colonial bloom occurs in an area and in a season that are usually characterised by the prevalence of diatoms. Mucilage is known for its embedding floating of POM and DOM, to which the quantity of scavenged organic matter increases with the age of mucilage [79, 80]. The concentration of other POM components, such as proteins, was not significantly higher than in the other areas, which suggests that the production of mucilage by *P. antarctica* was recent. Samples in the UML showed the lower F_v/F_m compared to below the UML. Thus, this suggests good adaptation of *P. antarctica* to low light conditions and nutrient availability, and an adequate amount of Fe, as reported by [71]. The levels of Fe detected [81] supports this hypothesis. Under Fe-replete regimes, compared to diatoms, *P. antarctica* is more able to efficiently use a large range of light levels, which are typical of a deep mixed layer [28, 82].

In the RoME 3 area, a second bloom was observed, which was confined in a wide UML (mean depth, 48 m) and characterised by biomass concentrations of up to 202 mg Chl-a m^{-2}. In this area, diatoms represented more than 90% of the entire phytoplankton community. *Pseudo-nitzschia* spp. were the most abundant diatoms, and they were found at the higher limit of their cell size, which indicates that the phytoplankton were in an active growth phase. Moreover, the F_v/F_m was the highest (mean, 0.55 ±0.09) and it was in the optimal range (0.45–0.65) reported for the Ross Sea [83], which suggests the onset of a phytoplankton bloom, not affected by limiting factors (such as Fe availability). During the study period, the uplift of the deeper waters that was favoured by the observed cyclonic circulation might have facilitated the episodic injection of deep Fe-rich waters into the euphotic zone [84]. The presence of recurrent mixing events can be also deduced by the low variability of photoprotective pigments within the UML.

An interesting finding of this study is the presence of large diatoms also in a wide UML, which contradicts the classic paradigm by which Antarctic diatoms generally accumulate in highly stratified waters. The high percentage of diatoms appears to be independent on the thickness of the UML (Figs 3 and 4) and the results of the PCA ordination stress that diatoms were positively correlated to melt-water percentages, whereas the opposite correlation was found for Haptophytes (Fig 6). This suggests that the melting processes might have a pivotal role in shaping the phytoplankton composition, more than the water column dynamics alone (at least in terms of the UML thickness). As climate change has a strong impact on the sea-ice dynamics at both global [85] and regional [86] scales, it might also have considerable effects on the ecology and biogeochemistry of the Ross Sea, altering the distribution of the two main functional groups. A recent study showed that high temperatures are correlated with high diatom abundance, and low temperatures match high *P. antarctica* [87], although it is not yet clear whether there is a causal mechanism behind this connection. Our study did not show any correlation between temperature and the relative contribution of *P. antarctica* and/or diatoms. Although correlation does not allow to infer cause-effect relationships, we hypothesise that rising ocean temperature, as expected from climate change predictions, might have a more relevant indirect effect on phytoplankton community structure through modulation of the ice dynamics, rather than only direct effects on cell physiology.

Trophic implications

The composition of the phytoplankton communities determines the fate and pathway of carbon through the oceanic systems [16–19] [88]. Considerable increases in phytoplankton

biomass and large size structure (micro-fraction accounting for 75% of the total biomass on average, independent of the functional groups) suggest that the Ross Sea in summer could now be extremely productive and might have a powerful impact on the trophic structure of the entire ecosystem (e.g., alterations in herbivore sizes, changes in pelagic-benthic coupling, presence of big mammals, change in penguin diet and others), as recently pointed out [89]. As the standing stock of phytoplankton was remarkably high in summer 2014, the question arises as to whether these organic materials would enter the classical Antarctic summer trophic chain or would have another fate. Before 2000, during summer, the offshore waters under ice-free conditions were characterised by low concentrations of phytoplankton biomass, which was characterised by a nano-size dominated community; these were coupled with a long trophic chain and an efficient microbial loop. Our results show that the phytoplankton features in summer 2014 were more similar to typical spring conditions, as characterised by the dominance of micro-phytoplankton fractions along the ice edge, which sustains the energy transfers through the Antarctic short trophic chain of 'diatoms-euphausiids-whales' [76] [90–92]. The low Pheao/Chl-a ratios and phaeophorbide concentrations (data not shown), as proxy of grazing activity [93, 94] and the presence of senescent (instead of grazed) phytoplankton cells, suggest the presence during summer 2014 of a relatively scarce trophic efficiency.

The significant correlations, with the quantitative and qualitative features of the POM, highlighted that phytoplankton drive the POM distribution and composition. In particular, diatoms had a major role in POM accumulation. This was mostly true in RoME 3, where the functional parameters of the phytoplankton community indicated active production, supported by favourable hydrodynamic conditions as well as micro- and macro-nutrient availability. This, however, allowed also a high qualitative value of POM. In this case, the bloom was at its early and intense phase, so consumers could not have started to feed on it.

RoME 1 was characterised by low photosynthetic efficiency with the presence of senescent cells, in agreement with the age of the bloom and the experienced long ice-free conditions. The high POC/Chl-a ratios and the moderate nutritional quality of POM agree with these features. A recent exploitation of this trophic resource by zooplankton was excluded, due to the low Phaeo/Chla-a ratios, but the senescent phytoplankton cells might host a microbial community that actively degrades POM in the absence of grazing activity. This explains the high protein content of POM, probably due to bacterial biomass.

In RoME 2, the low significance of the correlations suggests a decoupling between POM and phytoplankton. However, the low POC/Chl-a ratios in this area and the low grazing pressure still indicated a dominant role of phytoplankton. As previously mentioned, RoME 2 was characterised by a relevant presence of *P. antarctica*, which only partially contributes to the total quantity of POM, while it has a major role in determining the POM quality. Indeed, *P. antarctica* produces mucilage, which is composed of polysaccharides, with high carbohydrate content. The correlations with the qualitative features of POM (i.e., protein/carbohydrate ratio, POC/PON ratio) indicate low nutritional quality, and thus the summer *P. antarctica* production would be a moderate trophic supply [95], also for those grazers that can feed on mucilage aggregates [96]. Thus, the inefficient grazing on phytoplankton would be linked to the phytoplankton functional groups, composed of non-palatable or low nutritional value matter.

Our findings show an uncoupled increase in large diatoms and primary consumers (as revealed by the patterns of phaeopigments), independent of the phase of the bloom. On the other hand, the bloom decline appears to host an active microbial community, as revealed by the high protein contents of POM. This indicates that during the summer of 2014, the fate of primary production and carbon export could have been a lot different from those reported previously in the same area [67, 76, 97].

Conclusions

The considerable biomass and large size of the phytoplankton observed, in agreement with the recent literature, suggest relevant alterations in Ross Sea summer productivity. Moreover, the distribution of the main functional groups showed significant anomalies. The *P. antarctica* colonial bloom occurs in an area and in a season that are usually characterised by the prevalence of diatoms. The presence of large diatoms in a wide UML contradicts the classic paradigm of Antarctic diatom accumulation in highly stratified waters.

The imbalance between phytoplankton standing stocks and primary consumers, independent of the phase of the bloom, might dramatically alter the fate of the summer primary production and the carbon export in the Ross Sea. However, it is unclear what are the environmental factors that drive these extraordinary changes in primary production processes and the prevalence of different functional groups. Probably, a modification of Ross Sea hydrography will have a key role in reducing the limiting factors, and as consequence, in modifying the primary production processes.

Certainly, this present asset will affect not only the Ross Sea, but probably the entire Southern Ocean ecology, and subsequently it may have an impact at a global scale.

Supporting information

S1 Table. Sampling stations within each area of the RoME Project, corresponding geographic coordinates, bottom depth and sampling date.
(DOCX)

Acknowledgments

This study was carried out in the framework of the activities of the Italian National Programme for Antarctic Research, which provided financial and logistic support. We thank the officers, crew, and technical personnel on board the *R/V Italica* for their support during the seagoing operations. The authors are grateful to Federico Angelini and Giuseppe Arena for their help during the cruise, and Augusto Passarelli for logistic support in Italy. We are grateful to Antonio Pusceddu for valuable and constructive comments on the manuscript, and to anonymous referees for their suggestions. The authors thanks Fred Davey for according the use of Ross Sea bathymetry data [doi:10.1594/IEDA/100405].

Author Contributions

Conceptualization: OM VS.

Data curation: OM FB GB YC CM PR MS.

Formal analysis: OM YC CM FM.

Funding acquisition: OM CM PR.

Investigation: OM FB GB PR MS.

Project administration: OM MS.

Resources: OM CM PR MS.

Supervision: OM VS.

Visualization: OM FB FM YC.

Writing – original draft: OM VS FM YC MS.

Writing – review & editing: OM VS.

References

1. Field C, Mach K, Mastrandrea M, Barros R. Intergovernmental Panel on Climate Change (IPCC): Climate Change 2014: Impacts, Adaptation, and Vulnerability. Cambridge University Press 2014; pp. 1132.
2. Frölicher TL, Sarmiento JL, Paynter DJ, Dunne JP, Krasting JP, Winton M. Dominance of the Southern Ocean in anthropogenic carbon and heat uptake in CMIP5 models. J Climate 2015; 28 (2): 862–886.
3. Constable AJ, Melbourne-Thomas J, Corney SP, Arrigo KR, Barbraud C, Barnes DK, et al. Climate change and Southern Ocean ecosystems I: how changes in physical habitats directly affect marine biota. Global Change Biology 2014; 20: 3004–3025. https://doi.org/10.1111/gcb.12623 PMID: 24802817
4. Gutt J, Bertler N, Bracegirdle TJ, Buschmann A, Comiso J, Hosie G, et al. The Southern Ocean ecosystem under multiple climate change stresses—An integrated circumpolar assessment. Global Change Biology 2015; 21: 1434–1453. https://doi.org/10.1111/gcb.12794 PMID: 25369312
5. Schine CMS, van Dijken GL, Arrigo KR. Spatial analysis of trends in primary production and relationship with large-scale climate variability in the Ross Sea, Antarctica (1997–2013). J Geophys Res 2015;
6. Boyd PW, Doney SC, Strzepek R, Dusenberry J, Lindsay K, Fung I. Climate-mediated changes to mixed-layer properties in the Southern Ocean: Assessing the phytoplankton response. Biogeosciences 2008; 5: 847–864.
7. Trivelpiece WZ, Hinke JT, Miller K, Reiss CS, Trivelpiece SG, Watters GM. Variability in krill biomass links harvesting and climate warming to penguin population changes in Antarctica. PNAS 2011; 108 (18): 7625–7628. https://doi.org/10.1073/pnas.1016560108 PMID: 21482793
8. Turner J, Barrand NE, Bracegirdle TJ, Convey P, Hodgson DA. Antarctic climate change and the environment: an update. Polar Record 2013; 50: 237–259.
9. Arrigo KR, van Dijken GL, Strong AL. Environmental controls of marine productivity hot spots around Antarctica. J Geophys Res Oceans 2015; 120(8): 5545–5565.
10. Kennicutt Chown SL, Cassano JJ, Liggett D, Massom R, Peck LS, et al. Six priorities for Antarctic science (and supplementary information). Nature 2014; 512: 523–525.
11. Kennicutt Chown SL, Cassano JJ, Liggett D, Massom R, Peck LS, et al. A roadmap for Antarctic and Southern Ocean science for the next two decades and beyond. Antarctic Science 2015; 27: 3–18.
12. Fusco G, Budillon G, Spezie G. Surface heat fluxes and thermohaline variability in the Ross Sea and in Terra Nova Bay polynya. Cont Shelf Res 2009; 29: 1887–1895.
13. Arrigo KR, van Dijken G, Long M. Coastal Southern Ocean: A strong anthropogenic CO_2 sink. Geophys Rese Lett 2008; 35, L21602,
14. DiTullio GR, Smith WO Jr. Spatial patterns in phytoplankton biomass and pigment distributions in the Ross Sea. J Geophys Res 1996; 101: 18, 467–18, 478.
15. Smith WO Jr, Ainley DG, Arrigo KR, Dinniman MS. The Oceanography and Ecology of the Ross Sea. Annu Rev Mar Sci 2014; 6: 469–87.
16. Arrigo KR, Robinson DH, Worthen DL, Dunbar RB, DiTullio GR, van Woert M, et al. Phytoplankton community structure and the drawdown of nutrients and CO_2 in the Southern Ocean. Science 1999; 283: 365–367. PMID: 9888847
17. DiTullio GR, Grebmeier JM, Arrigo KR, Lizotte MP, Robinson DH, Leventer A, et al. Rapid and early export of *Phaeocystis antarctica* blooms in the Ross Sea, Antarctica. Nature 2000; 404: 595–598. https://doi.org/10.1038/35007061 PMID: 10766240
18. Sweeney C, Hansell DA, Carlson CA, Codispoti LA, Gordon LI, Marra J, et al. Biogeochemical regimes, net community production and carbon export in the Ross Sea, Antarctica. Deep-Sea Res II 2000; 47 (15–16): 3369–3394.
19. Smith WO Jr, Asper VA. The influence of phytoplankton assemblage composition on biogeochemical characteristics and cycles in the Southern Ross Sea, Antarctica. Deep-Sea Res I 2001; 48: 137–161.
20. Garrison DL, Gibson A, Kunze H, Gowing MM, Vickers CL, Mathot S, et al. The Ross Sea polynya project: diatom- and Phaeocystis-dominated phytoplankton assemblages in the Ross Sea, Antarctica, 1994–1996. In: DiTullio GR, Dunbar R editors. Biogeochemistry of the Ross Sea. Ant Res Ser 78. American Geophysical Union, Washington, DC 2003; 53–75.

21. Smith WO Jr, Dinniman MS, Tozzi S, DiTullio GR, Mangoni O, Modigh M, et al. Phytoplankton photosynthetic pigments in the Ross Sea: patterns and relationships among functional groups. J Mar Systems 2010; 82: 177–185.
22. Shields AR, Smith WO. Size-fractionated photosynthesis/irradiance relationships during *Phaeocystis antarctica*-dominated blooms in the Ross Sea, Antarctica. J Plankton Res 2009; 31 (7): 701–712.
23. Smith WO Jr, Dennett MR, Mathot S, Caron DA. The temporal dynamics of the flagellated and colonial stages of *Phaeocystis antarctica* in the Ross Sea. Deep-Sea Res II 2003; 50: 605–618.
24. Caron DA, Dennett MR, Lonsdale DJ, Moran DM, Shalapyonok L. Micro-zooplankton herbivory in Microzooplankton herbivory in the Ross Sea, Antarctica. Deep-Sea Res II 2000; 47: 15–16.
25. Mangoni O, Modigh M, Conversano F, Carrada GC, Saggiomo V. Effects of summer ice coverage on phytoplankton assemblages in the Ross Sea, Antarctica. Deep-Sea Res I 2004; 51: 1601–1617.
26. Smith WO Jr, Shields AR, Peloquin JA, Catalano G, Tozzi S, Dinniman MS, et al. Interannual variations in nutrients, net community production, and biogeochemical cycles in the Ross Sea. Deep-Sea Res II 2006; 53: 815–833.
27. Peloquin JA, Smith WO Jr. Phytoplankton blooms in the Ross Sea, Antarctica: interannual variability in magnitude, temporal patterns, and composition. J Geophys Res 2007; 112.
28. Arrigo KR, Mills MM, Kropuenske LR, van Dijken GL, Alderkamp A-C, Robinson DH. Photophysiology in Two Major Southern Ocean Phytoplankton Taxa: Photosynthesis and Growth of *Phaeocystis antarctica* and *Fragilariopsis cylindrus* under Different Irradiance Levels. Integr Comp Biol 2010; 50 (6): 950–966. https://doi.org/10.1093/icb/icq021 PMID: 21558252
29. Bertrand EM, Saito MA, Rose JM, Riesselman CR, Lohan MC, Noble AE, et al. Vitamin B12 and iron co-limitation of phytoplankton growth in the Ross Sea. Limnol Oceanogr 2007; 52: 1079–1093.
30. Feng Y, Hare CE, Rose JM, Handy SM, DiTullio GR, Lee PA, et al. Interactive effects of iron, irradiance and CO_2 on Ross Sea phytoplankton. Deep-Sea Res I 2010; 57: 368–383.
31. Franck VM, Brzezinski MA, Coale KH, Nelson DM. Iron and silicic acid concentrations regulate Si uptake north and south of the Polar Frontal Zone in the Pacific Sector of the Southern Ocean. Deep-Sea Res II 2000; 47: 3315–3338.
32. Xu K, Fu FX, Hutchins DA. Comparative responses of two dominant Antarctic phytoplankton taxa to interactions between ocean acidification, warming, irradiance, and iron availability. Limnol Oceanogr 2014; 59(6): 1919–1931.
33. Strzepek RF, Hunter KA, Frew RD, Harrison PJ, Boyd PW. Iron-light interactions differ in Southern Ocean phytoplankton. Limnol Oceanogr 2012; 57: 1182–1200.
34. de Baar HJ, de Jong JT, Nolting RF, Timmermans KR, van Leeuwe MA, Bathman U, et al. Low dissolved Fe and the absence of diatom blooms in remote Pacific waters of the Southern Ocean Mar Chem 1999; 66: 1–34.
35. Arrigo KR, Worthen DL, Robinson DH. A coupled ocean-ecosystem model of the Ross Sea: 2. Iron regulation of phytoplankton taxonomic variability and primary production. J Geophys Res 2003; 108.
36. Sedwick PN, Garcia N.S, Riseman SF, Marsay CM, DiTullio GR. Evidence for high iron requirements of colonial *Phaeocystis antarctica* at low irradiance. Biogeochemistry 2007; 83: 83–97.
37. Parkhill JP, Maillet G, Cullen JJ. Fluorescence-based maximal quantum yield for PSII as a diagnostic of nutrient stress. J Phycology 2001; 37: 517–529.
38. McMinn A and Hegseth EN. Quantum yield and photosynthetic parameters of marine microalgae from the southern Arctic Ocean, Svalbard. J Mar Biol Ass UK 2004; 84: 865–871.
39. Cheah W, McMinn A, Griffiths FB, Westwood KJ, Wright SW, et al. Response of Phytoplankton Photophysiology to Varying Environmental Conditions in the Sub-Antarctic and Polar Frontal Zone. PLoS ONE 2013; 8(8): e72165. https://doi.org/10.1371/journal.pone.0072165 PMID: 23977242
40. Murchie EH, Lawson T. Chlorophyll fluorescence analysis: a guide to good practice and understanding some new applications. J Experimental Botany 2013; 64(13): 3983–3998.
41. Boyd PW, Dillingham PW, McGraw CM, Armstrong EA, Cornwall CE, Feng Y-y, et al. Physiological responses of a Southern Ocean diatom to complex future ocean conditions. Nature Climate Change 2015; 6: 202–2013.
42. Alderkamp AC, Kulk G, Buma AGJ, Visser RJW, Van Dijken GL, et al. The effect of iron limitation on the photophysiology of *Phaeocystis antarctica* (Prymnesiophyceae) and *Fragilariopsis cylindrus* (Bacillariophyceae) under dynamic irradiance. J Phycol 2012; 48: 45–59. https://doi.org/10.1111/j.1529-8817.2011.01098.x PMID: 27009649
43. Nitsche F and Davey FJ. Ross Sea bathymetry grid (2005) based on Fred Davey's bathymetry map (2004). Integrated Earth Data Applications (IEDA). 2013;
44. Schlitzer R. Ocean Data View. 2017; odv.awi.de.

45. Rivaro P, Ianni C, Langone L, Ori C, Aulicino G, Cotroneo Y, et al. Physical and biological forcing on the mesoscale variability of the carbonate system in the Ross Sea (Antarctica) during the summer season 2014. J Mar Systems 2017; 166: 144–158.

46. Rivaro P, Abelmoschi ML, Grotti M, Magi E, Margiotta F, Massolo Set al. Combined effects of hydrological structure and iron and copper availability on the phytoplankton growth in Terra Nova Bay Polynya (Ross Sea, Antarctica). Deep-Sea Res I 2012; 62: 97–110.

47. Hansen HP, Grasshoff K. Automated chemical analysis. In: Grasshoff K, Ehrhardt M, Kremling K editors. Methods of seawater analysis. Weinheim Verlag Chemie. 1983; 347–370.

48. Hedges JI, Stern JH. Carbon and nitrogen determination of carbonate-containing solids. Limnol Oceanogr 1984; 29: 657–663.

49. Hartree EF. Determination of proteins: a modification of the Lowry method that gives a linear photometric response. Anal Biochem 1972; 48: 422–427. PMID: 4115981

50. Dubois M, Gilles KA, Hamilton JK, Rebers PA, Smith F. Colorimetric method for determination of sugars and related substances. Anal Chem 1956; 39: 350–356.

51. Saggiomo V, Santarpia I, Saggiomo M, Margiotta F, Mangoni O. Primary production processes and photosynthetic performance of a unique periantarctic ecosystem: the Strait of Magellan. Polar Biol 2011; 34(9): 1255–1267.

52. Holm-Hansen O, Lorenzen CJ, Holmes RW, Strickland JDH. Fluorometric determination of chlorophyll. J Cons Perm In. Explor Mer 1965; 30: 3–15.

53. Vidussi F, Claustre H, Bustillos-Guzman J, Cailliau C, Marty JC. Determination of chlorophylls and carotenoids of marine phytoplankton: separation of chlorophyll a from divinylchlorophyll a and zeaxanthin from lutein. J Plankton Res 1996; 18 (12): 2377–2382.

54. Mackey MD, Mackey DJ, Higgins HW, Wright SW. CHEMTAX-a program for estimating class abundances from chemical markers: application to HPLC measurements of phytoplankton. Mar Ecol Prog Ser 1996; 144: 265–283.

55. Wright SW, van den Enden RL, Pearce I, Davidson AT, Scott FJ, Westwood KJ. Phytoplankton community structure and stocks in the Southern Ocean (30–80˚E) determined by CHEMTAX analysis determined by HPLC pigment signatures. Deep-Sea Res II 2010; 57: 758–778.

56. Demmig-Adams B, Adams WW. Photoprotection and other responses of plants to high light stress. Ann Rev Plant Physiol Plant Mol Biol 1992; 43: 599–626.

57. Mangoni O, Carrada GC, Modigh M, Catalano G, Saggiomo V. Photoacclimation in Antarctic bottom ice algae: an experimental approach. Polar Biol 2009; 3 (32): 311–323.

58. Hutchins DA, Bruland KW. Iron-limited diatom growth and Si, N uptake ratios in a coastal upwelling regime. Nature 1998; 393: 561–564.

59. Utermöhl H. Zur vervollkommnung der quantitativen phytoplankton-methodik. Mitt Int Ver Theor Angew Limnol 1958; 9: 1–38.

60. Schreiber U, Schliwa U, Bilger W. Continuous recording of photochemical and non-photochemical chlorophyll fluorescence quenching with a new type of modulation fluorometer. Photosynthesis Res 1986; 10: 51–62.

61. Misic C, Covazzi Harriague A, Mangoni O, Cotroneo Y, Aulicino G, Castagno P. Different responses of the trophic features of particulate organic matter to summer constraints in the Ross Sea. J Mar Systems 2017; 166: 132–143.

62. Budillon G, Spezie G. 2000. Thermohaline structure and variability in the Terra Nova Bay polynya, Ross Sea. Antarctic Science 12 (4): 501–516.

63. Rusciano E, Budillon G, Fusco G, Spezie G. Evidence of atmosphere–sea ice–ocean coupling in the Terra Nova Bay polynya (Ross Sea-Antarctica). Cont Shelf Res 2013; 61: 112–124.

64. Cotroneo Y, Budillon G, Fusco G, Spezie G. Cold core eddies and fronts of the Antarctic Circumpolar Current south of New Zealand from in situ and satellite data. J Geophys Res Oceans 2013; 118 (5): 2653–2666.

65. DiTullio GR, Geesey ME, Leventer AR, Lizotte MP. Algal pigment ratios in the Ross Sea: implications for CHEMTAX analysis of Southern Ocean data. In: DiTullio GR, Dunbar R editors. Biogeochemistry of the Ross Sea. Ant Res Ser 78. American Geophysical Union, Washington, DC 2003; 279–293.

66. Arrigo KR, Worthen DL, Schnell A, Lizotte MP. Primary production in Southern Ocean waters. J Geoph Res 1998; 103 (15): 587–600.

67. Saggiomo V, Catalano G, Mangoni O, Budillon G, Carrada GC. Primary production processes in ice-free waters of the Ross Sea (Antarctica) during the austral summer 1996. Deep-Sea Res II 2002; 49: 1787–1801.

68. Hiscock MR, MR, Lance VP, Appill AM, Bidigare RR, Johnson ZI, Mitchell BG, et al. Photosynthetic maximum quantum yield increases are an essential component of the Southern Ocean phytoplankton response to iron. Proc Natl Acad Sci USA 2008; 105(12): 4775–4780. https://doi.org/10.1073/pnas.0705006105 PMID: 18349145

69. Strutton PG, Griffiths FB, Waters RL, Wright SW, Bindoff NL. Primary productivity off the East Antarctica (80–150˚E): January to March 1996. Deep-Sea Res II 2000; 47: 2327–2362.

70. Staehr PA, Henriksen P, Markager S. Photoacclimation of four marine phytoplankton species to irradiance and nutrient availability 2002; Mar Ecol Prog Ser 238: 47–59.

71. Van Leeuwe MA, Stefels J. Photosynthetic responses in *Phaeocystis antarctica* towards varying light and iron conditions. Biogeochemistry 2007; 83: 61–70.

72. van de Poll WH, Janknegt PJ, Van Leeuwe MA, Visser RJW, Buma AGJ. Excessive irradiance and antioxidant responses of an Antarctic marine diatom exposed to iron limitation and to dynamic irradiance. J Photochem Photobiol 2009; 94: 32–7.

73. Demmig-Adams B, Ebbert V, Mellman DL, Mueh KE, Schaffer L, Funk C, et al. Modulation of PsbS and flexible vs sustained energy dissipation by light environment in different species. Physiol Plant 2006; 127: 670–680.

74. van de Poll WH, Lagunas M, de Vries T, Visser RJW, Buma AGJ. Non-photochemical quenching of chlorophyll fluorescence and xanthophyll cycle responses after excess PAR and UVR in *Chaetoceros brevis*, *Phaeocystis antarctica* and coastal Antarctic phytoplankton. Mar Ecol Prog Ser 2011; 426: 119–131.

75. Jakob T, Goss R, Wilhelm C. Unusual pH-dependence of diadinoxanthin de-epoxidase activation causes chlororespiratory induced accumulation of diatoxanthin in the diatom *Phaeodactylum tricornutum*. J Plant Physiol 2001; 158: 383–390.

76. Saggiomo V, Carrada GC, Mangoni O, Ribera d'Alcalà M, Russo A. Spatial and temporal variability of size-fractionated biomass and primary production in the Ross Sea (Antarctica) during austral spring and summer. J Mar Systems 1998; 17: 115–127.

77. Kohut JT, Kustka AB, Hiscock M, Lam PJ, Measures C, Milligan A, et al. Mesoscale variability of the summer bloom over the northern Ross Sea shelf: A tale of two banks. J Mar Systems 2017; 166: 50–60.

78. Hatta M, Measures CI, Lam PJ, Ohnemus DC, Auro ME, Grand MM, et al. The relative roles of modified circumpolar deep water and benthic sources in supplying iron to the recurrent phytoplankton blooms above Pennell and Mawson Banks, Ross Sea, Antarctica. J Mar Systems 2017; 166: 61–72.

79. Danovaro R, Armeni M, Luna GM, Corinaldesi C, Dell'Anno A. Exo-enzymatic activities and dissolved organic pools in relation with mucilage development in the Northern Adriatic Sea. Sci Total Environ 2005; 353: 189–203. https://doi.org/10.1016/j.scitotenv.2005.09.029 PMID: 16225908

80. Del Negro P, Crevatin E, Larato C, Ferrari C, Totti C, Pompei M, et al. Mucilage microcosms. Sci Total Environ 2005; 353: 258–269. https://doi.org/10.1016/j.scitotenv.2005.09.018 PMID: 16242174

81. Rivaro P, Grotti M, Ardini F, Aulicino G, Cotroneo Y. Is dissolved iron distribution in the Ross Sea surface water affected by mesoscale physical structures? XXII Congresso dell'Associazione Italiana di Oceanologia e Limnologia 2015; Verbania Pallanza, Italy.

82. Mills MM, Kropuenske LR, Van Dijken GL, Alderkamp A-C, Berg GM, Robinson DH, et al. Photophysiology in two major Southern Ocean phytoplankton taxa: photosynthesis and growth of *Phaeocystis antarctica* (Prymnesiophyceae) and *Fragilariopsis cylindrus* (Bacillariophyceae) under simulated mixed layer irradiance. J Phycol 2010; 46: 1114–27.

83. Fragoso GM, Smith WO. Influence of hydrography on phytoplankton distribution in the Amundsen and Ross Seas, Antarctica. J Mar Systems 2012; 89 (1): 19–29.

84. Sedwick PN, Marsay CM, Sohst BM, Aguilar-Islas AM, Lohan MC, Long MC, et al. Early season depletion of dissolved iron in the Ross Sea polynya: Implications for iron dynamics on the Antarctic continental shelf. J Geophys Res 2011; 116, C12019,

85. Cerrone D, Fusco G, Simmonds I, Aulicino G, Budillon G. Dominant Covarying Climate Signals in the Southern Ocean and Antarctic Sea Ice Influence during Last Three Decades. J Climate 2017; dx.

86. Aulicino G. Fusco G, Kern S, Budillon G. Estimation of sea-ice thickness in Ross and Weddell Seas from SSM/I brightness temperatures. IEEE Transactions on Geoscience and Remote Sensing 2014; 52 (7): 4122–4140.

87. Liu X, Smith WO Jr. Physiochemical controls on phytoplankton distributions in the Ross Sea, Antarctica. J Mar Systems 2012; 94: 135–144.

88. Guglielmo L, Minutoli R, Bergamasco A, Granata A, Zagami G, Antezana T. Short-term changes in zooplankton community in Paso Ancho basin (Strait of Magellan): functional trophic structure and diel vertical migration. Polar Biol 2011; 34: 1301–1317.

89. Xavier JC, Brandt A, Ropert-Coudert Y, Badhe R, Gutt J, Havermans C, et al. Future Challenges in Southern Ocean Ecology Research. Frontiers in Mar Sci 2016;

90. Lancelot C, Hannon E, Becquevort S, Beth C, De Baar HJW. Modelling phytoplankton blooms in the Southern Ocean: dominant controls by light and iron in the Atlantic sector in austral spring 1992. Deep-Sea Res Part I 2000; 47: 1621–1662.

91. Carrada GC, Mangoni O, Russo GF, Saggiomo V. Phytoplankton size-fractionated biomasses in the Ross Sea. Spatial and temporal evolution during the austral spring. In: Faranda FM, Guglielmo L, Ianora A editors. Ross Sea Ecology, Italian Antarctic expeditions (1987–1995). Springer Berlin 2000; 205–216.

92. Saggiomo V, Carrada GC, Mangoni O, Marino D, Ribera d'Alcalà M. Physiological and ecological aspects of primary production in the Ross Sea. In: Ross Sea Ecology—Italian Antarctic expeditions (1987–1995). Faranda FM, Guglielmo L, Ianora A editors. Springer-Verlag, Berlin 2000; 247–258.

93. Shuman FR, Lorenzen CJ. Quantitative degradation of chlorophyll by a marine herbivore. Limnol Oceanogr 1975; 20: 580–586.

94. Collos Y, Husseini-Ratrema J, Bec B, Vaquer A, Lam Hoai T, Rougier C, et al. Pheopigment dynamics, zooplankton grazing rates and the autumnal ammonium peak in a Mediterranean lagoon. Hydrobiologia 2005; 550 (1): 83–93.

95. Pasqual C, Calafat A, Lopez-Fernandez P, Pusceddu A. Organic carbon inputs to the sea bottom of the Mallorca continental slope. J Mar Systems 2015; 148: 142–151.

96. Mathot S, Smith WO Jr, Carlson CA, Garrison DL. Estimate of *Phaeocystis* sp. carbon biomass: methodological problems related to the mucilaginous nature of the colonial matrix. J Phycol 2000; 36: 1049–1056.

97. Catalano G, Budillon G, La Ferla R, Povero P, Ravaioli M, Saggiomo V, et al. The Ross Sea. In: Liu K-K, Atkinson L, Quiñones R, Talaue-McManus L editors. Carbon and Nutrient Fluxes in Continental Margins: A Global Synthesis. Part II. Global Change: The IGBP Series. Springer Verlag 2010; 303–318.